Diurnal variability of nitrous oxide emissions from agricultural soils

Yuk Faat Wu

PhD

University of York

Environment and Geography

November 2021

Abstract

Nitrous oxide (N_2O) is a potent greenhouse gas with a rising atmospheric concentration largely due to the applications of nitrogen fertilisers globally. Development of mitigating strategies requires accurate estimations of N_2O emissions, however, estimates of N_2O emissions are uncertain due to its variability in space and time. An area of highest uncertainty is the diurnal variability of soil N_2O fluxes due to challenges of highly-frequent measurements. This research aimed to (1) investigate the prevalence of diurnal variability of N_2O flux from agricultural soils, (2) evaluate the efficacy of non-diurnal sampling intervals by comparisons with diurnal measurements of N_2O flux, and (3) examine the environmental and biological factors driving the diurnal variability of N_2O flux.

Through the systematic review of published N_2O flux data and field- and laboratory-based experiments, this research showed diurnal variability of N_2O flux is prevalent in agricultural soils, often exhibiting high diurnal amplitudes (>100%). Afternoon peaking of N_2O flux was the most common occurrence (~60% of the time) but its consistency can be impacted by changing field conditions such as interruption by rainfall. The review revealed that a single-daily flux measurements at 10:00 provided the best estimate of the daily mean value of N_2O emission (+2%), but with a risk of under- (-29%) or overestimations (+35%).

In field mesocosm experiments, diurnal N_2O fluxes were collected with a novel automated chamber system. The results of the first trial demonstrated that a single-daily flux measurements could adequately estimate N_2O emissions (+7%), whereas once-a-week basis measurements had large associated biases (-46 – +108%). Crucially, these experiments revealed that soil temperature showed little relationship with diurnal N_2O flux, whereas evidence of photosynthetic parameters driving diurnal variability of N_2O flux were found. The findings in the reductionist laboratory experiment, where fluctuations of soil temperature and moisture were minimised, further suggest PAR-driven plant metabolism is likely a driver of the diurnal variability of N_2O flux.

Table of Contents

List of Figures

List of Tables

List of Accompanying Materials

Supporting Information S1

Supporting Information S2

Acknowledgements

I would like to first thank the funding body of this research, the Natural Environment Research Council (NERC), and my hosting research institute, UK Centre for Ecology and Hydrology (UKCEH), for giving me the opportunity to conduct such interesting research.

My sincerest gratitude goes to my supervisors Prof Niall McNamara, Dr Jeanette Whitaker, Dr Sylvia Toet and Dr Christian Davies for their copious supports and advice throughout the past four years. Without them, this thesis would not have been possible. In particular, I would like to thank Niall for guiding me through my PhD. My thanks also go to the amazing people of the Plant-Soil Interactions group at UKCEH (Lancaster), Dafydd Elias, Simon Oakley, Kelly Mason, Amy Bradley, Aidan Keith, Rebecca Rowe, Sam Robinson and Sam Walrond, for all their help with my experiments, especially Dafydd for helping me with most of the technical issues in my PhD. Special thanks go to the facilities support personnel at UKCEH, Paul Jones and Luke Ireland, for helping me improve the design of my flow-through chambers used in Chapter 5.

This PhD journey has been an eye-opening experience. I have gained so much, not just academic knowledge and skills, but the amazing friends I have made along the way. Thank you, Rachel, for providing all the emotional supports I needed and keeping my sanity intact! George, John, Nye, Hannah, Holly, Vincent… I am sure I have missed some names here, but to everyone who has ever shared part of their life with me or helped me (emotionally or academically), even if it was just a few kind words, a small favour, or a piece of advice, please know that I am grateful.

Last but certainly not least, thank you Mum, for always being there for me. And to my beloved Tom and Sooty, thank you for being with me through thick and thin.

Author's declaration

I (Yuk Faat Wu) declare that this thesis is a presentation of original work, and I am the sole author. This work has not previously been presented for an award at this, or any other, University. All sources are acknowledged as References.

Chapter 2 consists of an original review undertaken by myself. The contribution of co-authors is as such: Amy Bradley performed part of the data extraction (Section 2.3.2); Niall McNamara, Jeanette Whitaker, Sylvia Toet and Christian Davies provided PhD supervision and detailed comments on the published manuscript.
Chapter 2 is published in *Global Change Biology* as: Wu, Y.-F., Whitaker, J., Toet, S., Bradley, A., Davies, C. A., & McNamara, N. P. (2021). Diurnal variability in soil nitrous oxide emissions is a widespread phenomenon. *Global Change Biology*, 27, 4950–4966. https://doi.org/10.1111/gcb.15791

The experimental set-up in Chapters 3 and 4 was facilitated by the members of the research group Plant-Soil Interaction at UK Centre for Ecology and Hydrology (Lancaster), including Niall McNamara, Dafydd Elias, Amy Bradley, Rebecca Rowe, Simon Oakley, Kelly Mason, and Aidan Keith. The development and design of the flow-through system were conducted by myself, with the help of Dafydd Elias and inputs of Niall McNamara.

1. General introduction

Extensive use of fossil fuels and various anthropogenic activities since the 19th century have led to exponential increases in the atmospheric concentrations of multiple greenhouse gases (GHGs), leading to the global warming crisis at present (Cassia et al., 2018). According to the National Oceanic and Atmospheric Administration (NOAA National Centers for Environmental information), the annual temperature anomalies of land and ocean surfaces has reached +0.98 °C in 2020. Furthermore, the global atmospheric concentrations of carbon dioxide (CO_2), methane (CH_4) and nitrous oxide (N_2O) have reached 416 ppm, 1873 ppb and 333 ppb in 2020 (Global Monitoring Laboratory), with growth rates of 2.3±0.5 ppm year^{-1}, 7.1±2.6 ppb yr^{-1} and 0.85±0.17 ppb yr^{-1}, respectively (Dlugokencky et al., 2018). The adverse impacts of global warming, including sea level rise and extreme climate events are detrimental to the socioeconomical and ecological well-being of the globe. It is projected roughly 10% of total economic value will be lost by 2050 if climate change is not alleviated (Swiss Re Institute, 2021). Furthermore, global biodiversity is under threat of climate change, as it is predicted up to 54% of species may be lost due to climate change (Urban, 2015).

1.1 Nitrous oxide in the atmosphere

Nitrous oxide is a natural atmospheric trace gas, yet it has the greatest global warming potential and the longest lifetime among the three major GHGs. Despite its relatively low atmospheric mixing ratio, the global warming potential of N_2O is 298 times higher than that of CO_2 over a 100 year time horizon with a lifetime of 114 years (Ehhalt et al., 2001; Ciais et al., 2013). To date, N_2O contributes 0.17 ± 0.03 W m^{-2} to the global radiative forcing (Myhre et al., 2013). Moreover, N_2O also catalyses the destruction of the stratospheric ozone layer (Ravishankara, Daniel and Portmann, 2009; Portmann, Daniel and Ravishankara, 2012), which is vital for filtering incoming ultraviolet radiation originating from the sun (Caldwell and Flint, 1994). It is speculated that the ongoing anthropogenic emissions of N_2O will hamper the recovery of the stratospheric ozone layer and will be the most important and largest ozone-depleting substance throughout the 21st century (Ravishankara, Daniel and Portmann, 2009).

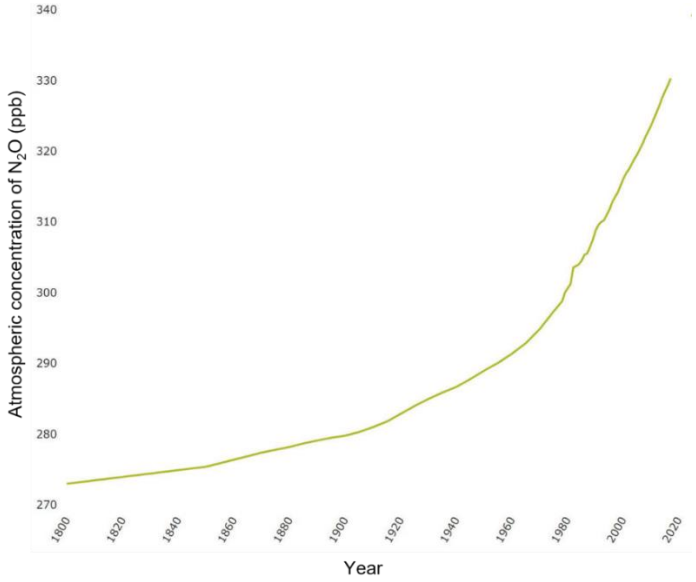

Figure 1.1. Trend in the atmospheric concentration of N_2O between 1800 and 2017, adapted from Global Monitoring Laboratory (2019)

1.2 Nitrous oxide emissions from agricultural soils

The invention of the Haber-Bosch process in the early 20th century, which converts the atmospherically abundant dinitrogen (N_2) into the plant available form ammonia (NH_3) at industrial scales, has transformed modern agriculture and boosted crop production by four times via N-enrichment in agricultural soils (Gruber and Galloway, 2008; Kissel, 2014; Stein and Klotz, 2016). The widespread applications of synthetic N fertilisers on agricultural soils have subsequently perturbed the global N cycle and led to a cascade of effects such as ecosystem acidification and eutrophication (Gruber and Galloway, 2008). However, contribution to global soil N_2O emissions remains one of the most adverse consequences of N fertiliser applications. Historic records from ice cores have shown a decreasing trend in the N stable isotope ratio ($\delta^{15}N$) in the atmospheric N_2O since 1940 (Figure 1.2) (Park et al., 2012), which indicates increasing N deposition onto soils, since the $\delta^{15}N$ ratio in biogenic N_2O emitted from soils is lower (Li and Wang, 2008; Felix and Elliott, 2013; Snider et al., 2015). With about 50% of the Earth's habitable land surfaces being used for agricultural purposes (Ellis et al., 2010), it is estimated 8.3 ± 2.5 Tg N_2O-N yr^{-1} are emitted from agricultural soils globally (Shukla et al., 2019). Although the implementations of policies and mitigation strategies have reduced N_2O emissions from agricultural soils in Europe in recent years (Petrescu et al., 2020), agriculture is still the main source of N_2O. At present, agricultural soils still contribute to over 70% of the N_2O emissions in the UK (Defra, 2019; Skiba et al., 2012).

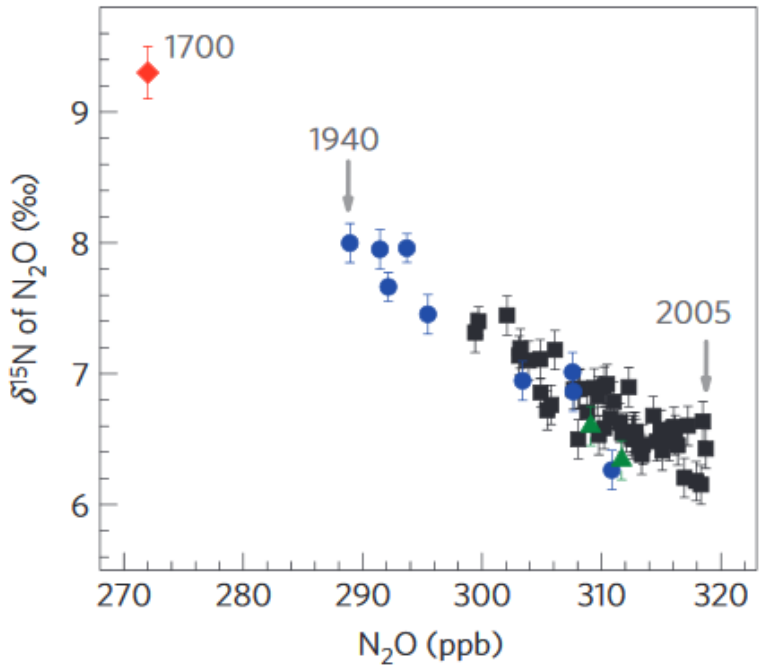

Figure 1.2. Historic record of N stable isotope ratio (δ15N) of atmospheric N2O indicating the increasing contribution of atmospheric N_2O of soil origin (adapted from Park et al. (2012))

1.3 Biological production of nitrous oxide in soils

Nitrogen (N) in soils exists in various organic and inorganic forms, which are in a constant state of transformation via various N-cycling processes. A portion of soil N is bound in soil organic matter (SOM), around 9 – 16% of SOM is comprised of proteins, peptides and amino acids (Stevenson and Cole, 1999). Proteins are usually depolymerised in soil by microbial extracellular enzymes (Schimel and Bennett, 2004), which then become N forms that are accessible to plants and soil microorganisms, such as oligopeptides and amino acids (Farrell et al., 2013; Hill, Farrell and Jones, 2012). Amino acids are prevalent in soil as they account for 32% to 50% of soil organic N (Senwo and Tabatabai, 1998). Excessive N uptake is usually mineralised and then released by microorganisms in the form of ammonium (NH_4^+), a substrate for nitrification (Schimel and Bennett, 2004).

The transformation of reactive nitrogen (Nr), including NH_3/NH_4^+, nitrate (NO_3^-), nitrite (NO_2^-), nitric oxide (NO), and N_2O, generally involves two major biological processes, namely nitrification and denitrification (Stein and Klotz, 2016). Nitrification and denitrification are primarily carried out by N-cycling archaea, bacteria and fungi (Pajares and Bohannan, 2016; Hayatsu, Tago and Saito, 2008). It is estimated approximately 70% of global N_2O emissions are contributed by microbial nitrification and denitrification (Syakila and Kroeze, 2011; Mrkonjic Fuka, Gesche Braker and Philippot, 2007). Apart from nitrification and denitrification, other biological processes that affect the balance of Nr

species include dissimilatory nitrate reduction to ammonium (DNRA) and anaerobic ammonium oxidation (Anammox). Figure 1.3 presents an overview of the interconnected pathways within the N cycle and the genes responsible for the production of the catalytic enzymes which bring about the N-cycling processes. Naturally, the soil N-cycle is highly complex and is regulated by various biological, physical and chemical factors, such as microbial community composition, substrate availability, redox potential, mycorrhizal associations and pH (Van Groenigen et al., 2015), which could consequently affect production and consumption of soil N_2O.

1.3.1 Nitrification

Although nitrification does not directly produce N_2O, they provide NO_2^- and NO_3^- substrates for subsequent denitrification and nitrifier denitrification (Martens, 2005; Zhu-Barker and Steenwerth, 2018). Under aerobic conditions, nitrification contributes substantially to N_2O emissions (Bremner and Blackmer, 1978), accounting for over 60% of the N_2O emissions (Liu et al., 2016; Uchida et al., 2013). It has been It is widely-recognised that nitrification can be autotrophic and heterotrophic depending on the types of nitrifiers (De Boer and Kowalchuk, 2001; Pedersen, Dunkin and Firestone, 1999; Zhang, Müller and Cai, 2015). Autotrophic nitrification is generally driven by nitrifying chemoautotrophs, which include ammonia-oxidising bacteria (AOB), ammonia-oxidising archaea (AOA) and nitrite oxidising bacteria (NOB); whereas heterotrophic nitrification is performed by heterotrophic nitrifying bacteria or fungi. Although autotrophic nitrification is generally considered as the principal nitrifiers in terrestrial ecosystems (Ussiri and Lal, 2012), recent studies have revealed that under acidic soil conditions, nitrification is predominantly heterotrophic (Pedersen, Dunkin and Firestone, 1999; Zhang et al., 2014). This is also because AOB are highly sensitive to acidity, ceasing growth below pH of 6.5 (Tarre and Green, 2004). It is also worth noting that heterotrophic nitrification can use both organic (e.g., amino acids) and inorganic N (e.g., NH_4^+) substrates (Honda et al., 1998; De Boer and Kowalchuk, 2001; Zhang et al., 2014), giving rise to its importance in ecosystems featuring organic acidic soils.

Nitrification encompasses the processes of NH_3 oxidation ($NH_3 \rightarrow NH_2OH/HNO \rightarrow NO_2^-$), and NO_2^- oxidation ($NO_2^- \rightarrow NO_3^-$), which are generally conducted under aerobic conditions (Ussiri and Lal, 2013). The first step of nitrification (i.e., NH_3 oxidation) is often described as the rate-limiting step of nitrification (Banning et al., 2015; Lehtovirta-Morley, 2018; Shen et al., 2012). It is carried out by two distinctive groups of microorganisms, ammonia-oxidising archaea and ammonia-oxidising bacteria, both capable of producing NH_3

monooxygenase encoded by the *amoA* gene (Lehtovirta-Morley, 2018). Little is known about the taxonomy of AOA, except that they are members of an archaeal phylum *Thaumarchaeota* (Schleper and Nicol, 2010; Zhalnina et al., 2012). Common genera of AOB in soils include genera *Nitrosomonas* and *Nitrococcus* (Holmes, Dang and Smith, 2019). Studies have found that AOA dominates in number in undisturbed neutral and acidic soils (Huang et al., 2021; Leininger et al., 2006; Prosser and Nicol, 2008, 2012), while AOB are more abundant and are responsible for ammonia oxidation in fertilised agricultural soils (Di et al., 2009; Meinhardt et al., 2018; Norton and Ouyang, 2019; Prosser and Nicol, 2012; Prosser et al., 2020).

During NO_2^- oxidation, NO_2^- is directly converted to NO_3^- by nitrite oxidoreductase encoded by the *nxrB* gene in NOB (e.g., *Nitrobacter*) (Vanparys et al., 2007; Pester et al., 2013). Similar to NH_3 oxidation, NO_2^- oxidation is also oxygen (O_2) dependent; however, under O_2-limited conditions, NO_2^- almost never accumulates to a level that is toxic to microorganisms and plants, except in low pH conditions (Bollag and Henninger, 1978; Ussiri and Lal, 2012). This is because NH_3 oxidation would be prohibited in the first place and existent NO_2^- would be converted to N_2O via nitrifier denitrification in anaerobic environments.

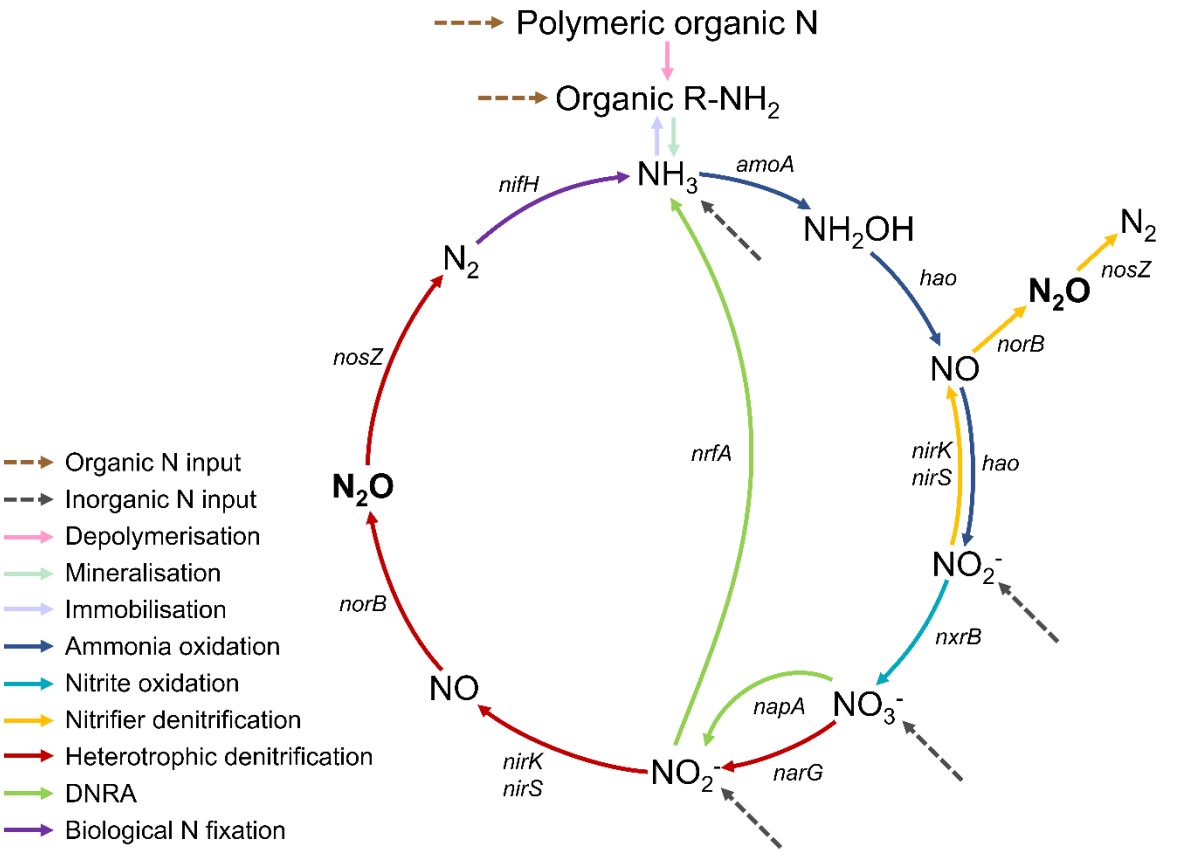

Figure 1.3. Main N-cycling processes (coloured arrows) and reactive N species in terrestrial ecosystems. Italicised terms represent the genes encoding the responsible enzymes facilitating the steps in the processes

1.3.3 Nitrifier denitrification

The importance of nitrifier denitrification in N_2O production has received increasing recognition in recent years. Studies have demonstrated up to 92% of total N_2O emissions from soils are produced via nitrifier denitrification in the presence of O_2 (Kool et al., 2010; Köster et al., 2015; Opdyke, Ostrom and Ostrom, 2009; Zhu et al., 2013). Not to be confused with coupled nitrification-denitrification, nitrifier denitrification is an alternative route following NH_3 oxidation carried out by NH_3 oxidisers which produces N_2O and N_2 (Figure 1.3), while coupled nitrification-denitrification refers to nitrification products (i.e., NO_2^- and NO_3^-) utilised by denitrifiers in conjunction (Wrage et al., 2001; Wrage-Mönnig et al., 2018). It is postulated that AOB employ nitrifier denitrification as a detoxification strategy to avoid the build-up of NO_2^- (Bouskill et al., 2012; Jung et al., 2014). In nitrifier denitrification, NO_2^- is first reduced to NO with NO_2^- reductase, which is commonly encoded by the *nirK* or *nirS* genes. The NO is then reduced to N_2O in the presence of nitric oxide reductase, which is encoded by the *norB* gene (Stein, 2011). In soil systems, N_2O emissions by nitrifier denitrification has been shown to increase with decreasing O_2 concentration from 21% to 0.5%, but below which contribution from nitrifier denitrification is negligible (Wrage et al., 2005; Venterea, 2007; Zhu et al., 2013). Nitrifier denitrification is also favoured by C limitation (Wrage et al., 2001; Wrage-Mönnig et al., 2018).

1.3.4 Denitrification

Heterotrophic denitrification, generally referred to as denitrification, is an important N_2O-yielding process in soil. Up to 35% of NO_3^- addition to soils could be lost to the atmosphere as N_2O via heterotrophic denitrification (Tiedje, 1988). Heterotrophic denitrification is a sequential process of the reduction of NO_3^- to N_2 (see Figure 1.3) catalysed by four types of reductase, which include NO_3^- reductase encoded by the *narG* gene, two mutually exclusive NO_2^- reductases encoded by the *nirS* and *nirK* gene, NO reductase encoded by the *norB* genes and N_2O reductase encoded by the *nosZ* genes (Sharma et al., 2005; Enwall et al., 2010; Ussiri and Lal, 2012).

A wide range of bacteria possesses the functional trait of heterotrophic denitrification. Most of these bacteria belongs to the genera of *Pseudomonas*, *Bacillus*, *Thauera* and *Paracoccus* (Ambus and Zechmeister-Boltenstern, 2007; Mrkonjic Fuka, Gesche Braker and Philippot, 2007). Certain genera of fungi have also been reported to be able to express *nir* and *nor* genes (Maeda et al., 2015), but they lack the *nosZ* gene that allows the reduction

of N_2O to N_2 (Hu, Chen and He, 2015). Anaerobic conditions are favourable to heterotrophic denitrification, which is when NO_3^- is used as a terminal electron acceptors in the formation of adenosine triphosphate in place of O_2 but NO_3^- is less energetically enriched which makes it less preferable (Maeda et al., 2015). Water-filled pore space is often used as a proxy for O_2 partial pressure in soil by researchers, since N_2O production has been found to positively correlate logarithmically with increasing water-filled pore space from 40% to 80% (Schindlbacher, Zechmeister-Boltenstern and Butterbach-Bahl, 2004; Bateman and Baggs, 2005; del Prado et al., 2006). Other favourable conditions include high available C and NO_3^- content (Burton et al., 2008; Firestone and Davidson, 1989; Martens, 2005; Wang, 2008; Weier et al., 1993). The final step of heterotrophic denitrification ($N_2O \rightarrow N_2$) does not always occur unless under extremely anoxic conditions, such as when water-filled pore space reaches above 90% (Chen et al., 2013), since the *nosZ* gene is inhibited by exposure to O_2 (Morley et al., 2008; Bergaust et al., 2010). Additionally, studies have shown that despite the substantial transcription of *nosZ* gene under acidic conditions (pH < 6.4), N_2O reductase expressed is non-functional, indicating low soil pH can prevent N_2O reduction (Hénault et al., 2019; Liu, Frostegård and Bakken, 2014).

1.3.5 Dissimilatory nitrate reduction to ammonium

Dissimilatory nitrate reduction to ammonium (DNRA) is a microbial process that competes against nitrifier denitrification and heterotrophic denitrification for N substrates (i.e., NO_3^- and NO_2^-), although the main product of DNRA is NH_3 instead. During DNRA, NO_3^- is first reduced to NO_2^- by NO_3^- reductase encoded by the *napA* gene; then, NO_2^- is reduced to NH_3 without any intermediates (Pandey et al., 2020). The process of DNRA is carried out by heterotrophic and anaerobic chemolithotrophic bacteria (Brunet and Garcia-Gil, 1996; Dalsgaard and Bak, 1994; Silver, Herman and Firestone, 2001), and it is known to take place in highly reduced conditions such as sediments (Bonin, 1996; Tiedje et al., 1983), as well as terrestrial ecosystems (Minick et al., 2016; Müller et al., 2009; Sgouridis et al., 2011; Silver, Herman and Firestone, 2001; Pandey et al., 2020). Albeit DNRA plays a significant role as a NO_3^- consumption process, its importance of N retention is often overlooked (van den Berg et al., 2016; Putz et al., 2018; Rütting et al., 2011). Similar to heterotrophic denitrification, DNRA is also favoured by O_2 limitation (van den Berg et al., 2017; Rütting et al., 2011). However, DNRA is only dominant under high C/NO_3^- and high NO_2^-/NO_3^- ratio (Pandey et al., 2020).

1.3.6 Regulating factors of nitrous oxide production

The dynamics among N-cycling processes (e.g., nitrification, nitrifier denitrification, heterotrophic denitrification and DNRA) will determine the net production or consumption of N_2O in soils and therefore the N_2O flux. The rates of these processes are regulated by essentially several factors, which broadly include the substrate availability of soil N, soil organic C content, soil moisture, O_2 partial pressure, soil temperature and pH. The most imperative regulating factor is soil N availability, especially NO_3^-, NO_2^- and NH_4^+, as they are the feedstock for N_2O-generating microbial processes (Firestone and Davidson, 1989). Secondly, soil O_2 partial pressure is a major controlling factor for denitrification, as denitrifiers would turn to use NO_3^-, NO_2^- and NO as electron acceptor for microbial respiration when O_2 becomes unavailable (Chen and Strous, 2013; Włodarczyk et al., 2021). Soil organic C, on the other hand, largely affects heterotrophic denitrification and DNRA by providing organic C for heterotrophic biomass assimilation, which in turn influences the capacity of heterotrophic denitrification and DNRA (Myrold and Tiedje, 1985; Baggs, Pihlatie and Cadisch, 2003). Studies have also found positive relationship between soil organic C content and ratio of N_2O production by heterotrophic nitrification in acidic soils (Zhang et al., 2014; Zhang, Müller and Cai, 2015). The positive effect of increased soil organic C on N_2O emission has been demonstrated in multiple studies using glucose addition (Azam et al., 2002; Wang et al., 2005; Wu et al., 2017a). It has been reported that soil organic C content correlates with the abundance of *nirS*-type denitrifiers (Enwall et al., 2010). Besides, the addition of soil organic C (especially in labile forms) can stimulate soil respiration (Cleveland et al., 2007; Jia et al., 2014; Wang et al., 2003), which subsequently consumes soil O_2 and creates aerobic conditions favourable to denitrification and nitrifier denitrification in soils (Ussiri and Lal, 2012). The quality of the soil organic C also shown to affect the fate of N substrates in soil. A meta-analysis by Chen et al. (2013) revealed that the positive effect of N_2O emission from plant residue amendment decreases with increasing C/N ratio of the plant residue, owing to the increase in N immobilisation with at high C/N ratios (i.e. > 45) as the non-denitrifying microbes compete N substrates against nitrifiers and denitrifiers for C assimilation.

The effect of soil moisture and soil physical properties (e.g., bulk density and texture), can also substantially influence O_2 partial pressure in soils (Butterbach-Bahl et al., 2013). For instance, soils with higher bulk densities and/or higher clay contents have lower porosities, which reduce the aeration in the soils and promote anaerobic N_2O production (Klefoth et

al., 2014). Water-filled pore space is commonly used as a proxy for soil O_2 level since the they are generally negatively correlated (Melling et al., 2014). Under high N conditions, increases in water-filled pore space have been shown to exponentially enhance N_2O emissions (Schindlbacher, Zechmeister-Boltenstern and Butterbach-Bahl, 2004; Smith et al., 1998), owing to the restriction of O_2 diffusion from the atmosphere into the soil, as well as the stimulation of soil respiration which further depletes soil O_2 (Chen et al., 2017; Suseela et al., 2012). Increases in water-filled pore space may also prevent the escape of N_2O produced in soils, potentially contributing to the temporal variability of N_2O flux. Production of N_2O via heterotrophic denitrification (i.e. NO → NO_2) generally occurs when water-filled pore space exceeds 60% (Davidson et al., 2000). Under O_2-limited conditions (0.5 – 3.0%), N_2O production via nitrifier denitrification and heterotrophic denitrification can increase over 80 times compared to that at 21% O_2 concentration, whereas in complete absence of O_2, heterotrophic denitrification is the sole source of N_2O (Zhu et al., 2013). Pulse emissions of N_2O were often observed following and during rainfall (Liu et al., 2014; Rowlings et al., 2015; van Haren et al., 2005; Waldo et al., 2019) or irrigation events (Kostyanovsky et al., 2019; Scheer et al., 2012; Zhang et al., 2012b).

The controls of soil temperature on soil N_2O production primarily rely on its direct influence on the kinetic reactions of the N_2O-genic microbial processes and on the growth of the N-cycling microbial communities (Abdalla, Smith and Williams, 2011; Lesschen et al., 2011; Mosier, 1994). Soil temperature also controls the biological consumption of soil O_2 partial pressure by governing the growth of aerobic heterotrophs, which indirectly affects the O_2 conditions favouring the processes of nitrification and denitrification (Butterbach-Bahl et al., 2013; Hénault et al., 2012). While both nitrification and denitrification have similar temperature dependencies (Wang et al., 2021), the temperature for the maximum rates of nitrification and denitrification has been shown to vary by climatic regions (Lai and Denton, 2018). The regulatory effects of soil temperature on the $N_2O/(N_2O + N_2)$ ratio are previously observed (Abdalla, Smith and Williams, 2011; Dalal et al., 2003; Sun et al., 2018), with exponential decreases in $N_2O/(N_2O + N_2)$ ratio with increasing soil temperature (Maag and Vinther, 1996). Reportedly, the maximum N_2O flux occurs at 35 °C, beyond which the N_2O flux starts to plumet due to increase N_2O reduction to N_2 (Lai and Denton, 2018).

On the other hand, soil pH can affects the rate of nitrifications and denitrification by means of inhibition of the expression of N-cycling genes (Suzuki, Dular and Kwok, 1974; Kyveryga et al., 2004; Liu et al., 2010; Huhe et al., 2016). Current knowledge on soil pH reveals that

low pH has a more apparent inhibitory effect on NH_3 oxidation by AOB and the last step of denitrification (i.e., $N_2O \rightarrow N_2$). However, high nitrification rates have been observed in acidic soils in many studies, which was attributed to the dominance of acid-tolerant AOA and heterotrophic nitrifiers (Islam, Chen and White, 2007; Zhang et al., 2012a; Hu, Xu and He, 2014; Liu et al., 2010). Often soils with low pH also feature higher $N_2O/(N_2O+N_2)$ ratio (Firestone, Firestone and Tiedje, 1980; van der Weerden et al., 1999; Čuhel et al., 2010), which indicates lower N_2O reduction ($N_2O \rightarrow N_2$) rates. This is largely due to the assembly of the NOS, an enzyme responsible for the reduction of N_2O, is inhibited in acidic soils (Bergaust et al., 2010; Bakken et al., 2012).

1.4 Measurement methods for soil N_2O emission

There exists a variety of methods that measure soil N_2O emissions, ranging from the small-scaled (< 1 m^2) chamber techniques to the micrometeorological technologies for field-scaled N_2O flux measurements, each with their own advantages and drawbacks. While many studies investigating soil N_2O fluxes have been conducted *ex situ* in laboratory settings, *in situ* field-based measurements often incorporate effects of climatic factors and better reflect the changing dynamics of soil N_2O flux in more realistic scenarios. Therefore, the following subsections will primarily focus on the existing common technologies for field-based measurements of soil N_2O emissions.

1.4.1 Static chamber technique

The static closed-chamber technique is a commonly practiced method (Ussiri and Lal, 2013), normally manually, for measuring soil N_2O fluxes. It is also referred to as the non-steady state chamber technique (Collier et al., 2014). The general procedures of the technique involve the installation of a chamber onto a soil surface pre-fitted with a base-ring over a length of time (usually up to an hour), forming an air-tight enclosure (headspace) and trapping gases emitted from the soil surface for the duration. Air samples in the headspace are collected at regular intervals (5- to 15-minute) with a syringe and evacuated vials, which are later analysed in the laboratory with gas chromatography to obtain the concentrations of the trace gas species of interest at the points of collection. The changes in gas concentration over the time of chamber placement are then used to calculate the gas flux. Compared to other flux measurement techniques, the static chamber technique is relatively low cost and easily deployed in different field conditions, which also allows for multiple deployments in the field to account for spatial variability of soil gas flux (Collier et al., 2014). Because of this, many researchers employ this technique for its versatility and suitability for small experimental plots (de Klein et al., 2020). However, due to its requirement for manual operation, flux measurements with the static chamber technique are often made at low temporal frequencies (usually weekly to monthly, sometimes daily) and rarely at sub-daily frequencies (Charteris et al., 2020; Ussiri and Lal, 2013), and therefore produce estimations of N_2O emission with larger uncertainties, since it may not capture the temporal variability of N_2O flux.

1.4.2 Automated chamber technique

A similar approach to measuring soil N_2O flux is the automated chamber technique, which has gained popularity in recent years (Zhao et al., 2018). Whilst the technique is not novel

(Schütz et al., 1989; Bronson, Neue and Singh, 1997), improvements made in rapid analytical technologies such as quantum cascade lasers (Brummer et al., 2017) and cavity ring-down spectroscopy (Grinfelde et al., 2017) have made automated chamber measurements more precise and robust (Grace et al., 2020; Grinfelde et al., 2017). Similar to the operating principle of the static chamber technique, the automated chamber technique derive soil gas fluxes by continuously measuring the changes in gas concentration within the chamber headspace over a programmed chamber closure time, ranging from several minutes to an hour, with a linear or non-linear regression model (Venterea et al., 2020). While manual installation and maintenance are still required, this technique allows long-term monitoring of soil N_2O fluxes at high-frequencies (several measurements a day), addressing the diurnal variability of N_2O flux (Flessa et al., 2002; Grace et al., 2020; Keane et al., 2018; Rowlings et al., 2015). Additionally, deployed automated chambers can be multiplexed, allowing near-simultaneous measurements of N_2O flux at different locations of a study area or of areas with different treatment applications (Barton et al., 2008; Keane et al., 2018, 2019; Marsden et al., 2018; Scheer et al., 2011; Schwenke et al., 2016). However, the cost of an automated chamber system is higher compared to that of static chambers (Grace et al., 2020).

1.4.3 Eddy covariance technique

The eddy covariance technique is micrometeorological method which provides near-continuous measurements of soil N_2O flux over a large landscape (Ussiri and Lal, 2013). The general basis of this technique relies on the simultaneous measurements of a trace gas concentration and vertical wind speed of eddies over an averaging period, and subsequently derive a net flux after the computation of the measured values (Hensen, Skiba and Famulari, 2013; McMillen, 1988). Like the automated chamber technique, the eddy covariance technique can provide high-frequency (sub-daily) real-time measurements of N_2O flux (Liang et al., 2018; Lognoul et al., 2019; Shurpali et al., 2016; Scanlon and Kiely, 2003). However, uniform topography is an important prerequisite for accurate flux measurements by the eddy covariance technique (Collier et al., 2014; Jones et al., 2011), which exclude certain landscapes and ecosystems from this technique. Additionally, as net N_2O fluxes are computed by averaging N_2O concentration changes over a large area since it only provides averaged net fluxes at field scale (flux footprint varies from 250m to 3 km) (Chu et al., 2021), this method overlooks the spatial heterogeneity of N_2O flux (Laville et al.,

1999; Loescher et al., 2006; Waldo et al., 2019), as well as lacks the ability for discrete measurements of N_2O flux from experimental plots.

1.5 Temporal variability of soil N_2O emission

Soil N_2O emissions are spatially and temporally variable by large owing to the inherent spatiotemporal heterogeneity of the N_2O-generating microbial processes in soils (Butterbach-Bahl et al., 2013; McDaniel et al., 2017), which are driven by a variety of interacting control including the aforementioned regulating factors (Butterbach-Bahl and Dannenmann, 2011). The spatiotemporal variability of soil N_2O flux exists in various scales ranging from microscopic to regional (Butterbach-Bahl et al., 2013; Chenu, Hassink and Bloem, 2001; Fóti et al., 2018; Nunan et al., 2003; Saikawa et al., 2014; van den Heuvel et al., 2009), and diurnal to interannual (Blackmer, Robbins and Bremner, 1982; Fóti et al., 2018; Ito et al., 2018; Khalil et al., 2007; Smith et al., 2004; Williams, Ineson and Coward, 1999). The spatiotemporal variability of N_2O flux, if unaddressed, can lead to highly certain estimates of N_2O emissions and impede the developments of N_2O mitigation strategies (Hénault et al., 2012). While understanding the spatial variability of N_2O flux presents its own challenges and such variability is an important characteristic of N_2O flux to consider, the scope of this thesis is to understand the temporal variability of N_2O flux, with a specific focus on diurnal variability. Given current global and regional estimates for N_2O emissions are calculated per annum, the following subsections will review the intra-annual variability of N_2O flux, namely the event-based, seasonal and diurnal variability of N_2O flux.

1.5.1 Event-based variability

Event-based variations in N_2O flux are usually related to climatically induced scenarios such as freeze-thaw and drought-rewetting events of soils (Barrat et al.; Bruijn et al., 2009; Chen et al., 1995; Ruser et al., 2006; Wagner-Riddle et al., 2017), as well as anthropogenic agricultural activities such as N fertilisation and irrigation. During the cycles of freeze-thaw and drought-rewetting, N_2O regulating parameters (e.g., water-filled pore space, O_2 partial pressure, soil N and soil organic C availability) increase drastically, leading to stimulation of N_2O-genic microbial processes (Butterbach-Bahl and Dannenmann, 2011). Additionally, changes in wind speed may also contribute to the short-term temporal variability of N_2O flux. Wind speed has been shown to positively affect N_2O flux, owing to its control on the dynamics of gas diffusion and advection in soils (Redeker, Baird and Teh, 2015; Zona et al., 2013).

Soils in regions of high latitudes and at high elevations are routinely frozen for during winter seasons and may be subject to frequent freeze-thaw cycles, which are also influenced by the diurnal patterns of soil temperature (Wagner-Riddle et al., 2010). Evidence from studies show that N_2O emitted during the freeze-thaw cycles can account for up to the majority of the total annual N_2O emission, although the percentages are highly variable depending on the ecosystems (Chen et al., 2018; Katayanagi and Hatano, 2012; Wagner-Riddle et al., 2017), ranging from 0% to 93% (Koga et al., 2004; Syväsalo et al., 2004). During the freeze-thaw cycles, physically and biologically 'locked' nutrients (i.e., organic C and N substrate) becomes available to soil N-cycling microbes due to microbial cell lysis and disruption of soil aggregates upon ice crystal formation (Congreves et al., 2017; Groffman et al., 2009; Schimel, Balser and Wallenstein, 2007; Wagner-Riddle et al., 2017). This leads to O_2 depletion due to stimulated soil respiration (Patel et al., 2021) and enhanced denitrification in ice-sealed soil, the entrapped N_2O is released upon thawing (Teepe, Brumme and Beese, 2001; Risk, Snider and Wagner-Riddle, 2013).

Soil N_2O production in the drought-rewetting cycles follow different mechanisms. During the prolonged dry periods (i.e., droughts), inorganic N accumulates in soil as a result of reduced plant N uptake and microbial N immobilisation (Parker and Schimel, 2011; Leitner et al., 2017; Zhang et al., 2017). Upon rewetting, the previously inaccessible N due to limited hydrological connectivity becomes available and the increased water-filled pore space (Harris et al., 2021; Gelfand et al., 2015). Pulse emissions of N_2O are often observed following rainfall events (Bell et al., 2016; Geng et al., 2017; Li, Frolking and Frolking, 1992; Liu et al., 2014). Similar to the 'Birch effect' (Birch and Friend, 1956), rewetting of soils rapidly enhances soil microbial activity including denitrification and heterotrophic respiration, along with the limited O_2 conditions induced by increased soil moisture, N_2O production is greatly enhanced (Borken and Matzner, 2009).

Nitrogen fertiliser applications on agricultural ecosystems are the main source of anthropogenic contributions to the global atmospheric increase of N_2O concentration (Bouwman, Boumans and Batjes, 2002). Pulse emissions of N_2O following applications of N fertilisers are commonly observed within several weeks in arable systems (Fuß et al., 2011; Kostyanovsky et al., 2019; Signor, Cerri and Conant, 2013). It is difficult to predict the episodic emissions of N_2O after N fertilisations since N_2O production is regulated by microbiological processes that are controlled by numerous environmental factors (Butterbach-Bahl et al., 2013), as well as the irrigation regimes following fertilisation (Wu

et al., 2017c). The timing of N fertiliser applications also can affect the N_2O emissions depending of the concurrent climate and N demand of the vegetation (Bell et al., 2016). For example, Thilakarathna et al. (2020) found significant reduction in total N_2O emissions from fields that received fertilisations in spring than those that received fertilisation in autumn. Split applications of fertilisers are sometimes advocated to reduce N_2O emissions (Bell et al., 2016; Burton et al., 2008), but its effectiveness is in question (Cardenas et al., 2019; Snyder et al., 2009).

1.5.2 Seasonal variability

Observations of large seasonal variations in N2O flux from arable systems have been reported in a number of studies(Chen et al., 2019; Choudhary, Akramkhanov and Saggar, 2002; Flessa, Dörsch and Beese, 1995; Kavdir, Hellebrand and Kern, 2008). Reportedly, up to 80% of the annual N2O evolution can occur in winter and spring months in temperate regions, where freeze-thaw cycles are featured in the two seasons (Chen et al., 2018; Flessa, Dörsch and Beese, 1995; Teepe, Brumme and Beese, 2001; Regina et al., 2004; Syväsalo et al., 2004; Wagner-Riddle and Thurtell, 1998). However, it is predicted that the freeze-thaw patterns in temperate regions will alter in the future as global warming progresses and higher frequency and intensity of rainfall will occur in growing seasons (Henry, 2008; Serquet et al., 2011; Griffis et al., 2017). Griffis et al. (2017) postulated that in a warming and wetting climate, spring thaw will account for less annual N_2O budget and approximately half of the annual N_2O budget will be evolved during early crop growth stages due to spring fertilisation, as studies have shown that over half of the annual N_2O emission can be evolved during the summer months during the crop vegetative period (Bremner, Robbins and Blackmer, 1980; Dhadli, Brar and Kingra, 2016).

1.5.3 Diurnal variability

The diurnal variability of N_2O flux refers to the variations in N_2O flux within a 24-hour period. Early observations of diurnal variations in N_2O flux were made decades ago (Blackmer, Robbins and Bremner, 1982; Christensen, 1983), however, the diurnal variability of N_2O flux has only gained increased research attention in recent years (Francis Clar and Anex, 2019; Keane et al., 2018, 2019; Lognoul et al., 2019; Shurpali et al., 2016; van der Weerden, Clough and Styles, 2013; Xu et al., 2016), likely because high-frequency flux measurement technologies have become more available. However, the diurnal variability of N_2O flux is often overlooked in current N_2O flux measurement practices (Charteris et al., 2020; De Klein and Harvey, 2015), despite study findings showing diurnal variations of N_2O flux

ranging between five- to ten-fold in magnitude (Christensen, 1983; Dobbie and Smith, 2003; Maljanen et al., 2002; Scheer et al., 2012; Shurpali et al., 2016; Williams, Ineson and Coward, 1999). In addition, the mechanisms behind the diurnal variability of N_2O flux are still poorly-understood. Typically, studies with observations of diurnal variations in N_2O flux attributed the diurnal oscillation of soil temperature to the diurnal pattern of N_2O fluxes, as N_2O fluxes were often peaked in the afternoon, which coincide with the diurnal fluctuations of soil temperature (Alves et al., 2012a; Blackmer, Robbins and Bremner, 1982; Livesley et al., 2008; Maljanen et al., 2002; Metivier, Pattey and Grant, 2009). As mentioned previously (Section 1.3.6), increase in soil temperature can stimulate microbial activity including N_2O-genic processes and microbial respiration. The increase in soil temperature during daytime likely contributes to the diurnal variations of N_2O flux.

However, some studies found stronger positive relationships between diurnal N_2O fluxes and photosynthetic parameters such as solar radiation (Christensen, 1983), photosynthetically active radiation (PAR; Keane et al., 2018), net ecosystem production (Keane et al., 2018) and gross primary production (Zona et al., 2013). Many studies that postulated positive correlations between soil N_2O fluxes and soil temperature did not take photosynthetic parameters into account, which could have exaggerated the effect of soil temperature by considering the effect of photosynthetic parameters as part of the effect of soil temperature. Undoubtedly, the increase in temperature would influence the rates of N_2O-genic processes as they are temperature dependent, with a temperature sensitivity (Q_{10}) between 1.4 and 3.4 (McKenney, Shuttleworth and Findlay, 1980; Yao et al., 2010; Phillips et al., 2015b). Yet, given its Q_{10} values, it is unlikely that the temperature effect alone could result in a diurnal variation of N_2O flux with five-fold or more of magnitude, as observed in many studies (Alves et al., 2012a; Keane et al., 2017; Laville et al., 2017; van der Weerden, Clough and Styles, 2013).

A theory posited by Christensen (1983) and Keane et al. (2018) suggests that plant photosynthesis may contribute to the diurnal variations of N_2O flux via increased root exudation of photosynthetically assimilated C during daytime. Since denitrifiers are heterotrophic and consume soil organic C to generate energy, exudation of photosynthate C would promote denitrification rate. Besides, root exudation of liable C can also deplete the O_2 in the rhizosphere via enhancing soil respiration (de Vries et al., 2019). Studies have provided demonstrated up to 40% of photosynthetically assimilated C are exuded into the rhizosphere (Canarini et al., 2019; Kuzyakov and Domanski, 2000), which are rapidly

respired within several hours of the photoperiods (Gavrichkova and Kuzyakov, 2010; Johnson et al., 2002; Kuzyakov and Cheng, 2001). The research evidence supports the theory that plant C inputs could also contribute to the diurnal variability of N_2O flux.

However, inconsistent diurnal patterns of N_2O flux have also been observed in literature. Shurpali et al. (2016) and Keane et al. (2019) observed daily maxima of N_2O flux occurring at night and oscillate asynchronously with the diurnal rhythm of PAR. It was posited that the long lag-time between the diurnal peaks of soil temperature/PAR and those of N_2O flux was due to N_2O production being at lower soil depths, which increased the time taken for N_2O to reach the soil surface (Smith et al., 1998). On the other hand, some studies measured diurnal N_2O fluxes but did not find any distinct diurnal patterns of N_2O flux (i.e., sinusoidal patterns with a daytime or night-time peak) (Ball, Scott and Parker, 1999; Du, Lu and Wang, 2006; Xu et al., 2016), whereas some studies presented contrasting evidence of the diurnal patterns of N_2O flux only occurring during high or low N_2O emissions periods (Francis Clar and Anex, 2019; Lognoul et al., 2019). The diurnal patterns of N_2O flux are also susceptible to interruption of non-diurnal events such the increase in soil moisture caused by rainfall (van der Weerden, Clough and Styles, 2013).

Given the large magnitudes of diurnal variability of N_2O flux, failure to address the diurnal variability of N_2O flux in flux measurement regimes could lead to increased uncertainty in the estimates of total emissions and N_2O budget (Shurpali et al., 2016), and could also hamper the developments and assessments of N_2O mitigation strategies. Although studies have suggested once daily measurements of N_2O flux in midmorning could capture N_2O fluxes close to the daily mean flux since it is the time of daily average soil temperature (Alves et al., 2012a; Charteris et al., 2020; Smith and Dobbie, 2001), the seemly irregular and unpredictable occurrences of diurnal pattern of N_2O flux would undermine this assumption. Furthermore, the mechanisms behind diurnal variability of N_2O flux are still poorly-understood. Knowledge of how diurnal variations of N_2O flux respond to potential environmental drivers are crucial to grasping a bettering understanding of the diurnal variability of N_2O flux.

1.6 Research aims

In this thesis, multiple aspects pertinent to the diurnal variability of soil N_2O flux were explored. The broad research aims of this thesis are as follows:

To investigate the prevalence of diurnal variability of N_2O flux – Diurnal variability of N_2O flux have been widely reported but few investigations on the prevalence of this phenomenon were conducted. Besides, inconsistent diurnal patterns of N_2O flux have been reported across and within existing studies. Understanding the persistence and occurrence frequency of different diurnal patterns of N_2O flux is crucial for explaining the significance of this phenomenon.

To evaluate the efficacy of different non-diurnal sampling intervals (e.g., daily and weekly) by comparisons with diurnal measurements of N_2O flux – Conventional measurement practices for soil N_2O flux do not account for the diurnal variations in N_2O flux and assume the flux measurements represent the average N_2O flux between measurement intervals. Adequacy of different N_2O flux sampling intervals, as well as estimations by emission factors, can be assessed with collected diurnal N_2O flux data.

To examine the potential environmental and biological factors driving the diurnal variability of N_2O flux – Current literature posits that diurnal variations in N_2O flux are primarily driven by soil temperature, however, some limited research has also suggested that plant related factors such as PAR driven photosynthesis and associated gross primary production may direct processes that promote diurnal N2O variation. For example, by altering the rates of root exudation and C supply to microbial communities. However, few studies have explored their discrete effects on the diurnal dynamics of N_2O flux (i.e., diurnal amplitude, pattern and peak timing) due to the strong diurnal coupling between the two variables under field conditions.

1.7 Overview of chapters

Chapter 2 reviewed and analysed diurnal N_2O flux data extracted from published literature, and provided evidence of common occurrences of diurnal patterns of N_2O flux (~60% daytime peaking, ~20% night-time peaking, addressing research aim 1), which vary with soil drainage property, water-filled pore space and land use. Further assessments in Chapter 2 also revealed that soil temperature only strongly correlates ($R \geq 0.7$) with diurnal N_2O flux a-third of the time, and single-daily flux measurements were best conducted at ca. 10:00 to avoid misestimations of cumulative N_2O emission, although the estimation uncertainties still persisted regardless of sampling time.

Chapter 3 assessed the diurnal variations in N_2O flux from fertilised, planted mesocosms in field conditions, with the use of an automated chamber system to perform diurnal N_2O flux measurements. Near-continuous diurnal N_2O fluxes revealed that estimating with the 1% emission factor (Hergoualc'h et al., 2019) underestimated cumulative N_2O emission by more than half, and flux sampling intervals beyond once daily could under- or overestimate cumulative N_2O emissions by -75% to +108% (addressing research aim 2). Consistent with the findings in Chapter 2, diurnal N_2O fluxes in Chapter 3 exhibited similar distributions of diurnal patterns of N_2O flux with high diurnal amplitudes of N_2O flux (> 100%) in 85% of the measurement days (corresponding to research aim 1). Further analyses in Chapter 3 revealed that variance in diurnal N_2O flux could be explained by soil moisture and gross primary productivity, but not soil temperature nor PAR (partly addressing research aim 3), prompting the experimental design in Chapter 4.

Using the pre-existing experimental set-up from Chapter 3, Chapter 4 explored the effects of soil warming and plant shading on the diurnal amplitude and peak timing of N_2O flux with a factorial experiment design (addressing research aim 3). Plant shading significantly reduced the diurnal amplitude of N_2O flux but only when soil warming was not applied concurrently. Soil warming did not have any significant effect of the diurnal amplitude of N_2O flux. However, plant shading and soil warming brought forward the most frequent flux peak time from 16:00 – 19:59 to 12:00 – 15:59. Interesting, while the relationship between diurnal amplitude of N_2O flux and daily cumulative solar radiation was significantly positive, the relationship between diurnal amplitude of N_2O flux and net ecosystem production (product of gross primary production – ecosystem respiration) was significantly negative. These findings hinted at the complex effects of the interactions between environmental and biological factors on the diurnal dynamics of N_2O flux, which are not well-understood.

Building on the basis of Chapter 4, Chapter 5 explored the discrete effects of different PAR levels on the diurnal dynamics of N_2O flux with a controlled laboratory set-up (addressing research aim 3). Under stable soil temperature and moisture conditions with 12-hour PAR photoperiods daytime peaking pattern of N_2O flux was more prevalent (75 – 84% of the time) than in the previous field-based experiments (Chapter 3 and 4). Increasing the PAR levels led to a significant increase in the diurnal amplitude of N_2O flux when the daily baseline fluxes (daily N_2O flux minima) were considered. On the other hand, reducing the PAR levels shifted the peak timing from 16:00 – 19:59 to 12:00 – 15:59, which was consistent with the finding in Chapter 4. Chapter 5 provided empirical evidence supporting the hypothesis that plant metabolism, independent of temperature, was a driver of diurnal variations of N_2O flux and contributed to the occurrence of daytime peaking of N_2O flux.

Chapter 6 provides a comprehensive discussion on the different aspects in relation to the diurnal variability of N_2O flux, by integrating the findings from the previous chapters and literature. Chapter 6 also highlights the knowledge gap that should be addressed in future research to improve the understanding on the complex mechanisms driving the diurnal variability of N_2O flux.

2. Diurnal variability in soil nitrous oxide emissions is a widespread phenomenon

This chapter is published as: Wu, Y.-F., Whitaker, J., Toet, S., Bradley, A., Davies, C. A., & McNamara, N. P. (2021). Diurnal variability in soil nitrous oxide emissions is a widespread phenomenon. *Global Change Biology*, 27, 4950–4966. https://doi.org/10.1111/gcb.15791

2.1 Abstract

Manual measurements of nitrous oxide (N_2O) emissions with static chambers are commonly practiced. However, they generally do not consider the diurnal variability of N_2O flux, and little is known about the patterns and drivers of such variability. We systematically reviewed and analysed 286 diurnal datasets of N_2O fluxes from published literature to: (i) assess the prevalence and timing (day or night peaking) of diurnal N_2O flux patterns in agricultural and forest soils; (ii) examine the relationship between N_2O flux and soil temperature with different diurnal patterns; (iii) identify whether non-diurnal factors (i.e. land management and soil properties) influence the occurrence of diurnal patterns; and (iv) evaluate the accuracy of estimating cumulative N_2O emissions with single-daily flux measurements.

Our synthesis demonstrates that diurnal N_2O flux variability is a widespread phenomenon in agricultural and forest soils. Of the 286 datasets analysed, ~80% exhibited diurnal N_2O patterns, with ~60% peaking during the day and ~20% at night. Contrary to many published observations, our analysis only found strong positive correlations ($R > 0.7$) between N_2O flux and soil temperature in one-third of the datasets. Soil drainage property, soil water-filled pore space (WFPS) level and land use were also found to potentially influence the occurrence of certain diurnal patterns. Our work demonstrated that single-daily flux measurements at mid-morning yielded daily emission estimates with the smallest average bias compared to measurements made at other times of day, however, it could still lead to significant over- or underestimation due to inconsistent diurnal N_2O patterns. This inconsistency also reflects the inaccuracy of using soil temperature to predict time of daily average N_2O flux. Future research should investigate the relationships between N_2O flux and other diurnal parameters such as photosynthetically active radiation (PAR) and root exudation, along with the consideration of the effects of soil moisture, drainage, and land use on the diurnal patterns of N_2O flux. The information could be incorporated in N_2O emission prediction models to improve accuracy.

2.2 Introduction

Nitrous oxide (N_2O) is a greenhouse gas (GHG) with a global warming potential 298 times that of carbon dioxide (CO_2) and a lifetime of over 110 years (Myhre et al., 2013). The atmospheric concentration of N_2O has increased from 273 ppb in 1800 to 330 ppb in 2017 (European Environment Agency, 2019) with agriculture being one of the biggest anthropogenic sources contributing 60 – 70% of anthropogenic N_2O emissions globally (Cowan et al., 2019). According to the Fifth Assessment by the Intergovernmental Panel on Climate Change (IPCC) (Ciais et al., 2013), global annual estimates for N_2O emissions from soils under natural vegetation and from agriculture are 6.6 (3.3 – 9.0) Tg N yr^{-1} and 4.1 (1.7 – 4.8) Tg N yr^{-1} respectively; equivalent to an uncertainty of ±43.2% and ±37.8%. There is significant potential to mitigate these agricultural N_2O emissions through improved land management (Winiwarter et al., 2018), however, the assessment of mitigation strategies requires accurate quantification of emissions which is currently lacking.

The temporal variability of soil N_2O flux contributes significantly to the uncertainty of emission estimates (Jungkunst et al., 2018; Lammirato et al., 2018). The three-tier system introduced by the IPCC classifies methodological approaches based on the quantity of information involved, where Tier 3 approaches consist of methods with the highest analytical complexity including direct flux measurements and complex models (Bickel et al., 2006; de Klein et al., 2006). However, these approaches generally ignore short-term temporal (i.e., diurnal) variability of N_2O flux (Giltrap, Li and Saggar, 2010; Grace et al., 2020), partly due to the computational challenges imposed by higher temporal resolutions, as well as the lack of diurnal N_2O flux data to validate the model predictions. Current guidance for measuring N_2O flux recommends that single-daily measurements are taken in mid-morning (ca. 10:00 h), since it corresponds closely to the time of daily average soil temperature and thus should represent the daily average flux if temperature is the main driver (Charteris et al., 2020; De Klein and Harvey, 2015; IAEA, 1992; Parkin and Venterea, 2010). However, it has been shown that diurnal variability of N_2O emissions is not solely controlled by soil temperature (Keane et al., 2018, 2019; Shurpali et al., 2016), thus mid-morning fluxes may not capture daily mean fluxes adequately. With exceptions such as ECOSYS (Metivier, Pattey and Grant, 2009), process-based simulation models of soil N_2O emissions (e.g. ECOSSE, DNDC and DAYCENT) (Cai et al., 2003; Del Grosso et al., 2001; Smith et al., 2010) are generally not configured to simulate diurnal variability of N_2O flux, as they take and produce daily averages of data inputs and outputs (Gilhespy et al., 2014). In

addition, the validation of model outputs are generally limited to single-daily or weekly N_2O flux measurements (Babu et al., 2006; Bell et al., 2012; Cai et al., 2003; Necpálová et al., 2015).

Although manual N_2O flux measurements at sub-daily frequencies are not commonly practised due to high costs of labour and time, they have provided evidence of diurnal variations in N_2O flux which have been shown to vary from five- to ten-fold in magnitude (Christensen, 1983; Dobbie and Smith, 2003; Maljanen et al., 2002; Scheer et al., 2012; Shurpali et al., 2016; Williams, Ineson and Coward, 1999). In addition, there has been significant technological advances in automated chamber systems in recent years, enabling real-time, *in-situ* N_2O flux measurements at sub-daily frequencies (Brummer et al., 2017; Keane et al., 2019). This has led to an increase in the availability of published sub-daily N_2O data across a range of agricultural and forest soils, which can be examined to assess the prevalence and timing of peak N_2O fluxes.

Regardless of manual or automated measurements, many studies reporting sub-daily data have observed a daytime peak in N_2O fluxes, often attributed to the diurnal patterns in soil temperature (Blackmer, Robbins and Bremner, 1982; Hosono et al., 2006; Liang et al., 2018; Scheer et al., 2014; van der Weerden, Clough and Styles, 2013; Williams, Ineson and Coward, 1999). However, a number of studies have reported night-time peaks of N_2O flux, that were out of phase with the timing of maximum soil temperature (Scheer et al., 2012; Shurpali et al., 2016; Smith et al., 1998; Zona et al., 2013). The temperature sensitivity (Q_{10}) of soil N_2O production measured in lab studies ranges from two to three (Christensen, 1983; Denmead, 1979; van der Weerden, Clough and Styles, 2013), which is at odds with the observed amplitudes in diurnal N_2O fluxes (e.g. over an order of magnitude for N_2O fluxes) and the associated soil temperature ranges (< 10 °C) in various studies (Christensen, 1983; Dobbie & Smith, 2003; Maljanen et al., 2002; Scheer et al., 2012; Shurpali et al., 2016; Williams et al., 1999). However, there has been very limited research on the drivers and mechanisms underpinning diurnal variation in N_2O fluxes, in part because the prevalence of diurnal N_2O flux variability, as a widespread phenomenon in global soils, has not been clearly demonstrated.

Quantifying the prevalence and understanding the drivers of diurnal N_2O flux variability would enable improvements in N_2O flux measurement strategies and N_2O emission estimation models, which are pivotal to the calculation of national N_2O budgets and the development and monitoring of N_2O mitigation strategies. To our knowledge, no study has

specifically addressed this challenge. We therefore conducted a systematic review and data synthesis of peer-reviewed publications to address the following research questions (RQ):

1. How common is diurnal variability in N_2O flux in cropland, grassland and forest soils, and do N_2O fluxes always follow the same pattern with a daytime peak?
2. Are soil N_2O fluxes strongly correlated with soil temperature regardless of the time of peaking?
3. Are diurnal N_2O flux patterns strongly associated with particular non-diurnal factors (e.g., soil abiotic properties and land use)?
4. Given that N_2O fluxes vary diurnally, how representative are single-daily measurements at mid-morning or any other time for estimating cumulative N_2O emissions?

2.3 Methods

We systematically identified peer-reviewed publications that reported sub-daily N_2O flux measurements from agricultural (cropland and grassland) and forest soils, and extracted N_2O flux and soil temperature data, dividing the data into individual datasets of 24-hour cycles. We first examined the prevalence of specific diurnal patterns of N_2O flux by normalising the N_2O fluxes of each dataset (Huang et al., 2014; Keane et al., 2018) and categorising the datasets into three pre-defined diurnal patterns: day-time peaking, night-time peaking and non-diurnal (RQ1). Since the basis of the current recommended sampling time for single-daily flux measurement relies on N_2O flux following the diurnal cycles of soil temperature, we also investigated the degree of correlation between N_2O flux and soil temperature by fitting a linear regression model to each dataset and calculating the correlation coefficient (RQ2). Then, we assigned the non-diurnal factors such as soil pH, bulk density, soil texture, N fertilisation, land use type, soil moisture and season of flux measurements provided in the literature to the corresponding datasets and examined whether diurnal patterns are associated with particular soil properties and/or management characteristics. (RQ3). Lastly, we compared the daily N_2O emission estimates calculated from single-daily measurements with those calculated from at least five sub-daily measurements (RQ4).

2.3.1 Literature search and inclusion criteria

A literature search was conducted on two major scientific literature databases – 'Web of Science Core Collection' and 'ScienceDirect', with the search terms list below. The 28th August 2019 was selected as the cut-off date, no literature searches were conducted after which.

- Title: ('greenhouse gas' OR 'N2O' OR 'nitrous oxide') AND ('flux' OR 'fluxes' OR 'emission' OR 'emissions')
- Abstract: 'diurnal' OR 'diel' OR 'high frequency' OR 'automated' OR 'automatic' OR 'high temporal' OR 'highly temporal'
- Anywhere: 'soil' OR 'soils'

A total of 314 journal articles (Web of Science: 215, ScienceDirect: 99) published between 1983 and 2019 were identified in the initial database search. Duplicate articles (n = 83) were subsequently removed, and a set of inclusion criteria to select studies eligible for data extraction. The inclusion criteria are listed as follows:

- N_2O flux measurements were performed on cropland, grassland or forest soils;
- Five or more N_2O flux measurements were taken in every 24-hour cycle;
- The first and last measurement points of each 24-hour cycle were within 00:00 – 03:59 and 20:00 – 23:59, respectively.

This resulted in a compilation of 46 journal articles eligible for data extraction (detailed in Supporting Information S1) and yielded 286 diurnal datasets of N_2O flux. Of the 286 datasets, 160 contained soil temperature (5 – 10 cm) data, 157 contained soil pH data, 115 contained bulk density data, 175 contained soil texture data, 135 contained soil moisture data and 261 contained data of season of flux measurements. Information on N fertilisation and land use were provided in all articles.

2.3.2 Data extraction and transformation

For each selected publication, N_2O flux and soil temperature (if provided) data were extracted from figures and converted into a numerical format using a data recovery tool – 'Engauge Digitizer' (Mitchell et al., 2020). Continuous time series graphs were first divided into individual datasets per 24-hour cycle (i.e. 00:00 – 23:59) with N_2O flux data standardised to μg N_2O-N m^{-2} h^{-1}. Hour and minute were also converted to decimal units (0.00 – 23.99 h). Where data were presented as 24-hours graphs of average or standardised N_2O flux (i.e. deviations from daily mean N_2O flux) over their measurement periods (e.g. 10 days), data from each graph was extracted as one dataset.

To investigate the diurnal patterns of N_2O flux, we followed the approach of Huang et al. (2014) and Keane et al. (2018), who eliminated the magnitude differences between days by normalising N_2O flux in every 24 hours (each dataset). Normalised N_2O flux data (N_2O_{norm}) were bound between 0.0 and 1.0 using the following equation (Eq. (2.1)):

$$N_2O_{norm,t} = \frac{N_2O_t - N_2O_{min}}{N_2O_{max} - N_2O_{min}}, \quad (2.1)$$

where $N_2O_{norm,t}$ is the normalised N_2O flux at one point in time (t), N_2O_t is the N_2O flux at t, N_2O_{min} is the minimum N_2O flux in a dataset, and N_2O_{max} is the maximum N_2O flux in a dataset.

2.3.3 Data analyses

2.3.3.1 Categorisation of diurnal patterns of N_2O flux

To determine the prevalence of different diurnal patterns of N_2O flux (RQ1), datasets were categorised as 'daytime peaking', 'night-time peaking' or 'non-diurnal' based on the following characteristics:

- Daytime peaking: N_2O flux increases in daytime and decreases at night-time, resembling a typical diurnal oscillation of soil temperature;
- Night-time peaking: N_2O flux decreases in daytime and increases at night-time, acting in contrast to a typical diurnal oscillation of soil temperature;
- Non-diurnal: N_2O flux fluctuates inconsistently or shows a continuous upward or downward trend throughout the diurnal cycle.

We developed and used three sets of objective conditions, listed below, to categorise datasets into diurnal patterns. Datasets that met all the conditions in a category were

classified as such. To avoid incorrect categorisation of non-diurnal datasets from a single occurrence of high or low flux during daytime or night-time, the conditions for daytime and night-time peaking required the occurrence of the two highest fluxes and the two lowest fluxes, respectively, to take place within the specified time ranges. Since daytime involves morning and afternoon, we specified the daytime range to be 04:30 – 19:30 h to capture both morning and afternoon peaking of N_2O flux, and subsequently defined two subcategories ('morning peaking' and 'afternoon peaking') within the daytime peaking category. The third condition ensured that over 50% of the total daily emission occur in daytime in daytime peaking datasets, and vice versa in night-time peaking datasets. Since the hours between the first and last flux measurements in datasets were often less than 24 hours, we adjusted the 50% threshold for each dataset using Eq. (2.2). We then calculated the percentage of emission within three 12-hour periods (04:00 – 16:00 h, 06:00 – 18:00 h and 08:00 – 20:00 h). The percentages of emission were calculated by dividing the emission within those 12-hour periods with the total emission of the dataset. The emission of each 12-hour period were computed using a trapezoidal integration function (in R package 'pracma').

For the daytime peaking category, two subcategories were defined to identify morning peaking and afternoon peaking of N_2O flux. The categorisation conditions for each diurnal pattern are listed below:

- Daytime peaking:
    1. Both the highest and second highest N_2O_{norm} occur between 04:30 – 19:30 h;
    2. The lowest N_2O_{norm} occurs between 00:00 – 09:00 or 18:00 – 00:00 h;
    3. The percentage of emission calculated within 04:00 – 16:00 h or 08:00 – 20:00 h is greater than the adjusted threshold (Eq. (2.2));
        - If percentage of emission calculated within 04:00 – 16:00 h exceeds the threshold and the afternoon emission percentage, the dataset is considered as 'morning peaking';

- If percentage of emission calculated within 08:00 – 20:00 h exceeds the threshold and the morning emission percentage, the dataset is considered as 'afternoon peaking'.

- Night-time peaking:

    1. Both the lowest and the second lowest N_2O_{norm} occur between 04:30 – 19:30 h;
    2. The highest N_2O_{norm} is between 00:00 – 09:00 h or 18:00 – 00:00 h;
    3. The percentage of emission calculated between 06:00 – 18:00 h is smaller than the calculated threshold.

- Non-diurnal:

    1. Dataset is neither daytime peaking nor night-time peaking.

$$Adjusted\ threshold = \frac{24}{Hours\ between\ the\ first\ and\ last\ measurement\ in\ dataset} \times 50\% \quad (2.2)$$

To determine whether the types of diurnal N_2O pattern are dependent on the magnitude of N_2O flux, datasets were categorised as high magnitude fluxes, where the maximum N_2O flux value was ≥ 100 μg N_2O-N m^{-2} h^{-1}, or low magnitude fluxes, where the maximum N_2O flux value was < 100 μg N_2O-N m^{-2} h^{-1} (Lognoul et al., 2019); and the proportions of each diurnal pattern within these categories was calculated.

2.3.3.2 N_2O flux and soil temperature

All statistical analyses of extracted data were performed in R version 3.6.1 (© The R Foundation).The correlation between N_2O flux and soil temperature in each diurnal pattern (RQ2) was examined by calculating the Pearson's correlation coefficients (R) between N_2O flux and soil temperature (5 – 10 cm soil depth) in the available data (n = 160). Additional soil temperature data points were generated by linearly interpolating the extracted soil temperature data. An R value between N_2O flux and interpolated soil temperature was computed using the correlation function (in R package 'ggpubr'). The datasets were then grouped according to their diurnal pattern.

2.3.3.3 Non-diurnal factors and diurnal N_2O flux patterns

To examine whether diurnal N_2O flux patterns are strongly associated with particular non-diurnal factors (RQ3), soil pH, bulk density, soil texture, N fertilisation, land use type, soil water-filled pore space (WFPS) and season of flux measurements data were used where available (Supplemental Table 1). Since only one of the extracted studies provided diurnal soil moisture data corresponding to its diurnal N_2O flux data (Du et al., 2006), a point-by-point diurnal relationship between soil moisture and N_2O flux (one similar to the N_2O-temperature relationship described in Section 2.3.2) could not be established and investigated in our analysis. Given the data structures of soil moisture provided by most of the studies (e.g. numerical indication of soil moisture ranges or soil moisture variations over the entire measurement period), we could only assign datasets into different soil WFPS level categories (i.e. ≤34.9%, 35-54.9%, 55-74.9% and ≥75%) according to the provided soil volumetric moisture content or WFPS data. Volumetric moisture content data were converted to WFPS levels using the bulk density value of the soil. Subsequently, the association between WFPS level category and diurnal N_2O flux pattern was examined.

Datasets originating from the same study site were assigned the same factor values or characteristics, unless specified otherwise. To investigate the association between diurnal patterns and non-diurnal factors, we assumed that all datasets and their diurnal patterns were independent from one another and plotted the distribution of numerical factors (i.e. pH and bulk density) in each diurnal pattern category, or the relative frequency of diurnal patterns in categorical factors (i.e. soil texture, N fertilisation, land use, soil WFPS level and season).

For numeric factors, datasets of soil pH (n = 157) and bulk density (n = 115) were grouped according to their diurnal pattern category. Boxplots showing the distribution of soil pH and bulk density in soils exhibiting the three diurnal patterns were produced, and the interquartile range and median of each category were extracted. The significant differences in soil pH and bulk density among the daytime peaking, night-time peaking and non-diurnal categories were tested using the Kruskal-Wallis test.

For categorical factors (i.e. soil texture, N fertilisation, land use, WFPS level and season), datasets were first grouped according to their parameter category (Table 2.1); then the proportions of each diurnal pattern in each parameter category were quantified and visualised in stacked bar charts. Only one dataset was collected during winter months, it was therefore not included in the analysis of seasonal effect on diurnal N_2O flux patterns. To reduce the number of soil texture groups and better visualise the effect of soil texture, datasets were reclassified into three soil classes according to their drainage property from the results of Groenendyk et al. (2015). These were defined as follows:

- Well drained: sand, loamy sand and silt;
- Imperfectly drained: sandy clay loam, silty clay, silty clay loam, silty loam and sandy loam;
- Poorly drained: clay, sandy clay, clay loam and peaty gley.

Table 2.1. Number of datasets with categorical parameters.

Season			Land use		
Spring	Summer	Autumn	Cropland	Grassland	Forest
98	138	24	210	43	33
N fertilisation		**WFPS level**			
Fertilised	Unfertilised	≤34.9%	35-54.9%	55-74.9%	≥75%
258	28	27	45	57	6
Soil drainage class					
Well drained		Imperfectly drained		Poorly drained	
8		137		30	

2.3.3.4 Calculation of biases of cumulative N_2O emissions with single-daily measurement at different sampling times

Using a single time-point sampling at different times of day to estimate cumulative daily emissions can significantly over- or underestimate cumulative emissions. To assess this bias, we compared the cumulative N_2O emissions estimated by single-daily measurement (C-N_2O_{single}) against those estimated by sub-daily measurements (C-$N_2O_{sub\text{-}daily}$) (RQ4). Positive and negative biases indicate over- and underestimations of N_2O emissions, respectively. As single-daily flux measurements take place in the morning or afternoon in standard practices, five sampling times (08:00, 10:00, 12:00, 14:00 and 16:00 h) were selected for the bias calculation. In each dataset, N_2O flux values at the five sampling times were linearly interpolated from the sub-daily N_2O fluxes provided by the database. C-N_2O_{single} values at the sampling times were calculated by multiplying the interpolated N_2O flux by 24, which then returned a daily C-N_2O for each sampling time in each dataset. The C-$N_2O_{sub\text{-}daily}$ value was calculated with the provided N_2O fluxes using a trapezoidal integration function (in R package 'pracma'). Since the sampling hours (i.e. number of hours between the first and last measurement in a day) in most datasets were less than 24, the daily C-$N_2O_{sub\text{-}daily}$ of each dataset was corrected by dividing the calculated C-$N_2O_{sub\text{-}daily}$ by the hours between the first and last measurement and then multiplying it by 24. For each dataset, the bias between C-N_2O_{single} (at a sampling time) and C-$N_2O_{sub\text{-}daily}$ was calculated using Eq. (2.3):

$$bias_{st} = \frac{C\text{-}N_2O_{single,st} - C\text{-}N_2O_{sub\text{-}daily}}{C\text{-}N_2O_{sub\text{-}daily}} \times 100\%, \quad (2.3)$$

In Eq. (2.3), $bias_{st}$ represents the bias of the single-daily measurement at a certain sampling time; C-$N_2O_{single,st}$ represents the cumulative daily N_2O emission calculated using interpolated N_2O flux at a certain sampling time; and C-$N_2O_{sub\text{-}daily}$ represents the cumulative daily N_2O emission calculated with the provided N_2O flux measurements using trapezoidal integration.

The mean value, upper and lower confidence interval (CI; 95%) of each $bias_{st}$ from all the datasets were generated using a nonparametric bootstrap function (in R package 'Hmisc') based on 1000 replications.

2.4 Results

2.4.1 Categorisation of diurnal patterns of N_2O flux

Out of the 286 datasets, 173 (60.5%), 55 (19.2%) and 58 (20.3%) were categorised as daytime peaking, night-time peaking and non-diurnal, respectively. Within the daytime peaking datasets (n = 173), 34 (19.8%) were classified as morning peaking and 138 (80.2%) as afternoon peaking. Daytime, afternoon peaking emissions were therefore the most commonly occurring diurnal pattern identified across all studies. In the high magnitude flux datasets (n = 131), 52.7% were categorised as daytime peaking, 18.3% night-time peaking and 29% as non-diurnal; whereas in the low magnitude flux datasets (n = 155), 67.1% were categorised as daytime peaking, 20% as night-time peaking and 12.9% as non-diurnal. The magnitude of N_2O flux has little effect on the diurnal pattern of N_2O flux. Line plots of the N_2O_{norm} and categorisation description of all datasets are supplied in Supporting Information S2.

2.4.2 Relationship between N_2O flux and soil temperature

In datasets with soil temperature data (n = 160), 80.6% had positive correlations ($0.002 \leq R \leq 1.0$) between N_2O flux and soil temperature at 5 – 10 cm depth (interpolated at N_2O flux measurement times) and 19.4% had negative correlations ($-0.8 \leq R \leq -0.02$). Only 33.1% of the 160 datasets showed strong positive correlations (i.e. $R > 0.7$). The interquartile ranges of R values for daytime peaking, night-time peaking and non-diurnal categories were 0.41 – 0.82, -0.19 – 0.15 and -0.03 – 0.67, respectively; whereas the median R values for the daytime peaking, night-time peaking and non-diurnal categories were 0.65, -0.06 and 0.32, respectively (Figure 2.1). This shows that daytime peaking datasets on average had stronger correlations than non-diurnal datasets. However, the wide range of R values in the daytime peaking category also implies that soil temperature is not consistently driving daytime N_2O flux peaks. Additionally, night-time peaking datasets only had a slightly negative R value on average which indicates little correlation exists between N_2O flux and soil temperature in night-time peaking datasets.

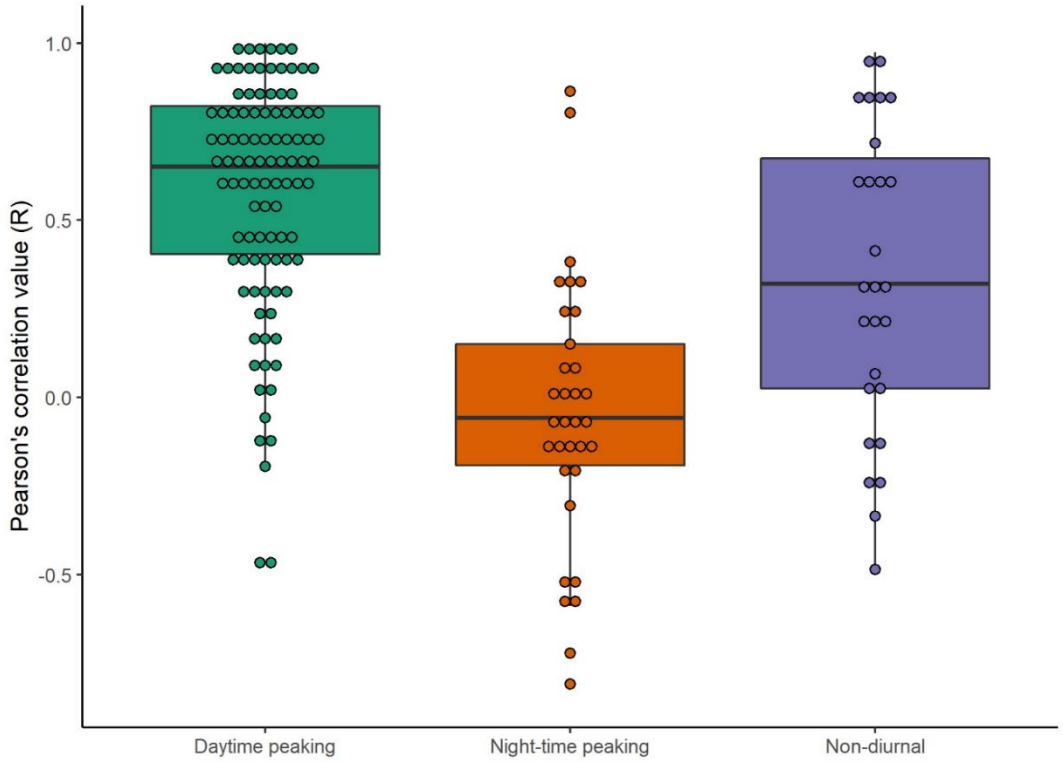

Figure 2.1. Differences in the relationship between soil temperature and N_2O fluxes in the three diurnal pattern categories. Boxes and whiskers represent the median (bold line in box), upper and lower quartile (top and bottom box line), maximum and minimum (top and bottom whisker) of Pearson's correlation coefficient (R) between N_2O flux and soil temperature (5 – 10 cm depth, interpolated at the times of N_2O flux measurement). Circles represent the R values of individual datasets.

2.4.3 Non-diurnal factors and diurnal patterns of N_2O

Soil pH in available datasets (n = 157) ranged from 3.0 to 8.6 (Figure 2a). The interquartile ranges of pH for daytime peaking, night-time peaking and non-diurnal categories were 5.9 – 7.4, 5.9 – 8.6 and 5.9 – 8.0, respectively. The median pH for the daytime peaking, night-time peaking and non-diurnal categories were 5.9, 7.2 and 5.9, respectively. No significant difference (p = 0.42) in soil pH was found among the diurnal pattern categories. However, the majority of daytime peaking and non-diurnal datasets, 59.6% and 64.3%, respectively, featured slightly acidic soils (i.e. pH at 5.0 – 7.0), with their median pH being 5.9; whereas a large portion (58.8%) of the night-time peaking datasets featured slightly alkaline soil (i.e. pH > 7.0) with a median of 7.2. The outliers in all three diurnal pattern categories (at pH = 3.0) were from the same study conducted on a forest soil (Figure 2.2a).

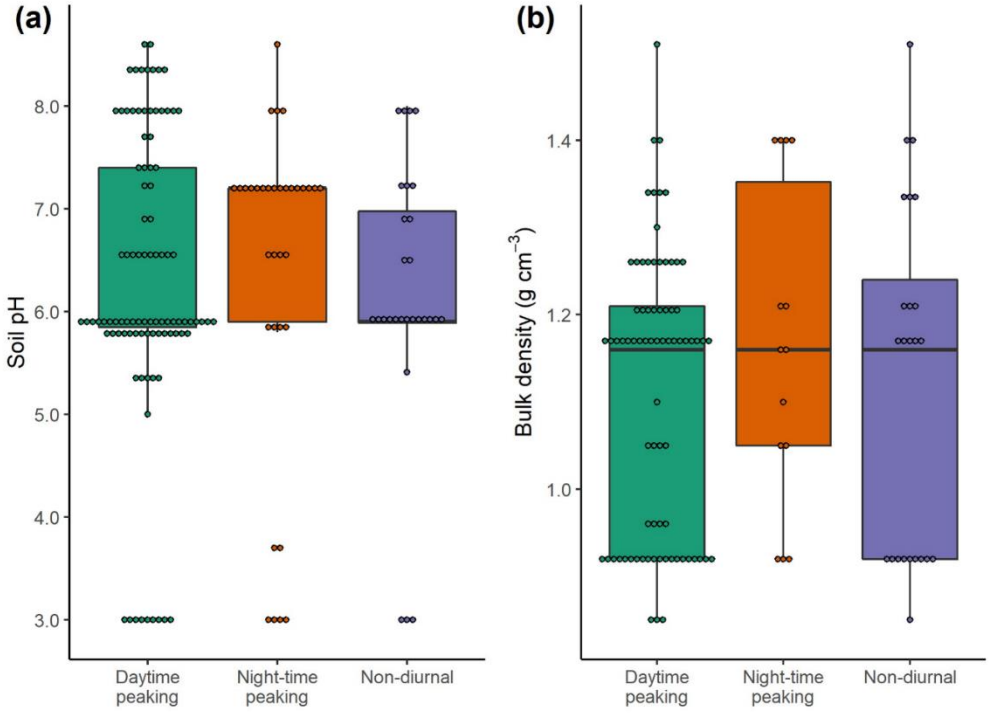

Figure 2.2. Distributions of (a) soil pH (n = 157) and (b) bulk density (n = 115) in the three diurnal pattern categories. Boxes and whiskers in (a) and (b) represent the median (bold line in box), upper and lower quartile (top and bottom box line), maximum and minimum (top and bottom whisker) of soil pH and bulk density, respectively. Circles in (a) and (b) represent the soil pH and bulk density values of soils from each dataset.

Only 115 of the 286 datasets included bulk density data. The interquartile ranges of bulk density for daytime peaking, night-time peaking and non-diurnal categories were 0.92 – 1.21 g cm^{-3}, 1.05 – 1.35 g cm^{-3} and 0.92 – 1.24 g cm^{-3}, respectively (Figure 2.2b). All three categories had the same bulk density median of 1.16 g cm^{-3}. No significant difference (p = 0.68) in soil bulk density was detected among the diurnal pattern categories either. Among the three soil drainage classes, both well drained and imperfectly drained soils were dominated by daytime peaking datasets, accounting for 62.5% and 60.6% of the corresponding soil drainage class category, respectively (Figure 2.3a). This was in agreement with the findings of soil WFPS categories, since datasets with WFPS ≤34.9% (n = 27) and 35-54.9% (n = 45) both predominantly showed daytime peaking patterns, accounting for over 70% in both WFPS level categories. Inversely, the majority of poorly drained soils were categorised as night-time peaking datasets (66.7%). Yet only datasets with WFPS level of 55-74.9% showed an increasing proportion of night-time peaking pattern (36.8%), whereas those with WFPS level ≥75% (n = 6) were dominated by daytime peaking patterns (83.3%). However, the datasets with WFPS level ≥75% did not provide information on their soil texture, and hence did not necessarily belong to poorly-drained soils.

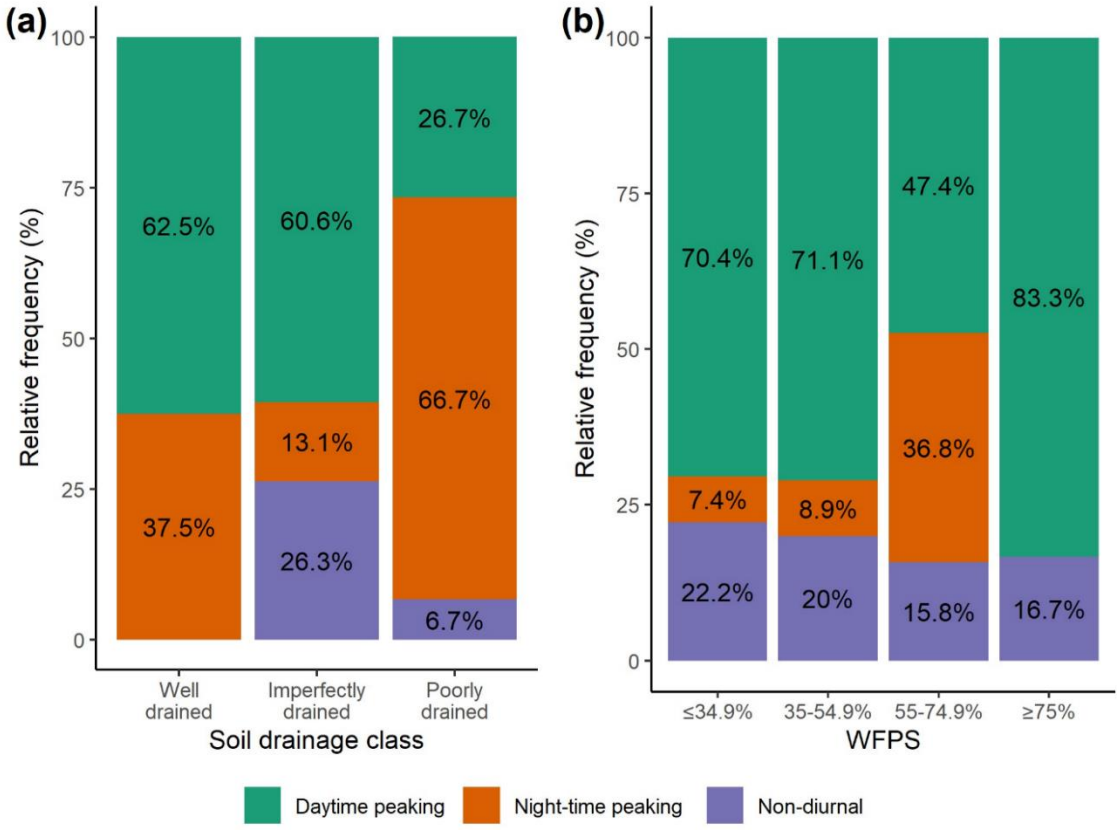

Figure 2.3. The relative frequency of diurnal N_2O flux patterns in (a) well drained (n = 8), imperfectly drained (n = 137) and poorly drained (n = 30) soils, and in (b) soils at WFPS level ≤34.9% (n = 27), 35-55% (n = 45), 55-74.9% (n = 57) and ≥75% (n = 6).

Datasets of fertilised soils (n = 258) showed a trend in diurnal pattern proportions similar to all datasets (Section 3.1), with daytime peaking, night-time peaking and non-diurnal datasets accounting for 58.9%, 20.5% and 20.5%, respectively (Figure 2.4a).

However, datasets of unfertilised soils (n = 28), exhibited a slightly different trend, with a larger daytime peaking proportion (75.0%) and a smaller night-time peaking proportion (7.1%). It should be noted that N fertilisation could have an autocorrelation with land use as unfertilised soils consisted entirely of grassland (n = 14) and forest soils (n = 15). Cropland and forest soils also exhibited proportions similar to the general ratio of 3:1:1 in diurnal patterns (Figure 2.4b). Cropland soils (n = 210) exhibited a slightly lower daytime peaking proportion (55.2%) than forest soils (n = 33, 66.7%). Grassland soils (n = 43), on the other hand, featured predominantly daytime peaking datasets (81.4%) with a much lower night-time peaking percentage (7.0%) compared to the other two land use types. Datasets collected in spring (n = 98) and autumn (n = 24) had similar proportions of daytime (~50%), night-time peaking (~20%) and non-diurnal (~30%) datasets, whereas those collected during summer months (n = 138) had a slightly larger proportion of daytime peaking datasets (62.3%) and a smaller proportion of non-diurnal datasets (16.7%) (Figure 2.4c).

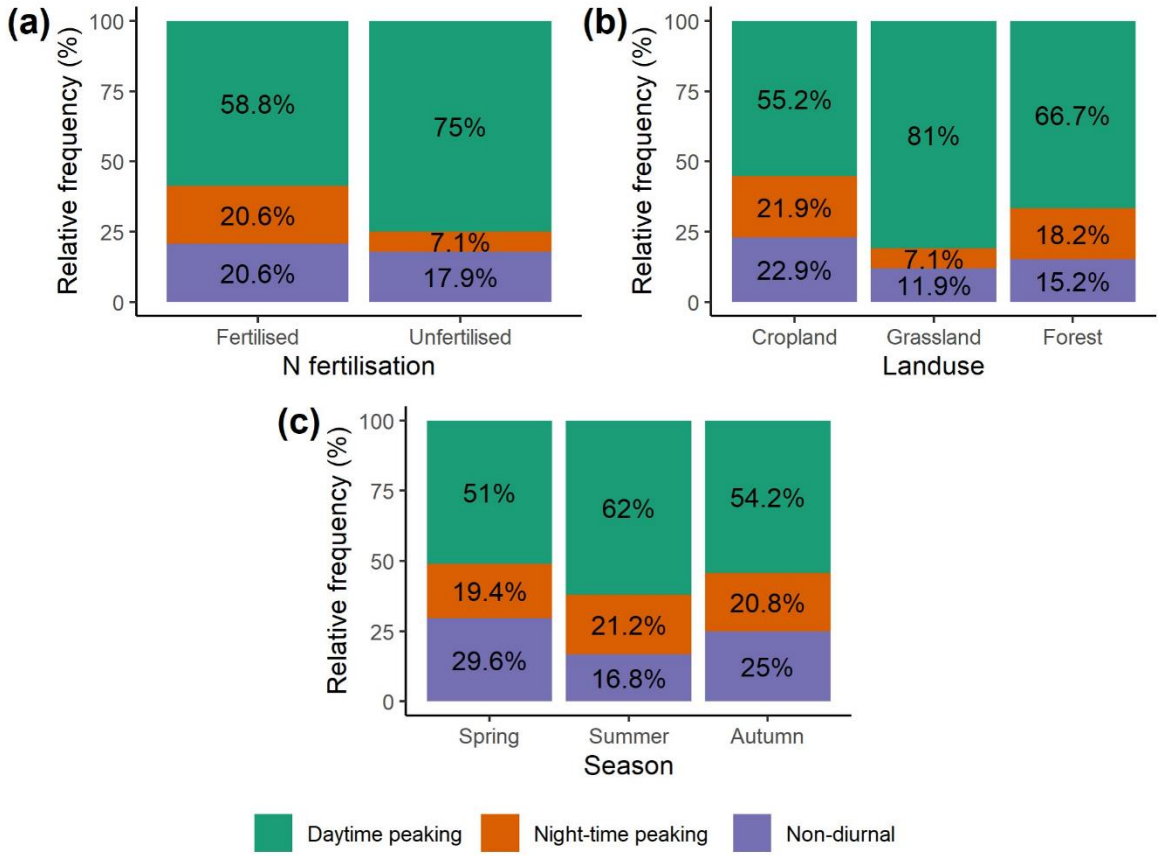

Figure 2.4. The relative frequency of diurnal N_2O flux patterns in (a) N fertilised (n = 258) and unfertilised (n = 28) soils, in (b) cropland (n = 210), grassland (n = 43), forest soils (n = 33), and in (c) spring (n = 98), summer (n = 138) and autumn (n = 24).

2.4.4 Calculation of estimation biases by single-daily measurements

The bootstrap results (Figure 2.5) showed that time of sampling significantly affected the magnitude of over- or underestimation (bias %) of cumulative N_2O emissions calculated at single time-points (single-daily measurements). Cumulative N_2O emissions estimated from a single time-point ($C\text{-}N_2O_{single}$) were most similar to those estimated from sub-daily measurements ($C\text{-}N_2O_{sub\text{-}daily}$) for the 10:00 h sampling time, illustrated by the small mean bias value (+2.1%) and relatively small CI (64.9%). In comparison, earlier and later sampling times generated greater over- or underestimations with larger uncertainties ranging between 79.5% and 118.8%. Sampling at 08:00 h resulted in a negative mean bias of -16.6%, whereas sampling at 12:00, 14:00 and 16:00 h resulted in positive mean biases of 32.1%, 47.7% and 58.8%, respectively.

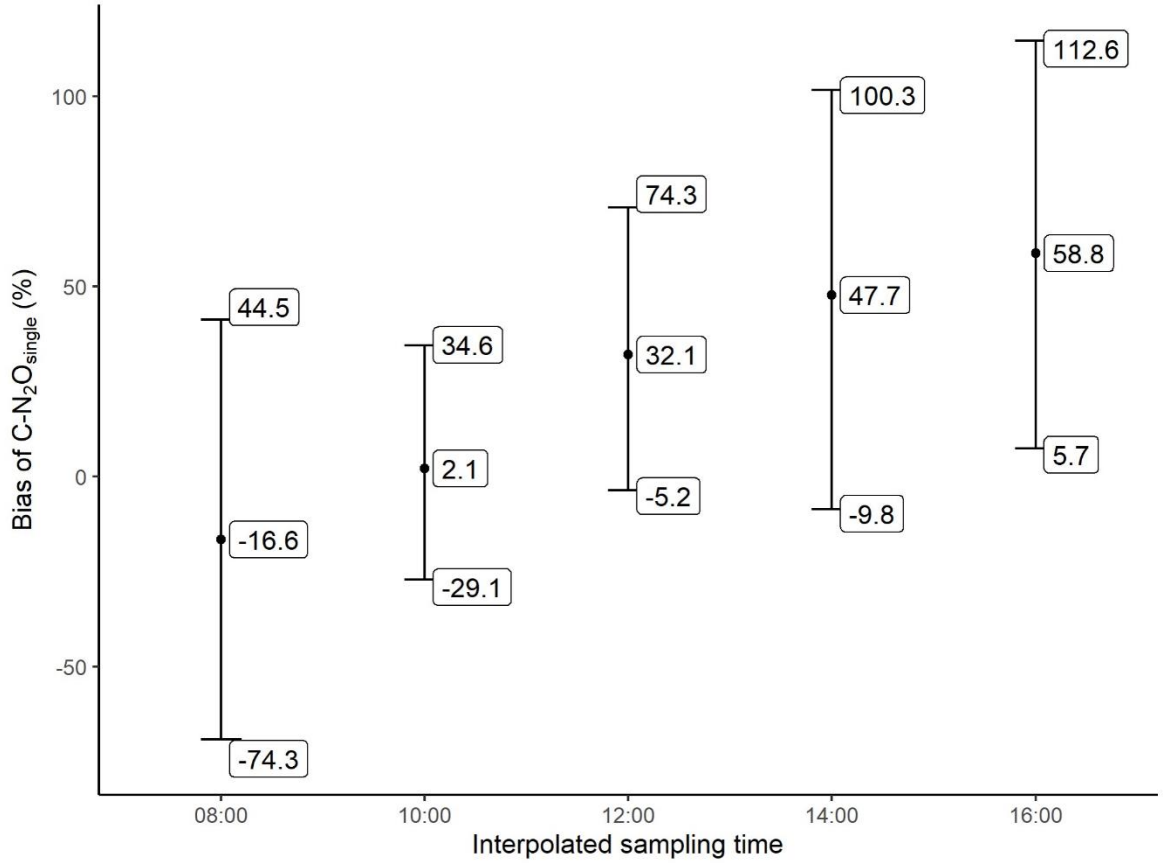

Figure 2.5. The effects of sampling time (interpolated) on the bias of C-N_2O_{single} (%) calculated against C-$N_2O_{sub\text{-}daily}$ from all datasets (n = 286); three annotated values are displayed above each sampling time. From top to bottom, they represent the upper CI, mean and lower CI (i.e. the bootstrap results based on 1000 replications) of percentage bias of C-N_2O_{single}.

2.5 Discussion

Our data synthesis has demonstrated that diurnal variability in N_2O flux is a widespread phenomenon, with daytime peaking dominating (~60%) across the reviewed land use types (cropland, grassland, and forest). However, daytime peaking was not found in all datasets with significant proportions of night-time peaking and non-diurnal pattern also identified, each accounting for ~20%. The relationship between N_2O flux and soil temperature was also revealed to be variable in the analysis, which contrasts with many literature's ascription of soil temperature to diurnal N_2O flux variations and hints that other diurnal or non-diurnal factors may also act as drivers or dampeners of diurnal variability. We showed that the relative occurrence of different diurnal patterns was strongly influenced by the drainage property of soil textural classes, with poorly drained soils featuring a majority of night-time peaking, and both well and imperfectly drained soils primarily exhibiting daytime peaking.

2.5.1 Daytime diurnal N_2O flux variability and the role of soil temperature

The current recommended approach to address diurnal variability of N_2O flux is to measure N_2O flux at 10:00 h or mid-morning where daily mean soil temperature occurs, to capture the daily mean N_2O flux (Charteris et al., 2020; de Klein & Harvey, 2015), since past literature has provided evidence supporting that N_2O flux is controlled by soil temperature (Alves et al., 2012a; Parkin, 2008; Smith and Dobbie, 2001). Using sub-daily data to estimate the uncertainty introduced by single-daily measurements revealed that the 10:00 h recommended sampling time (Charteris et al., 2020; de Klein & Harvey, 2015; IAEA, 1992; Parkin & Venterea, 2010) would most likely capture the daily average N_2O flux compared to other sampling times, since our study found diurnal N_2O fluxes peaking in the afternoon about half of the time (138 out of 286 datasets with a daytime-afternoon peaking pattern). However, due to the variability within the diurnal patterns of N_2O flux, sampling at 10:00h could still lead to significant over- or underestimation (Figure 2.5) when compared against sub-daily measurements, which more accurately capture diurnal variations of N_2O flux. This might be due to the absence of strong positive correlations ($R > 0.7$) between N_2O flux and soil temperature in 70% of the datasets. These findings suggest that soil temperature may not adequately represent diurnal variation in N_2O flux and imply that other diurnal variables could contribute to driving diurnal variation in N_2O flux.

A few studies have also observed diurnal peaks of N_2O flux preceding those of soil temperature (e.g. morning peaking of N_2O flux) (Akiyama and Tsuruta, 2003; Keane et al., 2018; Peng et al., 2019), and some reported a stronger relationship between N_2O flux and parameters driving photosynthesis such as solar radiation and photosynthetically active radiation (PAR) (Christensen, 1983; Keane et al., 2018; Shurpali et al., 2016). In those studies, plant inputs of labile organic C via root exudation driven by PAR were proposed as regulators of diurnal variations in N_2O flux (Keane et al., 2018; Keane et al., 2019; Shurpali et al., 2016). The potential influence of PAR mediated through plant metabolism is also supported by the study of Zona et al. (2013), where gross primary productivity explained 73% of diurnal N_2O variations in a growing season. However, Das et al. (2012) observed daytime peaks in N_2O flux with artificial PAR oscillations from bare soil in a temperature-controlled study, which they ascribed to soil surface warming resulting from the artificial PAR lighting. Their results, however, do not disprove the effect of root exudation of labile C on soil N_2O production, as both drivers could coincide in vegetated soil systems. Daytime activities such as irrigation, fertilisation and grazing could also influence diurnal N_2O flux

pattern. We found two extracted studies (dataset n = 14) that performed daily irrigation in the morning with one irrigated with fertiliser solution (Flessa et al., 2002; Hosono et al., 2006), and two other studies (dataset n = 7) that measured diurnal N_2O flux on actively grazed pastures (Wang et al., 2005; Williams, Ineson and Coward, 1999). This could lead to daytime peaking of N_2O flux that might not be caused by soil temperature or other potential diurnal drivers, since the increase in soil WFPS and/or N substrates (nitrate and ammonium) would promote denitrification and hence increase N_2O flux (Firestone & Davidson, 1989). Seasonal events such as freeze-thaw could also control to the occurrence of daytime peaking of N_2O flux. Peng et al. (2019) observed morning peaking of N_2O flux in a temperate forest during a freeze-thaw period in spring, whereas afternoon peaking of N_2O flux was observed in summer. However, the relative importance of these potential drivers to the diurnal variability of N_2O flux could not be established in this study, as it requires more comprehensive data collection of the mentioned drivers of diurnal resolutions which are currently unavailable.

2.5.2 Night-time N_2O flux diurnal variability and the role of soil temperature

Although night-time peaking of N_2O flux is uncommon (~20% of the datasets), its occurrence also contradicts the assumption of temperature as a main predictor. In a study that measured diurnal N_2O fluxes from a peaty gley soil, night-time peaking of N_2O flux was attributed to N_2O being produced at depth, creating a time lag of several hours between temperature-induced increases in N_2O production at depth and emissions at the surface (Smith et al., 1998). However, it is generally thought that N_2O production occurs mostly in the top few centimetres of the soils, even in peat soils (Goldberg, Knorr and Gebauer, 2008; Shcherbak and Robertson, 2019; Toma et al., 2011). Furthermore, N_2O produced at depth is likely consumed during upward diffusion (Goldberg, Knorr and Gebauer, 2008; Van Groenigen et al., 2005), especially under wet conditions with prolonged residence time, resulting in little emission of N_2O originated from deep subsurface soils (Clough et al., 2006). It is possible that night-time peaking of N_2O flux is a result of increased N_2O consumption during daytime. Soil oxygen (O_2) availability controls N_2O production ($NO \rightarrow N_2O$) and N_2O consumption ($N_2O \rightarrow N_2$), with the latter becoming more dominant when O_2 is severely limited (Castaldi, 2000; Knowles, 1982; McMillan et al., 2014; Morley et al., 2008; Schlüter et al., 2018). Increased O_2 consumption during daytime due to temperature-induced increases in soil respiration, coupled with the lack of O_2 supply in soils with restricted airflow, could result in lower N_2O flux during the day. As increased soil O_2 consumption

during daytime has been reported in various studies (Hamerlynck et al., January 12; Lu et al., 2013; Tang et al., 2003), and has been shown to positively correlate with soil temperature (Chuang, Lee and Chen, 2004; Wang et al., 2016) and photosynthetic rate (Neales and Davies, 1966), it is plausible that more N_2O in soils is consumed during the day than at night. This theory could also explain the larger proportion of night-time peaking emissions identified in poorly drained soils (Figure 2.3a), as N_2O reduction could surpass N_2O production during daytime in soils with limited air permeability. This hypothesis is also supported by evidence that night-time peaking of N_2O flux as well as N_2O uptake during daytime have been observed in vegetated wetlands featuring high percentages of soil WFPS and limited O_2 availability (Windham-Myers et al., 2018; Yu et al., 2012). Additionally, studies have found that plants exhibit higher uptake of soil nitrate and ammonium during the day (Geßler et al., 2002; Macduff and Bakken, 2003; Okuyama, Ozawa and Takagaki, 2015), which could also potentially contribute to the occurrence of night-time peaking of N_2O flux due to the reduction in substrates for nitrification and denitrification during daytime.

2.5.3 Biological pathway for diurnal N_2O flux amplification

Supported by several studies (Langarica-Fuentes et al., 2018; Oburger et al., 2014; Ueno and Ma, 2009; Wu et al., 2017b), we propose a biological pathway wherein the diurnal rhythms of root exudation of photosynthates could amplify diurnal N_2O fluxes beyond what can be explained by temperature alone. We suggest that root exudation during and after the photoperiod promotes denitrification activity, and hence increases N_2O production in soils. Denitrification and nitrifier denitrification are two main microbial processes driven by O_2 limitation (Bollmann and Conrad, 1998; Khalil, Mary and Renault, 2004; Zhu et al., 2013) that contribute to the majority of the N_2O production in soils (Kool et al., 2010; Opdyke, Ostrom and Ostrom, 2009; Wrage-Mönnig et al., 2018). Reduced soil O_2 concentration and increased soil respiration during daytime have been reported previously (Keane et al., 2019; Shurpali et al., 2016; Zimmermann et al., 2009). It is likely that during daytime, photosynthetically assimilated C is translocated to the plant roots and exuded into the rhizosphere, where potential denitrification activity is greater (Hamonts et al., 2013). Exuded C is then rapidly respired by heterotrophs (Kelting, Burger and Edwards, 1998; Sun et al., 2017), which subsequently depletes O_2 in the soil and drives denitrification and nitrifier denitrification (Knowles, 1982; Wrage et al., 2001). Several of our included studies have also shown diurnal N_2O fluxes to closely follow ecosystem respiration rates (CO_2 fluxes

measured by dark chambers) (Brumme and Beese, 1992; Flessa et al., 2002; Laville et al., 2017; Maljanen et al., 2002; Savage, Phillips and Davidson, 2014), highlighting the positive effects of ecosystem respiration on N_2O flux. Root exudation can also directly fuel N_2O production (Azam et al., 2002; Burton et al., 2008; Henderson et al., 2010), as most denitrifiers and some nitrifiers are heterotrophic and would consume the labile C in the exudate to gain energy. However, the exact effect of photosynthesis on the diurnal rhythm of root exudation is only partially understood. Although isotopic labelling experiments have reported rapid rhizosphere respiration of assimilated C (within two hours) upon plant exposure to light (Dilkes, Jones and Farrar, 2004; Gavrichkova and Kuzyakov, 2017), various time lags from less than an hour to more than a day between photosynthesis and soil respiration of assimilated C have been reported (Kuzyakov and Gavrichkova, 2010). Furthermore, soil temperature has been demonstrated to enhance root-derived C exudation rates (Yin et al., 2013; Zhang et al., 2016), which could explain the positive correlations between N_2O flux and soil temperature in some datasets. However, the temperature effects on root exudation has been shown to vary among species (O'Leary, 1966), and the time lag between soil temperature and root exudation is still unexplored thus far. Depending on the diurnal dynamics of soil O_2 concentration, N_2O flux might exhibit a daytime peaking or night-time peaking diurnal pattern. A field study in which night-time peaking diurnal N_2O patterns were observed from a poorly drained grassland soil also provided isotopic evidence suggesting a shift from nitrification in the early morning to denitrification in the afternoon (Yamulki et al., 2001). This shift in soil N-cycling processes concurs with the theory of increased root exudation of C during photoperiods promoting denitrification. Nonetheless, a thorough understanding of the diurnal behaviour of root exudation in different plant species in different soil conditions such as soil C and N availability and pH, is crucial to the understanding of how plants influence the dynamics of N_2O production and consumption through root exudation with current knowledge on this topic still limited (Kuzyakov and Gavrichkova, 2010). Furthermore, little research has been able to decouple PAR and soil temperature to demonstrate the sole effect of PAR on N_2O flux in vegetated soil systems.

2.5.4 Non-diurnal N_2O flux variability and the role of soil temperature

In the case of non-diurnal patterns, non-diurnal datasets overall showed a weak positive correlation ($0 < R < 0.7$) between N_2O flux and soil temperature (Figure 2.1); this could be explained by the immediate positive effect of N addition in some studies (Huang et al., 2014;

Kostyanovsky et al., 2019; Scheer et al., 2008). In experiments, fertilisation events often took place in the morning, which resulted in a continuous increase in N_2O flux in the following hours (Kostyanovsky et al., 2019; Šimek, Brůček and Hynšt, 2010; Smith et al., 1998). The upward trend of N_2O flux could coincide with soil temperature during daytime but lasts through the evening and night, resulting in a slight positive correlation between N_2O flux and soil temperature. The rest of the non-diurnal datasets with no visible trend was likely due to the disruption of the diurnal N_2O flux patterns caused by rainfall (Ball et al., 1999; Charteris et al., 2020; van der Weerden et al., 2013). It was reported that soil N_2O production declines substantially when soil WFPS reaches over 80% as denitrification shifts to completion (i.e. $N_2O \rightarrow N_2$) due to soil anoxia (Congreves et al., 2017; Davidson, 1993; Neill et al., 2005). As rainfall events do not have a diurnal rhythm and could obstruct O_2 influx into the soil by increasing the percentage soil WFPS, they could subsequently change the dynamics between soil N_2O production and consumption and therefore interrupt pre-existent diurnal patterns of N_2O flux.

2.5.5 Non-diurnal factors and diurnal variability of N_2O flux

The data synthesis reveals that the occurrence of specific diurnal patterns of N_2O flux may also be influenced by non-diurnal factors. Although no significant difference was found among the pH values of diurnal pattern categories (Figure 2.2a), the night-time peaking category exhibited a higher pH median value (pH = 7.2) than the daytime peaking and non-diurnal categories (pH = 5.9) (Figure 2.2a). This agrees with the findings of Hénault et al. (2019) and Čuhel et al. (2010), which demonstrated increased N_2O reduction activities (i.e. N_2O consumption) by denitrifers in alkaline conditions. Soils with higher pH could possess higher potentials for N_2O consumption and hence increased likelihoods of night-time peaking, owing to increased soil O_2 depletion during daytime by increased soil respiration (Makita et al., 2018; Tang et al., 2003), which subsequently leads to favourable conditions for N_2O reduction (Firestone and Davidson, 1989; Morley et al., 2008). The boxplot results of bulk density (Figure 2.2b) indicated that bulk density has little association with the occurrence of diurnal patterns, as we found similar median values and wide spreads of interquartile ranges of bulk density among the diurnal pattern categories with no significant difference between one another. Conversely, our findings of the proportion of diurnal patterns in soil drainage classes (Figure 2.3a) and WFPS levels (Figure 2.3b) suggest that soil gas diffusivity, which is regulated by both factors, could potentially determine the occurrence of specific diurnal patterns. The proportion of daytime peaking in well and

imperfectly drained soils was similar to that of the overall datasets (~60%); however, in poorly drained soils, the majority of the datasets were night-time peaking (67%). Similarly, proportions of daytime peaking datasets (~70%) were larger in soils with relatively low WFPS levels (i.e. ≤34.9% and 35-54.9%), than in soils with WFPS level of 55-75% (47%). Night-time peaking datasets also accounted for a higher proportion in soils with WFPS level of 55-75% (37%) compared to in soils with lower WFPS levels. Conversely, a majority of daytime peaking datasets (83%) and no night-time peaking dataset were observed in soils with WFPS level of ≥75%. However, this observation is unlikely to be conclusive given the small number of datasets with soil WFPS ≥75% (n = 6), which originated from two studies where one raised its soil WFPS to 80% in the morning at the start of the flux measurements (Kostyanovsky et al., 2019), and the other conducted flux measurements during a freeze-thaw period (Peng et al., 2019). Both would have led to increased soil WFPS, and thus N_2O flux during daytime. While none of the extracted studies observed diurnal oscillation in soil moisture (all measured at more than five cm depth), a study have found that soil moisture varies diurnally (slightly higher at night-time) at 1.5 cm depth (Reichman et al., 2013). This may contribute to the occurrence of night-time peaking of N_2O flux. Our findings of the increase in night-time peaking proportion in soils with reduced gas diffusivity support the theory suggested in Section 4.2, where we highlighted the possibility of N_2O consumption overtaking N_2O production during daytime under limiting O_2 conditions. In this review, poorly drained soils comprised soils with high clay or organic matter content (Section 2.2.3), which have been shown to have lower total porosity and gas diffusivity than well and imperfectly drained soils (Chamindu Deepagoda et al., 2011; Moldrup et al., 2000). Likewise, increase in WFPS reduces gas diffusivity of soils (Chamindu Deepagoda et al., 2011). Multiple studies have demonstrated the effect of gas diffusivity on N_2O flux, showing increasing N_2O flux when gas diffusivity reduces from 0.03 to 0.005, and decreasing N_2O flux when gas diffusivity goes below 0.005 (Balaine et al., 2016; Chamindu Deepagoda et al., 2019, 2020). Low gas diffusivity (< 0.005) can cause O_2 limitation in soil and subsequently prompt nitrifiers and denitrifiers to shift from N_2O production to consumption (Balaine et al., 2016; Bollmann and Conrad, 1998; Sutka et al., 2006). Since soil O_2 is less readily replenished in poorly drained soils and in soils with high WFPS, localised soil anoxia, where N_2O reduction overrides N_2O production, is likely to develop in these soils during daytime when soil respiration rate increases (Keane et al., 2017; Makita et al., 2018; Tang, Baldocchi and Xu, 2005). However, we have not found any study that

examined the effects of soil texture on the diurnal dynamics of soil O_2 concentration under the same conditions (e.g. bulk density, volumetric water content and vegetation), which leaves the relationship between soil texture and diurnal N_2O patterns still unclear. In addition, while the general regulatory effect of soil moisture and WFPS on N_2O flux is well-studied (Schindlbacher, Zechmeister-Boltenstern and Butterbach-Bahl, 2004), there is still little research focused on diurnal variations in soil moisture, along with its interactions with other diurnal variables such as soil temperature and soil respiration, leading to its effect on diurnal N_2O fluxes. For example, Denmead et al. (2010) observed diurnal oscillations of soil WFPS inverse to those of soil temperature, which could dampen the temperature effect on diurnal N_2O fluxes. Therefore, we suggest future research should collect diurnal data of soil moisture or WFPS, soil temperature and N_2O flux from soils of different textures and drainage properties to investigate the interactive effects of soil physical factors on diurnal N_2O fluxes.

Nitrogen fertilisation is another non-diurnal factor that was expected to have an effect on diurnal N_2O patterns, since many studies reported daytime peaking diurnal patterns only after the application of N fertilisers (Laville et al., 2017; Lognoul et al., 2019; Shurpali et al., 2016; Skiba et al., 1996). Yet, our findings (Figure 2.4a) show daytime peaking diurnal patterns occur more often in unfertilised soils than in fertilised soils, indicating that high soil N levels do not cause daytime peaking diurnal patterns. This is reiterated with the higher percentages of daytime peaking in low magnitude flux datasets (67%) than in high magnitude flux datasets (53%) (Section 3.1). Land use type has also been shown to govern the diurnal patterns of N_2O flux. Higher proportions of daytime peaking emissions were recorded in datasets with grassland (81%) and forest (67%) soils, compared to cropland (55%) soils (Figure 2.4b). Very little literature has reported the direct relationship between land use and the diurnal pattern of N_2O flux. One study that was conducted on a field consisting of two established land use systems (pasture and cropland) found greater gas diffusivity in the pasture than in the cropland (Kreba et al., 2017). This suggests that land use could indirectly influence the occurrence of diurnal N_2O patterns through changing the soil gas exchange dynamics. Future research should include similar experiments to test the effects of land use on the diurnal patterns of N_2O flux. Despite similar proportions of diurnal N_2O flux patterns being found among three seasons (Figure 2.4c), most of the diurnal N_2O flux datasets were collected during summer (n = 138) and spring (n = 98) months, with only a small number of datasets collected in autumn (n = 24) and winter (n = 1) months. This

may have resulted in a potential bias in the overall diurnal patterns of N_2O flux, as those in winter were not analysed due to the lack of data.

2.5.6 Potential bias of single-daily measurements

As discussed in Section 4.1, N_2O flux does not always follow the diurnal oscillation of soil temperature. Measuring N_2O flux at times of daily average soil temperature might not capture the daily average N_2O flux and could lead to over- or underestimation of daily fluxes. Our analysis (Figure 2.5) confirmed that 10:00 h was the optimal sampling time as it resulted in the smallest magnitude of under- or overestimation. This agrees with the recommended time of sampling suggested by several publications. However, there was still a significant uncertainty (CI ranged between -29% and +35%) as the single time-point sampling failed to capture the inconsistent occurrence of diurnal variations in N_2O flux. Most studies that suggested a recommended time of sampling based their extrapolations on their sub-daily N_2O flux measurement campaign(s) on a single field site which usually exhibited a more-or-less consistent diurnal pattern of N_2O flux for the duration of the campaign(s), which is often the duration of a season (Chang et al., 2016; Reeves and Wang, 2015; Savage, Phillips and Davidson, 2014; van der Weerden, Clough and Styles, 2013). However, some studies have shown differences in the diurnal behaviour of N_2O flux at different sites (Alves et al., 2012; Smith et al., 1998) and times of year (Shurpali et al., 2016; Zona et al., 2013). Besides, studies have also provided different recommended times of sampling. For instance, Parkin (2008) who measured N_2O emissions from a cropland found sampling at 12:00 h would only be 8% higher than the daily mean N_2O flux; whereas Smith and Dobbie (2001) measured N_2O emissions from two grassland sites and suggested sampling to take place at 03:00, 11:00 and 19:00 h, as it produced N_2O flux representative of the daily mean. This could be the result of varying diurnal patterns of N_2O flux in different ecosystems which further underlines the potential uncertainty of single-daily N_2O flux measurements. Hence, sub-daily flux measurements should be employed when possible to account for the diurnal variability of N_2O flux and accurately measure cumulative N_2O emissions.

2.6 Conclusion

Our work has, for the first time, conclusively demonstrated that diurnal variability of N_2O flux is a widespread phenomenon across agricultural and forest soils. Daytime peaking of N_2O flux was the most common diurnal pattern observed, but it did not consistently occur across soil drainage classes, soil WFPS levels, N fertilisation status, seasons and land use

types. This analysis has shown that single-daily measurements produce emission estimations with large uncertainties due to the inconsistency in diurnal N_2O flux patterns, with soil temperature only partially explaining diurnal variations in N_2O flux. There is a paucity of published data on diurnal variables (e.g. PAR, plant C inputs, soil moisture and N substrates) which may interact to influence diurnal N_2O fluxes, and this limits our understanding of the drivers of diurnal N_2O fluxes. The interactive effects of these variables, as well as other non-diurnal factors (e.g. land use and soil drainage property), on diurnal N_2O flux variations need to be addressed in future research. At present, analyses of the drivers of diurnal N_2O flux variability are limited by the lack of diurnal data on soil inorganic N content, soil labile C content and soil moisture. Collection and incorporation of such data into analyses of diurnal N_2O flux in future research will help address this and better predict the diurnal variability of N_2O flux.

Without a comprehensive understanding of the drivers of diurnal N_2O fluxes, our current ability to accurately model and upscale diurnal N_2O fluxes is limited. We do not know the persistence and occurrence of diurnal N_2O flux patterns over entire crop life cycles or seasons. In addition, the significance of diurnal variability of N_2O flux is still not acknowledged or addressed in national and global GHG emission reporting, contributing to N_2O emission estimate uncertainties and hindering the development of mitigation strategies. Nevertheless, recent developments in real-time monitoring of GHG fluxes have increased the availability of sub-daily N_2O flux data. This will play a key role in improving the accuracy of current model predictions of N_2O emission through emergent research on diurnal variability of N_2O flux.

3. Field observations of diurnal variations in soil nitrous oxide flux

3.1 Abstract

Nitrous oxide (N_2O) is a potent greenhouse gas largely emitted by soils. Soil N_2O fluxes are highly variable in time, over hourly, daily, and longer time scales. Failure to consider this variability from diurnal cycles could contribute to uncertainties in N_2O emission estimates. This study aimed to observe and assess the importance of addressing diurnal variability of N_2O flux for total N_2O emission calculation estimates, as well as examine the relationships of diurnal N_2O flux with measured biotic and abiotic variables. The measured variables were soil volumetric water content (VWC), soil temperature, photosynthetically active radiation (PAR) and gross primary productivity (GPP). Soil N_2O and CO_2 fluxes (subsequently partitioned to GPP) from field-situated fertilised mesocosms of forage rape (*Brassica napus* L.) were measured at sub-daily frequencies over 56 days.

A total of 84.58 mg N_2O m^{-2} (equivalent of 2.2% of N input) was emitted over the measurement period which was more than double the emission estimation using the current default emission factor (1% of N input). Our analysis also revealed that once-daily measurements of N_2O flux at ca. 10:00 was the only measurement interval that would produce an emission estimate with an acceptable bias (< ±10%) compared to semi-continuous diurnal measurements (ca. 10 per day). Other measurement intervals that are often utilised such as once every three days, weekly and fortnightly would risk under- or overestimation from -75% to +108%. High diurnal variations in N_2O flux were observed throughout the experiment, with more than 85% of the measurement days exhibiting > 100% of difference between daily minimum and maximum fluxes. A prevalence of daytime peaking diurnal N_2O patterns was also observed, exhibiting in > 60% of the measurement days.

Of the measured parameters, all but soil temperature significantly correlated ($p < 0.05$) with the four-hourly averages of N_2O flux, with VWC showing the highest correlation (Pearson's r = 0.273), followed by GPP (Pearson's r = 0.124) and PAR (Pearson's r = 0.110). Linear mixed-effects models revealed a large portion (> 50%) of the variance in log-transformed N_2O flux ($\ln(N_2O\ flux)$) were explained by day-to-day variations in flux magnitude, possibly owing to the changes in N substrate content by multiple fertilisations. A comparison of the models suggest the combination of VWC and GPP as fixed factors

provided the best prediction of ln(N_2O flux), hinting at the potential contribution of plant productivity on diurnal variations in N_2O flux, which has not been well-studied at present. Disassociating the diurnal coupling between soil temperature and GPP in future studies may provide more direct evidence of the individual effect of GPP on the diurnal dynamics of N_2O flux.

3.2 Introduction

Agriculture has been a major contributor to the rapid increase in atmospheric nitrous oxide (N_2O) concentrations since the 1800s due to the extensive applications of both organic and inorganic nitrogen (N) fertilisers on agricultural soils to boost crop and livestock yield. About 58% of anthropogenic N_2O emissions are of agricultural origins (Smith et al., 2007). Excessive inputs of N in soils subsequently lead to an increase in N_2O emissions through N-cycling microbial processes such as nitrification and denitrification. The Intergovernmental Panel on Climate Change (IPCC) in its Fifth Assessment Report estimated the global N_2O emissions from soils under natural vegetation and from agriculture to be 6.6 (3.3 – 9.0) Tg N yr^{-1} and 4.1 (1.7 – 4.8) Tg N yr^{-1}, respectively (Ciais et al., 2013).

In the UK, oil seed rape (*Brassica napus*) is one of the common agricultural crops, with a high N demand for growth and seed production (Hegewald et al., 2016; Ruser et al., 2017). As of 2020, a total 330,000 ha of land was used for oil seed rape cultivation in the UK (DEFRA, 2020). With a moderate fertilisation dosage of N, oilseed rape receives approximately 120 kg N ha^{-1} yr^{-1} (Weisler, Behrens and Horst, 2001). This converts to an annual N input of ~40 thousand tonnes in the UK, which could contribute significantly to N_2O emissions (Drewer et al., 2012; Keane et al., 2018; Ruser et al., 2017). The IPCC guidelines also suggest to estimate the annual N_2O emissions by multiplying the annual N inputs by an emission factor of 1% (Hergoualc'h et al., 2019). Since this emission factor is approximated based on field measurements or derived from model predictions of N_2O emissions (Bouwman, 1996; Smith, Bouwman and Braatz, 2000), it only accounts for the temporal variability of N_2O flux at the frequency in which the measurements or model validating dataset were made. Most field measurements at present do not consider the diurnal variability of N_2O flux (Jungkunst et al., 2018). With large uncertainties in the estimates of N_2O emissions, accurate N_2O emission inventories and the development of mitigation strategies is challenging (Dorich et al., 2020; Syakila and Kroeze, 2011).

Temporal variability of soil N_2O flux, especially short-term variations is considered a major cause of the large uncertainties in N_2O emission estimates (Del Grosso et al., 2012). Studies have uncovered strong day-to-day variations in N_2O flux (Barton et al., 2015; Lammirato et al., 2018; Richter et al., 2012), which the IPCC Tier 3 approaches such as direct flux measurements could potentially address if measurements were conducted on a daily basis. However, most of the current N_2O flux measurements by manual static chambers were performed at intervals ranging from once or twice per week to month (Barton et al., 2015;

Drewer et al., 2012; Parkin, 2008; Reeves and Wang, 2015; Skiba et al., 1998; Williams, Ineson and Coward, 1999), potentially missing the variations in N_2O flux in-between (Ball, Scott and Parker, 1999; Christensen, 1983; Dobbie and Smith, 2003; Scheer et al., 2012; Williams, Ineson and Coward, 1999). In a meta-analysis by Stehfest and Bouwman (2006), less than a third of the 464 included studies measured N_2O emissions on a daily or less than daily basis, and about half of the measurements were conducted at weekly or more than weekly frequencies. At this measurement resolution, even less consideration of the diurnal variability of N_2O flux is made, despite some studies reporting over an order of magnitude in diurnal N_2O flux variations (Ball, Scott and Parker, 1999; Christensen, 1983; Dobbie and Smith, 2003; Scheer et al., 2012; Williams, Ineson and Coward, 1999). Our own analysis of historic published data (Chapter 2) has shown that measuring once-a-day between 08:00 and 16:00 could result in a underestimation (down to -16%) or overestimation (up to 59%) of daily cumulative N_2O emission (Wu et al., 2021). In recent years, quantum cascade laser-based technologies have been increasingly available, which allow *in situ*, real-time measurements of atmospheric N_2O concentrations (Lebegue et al., 2016). By coupling with an automated chamber system (ACS), multiple N_2O flux measurements can be made within 24 hours, addressing the diurnal variations in N_2O emissions. Alternatively, micrometeorological methods such as the eddy covariance technique can be employed to provide continuous N_2O flux measurements, however, operation of eddy flux towers and processing of the collected data are more challenging compared to automated chamber measurements. Additionally, eddy covariance is most suitable for operation at the field scale (di Marco et al., 2005), whilst ACSs can incorporate experimental treatments by operating at the mesocosm/plots scale.

Regardless of the technique used, studies that measured N_2O fluxes from agricultural soils at high sub-daily frequencies often observed a daytime peaking pattern in the diurnal variations in N_2O emissions, characterised by low emissions in the early morning and peak emissions in the afternoon (Blackmer, Robbins and Bremner, 1982; Christensen, 1983; Clar and Anex, 2020; Keane et al., 2018; Scheer et al., 2014; van der Weerden, Clough and Styles, 2013; Williams, Ineson and Coward, 1999). This phenomenon is usually ascribed to the fluctuation of soil temperature, as N_2O flux is often positively correlated to soil temperature (Blackmer, Robbins and Bremner, 1982; Hosono et al., 2006; Liang et al., 2018; Scheer et al., 2014; van der Weerden, Clough and Styles, 2013; Williams, Ineson and Coward, 1999). Some studies, on the other hand, alluded to diurnal variations in N_2O flux

following the diurnal rhythms of photosynthetically active radiation (PAR), or a proxy of which such as solar radiation and gross primary productivity (GPP) (Christensen, 1983; Keane et al., 2018; Shurpali et al., 2016; Zona et al., 2013). Most of the studies that found strong associations between photosynthetic parameters (e.g., PAR, solar radiation and GPP) suggested that diurnal variations in N_2O flux might be driven by the C inputs from plants as a result of photosynthesis (Christensen, 1983; Keane et al., 2018; Shurpali et al., 2016). Studies have found that plants exude up to 40% of photosynthetically-fixed C into the rhizosphere (Badri and Vivanco, 2009; Newman, 1985; Prescott et al., 2020), which are released in various forms of organic compounds such as sugars, amino acids, fatty acids and phenolic compounds (Dennis, Miller and Hirsch, 2010; O'Brien et al., 2018). A study shows that oilseed rape transports 17 – 19% of its photosynthetically-fixed C to the roots and releases 30 – 34% of which into the rhizosphere (Shepherd and Davies, 1993). These easily decomposable root exudates are important energy sources for heterotrophic soil microbes including the majority of denitrifiers (Ai et al., 2020; Henry et al., 2008). The release of root exudates could also have secondary stimulating effect on denitrification by depleting soil O_2 in the rhizosphere upon aerobic respiration of root exudates by heterotrophs (Hu, Chen and He, 2015). It has been demonstrated that up to 86% of the root exudates were rapidly respired by soil microorganisms (Dilkes, Jones and Farrar, 2004; Hütsch, Augustin and Merbach, 2002; Pausch et al., 2013). In addition, a review study by Kuzyakov and Gavrichkova (2010) found that the lag time between photosynthesis and soil respiration of photosynthetically-fixed C is < 12.5 hours in herbaceous plants. This suggests that photosynthesis and the subsequent root exudation of labile C to soil microbes may regulate the temporal dynamics of N_2O production in soils.

Nevertheless, daytime peaking patterns of N_2O flux was not always observed in studies. Several studies also reported night-time peaking of N_2O flux that was out of sync with any photosynthetic parameter and soil temperature (Keane et al., 2019; Shurpali et al., 2016; Smith et al., 1998). On the other hand, several studies did not observe consistent diurnal patterns of N_2O flux at all (Ball, Scott and Parker, 1999; Du, Lu and Wang, 2006; Huang et al., 2014). The spread of daytime, night-time peaking and non-diurnal patterns of N_2O flux was recently quantified to be approximately 3:1:1 in a systematic review of 46 studies (Wu et al., 2021). This finding hints at the innate inconsistency in the diurnal patterns of N_2O flux, which is not well-studied as of now. One study attributed the inconsistency in diurnal patterns of N_2O flux to the events of rainfall (van der Weerden, Clough and Styles, 2013),

as the rise in soil moisture often stimulates N_2O pulse emissions and overrides the effects of diurnal variables.

1. Observe diurnal variations and patterns of N_2O flux,
2. Assess the importance of measuring N_2O fluxes at sub-daily frequencies (i.e., biases in total N_2O emissions using sub-daily measurements vs once daily/every three days/weekly/fortnightly measurements at 10:00), and
3. Explore the relationships between diurnal N_2O flux and other abiotic and biotic variables, including soil volumetric water content (VWC), soil temperature, PAR and GPP.

Based on the findings of overall diurnal patterns of N_2O flux (~60% of daytime peaking) in Chapter 2, it was hypothesised that daytime peaking of N_2O flux would be observed in approximately 60% of the measurement days. Based on literature findings mentioned above (Barton et al., 2015; Parkin, 2008; van der Weerden, Clough and Styles, 2013) and sampling time recommendations (Charteris et al., 2020; de Klein & Harvey, 2015; IAEA, 1992; Parkin & Venterea, 2010), it was also hypothesised that N_2O flux measurements at 10:00 once daily and every three days would yield biases of $< \pm 10\%$ in cumulative N_2O emission when compared to that calculated with sub-daily N_2O flux measurements, whereas those made at 10:00 weekly and fortnightly would result in unacceptable biases of $\geq \pm 10\%$. The $< \pm 10\%$ range was defined as acceptable bias in Barton et al. (2015). Furthermore, it was hypothesised that N_2O flux would exhibit significant and positive relationships with soil VWC, soil temperature, PAR and GPP, with soil VWC having the strongest relationship due to its control over soil O_2 level (main driver of denitrification), followed by soil temperature due to its positive effect on microbial activity (denitrification and nitrification) and PAR and GPP due to its potential regulation on root exudation of labile C (energy source for denitrification and heterotrophic respiration).

To assess these hypotheses, sub-daily measurements of N_2O flux were collected, along with collection of soil VWC, temperature, PAR and net CO_2 flux (for GPP partition) data at sub-daily frequencies. A field set-up using an ACS – Skyline2D, a similar system documented in Keane et al. (2018), was established. The mesocosm system was designed in a manner that subsequent work could incorporate field manipulation of drivers of diurnal N_2O emissions such as soil temperature and PAR (Chapter 4). Oil seed rape (*Brassica napus* L.) was used in the two field experiments (Chapter 4 and 5) as the study crop due to its significant presence as an agricultural crop and its potential contribution to N_2O emissions in the UK.

3.3 Methods

3.3.1 Experimental design and site description

A mesocosm experiment was conducted between 26 Jul 2018 and 24 Sept 2018 at the Hazelrigg Field Station, Lancaster, UK (54°1'N, 2°46'W). To observe diurnal variations in N_2O flux, flux measurements at sub-daily frequencies (9 to 11 measurements per day) were conducted with a set-up comprising an ACS (Skyline2D, University of York, York, UK) over a transect of 20 mesocosms, illustrated in Figure 3.1. The ACS was equipped with a transparent chamber (inner diameter = 40.7 cm, height = 62.0 cm, volume = 80,820 cm^3). A mobile laboratory housing a cavity ring-down spectrometer (CRDS) (Picarro G2508, Picarro Inc., Santa Clara, USA), was set up in the vicinity of the transect. The CRDS analysed and recorded the concentrations of N_2O in the gas stream from the chamber headspace at a frequency of approximately 1 Hz. Two lines of polyethylene tubing (Bev-A-Line, 1/4" inner diameter, 3/8" outer diameter, Cole-Parmer, St. Neots, UK), were connected between the chamber and the CRDS through the chassis; one served as the gas stream inlet from the chamber to the CRDS and the other as the outlet returning the gas stream from the CRDS to the chamber. Fluxes of N_2O and CO_2 and auxiliary data of VWC, soil temperature and PAR were collected from 26 Jul to 23 Sep 2018.

Mesocosms were composed of a bottom-draining cylindrical plastic pot (inner diameter: 40 cm, height: 38 cm), and an acrylic collar attached to the rim of the pot. Each mesocosm was filled with an alkaline cropland soil (pH = 8.36) with a texture of fine silt that was collected from a commercial farm in Lincolnshire, UK. A previous field experiment that observed daytime diurnal patterns of N_2O flux *in-situ* was conducted on this farm which cultivated oil seed rape (*Brassica napus* L.) at the time (Keane et al., 2018). The soil was homogenised by mixing before repacking into the mesocosms. Seeds of forage rape (*Brassica napus* L. "Interval", LG Seeds, Lincoln, UK) were sown in plug cells on 24 Jun 2018. Ten seedlings were transplanted to each mesocosm on 19 July 2018, which was one week prior to the start of the flux measurements. A soil temperature logger (HOBO Pendant® UA-002-64, Onset Corporation, MA, USA) was placed at 10 cm soil depth and a pre-calibrated volumetric moisture content (VWC) logger (Odyssey® Soil Moisture Logger, Dataflow Systems Ltd., Christchurch, NZ) was inserted 10 cm into the soil in each mesocosm.

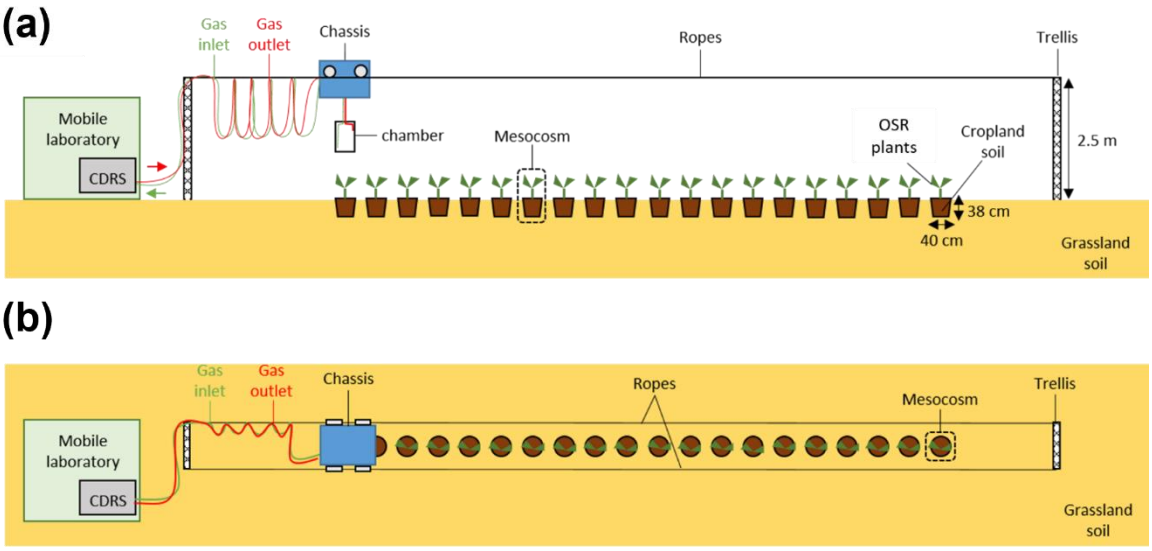

Figure 3.1. (a) Side and (b) top view illustration of the automated chamber system (ACS). The ACS consisted of two 2.5 m-tall trellises which were erected on both ends of the mesocosm transect (ca. 20 m apart), two parallel ropes that were mounted and tensioned between the metal trellises, and a motorised, computer-controlled Skyline2D chassis that hoisted and dropped a clear cylindrical chamber. Directly above each mesocosm, a magnet was placed in the rope to allow the recognition of the mesocosm locations by the chassis. The green and red arrow indicate gas inlet (chamber to CRDS) and outlet (CRDS to chamber).
Mesocosms were sunken into the field soil to the depth where the mesocosm soil surface was level with the field soil. To imitate the agricultural practice for forage rape farming, the mesocosms received three basal applications of a mineral N fertiliser (i.e., ammonium nitrate (NH4NO3)) at the rates of 70, 70 and 100 kg N ha-1 on 27 Jul, 22 Aug and 11 Sep 2018. The study site was amid a drought period (less than 0.2 mm of rainfall for over 15 consecutive days) at the beginning of the experiment, therefore, the mesocosms were irrigated daily between 26 Jul to 8 Aug 2018 to prevent drought-induced plant stress.

3.3.2 Measurements of N_2O and CO_2 fluxes and environmental parameters

During the experimental period, a non-steady state closed chamber measurement sequence that included a chamber enclosure time of 240 seconds and a flushing time of 130 seconds for each measurement, was programmed to measure all 20 mesocosms in a repeated cycle. The time for the completion of a cycle was approximately 2.25 hours. Upon the enclosure between the chamber and the mesocosm (Figure 3.2), a continuous circulation of gas stream was created between the chamber headspace and the CRDS. The concentrations of N_2O in the headspace during a chamber enclosure were recorded by the CRDS at approximately 1 Hz, generating a flux measurement. No gas flux measurements were made between 28th July 11:00 and 30th July 11:30 due to a disconnection of the inlet gas line caused by strong winds. Readings of PAR under the chamber top were recorded at one-minute intervals, whereas soil temperature (soil temperature) at 10 cm depth and VWC at 0-10 cm depth were recorded at five-minute intervals.

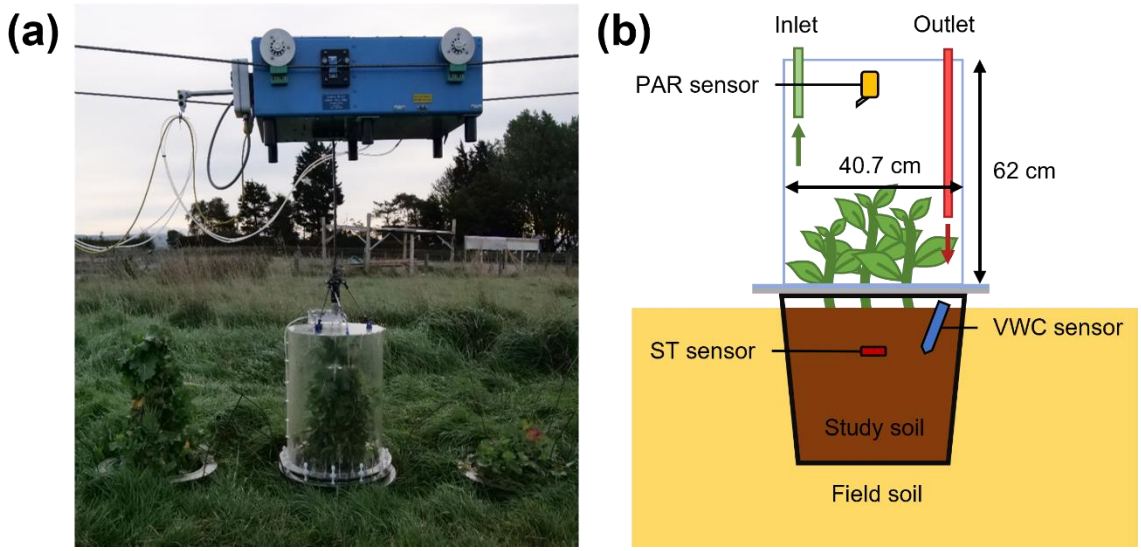

Figure 3.2. (a) Photograph of a mesocosm during a non-steady state closed chamber flux measurement performed by Skyline2D and (b) a side view diagram of a mesocosm and the Skyline chamber.

3.3.4 Data processing and statistical analyses

Data manipulation and visualisation were performed in RStudio (version 3.6.1, The R Foundation). Statistical analyses were conducted using jamovi (version 2.0.0, The jamovi project) with its inbuilt statistical packages. Gas concentration readings of N_2O and CO_2 during all chamber enclosures were converted to N_2O fluxes using a flux calculation package 'flux' in R (Jurasinski et al., 2015). To control the data quality of N_2O and CO_2 fluxes, linear regressions of N_2O with $R^2 < 0.1$ and automatic data points inclusion < 70% for each regression (indication of measurement disturbance) were considered zero flux, whereas linear regressions of CO_2 with $R^2 < 0.7$ and automatic data points inclusion < 70% were considered as bad flux measurements and discarded. The times of the fluxes were determined using the mean point of the regressions. Following this, CO_2 fluxes were partitioned into ecosystem respiration and GPP using the method detailed in Reichstein et al. (2005).

Data of environmental parameters (i.e., VWC, PAR and soil temperature) were then appended to the fluxes through linear interpolation. To account for the variability in N_2O fluxes between mesocosms, N_2O fluxes were first binned into four hourly bins, which were 02:00 (00:00 – 03:59), 06:00 (04:00 – 07:59), 10:00 (08:00 – 11:59), 14:00 (12:00 – 15:59), 18:00 (16:00 – 19:59), and 22:00 (20:00 – 23:59), and mean values of N_2O flux, VWC, soil temperature and PAR and their 95% confidence intervals were calculated. These mean values were used for data visualisation and statistical analyses. Diurnal variations in N_2O flux were then determined by the difference between the daily minimum and maximum mean N_2O flux of four hourly bins (hereby referred to as mean N_2O fluxes), which was

calculated as percentage increase by subtracting the maximum flux by the minimum flux, followed by the dividing with the minimum flux and multiplying by 100%.

To quantify the diurnal patterns of N_2O flux during the experiment, mean N_2O fluxes were split by individual days and each day was classified as either 'daytime peaking', 'night-time peaking', or 'non-diurnal', using the diurnal pattern categorisation method detailed in Wu et al. (2021). To further visualise to overall diurnal pattern of N_2O flux throughout the experiment, mean N_2O fluxes were first normalised following the method by Huang et al. (2014) and Keane et al. (2018), which removed the magnitude differences of N_2O flux between dates and allowed the observation of diurnal dynamics of N_2O flux. Then, the distributions of normalised N_2O fluxes of the four-hourly bins were plotted on a boxplot.

To compare the biases in cumulative N_2O emissions between sub-daily measurements and daily, every three days and weekly measurements, daily cumulative N_2O emissions of sub-daily measurements were first calculated using the mean N_2O fluxes of four hourly bins with trapezoidal integration (Keane et al., 2018), followed by a summation for the daily cumulative emissions to obtain a total emissions over the experimental period. The mean N_2O fluxes of the 10:00 four-hourly bins were multiplied by 24 for each day and summed up to calculate the total emission estimated by single-daily measurements. For measurements of once every three days, weekly, and fortnightly, multiple starting day scenarios were assumed (i.e., once every three days measurements would yield three total emission estimation scenarios since the start day could be on day 1, 2 or 3, weekly would yield seven scenarios and fortnightly would yield 14 scenarios). The daily cumulative N_2O emissions estimated by single-daily measurements were then taken at the respective intervals of the scenarios and propagated to the non-measurement dates. The biases in the total N_2O emissions between sub-daily measurements and daily, once every three days, weekly and fortnightly measurement scenarios were calculated using equation 2.3 in Chapter 2.

To examine the relationships between diurnal N_2O flux and abiotic and biotic variables, correlation coefficients (Pearson's r) were examined between mean N_2O flux and mean VWC, soil temperature, PAR and GPP. Due to the non-normality of the mean N_2O fluxes which could obscure the correlations, correlations with the ln(N_2O flux) were also investigated. Following this, three linear mixed-effects models were developed individually to assess the ability of soil temperature, PAR and GPP (as they showed considerable collinearity), along with VWC, to explain the variances in mean N_2O fluxes. To do so, the

Akaike Information Criterion (AIC; an estimator of out-of-sample prediction error and thereby indicates goodness of fit of a model), marginal R^2 (portion of variance explained by fixed effects) and p-values of the predictors of the three models were compared. In all three linear mixed-effects models, date of measurements was set as the random factor, whilst combinations of mean VWC and mean soil temperature, mean PAR or mean GPP were set as the fixed factors in their respective model. Zero mean PAR and GPP values (i.e., PAR and GPP at night) were excluded from the models since they could not explain the variances in night-time N_2O fluxes. The use of linear mixed-effects models was to account for the repeated measures of N_2O flux (i.e., multiple days of diurnal N_2O flux measurements), which were highly variable in magnitude, partly due to the N fertilisation events. To meet the assumption requirement of linear mixed-effects models (i.e., normality in model residuals), ln(N_2O flux) was used instead of mean N_2O fluxes, and ln(N_2O flux) ≤ 3.0 (equivalent of 20 μg m^{-2} h^{-1} of mean N_2O flux) were removed from the models to reduce the skewness towards low flux values. The normality of the models' residuals was tested with the Kolmogorov-Smirnov test. To visualise the fixed effects of the model predictors (i.e., mean VWC, soil temperature, PAR and GPP), observed values of ln(N_2O flux) were plotted against those of the predictors, followed by superimposing with the model-estimated values of ln(N_2O flux) at different levels of the predictors.

3.4 Results

Mean N_2O fluxes ranged between -20.6 ± 61.8 µg (mean ± standard error) N_2O m^{-2} h^{-1} and 829.6 ± 328.2 µg N_2O m^{-2} h^{-1} during the experiment (Figure 3.3a). Diurnal variations in N_2O flux observed in the experiment ranged from 21.4% to 13831.5%, with 87.0% (n = 47) of the measurement days exhibiting diurnal variations in N_2O flux > 100%. A total of 84.58 mg N_2O m^{-2} (equivalent of 5.38 kg N_2O-N ha^{-1}, or 2.2% of the total N inputs) were emitted throughout the experiment. Soil VWC at 0-10 cm varied from 27.5 ± 1.4% to 40.0 ± 1.7% with no clear diurnal pattern after the daily irrigation period (26 July to 8 August) (Figure 3.3b); whereas soil temperature at 10 cm ranged from 7.4 ± 0.2 °C to 23.5 ± 0.3 °C with diurnal differences ranging between 0.7 and 8.2 °C (Figure 3.3c). Daily maxima of PAR measured under chamber top ranged between 0.076 ± 0.010 mmol m^{-2} s^{-1} and 0.543 ± 0.045 mmol m^{-2} s^{-1} (Figure 3.3d), whereas that of GPP ranged between 2.08 ± 0.22 g m^{-2} h^{-1} and 4.89 ± 0.46 g m^{-2} h^{-1} (Figure 3.3e).

3.4.1 Biases in total cumulative N_2O emissions of measurement frequencies

The total N_2O emissions estimated using daily measurements at 10:00 resulted in a bias of +6.9% (Table 3.1, complete data table in Appendix II) which was within the acceptable bias defined by Barton et al. (2015), whereas with measurements of every three days resulted in biases between -1.9% and +15.0% depending on the starting day. Weekly measurements resulted in the largest and most variable biases ranging from -46.2% to +108.3%, with none of the days producing an estimate within the acceptable bias of within ± 10%. Similarly, fortnightly measurements produced large variable biases ranging from -74.6% to +89.9%, with only two of the starting day scenarios (scenario 6 and 7, Table 3.1) producing acceptable biases (+7.5% and -9.1%).

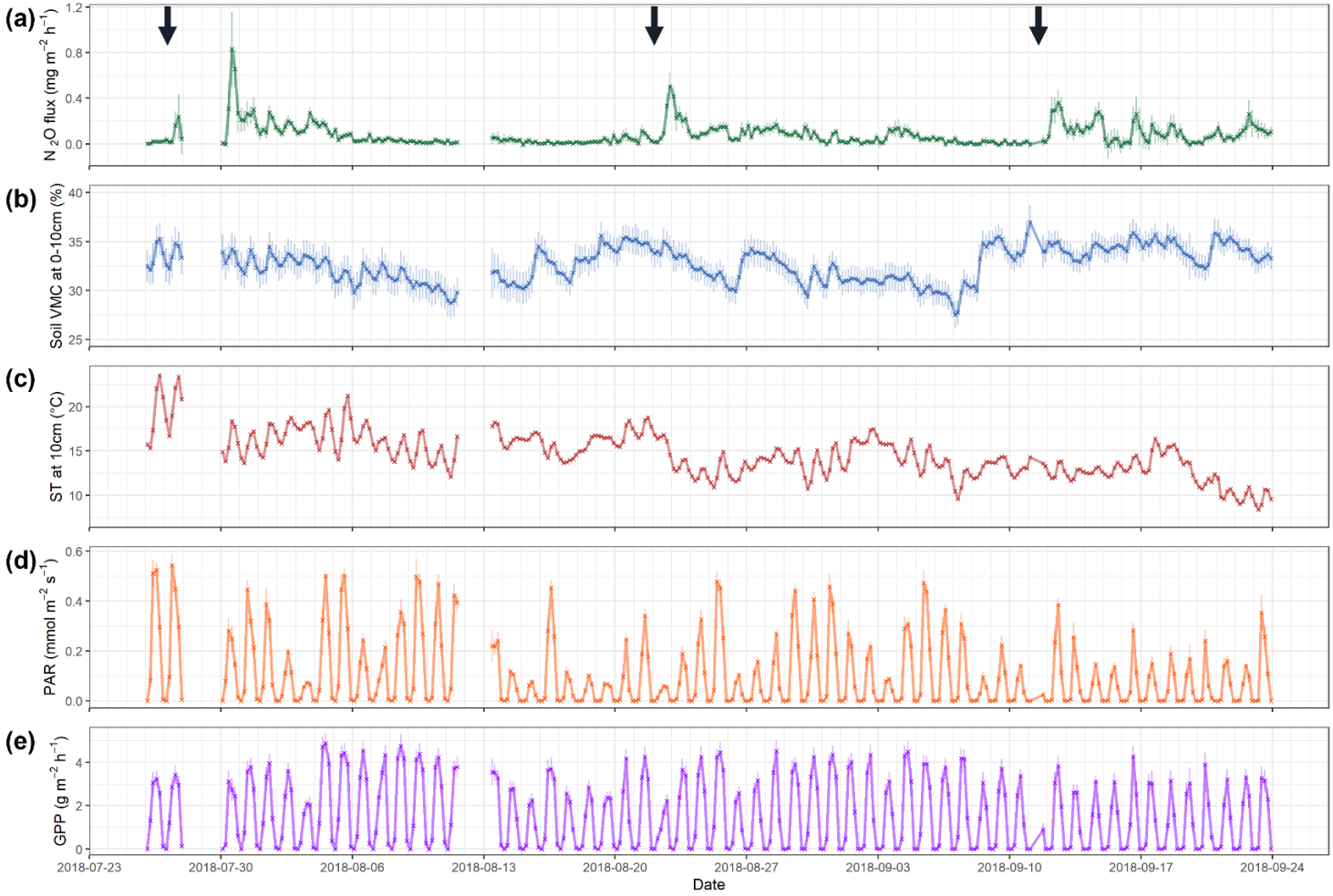

Figure 3.3. Timeseries of (a) N_2O flux, (b) soil volumetric content (VWC) at 0 – 10 cm, (c) soil temperature at 10 cm, (d) photosynthetically active radiation (PAR) under the chamber top and (e) GPP during the experiment. Crosses and vertical lines represent the mean values and 95% confidence intervals of four-hourly bins. Black arrows indicate the fertilisation events.

Table 3.1. Total N_2O emissions over the experimental period estimated with measurement scenarios of different intervals (single daily, once every three days, weekly and fortnightly at 10:00) and their biases when compared to the total N_2O emission estimated with sub-daily measurements.

Measurement frequency	**Total N_2O emission (mg N_2O m^{-2})**	**Bias (%)**
Sub-daily	84.58	NA
Single daily	90.41	+6.9
Every three days (scenario 1)	82.96	-1.9
Every three days (scenario 2)	89.44	+5.7
Every three days (scenario 3)	97.28	+15.0
Weekly (scenario 1)	53.55	-36.7
Weekly (scenario 2)	65.62	-22.4
Weekly (scenario 3)	45.53	-46.2
Weekly (scenario 4)	69.16	-18.2
Weekly (scenario 5)	176.15	+108.3
Weekly (scenario 6)	75.67	-10.5
Weekly (scenario 7)	123.16	+45.6
Fortnightly (scenario 1)	160.60	+89.9
Fortnightly (scenario 2)	152.85	+80.7
Fortnightly (scenario 3)	103.59	+22.5
Fortnightly (scenario 4)	68.63	-18.9
Fortnightly (scenario 5)	47.96	-43.3
Fortnightly (scenario 6)	90.93	+7.5
Fortnightly (scenario 7)	76.90	-9.1
Fortnightly (scenario 8)	95.41	+12.8
Fortnightly (scenario 9)	54.94	-35.0
Fortnightly (scenario 10)	118.46	+40.1
Fortnightly (scenario 11)	36.74	-56.6
Fortnightly (scenario 12)	63.96	-24.4
Fortnightly (scenario 13)	21.47	-74.6
Fortnightly (scenario 14)	65.16	-23.0

3.4.2 Categorisation of diurnal patterns of N_2O flux and overall diurnal pattern of N_2O flux during the measurement days

Mean N_2O fluxes exhibited daytime peaking pattern in 33 out of 56 days of complete measurements (61.1%) of flux measurements. Figure 3.4a shows an example of N_2O fluxes oscillating along with PAR and soil temperature for three consecutive days. It should be noted that the majority of daytime peaking days occurred outside the daily irrigation period. Night-time peaking pattern was only exhibited in 5 days (9.3%) and non-diurnal pattern were exhibited in 16 days (29.6%), as visualised in Figure 3.4b. The distributions of normalised N_2O fluxes in the four hourly bins further indicate an overall daytime peaking pattern of N_2O flux during the experiment (Figure 3.4c), with the 06:00 bin and the 14:00 bin having the lowest and highest distribution of normalised N_2O fluxes, respectively.

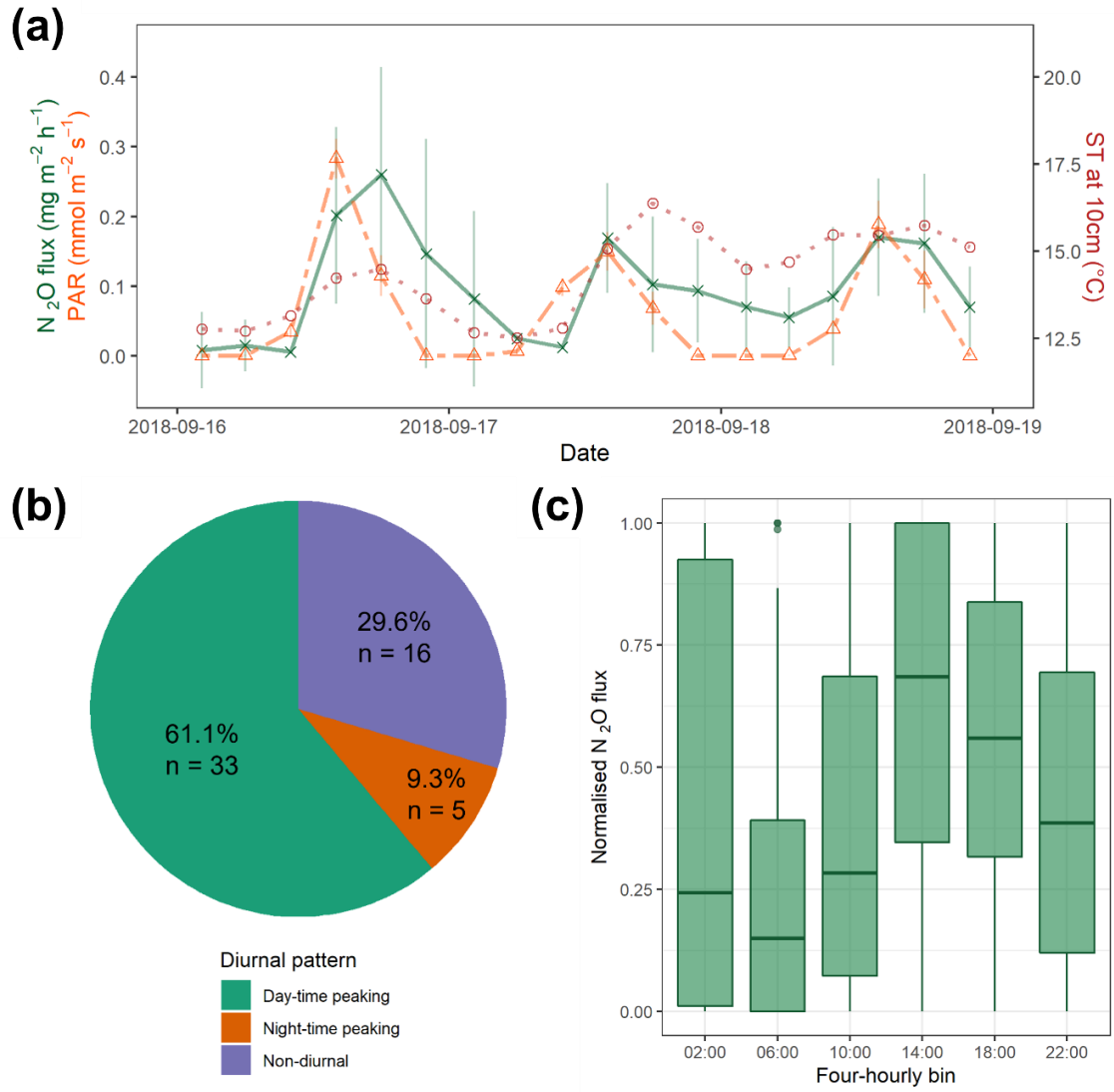

Figure 3.4. (a) Diurnal variations in mean N_2O flux (green crosses, solid line), PAR (orange triangles, dashed line) and soil temperature (red circles, dotted line) measured between 16 Sep and 18 Sep 2018. (b) Pie chart of the proportions of the three diurnal patterns (i.e., daytime peaking, night-time peaking, and non-diurnal) of N_2O flux; n indicates the number of days of which N_2O fluxes exhibited the respective diurnal pattern during the experiment. (c) Boxplot of normalised N_2O fluxes binned into six four-hourly bins indicating the overall diurnal pattern of N_2O flux during the experiment.

3.4.3 Correlation matrix and linear mixed-effects model of mean N_2O fluxes

The correlation matrix (Table 3.2, complete correlation matrix in Appendix I) shows both mean VWC and GPP significantly correlated with mean N_2O flux (VWC: $r = 0.273$, $p < 0.001$; GPP: $r = 0.130$, $p = 0.043$) and ln(N_2O flux) (VWC: $r = 0.264$, $p < 0.001$; GPP: $r = 0.219$, $p < 0.001$). Small Pearson's r values (between -0.1 and 0.1) and large p-values (> 0.5) were found in both mean N_2O flux and ln(N_2O flux) with mean soil temperature, indicating weak non-significant relationships. Mean PAR and GPP, on the other hand, both showed significant positive correlations ($r > 0.1$, $p < 0.05$) with mean N_2O flux and ln(N_2O flux).

Table 3.2. Correlation matrix of mean N_2O flux of four-hourly bins and log-transformed mean N_2O flux (ln(N_2O flux) against mean values of VWC, PAR and soil temperature of four-hourly bins. Values in bold indicate statistical significance.

	Mean N_2O flux	ln(N_2O flux)
	Pearson's r (p-value)	
ln(N_2O flux)	**0.766 (< 0.001)**	NA
VWC	**0.273 (< 0.001)**	**0.264 (< 0.001)**
Soil temperature	0.057 (0.296)	-0.035 (0.535)
PAR	**0.110 (0.043)**	**0.114 (0.042)**
GPP	**0.124 (0.023)**	**0.146 (0.009)**

The information of the three linear mixed-effect models is summarised in Table 3.3. Out of the three models, the GPP model had the lowest AIC (i.e., the least out-of-sample prediction error) of 296.4, indicating the best goodness of fit of the model estimations to the observed ln(N_2O flux) values. The AIC of the PAR model (327.6) was higher than that of the GPP model, whereas the soil temperature model had a comparatively much higher AIC (429.6). The marginal R^2 values of the models were not substantially different. The PAR model had the highest marginal R^2 (0.132), followed by the GPP model (0.122) and the soil temperature model (0.112). Mean VWC was a significant predictor in all three models; however, only GPP in the GPP model was also considered as a significant predictor and neither mean soil temperature or mean PAR was considered a significant predictor in their respective model.

Figure 3.5a to 3.5d show the scatter plots of the observed ln(N_2O flux) against mean VWC, soil temperature, PAR and GPP, respectively, along with model estimates of ln(N_2O flux) predicted at different levels of the parameters. A clear positive trend between ln(N_2O flux) and mean VWC can be observed (Figure 3.5a), whereas the positive relationship between ln(N_2O flux) and mean GPP appear more subdued (Figure 3.5d). Notably, the distribution of the observed ln(N_2O flux) against mean soil temperature (Figure 3.5b) is somewhat vertically congregated around 15 °C.

Table 3.3. Summary of model information of the three linear mixed-effects models. The formulae for soil temperature model, PAR model and GPP model are ln(N_2O flux) ~ 1 + VWC + soil temperature + (1|Date), ln(N_2O flux) ~ 1 + VWC + PAR + (1|Date), ln(N_2O flux) ~ 1 + VWC + GPP + (1|Date), respectively. Values of ln(N_2O flux), VWC, soil temperature, PAR and GPP are mean values of four-hourly bins. *: estimate and p-value are only applicable to the predictor of the respective model.

Model information	**Soil temperature model**	**PAR model**	**GPP model**
Model fit		Restricted maximum likelihood	
AIC	429.6	327.6	296.4
Marginal R^2	0.112	0.132	0.122
Conditional R^2	0.759	0.766	0.784
Observations	249	183	170
Number of dates	56	54	54
Predictor		*Estimate (p-value)*	
(Intercept)	**4.218 (< 0.001)**	**4.244 (< 0.001)**	**4.229 (< 0.001)**
VWC	**0.1589 (< 0.001)**	**0.198 (< 0.001)**	**0.175 (< 0.001)**
Soil temperature/PAR/GPP*	0.0382 (0.113)	0.339 (0.226)	**0.0678 (0.009)**

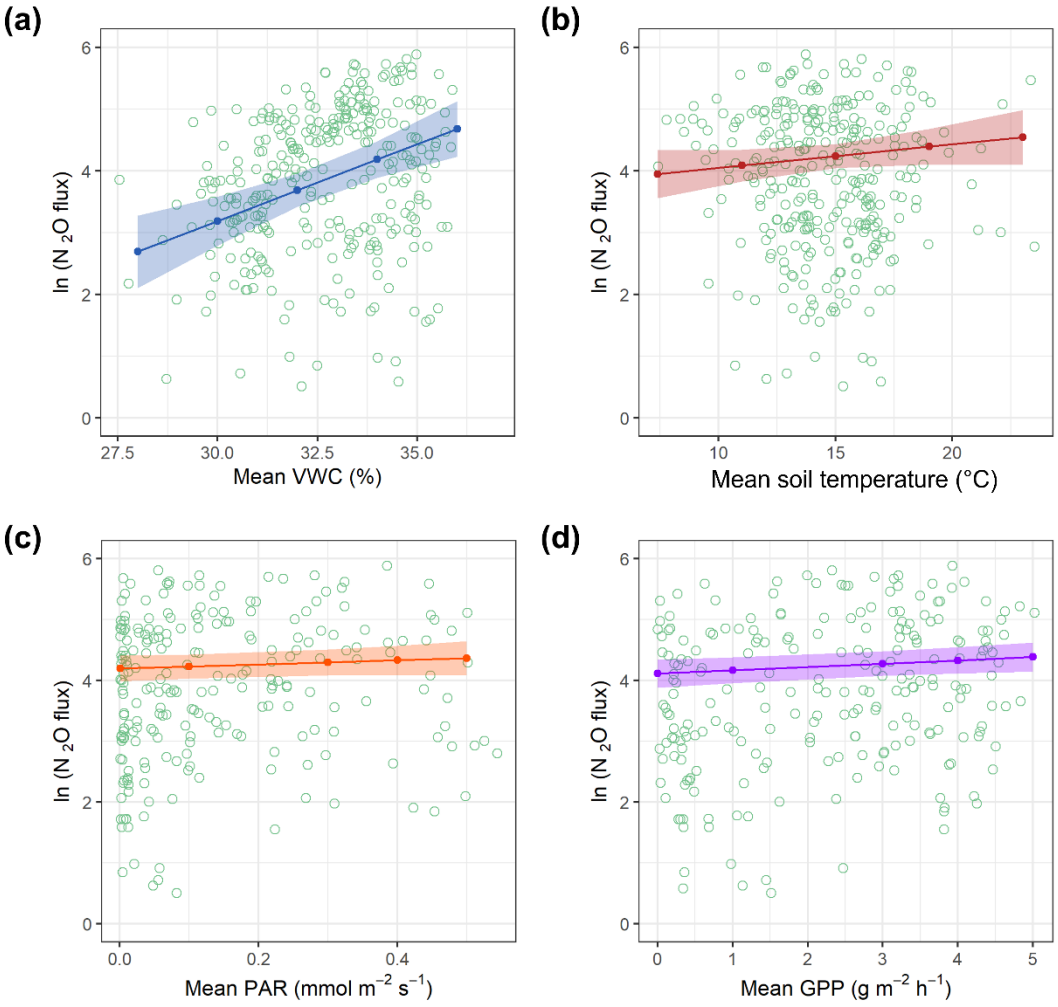

Figure 3.5. Scatter plots of the observed log-transformed mean N_2O fluxes (ln(N_2O flux)) (green open circles) against (a) mean VWC (of the GPP model), (b) mean soil temperature and (c) mean PAR and (d) mean GPP. Coloured dots and ribbons in (a) to (c) represent the ln(N_2O flux) values estimated by the liner mixed-effects model at different levels of the predictors and the 95% confidence interval limits (blue = VWC, red = soil temperature, orange = PAR, purple = GPP).

3.5 Discussion

This experiment tackled the challenges and limitations of measuring diurnal N_2O fluxes present in approaches otherwise with the use of an ACS. The implications of the experimental results could provide a better understanding of the drivers of diurnal variations in N_2O flux. This experimental set-up allowed future investigations of diurnal N_2O fluxes under treatments of manipulated diurnal variables (e.g., light intensity and soil temperature).

3.5.1 Importance of measuring diurnal variations in N_2O flux

High diurnal variations in N_2O flux were observed in this experiment, with differences between the daily minimum and maximum N_2O fluxes ranging up to 138 times and most days (> 87%) exhibited over 100% of diurnal variations in N_2O flux. Using the mean N_2O fluxes at the 10:00 four-hourly bins yielded a bias of +6.9% in total N_2O emission over the 56 measurement days, which is within the acceptable range of error defined by Barton et al. (2015) (±10%), who also revealed decreasing regularity of flux measurements could overestimated the total emission by up to 935%. This conforms the current guidance of sampling N_2O flux once-a-day in mid-morning around 10:00 to produce the most representative emission estimation (Charteris et al., 2020), as well as agrees with the findings of studies with similar assessments (Barton et al., 2015; Wu et al., 2021). However, the biases of total N_2O emission amplified with increased ranges of estimate as the measurement intervals widened. In the measurement regime of once every three days at 10:00, one out of three scenarios exhibited a bias of +15%, whereas weekly measurement frequencies (at 10:00) produced > ±10% biases in all seven scenarios, with under-estimations as low as -46% and overestimations as high as +108%. Likewise, 12 out of 14 scenarios of fortnightly measurement frequencies had > ±10% biases (-75% to +90%). This contrasts the indications by several studies that once every three days to weekly measurement frequencies could produce estimations with acceptable errors (Mosier et al., 1998; Reeves and Wang, 2015; Smith and Dobbie, 2001). Our findings also highlight the extent of uncertainty entailed in estimating N_2O emissions with flux measurements at longer than daily (up to monthly) intervals, which are still commonly practiced for N_2O emission reporting (Drewer et al., 2012, 2017; Harris et al., 2017; Hénault et al., 2019; Rochette, 2011). However, in the recent guidelines for N_2O emission sampling methods,

Charteris et al. (2020) also recommended varying the frequency of flux measurements based on whether emission peaks are expected (e.g., rainfall and fertilisation events), which may better capture the day-to-day and potentially diurnal variations in N_2O emissions.

Reporting of inaccurate N_2O emission estimates could further impede the accurate calculation of the emission factor, since the current default emission factor of 1% suggested by the IPCC was based on the summaries by Bouwman (1996), who extracted N_2O emission data from past studies with measurement intervals between three days to a month. Our results of sub-daily flux measurements however show that 2.2% of the applied N was emitted as N_2O in 56 days, highlighting the substantial shortfall of the recommended emission factor of 1%.

The magnitude of the biases by infrequent measurements in this study was partially due to the failure to capture the high magnitude, day-to-day variations in N_2O flux, leading to under- or overestimation of total emission by assumption of transient fluxes over extended periods of time. Even with single daily flux measurements at 10:00, the risk of under- or overestimation still persists given the diurnal variability of N_2O flux and the inconsistency of diurnal N_2O patterns. Wu et al. (2021) found single daily flux measurement at 10:00 although produced the smallest bias on average among other times of day, it still led to a potential underestimation of -29% and overestimation of +35%. At present, diurnal variability of N_2O flux is not considered in common prediction models such as DNDC and DAYCENT (Cai et al., 2003; Del Grosso et al., 2012) or manual measurements by static chambers (Pavelka et al., 2018). The potential uncertainty in N_2O emission estimates caused by the overlooking of diurnal variations in N_2O flux could hinder the development of mitigation strategies and land management practices (Lammirato et al., 2018; Venterea et al., 2012). Additionally, collections of diurnal N_2O flux data could provide information for the improvement of existing process-based models.

3.5.2 Diurnal patterns of N_2O flux

Over the experimental period, N_2O fluxes exhibited daytime peaking diurnal patterns in about 61% of the days. This agrees with the findings of Wu et al. (2021), where 286 days of diurnal N_2O flux data from 46 published studies were classified into three diurnal pattern categories (i.e., daytime peaking, night-time peaking and non-diurnal) and found daytime

peaking patterns in ~60% of the diurnal datasets. The similarity in the proportions of daytime peaking patterns in this experiment and those of the global dataset in Wu et al. (2021) (Chapter 2) suggests that diurnal patterns of soil N_2O flux may not be spatially driven. This is further supported by the study by Alves et al. (2012b), which found similar diurnal patterns of N_2O flux (daytime peaking) in two geographically distinct field sites (Edinburgh, UK and Seropédica, Brazil). The proportions of night-time peaking and non-diurnal patterns in this experiment were lower (~9%) and higher (~30%), respectively, than the reported proportions of ~20% by Wu et al. (2021) (Chapter 2). This discrepancy could be explained by the drainage property of the study soil (fine silt). Silt is classified as an imperfectly drained soil according to Groenendyk et al. (Groenendyk et al., 2015); and imperfectly drained soils were reported to have a lower proportion of night-time peaking patterns (~13%) and a higher proportion of non-diurnal patterns (~26%) in the results of the study by Wu et al. (2021). Non-diurnal events including fertilisation and rainfall have been shown to obscure the daytime peaking patterns and give rise to non-diurnal patterns of N_2O flux in previous studies (Clar and Anex, 2020; van der Weerden, Clough and Styles, 2013; Kostyanovsky et al., 2019). This is owing to the rapid increases in soil N availability and VWC, which stimulate soil N_2O production within hours and trigger pulse emissions of N_2O (Fuß et al., 2011; Geng et al., 2017). Pulse emissions of N_2O are episodic and have been observed to last for more than 24 hours (Ball, Crichton and Horgan, 2008) and could override any diurnal effect by PAR and soil temperature (van der Weerden, Clough and Styles, 2013). Despite the inconsistency in diurnal patterns, daytime peaking patterns of N_2O flux were still common occurrences during the experiment, with diurnal N_2O fluxes most likely to peak between 12:00 and 16:00, as shown by the distribution of normalised N_2O fluxes at the 14:00 bin (over 50% at > 0.6) in Figure 3.4c.

3.5.3 Potential drivers of diurnal N_2O flux

The significant positive relationships of mean N_2O flux and ln(N_2O flux) with mean VWC in the correlation matrix (Table 3.2) and linear mixed-effects models (Table 3.3) indicate that VWC is the dominant driver of diurnal N_2O fluxes out of the abiotic and biotic variables measured. This agrees with the findings of various studies, where a strong positive effect of soil moisture on N_2O flux is reported (Butterbach-Bahl et al., 2013; Davidson and Verchot, 2000; Schindlbacher, Zechmeister-Boltenstern and Butterbach-Bahl, 2004). Soil VWC,

which controls soil water-filled pore space, has been shown to govern soil aeration by limiting gas diffusion from the atmosphere into the soil profile, and subsequently stimulate N_2O production in soils through O_2 depletion (Balaine et al., 2013; van der Weerden, Kelliher and Klein, 2012). Studies have also shown that even under drier conditions (water-filled pore space at 30 – 70%), N_2O production can still take place due to nitrifier denitrification (Bracken et al., 2021; van Haren et al., 2005). Nevertheless, diurnal N_2O fluxes showed a majority of daytime peaking patterns throughout the experiment, whereas VWC only oscillated diurnally during the initial irrigation period (26 July to 8 August). Therefore, VWC was unlikely the predominant contributor of the occurrences of daytime peaking of N_2O flux.

Contrary to the typical attribution of soil temperature as the main driver of diurnal variations in N_2O flux in a multitude of literature (Blackmer, Robbins and Bremner, 1982; Hosono et al., 2006; Liang et al., 2018; Scheer et al., 2014; van der Weerden, Kelliher and Klein, 2012; Williams, Ineson and Coward, 1999), mean soil temperature showed weak correlations ($r < 0.1$) with mean N_2O flux and no significance ($p > 0.05$) with ln(N_2O flux) in the correlation matrix. Similarly, mean soil temperature was not considered a significant predictor ($p = 0.113$) in its linear mixed-effects model (i.e., soil temperature model), which also showed the highest AIC and marginal R^2 compared to the other two models. This indicates the model had the lowest goodness of fit to the observed data and explained the least data variance. A congregation of observed ln(N_2O flux) at around 15 °C in the fixed-effect plot (Figure 3.5b) further illustrates the lack of a strong relationship between diurnal N_2O flux and soil temperature. Although laboratory studies have demonstrated N_2O production to have a temperature sensitivity (Q_{10}) of around 2.0 (Castaldi, 2000; Phillips et al., 2015a), which in theory should account for at least some part of the diurnal variations in N_2O flux, our results showed that the explanatory strength of soil temperature in this experiment was not sufficient to be considered significant. Studies have shown that the majority of N_2O emissions (> 60%) originate from 0 – 20 cm soil depth (Shcherbak and Robertson, 2019; Toma et al., 2011; Zuo et al., 2022). The observations of > 100% diurnal variations in N_2O flux in 87% of the measurement days with prevalent daytime peaking patterns, where the diurnal differences in soil temperature at 10 cm never exceeded 10 °C, suggest that diurnal variations in N_2O flux were not strongly controlled by soil temperature

at 10 cm or below. Diurnal variations in soil temperature near soil surface (0 – 9 cm) or other diurnal factors such as photosynthetic parameters might regulate the occurrence of daytime peaking of N_2O flux.

Compared to mean soil temperature, both mean PAR and GPP showed more positive ($r > 0.1$) and significant relationships ($p < 0.05$) with mean N_2O flux and ln(N_2O flux) in the correlation matrix. Both the PAR model and the GPP models had lower values of AIC (327.6 and 296.4, respectively) and higher values of marginal R^2 (0.132 and 0.122, respectively) than the soil temperature model, indicating a better model fit. However, mean PAR was not considered a significant predictor in its linear mixed-effects model, whereas mean GPP was. This hints that GPP was a stronger driver of diurnal N_2O fluxes than PAR and soil temperature, possibly due to its influences on the microbial N_2O production mechanisms in soils. As labile C is more available in the rhizosphere, the bacterial community therein is typically copiotrophic and fast-growing (Dennis, Miller and Hirsch, 2010; Ridl et al., 2016; Uksa et al., 2015). A study by Okubo et al. (2016) showed that *Brassicaceae* plants exude on average 7.7 mg g^{-1} root of sugars despite being non-mycorrhizal. Additionally, studies have shown that the chemical compositions of the root exudates vary with plant species (Jones, Hodge and Kuzyakov, 2004; Nguyen, 2009; O'Brien et al., 2018), which might shape the structure of the microbial community in the rhizosphere. For example, in oilseed rape, the bacterial community of its rhizosphere is dominated by the *Xanthomonas*, *Rhizobium*, *Pseudomonas* and *Flavobacterium* genera (de Campos et al., 2013), which all contain heterotrophic aerobic and/or anaerobic denitrifying species (Abdelhamed et al., 2021; Chèneby et al., 2000; Pishgar et al., 2019). Therefore, soil N_2O production could likely follow the diurnal rhythms of root exudation, which lags several hours behind photosynthesis in herbaceous plants (Bahn et al., 2009; Makita, Kosugi and Kamakura, 2014), of the oilseed rape plants in this study.

However, while some studies found > 60% of the variances in N_2O flux were explained by PAR or GPP (Keane et al., 2018; Zona et al., 2013), in this experiment, GPP along with VWC only explained ~12% of the variance in N_2O flux (Table 3.3). Instead, > 50% of the variances in N_2O flux were explained by day-to-day variations in N_2O flux magnitude, as indicated by the differences between conditional R^2 and marginal R^2 in the three linear mixed-effects models (date was set as a random factor). This was likely caused by the changes in soil N

substrate content from the multiple fertilisation events, which is a dominant driver of soil N_2O production (Firestone and Davidson, 1989). Still, our results suggest that GPP could play a role in regulating the diurnal variations in N_2O flux, and the inclusion of GPP in processed-based prediction models of N_2O emission such as DNDC and DayCent (GPP is not included as an input component at present (Del Grosso et al., 2012; Li et al., 2006)) could help produce more accurate estimations. However, more direct evidence of the positive influences on plant productivity on diurnal N_2O flux is needed to justify the inclusion, which will require dissociating photosynthetic parameters from other diurnal covariables such as soil temperature that could also regulate N_2O flux. Effort to diminish diurnal fluctuations of soil temperature from day and night cycles has been proven challenging, even in controlled laboratory conditions (Das et al., 2012). Future studies could apply soil warming and/or plant shading treatments in mesocosm experimental set-up such as one in this study to deviate the diurnal amplitudes of soil temperature and PAR/GPP in order to separate the effects of both variables.

3.6 Conclusion

In this study, we investigated the importance of considering diurnal variations in N_2O flux in N_2O emission calculations and explored several potential drivers of diurnal N_2O flux. Through the use of an automated chamber measurement system, large diurnal variations in N_2O flux were observed. Our results show that single-daily measurements at 10:00 could estimate total N_2O emission with an acceptable bias, but any measurement intervals beyond once-a-day will risk large over- or underestimations owing to the large day-to-day variations in N_2O flux, which accounted for a large portion of temporal variances of N_2O flux. Distinctive daytime peaking diurnal patterns of N_2O flux were observed on most days of the experiment, but variations in diurnal patterns were also observed. They were likely caused by non-diurnal factors such as rainfall. Of the measured environmental variables, VWC was the strongest driver of N_2O flux, followed by GPP and then PAR. However, correlation matrix and linear mixed-effects model results showed no significant relationship between N_2O flux and soil temperature, contrasting typical literature ascriptions. Further investigation of the separated effects of plant productivity and soil temperature could help understand the underpinning mechanisms driving diurnal variations in N_2O flux.

4. Effects of soil warming and plant shading on the diurnal variability of nitrous oxide emissions

4.1 Abstract

Diurnal variations in soil nitrous oxide (N_2O) flux have been shown to correlate with soil temperature as well as other photosynthetic parameters; however, the mechanistic basis of their relationships has not been established. This study aimed to explore the effects of a photosynthetic parameter (solar radiation) and soil temperature on the diurnal amplitude and peak timing of N_2O flux.

A field mesocosm experiment was conducted with plant shading and soil warming treatments applied over a series of 3-day interventions, along with the sub-daily measurements of N_2O flux and subsidiary variables. The results showed that during treatment periods, plant shading significantly reduced ($p = 0.042$) the diurnal amplitude of N_2O flux by 34%, whereas soil warming did not affect the diurnal amplitude of N_2O flux. Daytime peaking of diurnal N_2O fluxes was common (54% to 63%) but not consistent across treatments. Under no plant shading and soil warming, the diurnal peaks of N_2O flux tended to occur in late afternoon (16:00 – 19:59), accounting for 39% of the occurrences. Plant shading altered the peak timing of diurnal N_2O flux by significantly reducing (15%, adjusted residuals = -2.29) the diurnal peak occurrences in late afternoon (16:00 – 19:59) and significantly increasing (19%, adjusted residuals = 1.97) the diurnal peak occurrences at night (20:00 – 23:59). Further analyses revealed that daily cumulative solar radiation had a significant positive effect ($p = 0.018$), whilst daily cumulative net ecosystem production had a significant negative effect ($p = 0.001$) on the diurnal amplitude of N_2O flux.

The findings of this experiment alluded to the diurnal controls of plant-mediated metabolisms in soils on the diurnal amplitude and pattern of N_2O flux, which might be linked to photosynthesis. However, it is still unclear how soil biochemical properties (e.g., labile C and inorganic N content, soil O_2 concentration) change over diurnal courses and how photosynthesis-related mechanisms lead to such changes since daily cumulative solar radiation and net ecosystem production (NEP) explained little of the variance in diurnal amplitude of N_2O flux.

4.2 Introduction

Diurnal variability of nitrous oxide (N_2O) flux from soils has been widely observed, with some studies reporting diurnal variations in N_2O flux of up to 10-fold (Christensen, 1983; Dobbie and Smith, 2003; Maljanen et al., 2002; Scheer et al., 2012; Shurpali et al., 2016; Williams, Ineson and Coward, 1999). This could impede the accuracy of N_2O emission estimates if diurnal variability of N_2O flux is not considered. Past observations of diurnal variations of N_2O flux have mostly been attributed to the diurnal oscillation of soil temperature due to the observations of a consistent pattern of daytime peaking of N_2O flux, which is concurrent with soil temperature (Blackmer, Robbins and Bremner, 1982; Scheer et al., 2012; van der Weerden, Clough and Styles, 2013; Williams, Ineson and Coward, 1999). This has subsequently led to the recommendation of taking single-daily measurements of N_2O flux in mid-morning (ca. 10:00 h) to obtain the daily average N_2O flux rate, since it is also when soil temperature is at its daily average in most cases (Charteris et al., 2020; De Klein and Harvey, 2015). However, the magnitude of diurnal soil N_2O emissions (Christensen, 1983; Dobbie and Smith, 2003; Maljanen et al., 2002; Scheer et al., 2012; Shurpali et al., 2016; Williams, Ineson and Coward, 1999) far exceed what can be explained by the expected temperature sensitivity (Q_{10}) of 2 – 4 for N_2O production (Ding, Sun and Huang, 2019; Myrstener, Jonsson and Bergström, 2016; Phillips et al., 2015a; Vicca et al., 2009), suggesting other factors may also interact to drive the phenomenon. In addition, some studies have observed night-time peaking patterns of N_2O flux that is out-of-phase with soil temperature (Keane et al., 2019; Scheer et al., 2012; Shurpali et al., 2016; Zona et al., 2013), which suggests other diurnal variables may govern the peaking timing of N_2O flux. While some factors such as mineral nitrogen (N) availability and soil moisture have a strong influence on N_2O production these factors do not show diurnal trends (Papastylianou, 1995; Roxy, Sumithranand and Renuka, 2010), and therefore, are unlikely to regulate the diurnal patterns of N_2O flux.

Some studies have instead suggested plant photosynthetic activity as a controlling factor of the diurnal variability of N_2O flux. Christensen (1983) observed daytime peaking of N_2O flux and found days with high diurnal variability in N_2O flux coincided with days with high solar radiation. Keane et al. (2018) also found diurnal peaks of N_2O flux preceding those of soil temperature and a stronger coupling between N_2O flux and photosynthetic parameters including photosynthetically active radiation (PAR) and net ecosystem production (NEP).

Other studies have found positive correlations between N_2O flux and gross primary productivity (Shurpali et al., 2016; Zona et al., 2013). These findings hint at the positive effect of plant productivity on N_2O flux. Plants have been shown to exude up to a third of the daily photosynthetically fixed C in the form of root exudates (Badri and Vivanco, 2009; Chabbi and Rumpel, 2009; Kaiser et al., 2015), which could subsequently stimulate N_2O production in the rhizosphere by providing labile C sources (Bahn et al., 2009; Koo et al., 2005; van Hees et al., 2005) to heterotrophic respiration and denitrification (Azam et al., 2002; Wang et al., 2005), as more than 60% of the total N_2O emissions has been observed to originate from the rhizosphere (Xing et al., 2021). Root exudation of C is often proxied by microbial respiration in the rhizosphere due to the rapid rhizomicrobial respiration of exuded C (Hill et al., 2007; Kuzyakov and Gavrichkova, 2010). While plants can exude up to 40% of their photosynthetically fixed C into the rhizosphere (Canarini et al., 2019; Kuzyakov and Domanski, 2000), the chemical compositions of root exudates are known to vary with plant species which can subsequently impact the soil microbial communities including those of nitrifiers and denitrifiers (Li et al., 2017; Ruiz-Rueda, Hallin and Bañeras, 2009; Zhou et al., 2020). Glucosinolates are a group organic compounds typically found in the root exudates of *Brassicaceae* plants, which have antifungal and antibacterial properties (Aires et al., 2009; Mithen, Lewis and Fenwick, 1986; Tierens et al., 2001), and have been suggested to explain *Brassicaceae* plants' inability to form arbuscular mycorrhizae (Roberts and Anderson, 2001; Vierheilig et al., 2000). A study by Bressen (2009) found that root exudation of glucosinolates significantly impacted the structure and composition of the soil fungal communities and two bacterial families (*alphaproteobacterial* and *Rhizobiaceae*). This might shift the rhizomicrobial communities of *Brassicaceae* plants towards glucosinolates-tolerant fungal and bacterial species, such as N-fixing *Azorhizobium caulinodan*s (Gough et al., 1997; O'Callaghan et al., 2000), bacterial denitrifying *Bacillus subtilis* (Brabban and Edwards, 1995) and ectomycorrhizal denitrifying *Paxillus involutus* (Dąbrowska et al., 2021; Prendergast-Miller, Baggs and Johnson, 2011; Zeng, Mallik and Setliff, 2003).

Diurnal oscillations of rhizosphere respiration was demonstrated in a pulse-labelling experiment by Kuzyakov and Cheng (2001), suggesting similar diurnal oscillations of root exudation. This further alludes to the regulatory effects of plant productivity on the diurnal variations of N_2O flux. However, the effects of plant productivity on diurnal N_2O flux are

still unclear. A close diurnal coupling between net primary production and soil N uptake was demonstrated in a study (Riley, Zhu and Tang, 2018), which suggests the diurnal oscillation of plant productivity could instead dampen the diurnal amplitude of N_2O flux due to the increased N uptake by plant roots during photoperiods and subsequently reductions in N substrate availability for N_2O production. This is supported by the study by Schützenmeister et al. (2020), who demonstrated reduced cumulative N_2O emissions and diurnal amplitude of N_2O flux from planted mesocosms under light conditions compared to dark conditions. On the other hand, experimental evidence has also brought the effects of plant productivity on diurnal N_2O flux into question. Das et al. (2012) observed similar diurnal patterns of N_2O flux in both grass-grown and bare soil, and suggested the potential effects of PAR cycle leading to root exudation did not cause the diurnal variations of N_2O flux; instead, the observed diurnal variations in N_2O flux were attributed to the fluctuations of soil temperature caused by the heat from the light sources. At present, the effects of photosynthesis on the diurnal variations and patterns of soil N_2O flux are still poorly understood. Although recent studies have considered and investigated the relationship of soil N_2O flux with PAR and NEP (Keane et al., 2018; Shurpali et al., 2016; Zona et al., 2013), direct evidence indicating the sole effects of photosynthetic parameters (e.g. PAR, solar radiation, NEP, and etc.) on the diurnal amplitudes and peak timing of N_2O flux is still lacking. This is partly because photosynthetic parameters and soil temperature often covary on a diurnal scale. Even in a controlled laboratory environment, decoupling photosynthetic parameters and soil temperature remains a challenge (Das et al., 2012).

Building on the observations of diurnal N_2O fluxes made in Chapter 3, this experiment aimed to answer the research questions below:

1. Do plant shading and soil warming, individually or in combination, affect the magnitude and peak timing of diurnal variations in N_2O flux?
2. Can environmental and biological variables explain the magnitude of diurnal variations in N_2O flux?

It was hypothesised that mesocosms receiving soil warming would exhibit significant increases in diurnal amplitudes (i.e., magnitude of diurnal variations) of N_2O flux and daily cumulative N_2O emissions, compared to those without soil warming, whereas mesocosms receiving plant shading would exhibit significant reductions in diurnal amplitudes of N_2O flux and daily cumulative N_2O emissions, compared to those without plant shading. In

addition, it was hypothesised that daily average soil VWC, daily average soil temperature, daily cumulative solar radiation and daily cumulative NEP would show significantly positive relationships with diurnal amplitudes of N_2O flux in all mesocosms.

To address the research questions and hypotheses above, the field mesocosm experimental design in Chapter 3 was adapted and modified to test the contribution and interaction of soil temperature and solar radiation on diurnal N_2O flux. Different magnitudes of diurnal variations in soil temperature and photosynthetic parameters were created during treatment application periods, allowing the investigation of the separate effects of soil temperature and photosynthetic parameters on the diurnal variations and patterns of soil N_2O flux. In this experiment, environmental variables including soil temperature and solar radiation and soil volumetric water content (VWC) were collected at sub-daily frequencies. Details of the experimental set-up are elaborated in Section 4.3.

4.3 Methods

4.3.1 Experimental design and site description

To investigate the effects of plant shading and soil warming on diurnal soil N_2O fluxes, a factorial experiment was conducted with 20 field-situated mesocosms planted with forage rape (*Brassica napus* L.). Treatments of plant shading and soil warming were repeatedly imposed on a campaign basis of 3 consecutive days during the experiment. The experiment was conducted between 6 Aug and 25 Sept 2019, with seven periods of treatment application, at Hazelrigg Field Station, Lancaster, UK (54°1'N, 2°46'W). Table 4.1 lists the dates of events which took place during the experiment. Measurements of N_2O and CO_2 fluxes were made with an automated chamber system.

Table 4.1. Chronological sequence of events of and before the experiment and their dates.

Events	Dates
Mesocosm soil repacking	10 Jun – 14 Jun
Crop seeds sowing	10 Jul
Seedlings thinning	23 Jul
Start of experiment	6 Aug
First fertilisation	6 Aug
Treatment period 1	6 Aug – 8 Aug
Treatment period 2	13 Aug – 15 Aug
Second fertilisation	20 Aug
Treatment period 3	20 Aug – 22 Aug
Treatment period 4	24 Aug – 26 Aug
Treatment period 5	31 Aug – 2 Sept
Third fertilisation	2 Sept
Treatment period 6	5 Sept – 7 Sept
Treatment period 7	13 Sept – 15 Sept
End of experiment	25 Sept

The soil used in this experiment was from an arable field planted with *Brassica napus* where strong diurnal patterns of N_2O flux were reported (Keane et al., 2018). The soil had a texture of fine silt with a bulk density (0 – 10 cm depth) of 1.08 ± 0.01 g cm^{-3} (mean ± standard error) and pH of 8.36 ± 0.02 (mean ± standard error). Each mesocosm (of 20) comprised a bottom-draining cylindrical pot (inner diameter: 40 cm, height: 38 cm) and were sunken into the ground of the grassland field on a transect along the north-south axis. The soil used was previously grown with forage rape and received a total of 240 kg N ha^{-1} ammonium nitrate (NH_4NO_3) in another mesocosm experiment conducted in 2018 (Chapter 3). The soil was homogenised by mixing and repacking into the pots two months prior to the start of the experiment (10 – 14 Jun).

One month prior to the experiment (10 Jul 2019), forage rape seeds (*Brassica napus* L. "Interval", LG Seeds, Lincoln, UK) were sown in the mesocosms at a rate of approximately 20 seeds per mesocosm. Plants were subsequently thinned to four individuals per mesocosm at their leaf development stage (AHDB, 2021) to mimic the crop density in agricultural practice (LG Seeds, 2019). Over the duration of the experiment (6 Aug to 25 Sept 2019), the crop developed from the leaf development stage to the stem elongation stage (AHDB, 2021).

4.3.2 Fertilisation and Treatment applications

All mesocosms received three basal applications of NH_4NO_3 at a rate of 100 kg N ha^{-1} on 6 Aug, 19 Aug, and 2 Sept, as well as an application of phosphorus and potassium at a rate of 25 kg ha^{-1} on 6 Aug with ammonium dihydrogen phosphate ($NH_4H_2PO_4$) and potassium chloride (KCl), respectively, according to the recommended fertilisation practice for forage rape (LG Seeds, 2019).

During the experiment, intermittent treatments of soil warming and plant shading were implemented to mesocosms over seven treatment periods, each period lasting for three consecutive days (Table 4.1). Treatment periods were one to five days apart. Breaks between treatment applications were implemented to limit microbial acclimation to the increased soil temperature (Bradford, 2013). The experimental set-up during a treatment period is shown in Figure 4.1. The mesocosms were divided into four mesocosm groups, each receiving a combination of soil warming and plant shading during the treatment periods; the coding of the mesocosm groups and the respective treatments are listed in Table 4.2.

Soil warming cables in the soil warming groups (W and SW) were switched on from 10:00 to 16:00 during treatment periods with the aim to increase soil temperature to > 20 °C in daytime. During the repacking of the mesocosms, soil warming cables (50W Soil Warming Cable, BioGreen, Germany) were laid at 15 cm soil depth of the mesocosms of the soil warming groups (W and SW). Shading cages (top-open, 1.0 m (h) × 0.6 m (l) × 0.6 m (w)) made from polyvinyl chloride poles and polyethylene shade mesh (50% Shade Netting, True Products, UK) were installed around the plant shading groups (S and SW) over the duration of each treatment period. Outside the treatment periods, no plant shading or soil warming was applied to the mesocosms.

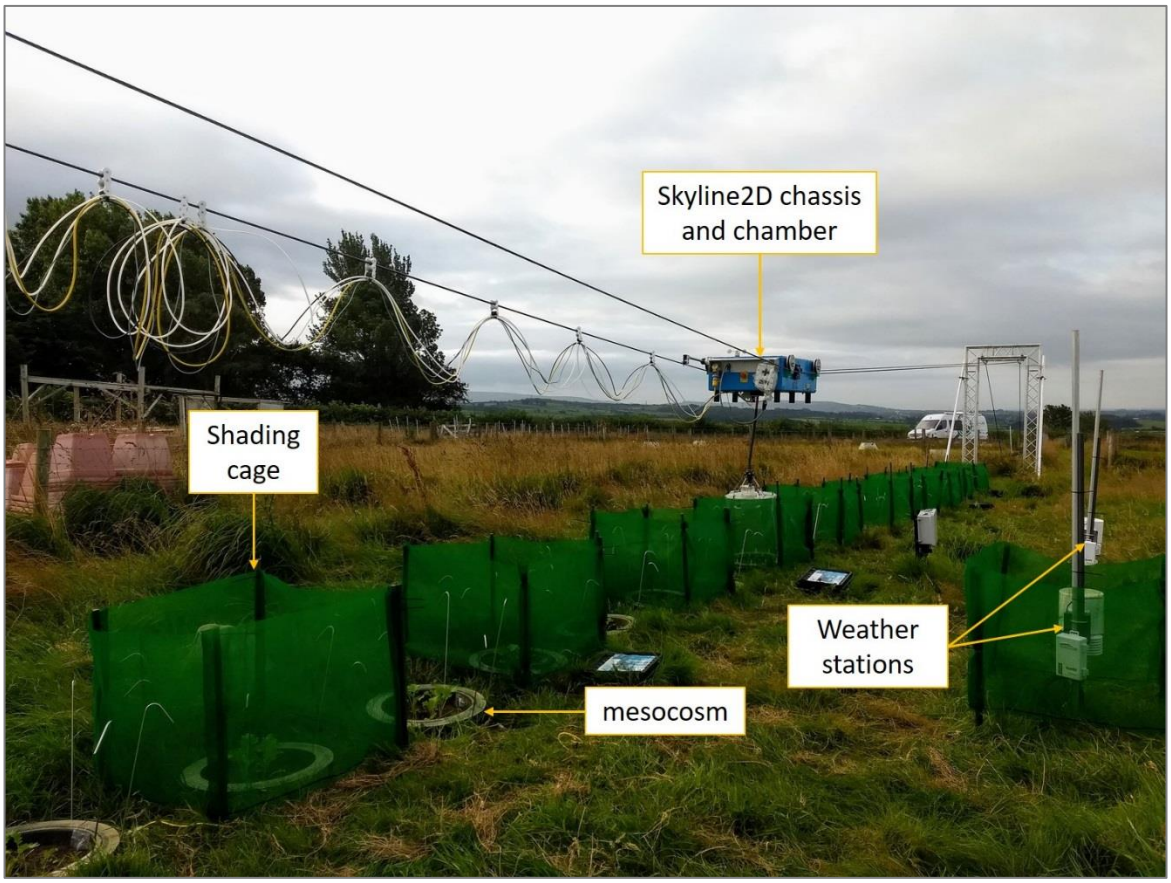

Figure 4.1. Photograph of the experimental set-up during treatment periods.

Table 4.2. Mesocosm group codes and their corresponding plant shading and soil warming treatment during the treatment periods in the experiment.

Mesocosm group codes	Treatments
CTRL	No plant shading or soil warming (i.e., control)
S	Plant shading only
W	Soil warming only
SW	Plant shading and soil warming

4.3.3 Measurements of N_2O flux, CO_2 flux and other environmental variables

An automated chamber system (Skyline2D, University of York, UK) equipped with a transparent, closed-dynamic (non-steady state) chamber was installed over the transect of the mesocosms to measure N_2O and CO_2 fluxes from the mesocosms at diurnal frequencies. The details of the set-up and the principle of the automated chamber system are specified in Chapter 3.3.1. The automated chamber measured the mesocosms on a sequenced cycle over the duration of the experiment. In a flux measurement, the chamber was hoisted down and formed an enclosure lasting for five minutes over the measured mesocosm. Readings of N_2O and CO_2 concentration inside the chamber during a chamber closure were recorded at

a frequency of ca. 1 Hz by a cavity ring-down spectrometer (Picarro G2508, Picarro Inc., Santa Clara, USA), and were later converted to flux rates during data processing. Soil temperature and VWC were measured at 10 cm soil depth (TDT SDI-12, Acclima Digital, USA) at one-minute intervals. Solar radiation was measured at one-minute intervals at 0.5 m above ground with a weather station (DWS Decagon Weather Station, Decagon Devices, USA) adjacent to the transect of the mesocosms. Solar radiation readings of shading treatment were taken with another weather station of the same model within a shading cage (Figure 4.1). The two weather stations were assessed before the experiment to produce statistically similar readings under the same weather conditions to avoid biases in solar radiation readings between instruments.

4.3.4 Data processing and analyses

All data processing, visualisation and statistical analyses were performed in R (version 3.6.1, The R Foundation) and Microsoft Excel (version 2110, Microsoft 365). Raw data from the cavity ring-down spectrometer were converted to N_2O and CO_2 fluxes using a flux calculation package 'flux' in R (Jurasinski et al., 2015). Quality control of N_2O and CO_2 fluxes was achieved by checking the R^2 value and the proportion of data points used for the linear regression fitting of each flux calculation. For N_2O, fluxes with an R^2 value < 0.1 and a data point proportion < 70% were considered as zero flux. For CO_2, fluxes with an R^2 value < 0.7 and a data point proportion < 40% were discarded. Since the automated chamber system was equipped with a clear chamber, the measured CO_2 fluxes thus represent the net ecosystem exchange rates of the mesocosms (Zhao et al., 2018). Net ecosystem production (NEP) rates were converted from measured CO_2 fluxes, since clear chamber measurements were made. Daily cumulative N_2O emissions, solar radiation, NEP of each mesocosm were calculated using the trapezoidal function with their respective diurnal measurements over every 24-hour period. The magnitude of diurnal variations in N_2O flux was defined as diurnal amplitude of N_2O flux, which was calculated by the subtraction of the daily maximum N_2O fluxes by the daily minimum N_2O fluxes of the corresponding date and mesocosm.

Addressing the first part of research question 1, linear mixed-effect modelling ('lme' function in R package 'nlme') was used to assess the marginal fixed effects of the daily average VWC, plant shading, soil warming and the interaction between plant shading and soil warming on the diurnal amplitudes of N_2O flux during treatment periods, with

mesocosm set as the random effects and experimental day as the autocorrelated covariate within each mesocosm. The inclusion of daily average VWC was to account for the variance in diurnal amplitude of N_2O flux caused by between-date variations in average VWC, which were independent to treatments and autocorrelation of experimental day in the random effects. To meet the assumption of linear mixed-effect modelling (i.e., normality in the model residuals), the diurnal amplitudes of N_2O flux were first log-transformed (natural) before modelling. To test whether the effects of treatments were consistent on the daily cumulative N_2O emissions, the same model formula was repeated but with log-transformed daily cumulative N_2O emission as the dependent variable.

To examine the treatment effects on the peak timing of diurnal N_2O fluxes, diurnal N_2O fluxes of each mesocosm during treatment periods were first binned into four-hourly bins based on the timing of the fluxes to allow statistical comparisons. The four-hourly bins included 02:00 (00:00 – 03:59), 06:00 (04:00 – 07:59), 10:00 (08:00 – 11:59), 14:00 (12:00 – 15:59), 18:00 (16:00 – 19:59), and 22:00 (20:00 – 23:59). Then, diurnal N_2O fluxes were averaged within each bin and normalised with the method stated in Chapter 2 (Equation 2.1), which remove the differences in flux magnitude among mesocosms and dates. Boxplots of normalised N_2O fluxes of the mesocosm groups were produced to visualise their overall diurnal patterns. Next, the differences in peak timing of N_2O flux in the mesocosm groups were assessed. This was achieved by counting the occurrences of daily maxima of N_2O flux in each four-hourly bin and compiling the data into a contingency table, followed by a chi-square test (CHISQ.TEST in Excel) of the observed values against the expected values of peak occurrence. As a post-hoc test, an expected frequency was calculated for every four-hourly bin in every treatment group (i.e., a cell in the contingency table) using the total of each row and column of the contingency table (Agresti, 2002). An adjusted residual (z score equivalent) in each mesocosm group in each four-hourly bin was then calculated by the comparison between the observed and the expected frequency for each cell. When the absolute value of the adjusted residual was > 1.96, it was considered as statistically significant (Sharpe, 2019).

Linear mixed-effects modelling was used to assess the effects of environmental (VWC, soil temperature and solar radiation) and biological (NEP) variables on the diurnal amplitude of N_2O flux. The fixed effects terms of the model included daily average VWC, daily average soil temperature, daily cumulative solar radiation and daily cumulative NEP, whereas the

random effect terms were mesocosm and the autocorrelation of experimental day within each mesocosm. Variance inflation factors (< 2.0) of the fixed effects terms were checked to ensure fixed effects terms were not collinear before the inclusion into the model. To understand the relative importance (effect size) of the fixed effects in the subsequent model, their partial eta squared (η_p^2) values were estimated with the F statistics of the fixed effects terms.

4.4 Results

The automated chamber system collected sub-daily N_2O fluxes at frequencies of approximately 9 – 11 per day from each mesocosm during the experiment. Eight days (9 – 11, 13, 14, 20 – 22 Aug) of the flux data were lost due to instrumental failures in the experiment. Throughout the experiment, N_2O fluxes ranged from -0.66 to 1.68 mg N_2O m^{-2} h^{-1}, as shown in Figure 4.2a. High N_2O fluxes (> 1.0 mg N_2O m^{-2} h^{-1}) were observed mostly after the second and third fertilisation event. High diurnal variability of N_2O fluxes was also observed, as the diurnal amplitudes of N_2O flux were large and variable during experiment, ranging from 10 to 8,349 µg m^{-2} h^{-1}. Soil VWC ranged between 16% and 48% during the experiment, with no clear diurnal trends (Figure 4.2b). Treatment applications effectively altered the diurnal amplitude of soil temperature and solar radiation during treatment periods (Figure 4.2c and 4.2d). During treatment periods, the warming treatment increased the daily maxima of soil temperature in the W and SW group to 21.6 – 25.8 °C (up to 50% increase), as opposed to those in the CTRL and S group which were 13.8 – 21.9 °C. The shading treatment, on the other hand, reduced the daily maxima of solar radiation by 0.04 – 0.81 kW m^{-2} (up to 79% reduction) in the S and SW group. Outside treatment periods, soil temperature and solar radiations between groups showed no significant differences.

4.4.1 Treatment effects of soil warming and plant shading on diurnal amplitude of N_2O flux and daily cumulative N_2O emission

The information of the linear mixed-effects models (Table 4.3) indicated that, during the treatment periods, only plant shading significantly reduced the log-transformed diurnal amplitude of N_2O flux by an estimated marginal mean of 0.42 ($F_{1,16}$ = 2.032, p = 0.042) but not the daily cumulative N_2O emission (Figure 4.3). This equated to a mean reduction of 34.3% in the actual diurnal amplitude of N_2O flux after the exponential conversion. Soil warming and the interaction between plant shading and soil warming did not result in significant effects on the diurnal amplitude of N_2O flux during the treatment periods (Table 4.3). Neither plant shading, soil warming nor the interaction between plant shading and soil warming had any significant effects (p > 0.05) on the daily cumulative N_2O emission (Table 4.3). The details of the model information are provided in Appendix II.

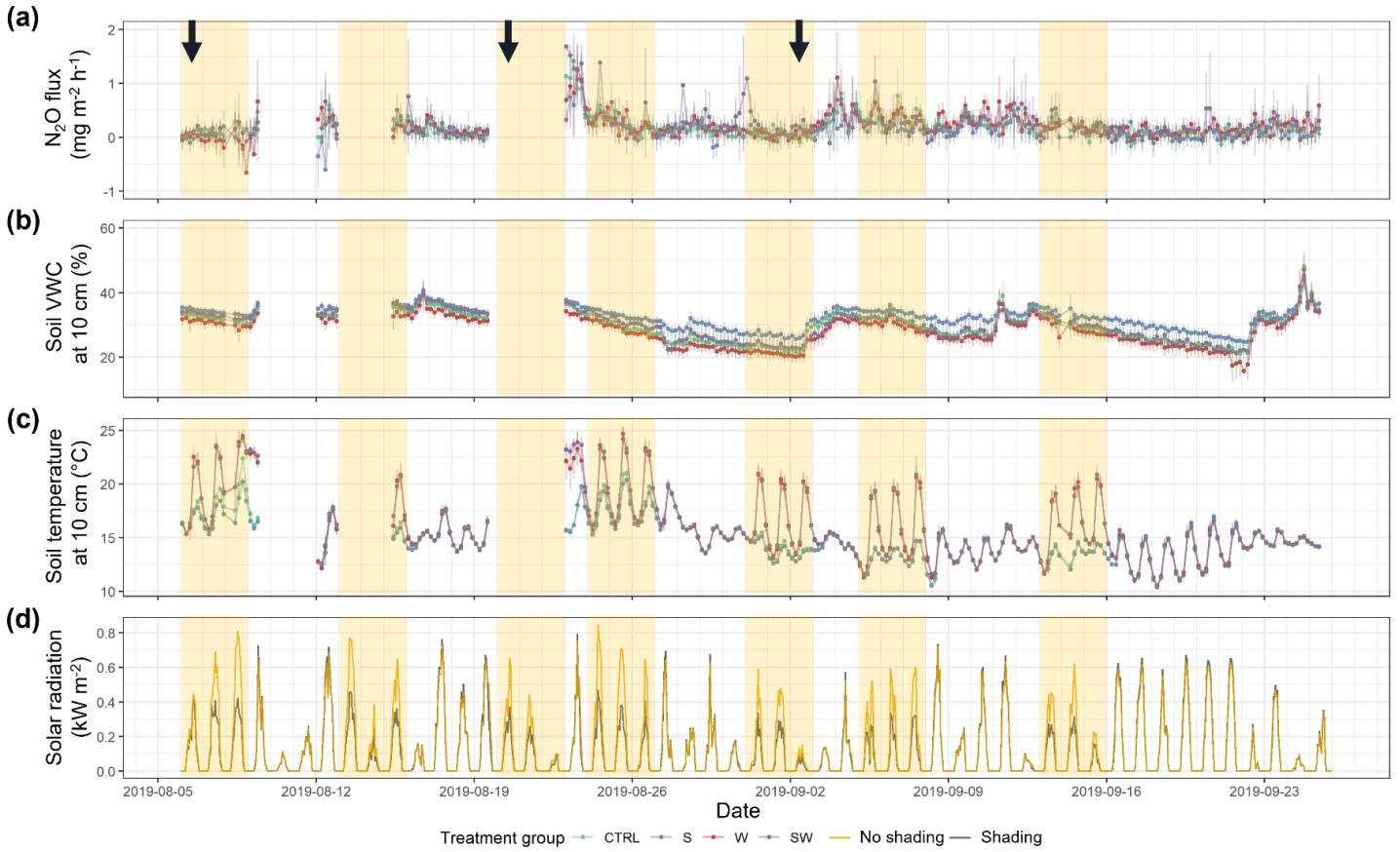

Figure 4.2. Timeseries of (a) N_2O flux, (b) soil volumetric content (VWC), (c) soil temperature and (d) solar radiation over the duration of the experiment. Dots and vertical lines in (a-c) represent the mean values and 95% confidence intervals of four-hourly bins. Mesocosm groups in (a-c) are indicated by different colours, whereas in (d) mesocosm groups without shading (CTRL, W) and with shading (S, SW) are represented by orange and blue, respectively. Black arrows indicate the fertilisation events. Light yellow bands indicate treatment application periods. Dates with missing points and broken lines in (a) to (c) indicate dates with instrument failure.

Table 4.3. Model information of the four linear mixed-effects models examining the treatment effects of plant shading, soil warming and the interaction between on the log-transformed diurnal amplitude of N_2O flux and daily cumulative N_2O emission, during and outside treatment periods. The syntaxes of the mixed models were: lme(fixed = ln(diurnal amplitude of N_2O flux) or ln(daily cumulative N_2O emission) ~ daily average VWC + plant shading + soil warming + plant shading:soil warming, random = ~1|mescosm, correlation = corAR1(form = ~experimental day|mesocosm), method = 'REML').

Log-transformed diurnal amplitude of N_2O flux during treatment periods					
Observations			290		
Marginal R^2 / Conditional R^2			0.081/0.081		
Predictors	*Estimate*	*DF*	*den DF*	*F*	*p-value*
(Intercept)	4.07	1	269	7082	**<0.001**
Daily average VWC	0.05	1	269	8.732	**<0.001**
Plant shading	-0.42	1	16	2.032	**0.042**
Soil warming	0.06	1	16	4.015	0.762
Plant shading:Soil warming	0.44	1	16	2.708	0.119
Log-transformed daily cumulative N_2O emission during treatment periods					
Observations			285		
Marginal R^2 / Conditional R^2			0.103/0.103		
Predictors	*Estimate*	*DF*	*den DF*	*F*	*p-value*
(Intercept)	5.70	1	264	12052	**<0.001**
Daily average VWC	0.07	1	264	18.030	**<0.001**
Plant shading	-0.36	1	16	0.506	0.100
Soil warming	-0.01	1	16	2.373	0.958
Plant shading:Soil warming	0.48	1	16	2.780	0.115

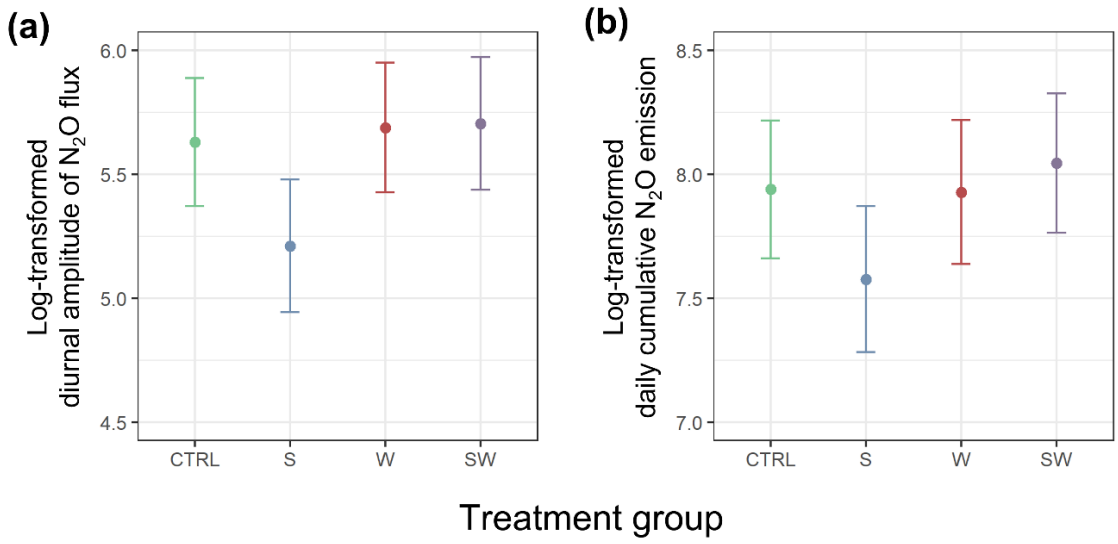

Figure 4.3. Estimated marginal means and 95% confidence intervals of (a) log-transformed diurnal amplitude of N_2O flux and (b) log-transformed daily cumulative N_2O emission of the four mesocosm groups (CTRL, S, W and SW) during treatment periods.

4.4.2 Treatment effects of soil warming and plant shading on peak timing of diurnal N_2O flux

All mesocosm groups showed primarily diurnal daytime of N_2O flux during treatment periods, with the diurnal peaks of N_2O flux predominantly in the four-hourly bins of 18:00 (i.e., 16:00 – 19:59) in the CTRL (38.5%) and the SW group (28.1%) and 14:00 (i.e., 12:00 – 15:59) in the S (29.2%) and the W group (32.3%, Figure 4.4, Table 4.4). Each mesocosm exhibited a single daily flux peak on most of the days during treatment periods, but the timing of the flux peak varied between days, which contributed to the seemingly secondary diurnal peak in the overall diurnal patterns (e.g., CTRL group at the 06:00 bin, Figure 4.4a). The chi-square test of the diurnal peak frequencies indicated there were significant differences ($p = 0.005$) between the observed frequencies the expected frequencies (calculated from the contingency table) of diurnal peaks in some of the treatment groups and some of the four-hourly bins. The results of the adjusted residuals (Table 4.4) showed that the CTRL group exhibited significantly higher diurnal peak frequency at the 18:00 bin (38.5%, adjusted residual = 2.81) than the expected peak frequency, whereas the S group exhibited significantly lower frequencies at the 06:00 bin (4.2%, adjusted residual = -2.24) and the 18:00 bin (15.3%, adjusted residual = -2.29), and a significantly higher frequency at the 22:00 bin (adjusted residual = 1.97) than the expected peak frequencies. The SW group also exhibited a significantly higher frequency (than expected) of diurnal peaks at the 10:00 bin (16.9%, adjusted residual = 2.50). On the other hand, diurnal peak frequencies of the W group were not significantly different to the expected frequencies at all four-hourly bins.

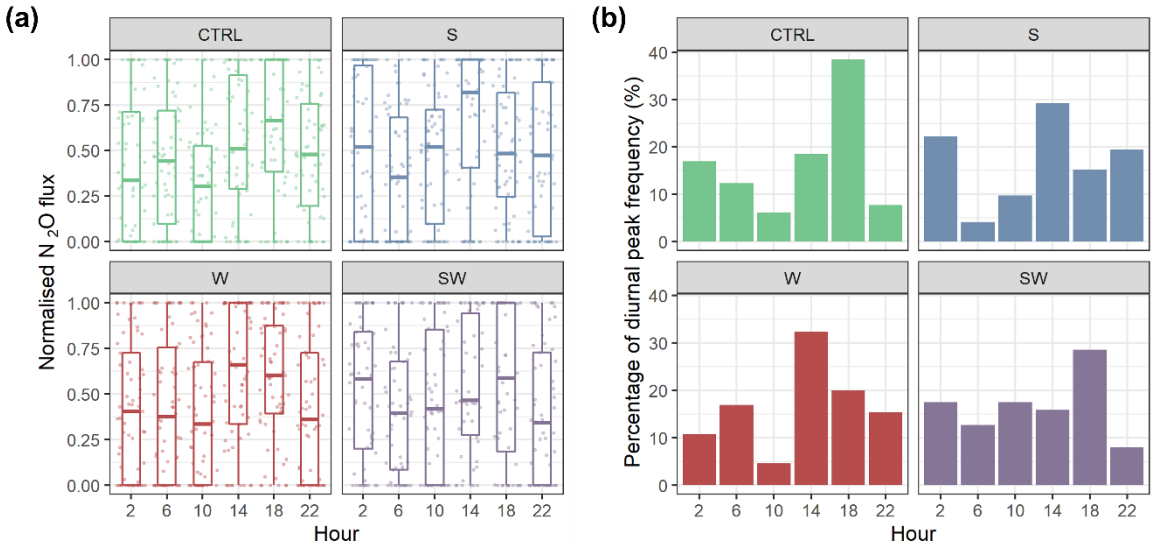

Figure 4.4. (a) Overall diurnal patterns of N_2O flux of the mesocosm groups and (b) percentage of diurnal N_2O flux peak frequency of the four-hourly bins during treatment periods.

Table 4.4. Contingency table for the chi-square test (p = 0.005) of independence of peak frequency of diurnal N_2O flux of the mesocosm groups at the six four-hourly bins. Values of expected frequency were calculated from the row total and column total of the contingency table. Absolute values of adjusted residuals are bolded when > 1.96, which denotes statistical significance between observed and expected frequency with a cell.

Four-hourly bins		**Mesocosm groups**				**Total frequency**
		CTRL	**S**	**W**	**SW**	
02:00	Observed frequency	11	16	7	11	45
	Frequency percentage	16.9%	22.2%	10.8%	17.5%	
	Expected frequency	11.0	12.2	11.0	10.7	
	Adjusted residual	-0.01	1.39	-1.54	0.12	
06:00	Observed frequency	8	3	11	8	30
	Frequency percentage	12.3%	4.2%	16.9%	12.3%	
	Expected frequency	7.4	8.2	7.4	7.1	
	Adjusted residual	0.29	**-2.24**	1.64	0.40	
10:00	Observed frequency	4	7	3	11	25
	Frequency percentage	6.2%	9.7%	4.6%	16.9%	
	Expected frequency	6.1	6.8	6.1	5.9	
	Adjusted residual	-1.04	0.10	-1.53	**2.50**	
14:00	Observed frequency	12	21	21	10	64
	Frequency percentage	18.5%	29.2%	32.3%	15.4%	
	Expected frequency	15.7	17.4	15.7	15.2	
	Adjusted residual	-1.23	1.17	1.77	-1.76	
18:00	Observed frequency	25	11	13	18	67
	Frequency percentage	38.5%	15.3%	20.0%	27.7%	
	Expected frequency	16.4	18.2	16.4	15.9	
	Adjusted residual	**2.81**	**-2.29**	-1.13	0.69	
22:00	Observed frequency	5	14	10	5	34
	Frequency percentage	7.7%	19.4%	15.4%	7.7%	
	Expected frequency	8.3	9.2	8.3	8.1	
	Adjusted residual	-1.43	**1.97**	0.71	-1.33	
Total frequency		65	72	65	63	265

4.4.3 Effects of environmental and biological variables on the diurnal amplitude of N_2O flux

All environmental and biological variables (daily average VWC, daily average soil temperature, daily cumulative solar radiation and daily cumulative NEP) had significant effects ($p < 0.05$) on the diurnal amplitude of N_2O flux (Table 4.5). The effects of daily average VWC (estimate = 0.05, $F_{1,266} = 8.722$, $p = 0.002$) and daily cumulative solar radiation (estimate = 0.10, $F_{1,266} = 3.265$, $p = 0.018$) were significantly positive (Figure 4.5b and 4.5d), whereas those of daily average soil temperature (estimate = -0.07, $F_{1,266} = 0.907$, $p = 0.026$) and daily cumulative NEP (estimate = -0.02, $F_{1,266} = 11.50$, $p = 0.001$) were significantly negative (Figure 4.5c and 4.5e). Comparatively, daily cumulative NEP had the largest effect size ($\eta_p^2 = 0.04$), followed by daily average VWC ($\eta_p^2 = 0.03$), daily cumulative solar radiation ($\eta_p^2 = 0.01$) and daily average soil temperature ($\eta_p^2 = 0.003$). However, the explanative power of the model was low to begin with (marginal $R^2 = 0.09$, conditional $R^2 = 0.132$)

Table 4.5. Model information of the linear mixed-effects model investigating the fixed effects of daily average VWC, daily average soil temperature, daily cumulative solar radiation, and daily cumulative NEP on the log-transformed diurnal amplitude of N_2O flux during the treatment periods. The syntax of the mixed model was: lme(fixed = ln(diurnal amplitude of N_2O flux) ~ daily average VWC + daily average soil temperature + daily cumulative solar radiation + daily cumulative NEP, random = ~1|mescosm, correlation = corAR1(form = ~experimental day|mesocosm), method = 'REML').

Log-transformed diurnal amplitude of N_2O flux throughout the experiment						
Observations			290			
Marginal R^2 / Conditional R^2			0.090/0.132			
Predictors	*Estimate*	*DF*	*den DF*	*F*	*p-value*	η_p^2
(Intercept)	4.81	1	266	4831	**<0.001**	-
Daily average VWC	0.05	1	266	8.722	**0.002**	0.03
Daily average soil temperature	-0.07	1	266	0.907	**0.026**	0.003
Daily cumulative solar radiation	0.10	1	266	3.265	**0.018**	0.01
Daily cumulative NEP	-0.02	1	266	11.50	**0.001**	0.04

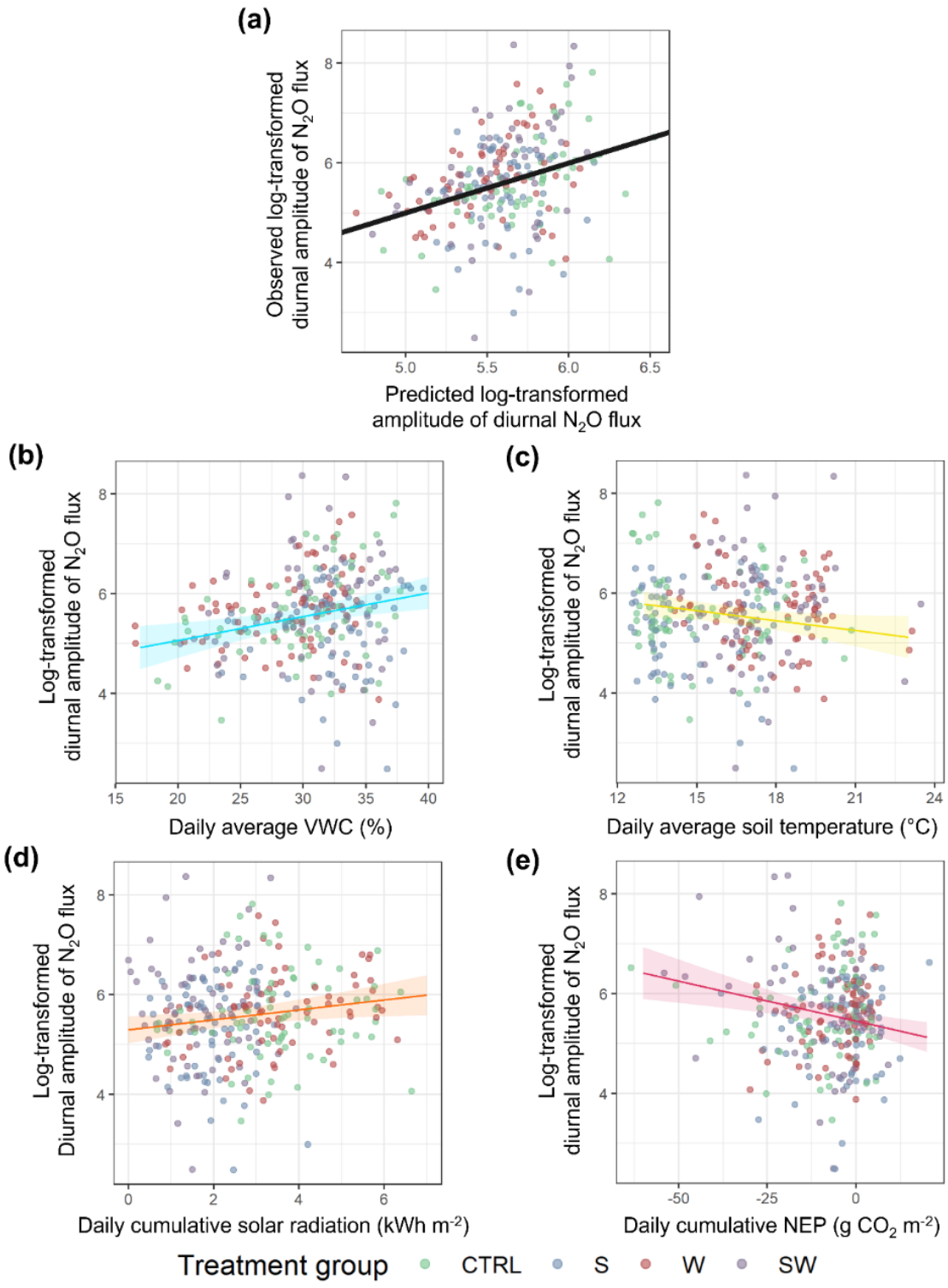

Figure 4.5. (a) Scatter plot of the observed log-transformed diurnal amplitude of N_2O flux against that predicted by the linear mixed-effects model, the black solid line indicates the one-to-one ratio. (b-e) Marginal fixed effects plots of (b) daily average VWC, (c) daily average soil temperature, (d) daily cumulative solar radiation, and (e) daily cumulative NEP on the log-transformed diurnal amplitude of N_2O flux. Coloured lines and ribbons in (b-e) indicate the marginal effects and its 95% confidence intervals of the respective fixed effects terms in the model, whereas dots indicate the observed log-transformed diurnal amplitudes of N_2O flux against the fixed-effects terms.

4.5 Discussion

In this experiment, the two commonly attributed diurnal environmental covariables of diurnal variations in N_2O flux (i.e., soil temperature and solar radiation) were dissociated by plant shading and soil warming treatments. Plant shading alone reduced the diurnal amplitude of N_2O flux, but not the daily cumulative N_2O flux, whereas both soil warming and the combined treatment of plant shading and soil warming did not affect the diurnal amplitude of N_2O flux and the daily cumulative N_2O flux.

All mesocosm groups exhibited overall daytime peaking patterns of normalised N_2O flux (Figure 4.4a), which were in line with the findings in Chapter 2 and 3, where normalised N_2O fluxes were found to peak in daytime most of the time (~60%). The overall diurnal patterns of each mesocosm group also largely resembled their distribution of diurnal flux peak frequencies at the four-hourly bins (Figure 4.4b). While the majority of diurnal peaks of N_2O flux occurred in daytime at the 14:00 and 18:00 four-hourly bins, diurnal peaks of N_2O flux still occurred at night-time up to 17% of the time (using CTRL group as reference in Table 4.4). The occurrence of night-time peaking of N_2O flux were also observed in past studies (Keane et al., 2019; Shurpali et al., 2016; Smith et al., 1998), which attributed it to several potential causes including increased rates of N_2O reduction ($N_2O \rightarrow N_2$) facilitated by increased supply of root-derived C to denitrifiers during daytime (Keane et al., 2019; Shurpali et al., 2016), and N_2O production being deeper in the soil, leading to longer time taken for N_2O to escape from the soil (Smith et al., 1998). Alternatively, rainfall events (non-diurnal) could also trigger the short-term burst of N_2O flux at anytime of day and interrupt any existing diurnal patterns of N_2O flux (van der Weerden, Clough and Styles, 2013).

4.5.1 Treatment effects on diurnal amplitude of N_2O flux and daily cumulative N_2O emission

During treatment periods, plant shading on average reduced the diurnal amplitude of N_2O flux by more than a third (estimate = -0.42, $F_{1,16}$ = 2.032, p = 0.042; Figure 4.3a, Table 4.3). It was likely that the impositions of plant shading suppressed the diurnal amplitude of N_2O flux during treatment periods. Current understanding of the mechanisms behind the effects of plant shading on N_2O emission is still lacking due to the limited literature on the topic. Only one study thus far has provided experimental evidence of significant reduction in the diurnal amplitude of N_2O flux and daily cumulative N_2O emission from soils cultivated with shaded soybean plants compared to those with non-shaded soybean plants (Yang and Cai, 2006). The inhibitive effects of plant shading on the diurnal amplitude of N_2O flux were

attributed to the reduction in soil respiration caused by reduced root exudation rates. It has been demonstrated that the absence of light substantially dampened the diurnal amplitudes of root-derived CO_2 efflux, which was mainly driven by root exudation of labile C (Kuzyakov and Cheng, 2001). Since heterotrophic denitrification is the major process responsible for N_2O production in soils (McLain and Martens, 2006), root exudation of photosynthetically-fixed C could fuel heterotrophic denitrifiers and govern soil N_2O production in the rhizosphere (Kuzyakov and Cheng, 2001; Kuzyakov and Gavrichkova, 2010; Yin et al., 2013), a hotspot for denitrifying activity (Smith and Tiedje, 1979). It is claimed that up to 40% of the photosynthetically fixed C can be released as root exudates (Badri and Vivanco, 2009; Chabbi and Rumpel, 2009; Gargallo-Garriga et al., 2018; Guyonnet et al., 2018; Kaiser et al., 2015; Shepherd and Davies, 1993), a reduction in photosynthesis by plant shading could lower the quantity of photosynthate C exuded into the rhizosphere, and subsequently reduce soil N_2O flux. While direct evidence of this mechanism has not be reported in literature, observations in studies provide rational evidence suggesting the possibility of such mechanism. A study by Ma et al. (2020) showed that under increased GPP, the magnitude and diurnal amplitude of soil respiration rate also increased, which could subsequent lead to an increase in the magnitude and diurnal amplitude of denitrification. A study by Dechassa and Schenk (2004) also observed significant increases in root exudation rate of organic anions by cabbage plants (*Brassica oleracea*) during photoperiods, with extremely low exudation rates of citrate, malate and succinate during darkness. This supports the reducing effect of plant shading on the diurnal amplitude of N_2O flux observed in this experiment. It is found that ectomycorrhizal fungi such as *Paxillus involutus* can receive up to 25% of the primary productivity of their host plants as symbionts (Hobbie, 2006), and further provide exuded C to bacterial denitrifiers within the mycorrhizosphere, subsequently stimulating N_2O production (Prendergast-Miller, Baggs and Johnson, 2011). A study has shown that, while root exudates of *Brassicaceae* plants, namely glucosinolates, are antimicrobial, the metabolites of glucosinolates can stimulate the hyphal growth of the denitrifying ectomycorrhizal fungus *Paxillus involutus* (Zeng, Mallik and Setliff, 2003).

However, in this experiment plant shading did not result in any significant difference in the daily cumulative N_2O emission (albeit $p = 0.100$). This suggests plant shading affected the diurnal dynamics of soil N_2O flux a larger extent but less so the quantity of N denitrified on

a daily timespan. Daily cumulative N_2O emissions were more likely governed by soil VWC ($p < 0.001$, Table 4.3), which regulates soil O_2 content (Balaine et al., 2013), and potentially the N substrate availability in the soil (Burton et al., 2008; Ruser et al., 2001).

On the contrary, soil warming did not have any significant effect on the diurnal amplitude of N_2O flux (estimate = 0.06, $F_{1,16}$ = 4.015, p = 0.762) or daily cumulative N_2O emission (estimate = 2.373, $F_{1,16}$ = -0.01, p = 0.958), despite expectations based on common ascription of diurnal variations in N_2O flux to soil temperature in various literature (Blackmer, Robbins and Bremner, 1982; Hosono et al., 2006; Liang et al., 2018; Scheer et al., 2014; van der Weerden, Clough and Styles, 2013; Williams, Ineson and Coward, 1999). This finding indicates diurnal fluctuations in soil temperature in this study contributes little to the diurnal amplitude of N_2O flux, despite findings in other studies suggest otherwise (Alves et al., 2012a; Blackmer, Robbins and Bremner, 1982; Scheer et al., 2014). The collinearity between photosynthetic parameters (e.g., PAR and solar radiation) could have led to the attributions of diurnal variations in N_2O flux to the soil temperature since many historical studies did not consider the relationship between N_2O flux and photosynthetic parameters (Alves et al., 2012a; Flessa et al., 2002; Laville et al., 2017; Lognoul et al., 2019). Interestingly, significant reduction in the diurnal amplitude of N_2O flux was not observed in the SW group (Figure 4.3a), which suggests the reducing effects of plant shading was somehow negated by soil warming, given soil warming alone did not stimulate higher diurnal amplitude of N_2O flux. It is unclear how soil warming prevents the changes in plant metabolisms belowground brought about by reduced photosynthesis. Investigating the diurnal variations in labile C content in planted soils subjected to plant shading and soil warming might reveal more information.

4.5.2 Treatment effects on peak timing of diurnal N_2O flux

In the CTRL group, the normalised N_2O fluxes peaked most frequently (38.5% of the measurements) between 16:00 and 20:00 (four-hourly 18:00 bin. This indicated the diurnal peaks of N_2O flux lagged behind solar radiation by a few hours (solar radiation usually peaked around mid-day) under natural environmental conditions. This time lag may be explained by the time spent on the translocation and exudation of photosynthetically-fixed C from plant roots, given the assimilation of C by photosynthesis and microbial respiration of exuded C are both rapid processes (Kuzyakov and Gavrichkova, 2010). Multiple studies have found the time lag between photosynthesis and soil efflux of photosynthate C to

range between one to 12 hours in agricultural crops (Dilkes, Jones and Farrar, 2004; Gavrichkova and Kuzyakov, 2010; Kuzyakov and Cheng, 2001; Kuzyakov and Domanski, 2002; Xu et al., 2008). However, the most common peaking timing of diurnal N_2O flux in the CTRL group (18:00 bin) in this experiment was later by a few hours than the peaking timing of diurnal N_2O flux found in Chapter 3 (in the 14:00 bin) and in another similar study with *Brassic napus* (12:00 – 14:00) (Keane et al., 2018). This may be caused by the different climatic scenarios between this experiment and the experiment in Chapter 3, as rainfall events were more frequent during this experiment. Yue et al. (2018) showed the diurnal peaks of soil respiration shifted from 13:00 to 17:00 after rainfall events, which could explain the occurrences of diurnal peaks of N_2O flux being in 16:00 – 19:59 in this study.

Compared to the expected frequencies of diurnal N_2O peaks of each four-hourly bin, plant shading significantly reduced the diurnal peak frequency at the 18:00 bin (adjusted residual = -2.29) and at the 06:00 bin (adjusted residual = -2.24) but significantly increased the diurnal peak frequency at the 22:00 bin (adjusted residual = 1.97) in the S group, and significantly increased the diurnal peak frequency at the 10:00 bin (adjusted residual = 2.50) in the SW group. Current understanding on the effects of plant shading on the diurnal patterns of N_2O flux as well as root exudation is limited. Two studies have demonstrated under dark conditions, the diurnal peak of root exudation was substantially dampened (Reichman and Parker, 2007; Zhao et al., 2021), whereas in the study by Bahn et al. (2009), shading was shown to delay the diurnal peak of root-derived C respiration by several hours. This might explain the increased variability of peak timing of N_2O flux via influencing the diurnal rhythm of root exudation of C. The increased diurnal peak frequency at the 22:00 bin may also be attributed to increased root respiration at night which might have outweighed the effects of daytime peaking root exudation pattern in the shaded mesocosms, since root respiration also consumes soil O_2 and in turn drives N_2O production. Increases in root respiration rates at night-time have been observed in several studies (Li et al., 2010, 2011; Makita et al., 2018). In the study by Li et al. (2011), night-time peaking of root respiration was observed separately from daytime peaking of soil microbial respiration, which was largely driven by root exudation and decomposition of C. This further suggests other components of rhizosphere respiration (e.g., root respiration) could contribute to the diurnal variability of N_2O flux.

The W group exhibited the highest frequency of diurnal peaks (32.3%) at the 14:00 bin instead of the 18:00 bin (Figure 4.4b), albeit the frequencies of diurnal peaks at all four-hourly bins are statistically similar to the expected frequencies. The shifting of the diurnal peaks might be the result of soil warming between 10:00 and 16:00 prompting higher microbial activity including denitrification (Phillips et al., 2015a; Lloyd and Taylor, 1994; Winkler, Cherry and Schlesinger, 1996) at the 14:00 bin (12:00 – 15:59) than at the 18:00 bin (16:00 – 19:59). It should also be noted that soil warming did not significantly increase the diurnal amplitude of N_2O flux, indicating the quantity of denitrification 'fuels' available for microbes such as inorganic N and labile C may not have been enhanced by soil warming. This was substantiated in a study which found no effect by daytime soil warming on the soil CO_2 efflux (Xia et al., 2009).

4.5.3 Effects of environmental and biological variables on diurnal amplitude of N_2O flux

All the investigated environmental and biological variables (i.e., daily average VWC, daily average soil temperature, daily cumulative solar radiation and daily cumulative NEP) were found to have significant effects ($0.001 \leq p \leq 0.026$) on the diurnal amplitude of N_2O flux (Table 4.5). However, the fixed effects variables in linear mixed-effects model explained only a small proportion of the variance in the diurnal amplitude of N_2O flux (marginal R^2 = 0.09), which suggests a large proportion of the variance were caused by other factors outside these variables. Other factors such as the changes in the soil N substrate content could have contributed to the variances in the diurnal amplitude of N_2O flux. During the experiment, high diurnal fluctuations of N_2O flux were often observed after the fertilisation events (Figure 4.2a), which would not have been explained by the investigated variables.

The positive marginal effects of daily average VWC on the diurnal amplitude of N_2O flux (estimate = 0.05, $p = 0.002$, $\eta_p^2 = 0.03$, Figure 4.5b) were in agreement with the findings of various studies (Dobbie and Smith, 2003; van Haren et al., 2005; Wang and Cai, 2008; Ussiri and Lal, 2013), where soil N_2O flux was found to increase with VWC or water filled pore space. It has been demonstrated in studies that soil moisture restricts O_2 supply from the atmosphere into the soil (Balaine et al., 2013) and increases the number of anaerobic microsites favourable for denitrification (Schindlbacher, Zechmeister-Boltenstern and Butterbach-Bahl, 2004). Microbial activity in general is also enhanced by increased soil moisture (Or et al., 2007). The increase in daily average VWC could in turn amplify the extent of diurnal variations of soil N_2O flux, as other soil O_2-consuming variables (e.g.,

microbial respiration of plant-exuded C and root respiration) oscillate diurnally (Makita et al., 2018).

On the contrary, daily average soil temperature had a negative marginal effect on the diurnal amplitude of N_2O flux in this experiment (estimate = -0.07, Figure 4.5c). However, although the effect was significant (p = 0.026), it was substantially smaller than the other investigated variables (η_p^2 = 0.003) by comparison. This finding was consistent with the lack of significant effects of soil warming on the diurnal amplitude of N_2O flux shown previously (Table 4.3) but contrasted the positive correlation between diurnal N_2O flux and soil temperature found in historical studies (Blackmer, Robbins and Bremner, 1982; Scheer et al., 2014; Skiba et al., 2013). The lack of a strong effect of soil temperature on the diurnal amplitude of N_2O flux may be due to other factors such as the aforementioned changing soil N content caused by fertilisation which could have overridden the diurnal effects of soil temperature (Francis Clar and Anex, 2019). On the contrary, the effect of daily cumulative solar radiation on the diurnal amplitude of N_2O flux were significantly positive but its effect size was also relatively small (estimate = 0.10, p = 0.018, η_p^2 = 0.01, Figure 4.5d). It has also been shown that solar radiation positively regulates the quantity of root exudates via the control of photosynthetic assimilation of C (Dechassa and Schenk, 2004; Nakayama and Tateno, 2018). The increase in quantity of root exudates could also amplifies the diurnal peaks of root exudation and subsequently diurnal amplitude.

Conversely, daily cumulative NEP had a significant negative effect (estimate = -0.02, p = 0.001, Figure 4.5e) on the diurnal amplitude of N_2O flux with the largest effect size (η_p^2 = 0.04) of all the variables. This confounds the positive effect of daily cumulative solar radiation discussed previously, as it was expected that daily cumulative NEP would be positively correlated with daily cumulative solar radiation and thus resulting in a positive effect. However, further examination revealed no significant correlations between the two variables (Appendix II). This might be because NEP is the result of gross primary productivity minus ecosystem respiration (Kirschbaum et al., 2001), the latter is positively affected by gross primary productivity due to increased exudation of photosynthetic-fixed C and the subsequent priming effect of soil organic C (Helal and Sauerbeck, 1986; Kuzyakov and Cheng, 2001; Larsen et al., 2007). Consequently, daily cumulative solar radiation may not represent daily cumulative NEP. The lower/more negative NEP suggests higher ecosystem respiration, which is a key indicator for soil microbial activities (Phillips and Nickerson, 2015)

including denitrification (Braker, Schwarz and Conrad, 2010; Phillips et al., 2015a) and heterotrophic respiration (Carey et al., 2016; Peterjohn et al., 1994). The former microbial process directly contributes to N_2O production in soil (Firestone and Davidson, 1989), whereas the latter indirectly promotes denitrifying activity by creating O_2-limiting conditions in soils (Butterbach-Bahl et al., 2013; Khalil, Mary and Renault, 2004). Ecosystem respiration has been shown to oscillate diurnally and is modulated by photosynthesis (Larsen et al., 2007; Tang, Baldocchi and Xu, 2005). Multiple studies have found strong diurnal couplings between soil N_2O flux and ecosystem respiration (Keane et al., 2019; Kostyanovsky et al., 2019; Šimek, Brůček and Hynšt, 2010), which could explain the negative effect of daily cumulative NEP on the diurnal amplitude of N_2O flux (Figure 4.5e). Whilst NEP could be partitioned into ecosystem respiration and gross primary production by proxy a temperature response function (Keane et al., 2019; Reichstein et al., 2005), it was not applicable in this experiment due to the soil warming treatment causing abnormal diurnal fluctuations of soil temperature.

4.6 Conclusion

This study investigated the effects of plant shading and soil warming on the diurnal dynamics of N_2O flux. Plant shading significantly reduced the diurnal amplitude of N_2O flux, as well as altered the peak frequencies of diurnal N_2O flux by significantly increasing the occurrences of diurnal peak at night (20:00 – 23:59) and significantly reducing those in late afternoon (16:00 – 19:59). These findings indicated plant-mediated effects brought about by photosynthetic activity could potentially regulate diurnal N_2O flux. Soil warming had little effects on the diurnal amplitude of N_2O flux, which was further supported by the very weak negative effects (albeit significant) of daily average soil temperature on the diurnal amplitude of N_2O flux. However, soil warming counteracted the reducing effect of plant shading on the diurnal amplitude of N_2O flux, suggesting the effects of soil warming might be circumstantial. Daily cumulative NEP had the strongest negative effect on the diurnal amplitude N_2O flux, which suggests diurnal amplitude of N_2O flux may be positively affected by ecosystem respiration.

The results of this experiment suggest that the diurnal amplitude of N_2O flux was partly influenced by photosynthetic parameters, possibly via their diurnal controls on root exudation of photosynthate C and/or the subsequent effects of diurnal variations in root-derived C content on soil respiration rate and soil O_2 concentration. On the other hand, soil

temperature did not show regulatory effects on the diurnal amplitude of N_2O flux under the field mesocosm conditions and crop species in this experiment. The field conditions also entailed temporal variability of other non-diurnal drivers of N_2O flux such as soil moisture, which could override the diurnal effects of photosynthetic parameters. To study the effects of photosynthetic activity on diurnal N_2O fluxes would require minimising the diurnal variations of other factors (e.g., soil moisture and temperature) in a controlled environment.

5. Plant-mediated effects of photosynthetically active radiation on diurnal variations in soil nitrous oxide flux

5.1 Abstract

It is known that nitrous oxide (N_2O) fluxes from soil exhibit high temporal variability, especially on a diurnal scale. Diurnal variations in N_2O flux have often been associated with the diurnal fluctuations of soil temperature but photosynthetic parameters such as photosynthetically active radiation (PAR) may also regulate diurnal variations in N_2O flux.

This study assessed the discrete effects of PAR on diurnal soil N_2O flux under controlled conditions which minimised fluctuations in soil temperature and soil moisture. Fifteen fertilised grassland mesocosms were established in a controlled-temperature environment with a 12-hour photoperiod. Mesocosms were split into three treatment groups (High PAR, Medium PAR and Low PAR) and underwent three experimental periods (in chronological order: pre-treatment at Medium PAR – 5 days, treatment PAR groups – 7 days and post-treatment – 5 days at Medium PAR). Diurnal N_2O fluxes were measured by semi-continuously to assess the effects of PAR on the diurnal dynamics (patterns, peak timing, and amplitude) of N_2O flux.

The results showed that when variations in temperature and soil moisture were minimised, daytime peaking patterns of N_2O flux were still prevalent across all PAR treatments and experimental periods. Compared to field observations, the diurnal patterns of N_2O flux in this experiment were more consistent. Reducing PAR level shifted the flux peak timing from late afternoon to early afternoon, while exposure to high PAR level significantly increased the diurnal amplitude of N_2O flux. Further analysis revealed a significant positive, albeit weak, relationship between cumulative net ecosystem production (NEP) during the photoperiod and standardised diurnal amplitude of N_2O flux ($p = 0.004$, adjusted $R^2 = 0.029$).

This experiment provides empirical evidence to support the hypothesis that plant metabolism, independent of temperature, is a driver of diurnal variations of N_2O flux and contributes to the occurrence of daytime peaking of N_2O flux. Future research investigating the variations in soil biochemical properties in response to the diurnal rhythm of photosynthesis could provide revealing information on the mechanisms behind diurnal variability of N_2O flux.

5.2 Introduction

Decades of extensive nitrogen (N) inputs into agricultural soils have contributed to increases in the atmospheric concentration of nitrous oxide (N_2O), a potent greenhouse gas and a catalyst for the destruction of stratospheric ozone (Ciais et al., 2013; Reay et al., 2012). Two biological processes, nitrification and denitrification, govern the majority of N_2O production in soils (Smith, 2017), by converting soil inorganic N directly and indirectly to N_2O via chains of biological reactions (Barnard, Leadley and Hungate, 2005; Butterbach-Bahl et al., 2013). The two processes are performed mainly by soil microbes and are regulated by environmental conditions such as soil oxygen (O_2) status and temperature (Firestone and Davidson, 1989). Additionally, both processes are fuelled by organic carbon (C) content, as most denitrifiers and some nitrifiers are heterotrophs (Castignetti and Hollocher, 1984; Liu et al., 2019; Zhang, Müller and Cai, 2015).

Accurate estimations of soil N_2O emissions are vital to the calculation of national N_2O inventories and the development of mitigation strategies. However, due to the high spatiotemporal variability of soil N_2O flux, current emission estimation methods such as manual chamber measurements and process-based prediction models produce estimates with high uncertainty (Lammirato et al., 2018; Stehfest and Bouwman, 2006). Part of the uncertainty is contributed by the diurnal variability of N_2O flux, which common manual N_2O flux sampling practices and prediction models do not address (Alves et al., 2012a; Necpálová et al., 2015; Shurpali et al., 2016; van der Weerden, Kelliher and Klein, 2012). Literature have reported high diurnal variations in soil N_2O flux, reaching a diurnal difference up to ten times between the daily minimum and maximum flux (Christensen, 1983; Dobbie and Smith, 2003; Keane et al., 2018; Maljanen et al., 2002; Scheer et al., 2012; Shurpali et al., 2016). Understanding the drivers of diurnal variations in N_2O flux is imperative, as it will help improve current estimation methods for soil N_2O emissions such as process-based models and direct measurement regimes.

Additionally, difference in land management systems may result in preferential diurnal patterns of N_2O flux. In Chapter 2, daytime peaking patterns of N_2O flux were found more commonly in grassland ecosystems (81%) than arable ecosystems (55%). Compared to arable ecosystems, permanent grassland ecosystems were found to have higher denitrifying bacteria abundance and denitrifying enzyme activity (Hirsch et al., 2017; Miller et al., 2009), indicating the microbial communities under permanent grasses could be more

efficient in denitrification and N_2O production. Studies found that grassland species such as *Poa pratensis* and *Lolium perenne* exude high amounts of organic acids (e.g., N-acetylglucosamine, succinate, serine, glycine, etc.) (Dietz et al., 2020; Paynel, J Murray and Bernard Cliquet, 2001), which have stimulatory effects on microbial denitrification (Maurer et al., 2021). This suggests higher denitrification capabilities of grassland ecosystems. In addition, studies have shown that two bacterial phyla *Alphaproteobacteria* and *Verrucomicrobia* (largely *Chthoniobacter flavusi*) are more dominant in permanent grassland soils, compared to arable soils (Florian et al., 2021; Hirsch et al., 2017; Karimi et al., 2018). Both phyla contain species capable of denitrification (Bárta et al., 2017; Cua and Stein, 2014; Coyotzi et al., 2017; Heylen et al., 2007; Wang et al., 2017).

Diurnal N_2O fluxes are often reported to follow a daytime peaking pattern featuring diurnal peaks in the afternoon, which are typically attributed to the diurnal oscillation of soil temperature (Blackmer, Robbins and Bremner, 1982; Hosono et al., 2006; Scheer et al., 2014; Skiba and Smith, 2000; van der Weerden, Clough and Styles, 2013; Williams, Ineson and Coward, 1999). However, several studies have observed stronger relationships between diurnal N_2O fluxes and photosynthetic parameters (e.g., photosynthetically active radiation (PAR), solar radiation and net ecosystem production (NEP)) and suggested plant photosynthetic activity could drive diurnal N_2O fluxes via root exudation of photosynthate C (Christensen, 1983; Keane et al., 2018; Shurpali et al., 2016; Zona et al., 2013). A previous laboratory experiment by Das et al. (2012) investigated the effects of PAR on diurnal variations in N_2O flux. The authors refuted the theory that PAR has a diurnal effect on soil N_2O flux via stimulation of root exudation as they found daytime peaking of N_2O flux from both planted and unplanted soils and postulated the diurnal fluctuations of soil temperature caused by the heat from the grow lights were the cause of the diurnal variations in N_2O flux. However, this conclusion is potentially inaccurate and misleading, since their findings only showed that the diurnal variations in N_2O flux from the planted soils could be driven by both PAR and soil temperature, whereas soil temperature was the only diurnal driver of N_2O flux from the unplanted soils. Often soil temperature is autocorrelated with PAR or solar radiation, meaning it could obscure the potential diurnal effects of photosynthetic activity on soil N_2O flux if it was the only diurnal variable considered. In fact, many field studies of planted ecosystems have reported a temperature sensitivity (Q_{10}) of soil N_2O production of over three (Akiyama and Tsuruta, 2002; Blackmer,

Robbins and Bremner, 1982; Dobbie and Smith, 2003; Parkin and Kaspar, 2006), whereas laboratory studies of unplanted soils found that the Q_{10} of soil N_2O production was only about two (Castaldi, 2000; Phillips et al., 2015a). This mismatch in the Q_{10} of N_2O production between planted and unplanted systems suggests the need to investigate the effects of photosynthetic activity on diurnal variations in N_2O flux without the confounding effects of soil temperature. The ubiquity of a diurnal pattern of N_2O flux is uncertain. While many studies have consistently observed daytime peaking (in the afternoon) of diurnal N_2O fluxes in planted ecosystems under field conditions (Akiyama and Tsuruta, 2002; Christensen, 1983; Hosono et al., 2006; Keane et al., 2018; Smith et al., 1995), some have observed consistent night-time peaking of diurnal N_2O fluxes (Keane et al., 2019; Scheer et al., 2012; Shurpali et al., 2016), whereas others did not observe any diurnal patterns (Ball, Scott and Parker, 1999; Yao et al., 2009). The consistency of diurnal patterns of N_2O flux appears context specific, Francis Clar and Anex (2019) reported the daytime peaking of diurnal N_2O fluxes only occurred during low emissions periods (defined as days with N_2O fluxes ≤ 3.0 mg m^{-2} h^{-1} in the study) and no diurnal patterns were exhibited during high emissions periods after N fertilisation. However, the opposite observations were reported by (Lognoul et al., 2019), indicating that diurnal patterns of N_2O flux are independent from soil N levels. Some studies instead observed interruption of diurnal N_2O patterns by rainfall events (Reeves and Wang, 2015; van der Weerden, Clough and Styles, 2013), and postulated the reduction in soil O_2 status triggered pulse fluxes of N_2O which overrode the diurnal N_2O patterns regardless of the time of day.

As substantiated by the findings of Chapter 2 to 4, diurnal variability of N_2O flux is a common phenomenon but the underlying mechanisms are unknown. What remains unclear is, whether PAR-driven plant metabolism contributes to the occurrence and magnitude of diurnal N_2O variations independently of temperature. The following research questions were proposed:

1. Does a regular photoperiod induce consistent daytime peaking of N_2O flux when variations in soil temperature and moisture are minimised?
2. Does the level of PAR regulate daily cumulative N_2O emissions and the diurnal amplitude of N_2O flux?
3. Is the diurnal amplitude of N_2O flux influenced by plant productivity in response to PAR?

It was hypothesised that consistent daytime peaking of N2O flux would be observed under a regular photoperiod with minimised temporal variations in soil temperature and moisture. Additionally, it was hypothesised that daily cumulative N2O emissions and diurnal amplitude of N2O flux would increase along with increasing levels of PAR, which would be explained by increased daily cumulative NEP brought about by increased PAR levels.

To address the research questions and hypotheses, a laboratory experiment was devised where planted soil cores were exposed to different levels of PAR, under controlled environment conditions which minimised variations in soil temperature and moisture to decouple the impacts of temperature and plant metabolism. The experimental set-up is detailed in Section 5.3.

5.3 Method

5.3.1 Soil description and experimental design

For this experiment, 15 soil cores were collected and exposed to three levels of PAR (n=5) under controlled environmental conditions and N_2O fluxes were monitored before, during and after PAR treatments. The study soil was taken from an agricultural grassland (dominant species: *Agrostis stolonifera* and *Poa trivialis*) in Preston, UK (53°51'08.5" N, 2°47'15.5" W). The field had been used for silage production and received an annual fertilisation of 81 kg N ha^{-1}, 24 kg S ha^{-1} and 3,000 gallons $acre^{-1}$ of cattle slurry. The texture of the soil was sandy clay loam, with a bulk density of 1.00 g cm^{-3} and a pH of 7.14. The soil had an initial ammonium (NH_4^+) and nitrate (NO_3^-) concentration of 6.8 ± 0.2 µg g^{-1} and 5.0 ± 0.3 µg g^{-1}, respectively. The total C and N content of the soil was 2.08% and 0.21%, respectively.

The fifteen cores of intact vegetated topsoil were collected with cut PVC pipes (20 cm outer diameter, 19 cm inner diameter and 15 cm height) on 6 Jun 2021. To prevent gas and liquid exchange through the bottom of the mesocosms during the experiment, the soil cores were transferred into another set of bottom-sealed PVC pipes of the same dimensions prior to the experiment.

The laboratory experiment was conducted between 12 Jun and 29 Jun 2021. Prior to the start of the experiment, vegetation in the mesocosms was cut to 5 cm above the soil surface to mimic the farm's silage production practice. All mesocosms were fertilised with a basal application of 70 kg N ha^{-1} of ammonium nitrate and received 500 ml of deionised water before the start of the experiment. The 15 mesocosms were randomly divided into three treatment groups, namely, High PAR (715 ± 35 µmol m^{-2} s^{-1}), Medium PAR (415 ± 16 µmol m^{-2} s^{-1}) and Low PAR (132 ± 5 µmol m^{-2} s^{-1}). The five replicate mesocosms in each treatment group were situated in a three-sided cubicle under a grow light with adjustable light intensities (300W Daylight LED Grow Light, Maxibright, UK). The grow lights were placed 50 cm above the vegetation surface and were switched on and off at 6:00 and 18:00, providing a 12-hour daily photoperiod. To minimise the diurnal fluctuations of soil temperature, all mesocosm chambers and the air mixing chamber were housed in a room with a controlled temperature of 20.0 ± 1.0 °C. Additionally, mesocosms in each treatment block were immersed in a water bath (12 cm height), which acted as a heat sink.

A soil temperature sensor (10kΩ Thermistor, EPCOS, Germany) and soil moisture sensor (Analog Capacitive Soil Moisture Sensor, DFRobot Gravity, China) were installed at 5 cm and 0 – 6 cm soil depth of each mesocosm, respectively, and wired through the chamber wall to their respective data loggers (Arduino Uno, Arduino, Italy). Soil temperature and volumetric water content (VWC) were recorded at 1-minute intervals. A semi-continuous greenhouse gas monitoring system was developed for this experiment. Briefly, clear acrylic flow-through chambers (20 cm outer diameter, 19.4 cm inner diameter, 20 cm height) were placed over the vegetation and sealed onto each mesocosm for the duration of the experiment. The inlets of the flow-through chambers were connected to an air mixing chamber via polyethylene tubing (1/4 inch outer diameter, 1/8 inch inner diameter Bev-A-Line Transfer Tubing, Thermoplastic Processes Inc., USA), whereas the outlets were connected to a 16-channel rotary valve with water traps and flow meters in between. The external vacuum pump and the cavity ring-down spectrometer (CRDS) (G2508, Picarro Inc., USA) pump continuously pulled gas from the inlet of the air mixing chamber, through the flow-through chambers, water traps and mechanical flow meters (gas flow rate set to approximately 100 ml min^{-1}) to the 16-channel rotary valve. The air mixing chamber had one inlet (connected to a PVC tube to the outside) and 16 outlets (one to the rotary valve and 15 to the flow-through chambers). The rotary valve was sequenced to direct gas flow from one chamber for eight minutes to the CRDS and the rest to the external vacuum pump in a loop. Figure 5.1 illustrates the set-up of flow-through system in the experiment. During the experiment, the CRDS measured and recorded the N_2O and CO_2 gas concentrations (at approximately 1 Hz frequencies) from the mesocosm chambers in each PAR treatment group in sequence, which was followed by a measurement of the atmospheric air from the air mixing chamber, and then to the next treatment block.

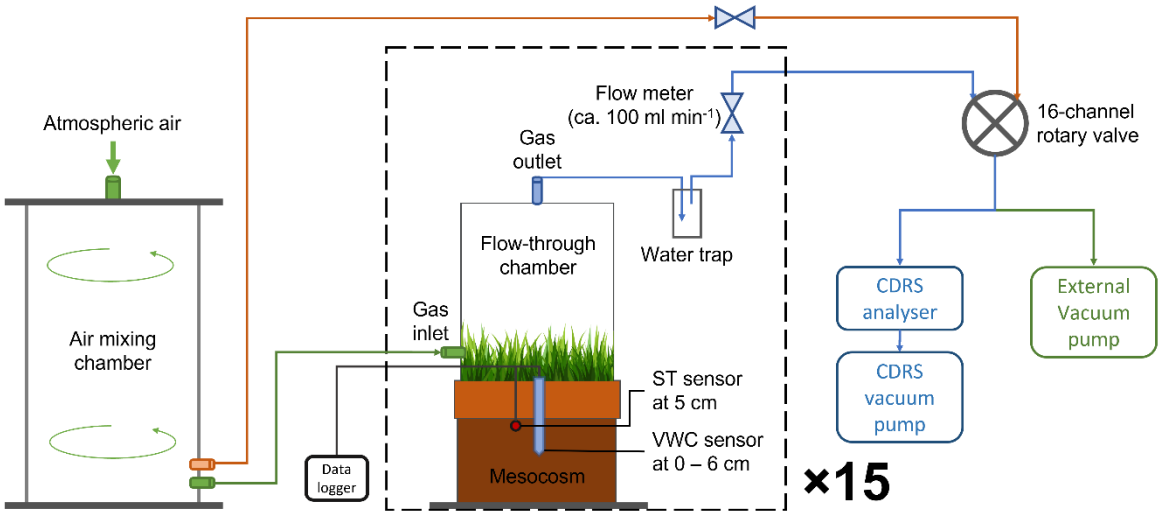

Figure 5.1. Diagram of the steady-state flow-through (open dynamic) chamber system chamber system developed for this experiment. Fifteen mesocosms were connected to the mixing chamber and to the 16-channel rotary valve via gas inlet and outlet, respectively. The sixteenth gas line of the mixing chamber (orange) was connected directly to the rotary valve. Gas lines to the rotary valve were reduced to approximately 100 ml min^{-1} by flow restrictors. The rotary valve directed one gas line to the CRDS analyser at a time for 8 minutes and the rest to the vacuum pump (exhaust), before switching to the next gas line.

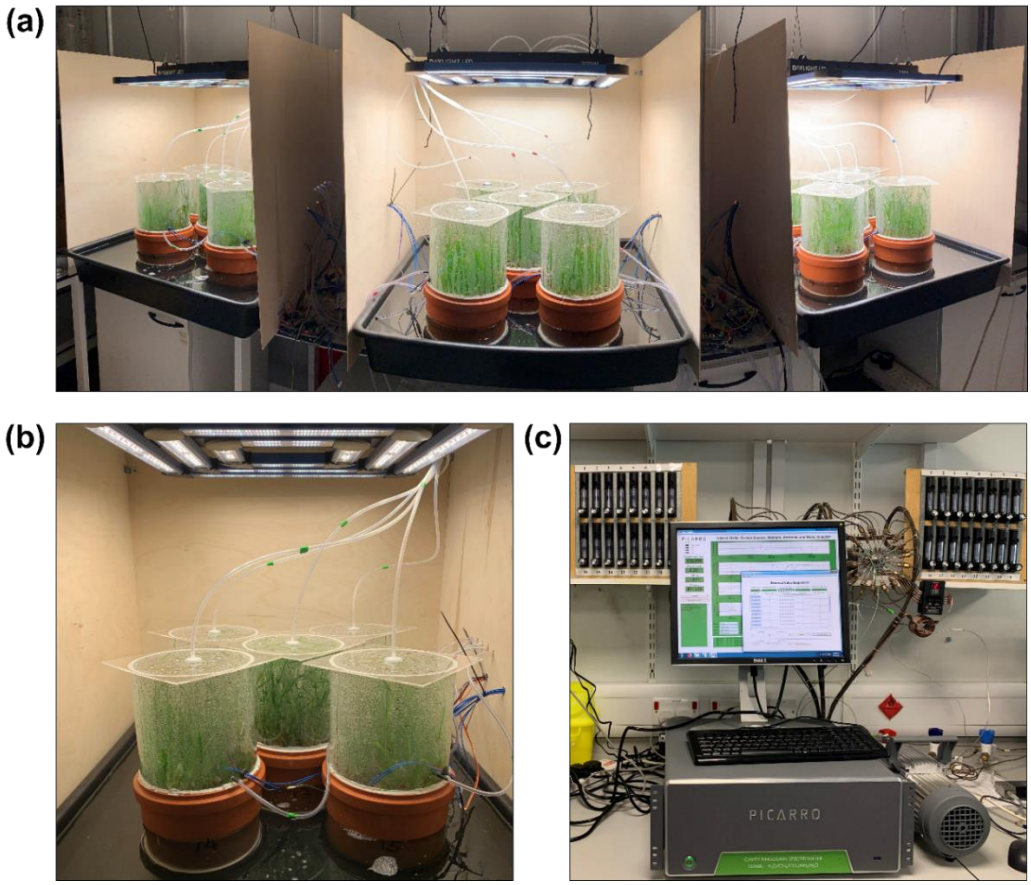

Figure 5.2. Photographs of (a) the experimental set-up during the treatment period, (b) a cubicle containing five replicate mesocosms of a treatment group, and (c) the gas line connections to the rotary valve, flow meters and CRDS.

5.3.2 Experimental procedures

The experiment was divided into three time periods: the pre-treatment period (5 days), treatment period (7 days) and post-treatment period (5 days). The design of a pre-treatment and post-treatment period was first to allow mesocosms to acclimatise to the laboratory conditions and then to observe any carried-over effects of treatments, respectively. During the pre-treatment period, all three treatment groups received a medium PAR level during photoperiods, equivalent to a PAR flux of 415 ± 16 µmol m^{-2} s^{-1} at the vegetation surface. During the treatment period, the High PAR group received a higher PAR level of 715 ± 35 µmol m^{-2} s^{-1}, and the Low PAR group a lower PAR level of 132 ± 5 µmol m^{-2} s^{-1}, whereas the PAR level in the Medium PAR group remained unchanged. In the post-treatment period, all three groups had their PAR levels reverted back to the medium PAR level. At the end of the experiment, aboveground biomass as a measure of productivity was harvested from all mesocosms, dried in the oven at 105 °C for 48 hours, and weighed. Soil samples were collected from the 0 – 5 cm topsoil for soil ammonium and nitrate concentrations and total C and N analyses. Soil ammonium and nitrate concentrations were determined using colorimetric methods (Ringuet, Sassano and Johnson, 2011) with 0.5 M potassium sulphate extracts of fresh soil samples. A dry combustion analyser (TruSpec CN, LECO Corporation, Michigan, USA) was used to determine the total C and N content of the soil samples (Wright and Bailey, 2001).

5.3.3 Data processing and statistical analyses

All data processing, visualisation and statistical analyses were performed in RStudio (version 3.6.1, The R Foundation). For N_2O and CO_2 flux computations, a mean value of N_2O and CO_2 concentration was calculated for every measurement using the intermediate 6 minutes of gas concentration readings, which were then converted to gas flux with equation 5.1 (McGinn, 2006):

$$F = \frac{f}{A_{soil}} \times (C_{out} - C_{in}) \quad (5.1)$$

Where F is the N_2O or CO_2 flux (g m^{-2} s^{-1}), f is the flow rate to the mesocosm chambers (m^3 s^{-1}), A_{soil} is the soil area (m^2), C_{out} is the concentration of N_2O or CO_2 in the outflow (i.e., gas flow from the mesocosm chamber, g m^{-3}) and C_{in} is the concentration of N_2O or CO_2 in the inflow (i.e., the previous measurement of gas flow from the air mixing chamber, g m^{-3}). As a measure of data quality control, N_2O and CO_2 fluxes falling between the detection limits

of the CRDS were considered as zero fluxes. The detection limits are ± 9.15 μg m^{-2} h^{-1} and ± 0.365 mg m^{-2} h^{-1} for N_2O and CO_2 fluxes, respectively.

Daily cumulative N_2O emissions and diurnal amplitudes of N_2O flux (actual and standardised, defined below) of each mesocosm were first calculated to test the effects of the differences in PAR level on the magnitude of daily cumulative N_2O emission and diurnal amplitude of N_2O flux. Daily cumulative N_2O emissions were calculated by trapezoidal integration of measured diurnal N_2O fluxes over every 24-hour cycle. Actual diurnal amplitudes of N_2O flux were calculated by subtraction of the daily maximum N_2O fluxes by the corresponding daily minimum N_2O fluxes. Since large differences (up to an order of magnitude) in the magnitude of N_2O fluxes were observed between mesocosms within and between treatment groups, despite the randomisation of the mesocosms and being under similar environmental conditions (i.e., during the pre-treatment period), the diurnal amplitudes of N_2O flux were further standardised to allow appropriately-scaled comparisons relative to the magnitude of the minimum flux. Similar approaches were used in past studies (Lognoul et al., 2019; Reeves and Wang, 2015; Reeves et al., 2016). Standardised diurnal amplitude of N_2O flux (%) were calculated by dividing the actual diurnal amplitudes N_2O flux by their daily minimum N_2O fluxes, which were assumed as the daily baselines of N_2O flux. Linear mixed-effects models were used to investigate the effects of PAR levels, experimental periods and the interaction between PAR levels and experimental periods (as fixed effects terms) on the daily cumulative N_2O emission and actual diurnal amplitude of N_2O flux, with mesocosm as the random effect term and experimental day as an autocorrelated variable within the random effect of mesocosm. For standardised diurnal amplitude of N_2O flux, a linear regression model was used since the effects of mesocosm and day of experiment were removed through standardisation. Since linear mixed-effects model and linear regression model assume normality of model residuals, log-transformed (natural) of daily cumulative N_2O emissions and actual and standardised diurnal amplitudes of N_2O flux were used as the model dependent variables instead. To test the significant differences between treatment groups within each treatment period and between treatment periods within each treatment group, Tukey pairwise comparisons (estimated marginals means for the linear mixed-effects models, means for the linear regression model) were performed as post-hoc tests.

The effects of plant productivity on the diurnal amplitude of N_2O flux were examined with both the log-transformed actual and standardised diurnal amplitudes of N_2O flux. Due to the experimental design resulting limited variations in soil temperature, it was inapplicable to partition gross primary productivity and ecosystem respiration from net ecosystem exchange of CO_2 (Reichstein et al., 2005). Therefore, cumulative NEP during the photoperiod (06:00 – 12:00) of daily cycles were calculated and assumed as the daily cumulative measurements of plant productivity. A linear mixed-effects model and a linear regression model was used for the actual and standardised diurnal amplitude of N_2O flux, respectively. Cumulative NEP during photoperiod was used as the only explanatory variable in both models, with the linear mixed-effects model having the same random effect terms defined previously.

To inspect the diurnal patterns of each PAR treatment group during the three experimental periods, diurnal N_2O fluxes of all the mesocosms were first normalised, which removed the effects of magnitude differences in N_2O flux between mesocosms and between dates. The normalisation method used is described in Chapter 2.2. Normalised N_2O fluxes were plotted separately by treatment groups and experimental periods; a locally estimated scatterplot smoothing (LOESS; span = 0.6) curve was superimposed onto the scatterplot for each group.

To assess the consistency of peak timing of diurnal N_2O fluxes, the peak times of all mesocosms were quantified by binning the daily N_2O flux maxima (i.e., normalised N_2O = 1.0) into six four-hourly bins accordingly. The four-hourly bins were defined as 02:00 (00:00 – 03:59), 06:00 (04:00 – 07:59), 10:00 (08:00 – 11:59), 14:00 (12:00 – 15:59), 18:00 (16:00 – 19:59), and 22:00 (20:00 – 23:59). The frequencies of diurnal peaks in each four-hourly bin were then counted by treatment group and summarised into percentages.

Soil ammonium and nitrate concentration, total C and N and aboveground biomass of all mesocosms after the experiment were compared by treatment groups using one-way analysis of variance (ANOVA).

5.4 Results

5.4.1 N_2O fluxes, soil and plant properties

Over the whole experiment, the Low PAR group emitted the highest total amount of N_2O (214.3 ± 97.9 mg m^{-2}, mean ± 95% confidence intervals (CI)), followed by the Medium PAR (133.0 ± 77.5 mg m^{-2}) and the High PAR group (33.8 ± 5.2 mg m^{-2}). All three treatment groups showed gradual increases of three times or more in daily cumulative N_2O emissions from the pre-treatment period to the post-treatment period (Table 5.1, Figure 5.3a). Similar increasing trends were also found in the actual diurnal amplitudes of N_2O flux of the three groups, with the differences between the pre-treatment and the post-treatment period being approximately two to three times (Table 5.1).

However, when standardised, the Low PAR group showed a decrease in diurnal amplitude throughout the three periods (98.6% ± 69.1% to 34.1 ± 11.5%), whereas the Medium PAR group had similar standardised diurnal amplitude of N_2O flux in the pre-treatment (58.0% ± 10.4%) and treatment period (52.9% ± 11.8%), and an increase in the post-treatment period (79.6% ± 66.2%, Table 5.1). The High PAR group on the other hand, showed an increase in standardised diurnal amplitude of N_2O flux from the pre-treatment (54.3% ± 10.5%) to the treatment period (84.4% ± 16.2%), which reduced in the post-treatment period (47.7% ± 12.5%). Detailed analyses of the treatment effects on daily cumulative N_2O emission and diurnal amplitude of N_2O flux are reported in Section 5.4.3.

In addition, large variances in the magnitude of N_2O flux (up to an order of magnitude) were observed consistently in two of mesocosms in the Medium and High PAR group (Table 5.1), which started from the pre-treatment period (Detailed statistics supplied in Appendix III). This consequently led to the comparatively larger means and confidence intervals of the daily cumulative N_2O emissions and actual diurnal amplitudes of N_2O flux in the Medium PAR and Low PAR group.

Table 5.1. Means and 95% confidence intervals of the daily cumulative N_2O emissions (mg m^{-2}), actual (µg m^{-2})and standardised diurnal amplitude of N_2O flux (%) of the Low PAR, Medium PAR and High PAR group in the pre-treatment, treatment and post-treatment period. For the pre-treatment and post-treatment periods, the number of observations of each group was 25; for the treatment period, the number of observations was 35.

Treatment groups	*Daily cumulative N_2O emission (mean ± 95% CI, **mg m^{-2}**)*		
	Pre-treatment	Treatment	Post-treatment
Low PAR	4.15 ± 0.93	14.19 ± 5.30	19.03 ± 5.84
Medium PAR	1.68 ± 0.70	8.51 ± 3.90	13.02 ± 6.00
High PAR	1.08 ± 0.20	1.69 ± 0.31	3.40 ± 0.73
Treatment groups	*Actual diurnal amplitude of N_2O flux (mean ± 95% CI, **µg m^{-2}**)*		
	Pre-treatment	Treatment	Post-treatment
Low PAR	99.2 ± 59.5	146.0 ± 52.5	218.0 ± 77.0
Medium PAR	36.3 ± 17.7	103.0 ± 38.1	110.0 ± 41.0
High PAR	19.4 ± 3.8	48.4 ± 13.1	49.8 ± 12.5
Treatment groups	*Standardised diurnal amplitude of N_2O flux (mean ± 95% CI, **%**)*		
	Pre-treatment	Treatment	Post-treatment
Low PAR	98.6 ± 69.1	43.8 ± 10.1	34.1 ± 11.5
Medium PAR	58.0 ± 10.4	52.9 ± 11.8	79.6 ± 66.2
High PAR	54.3 ± 10.5	84.4 ± 16.2	47.7 ± 12.5

The experimental set-up was designed to minimise fluctuations in soil temperature. This was successful with diurnal fluctuations in soil temperature at 5 cm soil depth being ± 1.4 and ± 0.3 °C, in the High PAR and Low PAR group in the treatment period, respectively (Figure 5.3c). Soil VWC remained stable with no diurnal fluctuations during the experiment, ranging between 49.5% and 52.5% among mesocosms (Figure 5.3d). Total soil C and N, soil NH_4^+ and NO_3^- and aboveground biomass analysed at the end of the experiment were not significantly different between PAR treatments (Table 5.2).

Table 5.2. Soil ammonium (NH_4^+), nitrate (NO_3^-), total soil C and N and oven-dried (at 105 °C) aboveground biomass (mean ± 95% confidence intervals; n = 5) of PAR treatments at the end of the experiment.

Treatment group	*mean ± standard error*				
	Soil NH_4^+ (μg g^{-1})	Soil NO_3^- (μg g^{-1})	Soil total C (%)	Soil total N (%)	Aboveground biomass (g)
High PAR	73.4 ± 24.3	74.4 ± 10.7	5.35 ± 0.79	0.53 ± 0.08	5.52 ± 0.38
Medium PAR	68.3 ± 16.4	80.2 ± 26.7	4.65 ± 0.53	0.45 ± 0.05	5.62 ± 0.54
Low PAR	81.0 ± 51.1	67.1 ± 18.8	4.49 ± 0.72	0.43 ± 0.07	4.81 ± 1.00

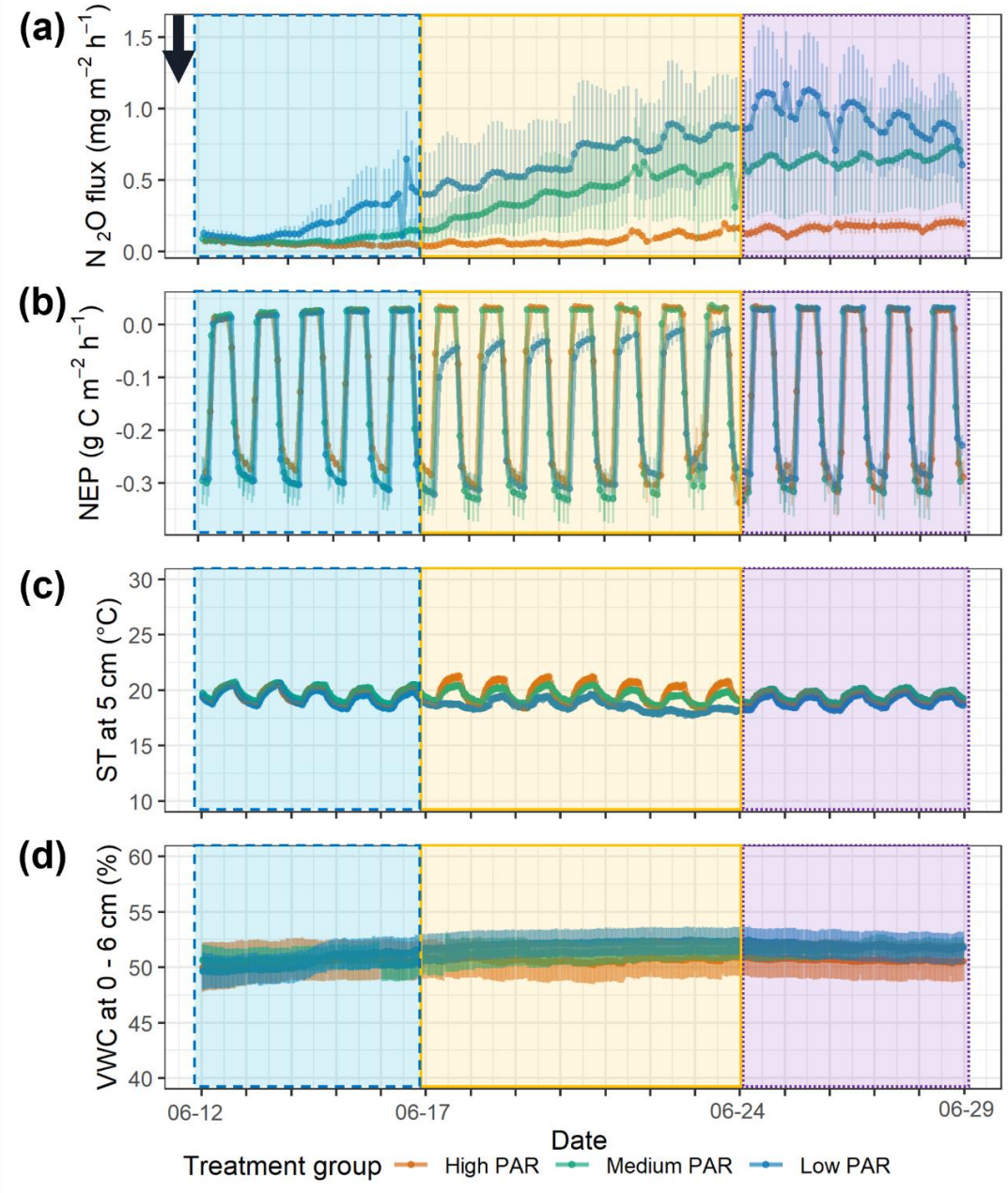

Figure 5.3. Time series of actual (a) N_2O flux, (b) net ecosystem production (NEP), (c) soil temperature (soil temperature) at 5 cm (°C) and (d) soil volumetric content (VWC) at 0 – 6 cm of the three treatment groups (high PAR – orange circle, medium PAR – green square, low PAR – blue triangle) over the experimental periods (pre-treatment – light blue shade, dashed line; treatment – yellow shade, solid line; post-treatment – purple shade, dotted line). The arrow indicates the time of the fertilisation of 70 kg N ha^{-1} of ammonium nitrate.

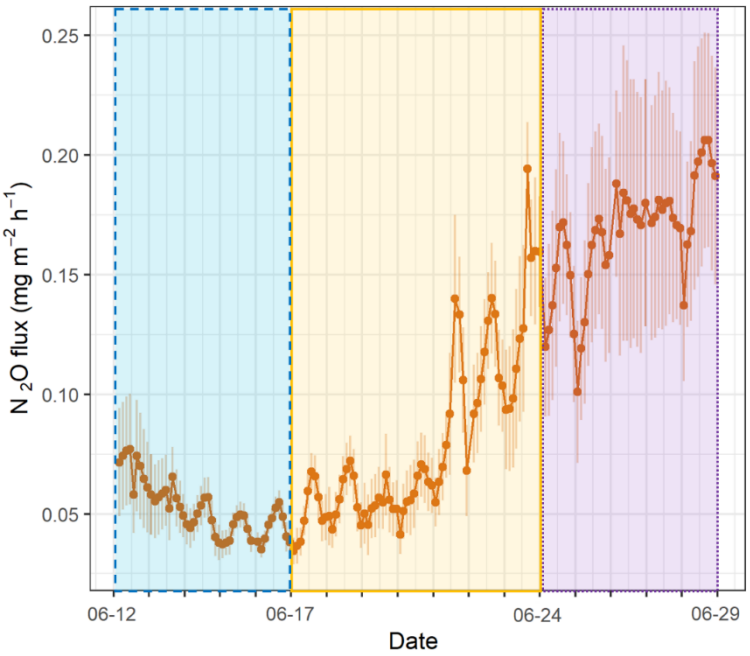

Figure 5.4. The time series of N_2O flux of the High PAR treatment group on appropriate scaling. Light blue dashed line box represents the pre-treatment period, yellow solid line box represents the treatment period, and purple dotted line box represents the post-treatment period.

5.4.2 Diurnal patterns and peak timing of N_2O flux

To evaluate the consistency of diurnal patterns of N_2O flux, N_2O flux data were normalised and then plotted, followed by the binning of the times of daily N_2O flux maxima (Section 5.3.3). Throughout all three periods, diurnal N_2O fluxes of the three groups exhibited a daytime peaking pattern with the majority of peak times between 10:00 and 18:00 (Figure 5.5a, 5.5c and 5.5e). Binning of the peak flux times revealed that the majority of the diurnal peaks in the 14:00 bin was constituted by the High PAR group from pre-treatment to post-treatment period and the Low PAR group in the treatment and post-treatment period, whereas the majority of those in the 18:00 bin comprised the Medium PAR group in all three periods (Figure 5.5b, 5.5d and 5.5f). The High PAR group predominantly exhibited its diurnal peaks in the 14:00 bin (48.0 – 65.7% out of 100%) in all three periods, with the highest percentage of occurrence frequency during the treatment period at 65.7% (Figure 5.5d). The Medium PAR group primarily exhibited its diurnal peaks at the 18:00 bin (44.1 – 84.0% out of 100%) with the highest percentage of occurrence frequency also during the treatment period at 84.0% (Figure 5.5d). On the other hand, the Low PAR group initially exhibited the highest frequency of its diurnal peaks in the 18:00 bin (32.0% out of 100%), which shifted to the 14:00 bin in the treatment (42.9%) and post-treatment period (56.1%).

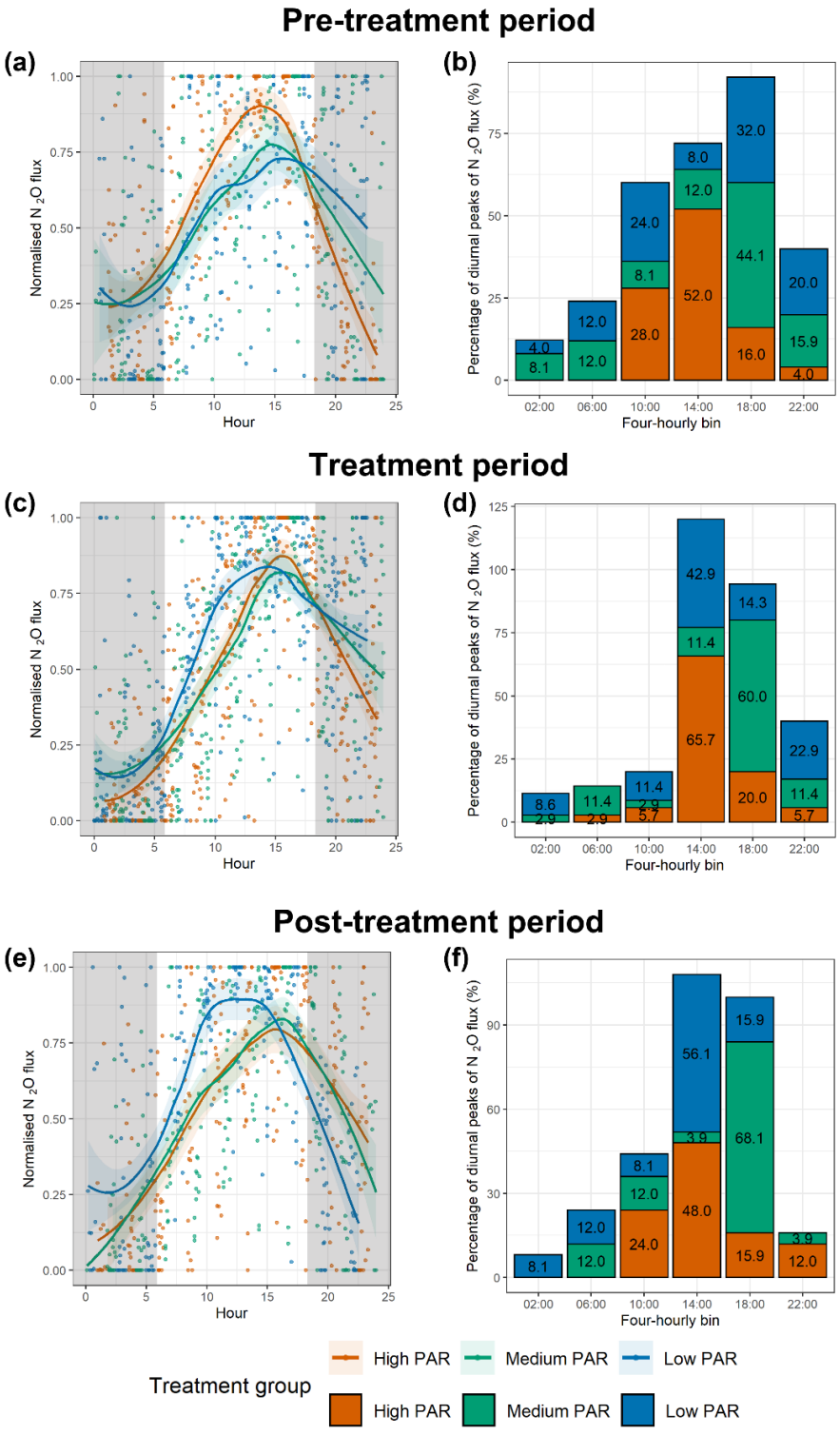

Figure 5.5. Diurnal patterns of normalised N_2O flux in High PAR (orange dots and lines), Medium PAR (green dots and lines) and Low PAR (blue dots and lines) group during the (a) pre-treatment period, (c) treatment period, and (e) post-treatment period; unshaded and shaded areas indicate light and dark periods, respectively; and stacked bar charts of percentage frequency of diurnal peaks of N_2O flux in four-hourly bins in the High PAR (orange bars), Medium PAR (green bars) and Low PAR (blue bars) during the (a) pre-treatment period, (c) treatment period, and (e) post-treatment period. The total percentage of each group in each period is 100% and the total number of observations of each group is 25 in the pre-treatment and post-treatment period and 35 in the treatment period.

5.4.3 Treatment effects on daily cumulative N_2O emission and diurnal amplitude of N_2O flux

To compare the effects of PAR level on daily cumulative N_2O emissions and the diurnal amplitude of N_2O flux (actual and standardised), log-transformed data between groups were compared for the three periods, as well as between the three periods within each group. In the daily cumulative N_2O emission and actual diurnal amplitude of N_2O flux, no significant difference was found among the Low PAR, Medium PAR and High PAR group in all three periods ($p > 0.05$, Figure 5.6a and 5.6b). In the standardised diurnal amplitude of N_2O flux, the only significant differences were found in the treatment period, where the High PAR group showed significantly higher standardised diurnal amplitude of N_2O flux than the Medium PAR (estimate = 0.652, $p = 0.011$) and the Low PAR group (estimate = 0.852, $p < 0.001$, Figure 5.6c).

Over the experimental periods, only the Medium PAR group exhibited a significant increase in the daily cumulative N_2O emission between the pre-treatment and post-treatment period (estimate = 0.571, $p = 0.023$, Figure 5.6a). In terms of actual diurnal amplitude of N_2O flux, the Low PAR group showed a significant increase between the pre-treatment and post-treatment period (estimate = 0.947, $p = 0.014$, Figure 5.6b), the Medium PAR group showed significant increases between the pre-treatment and treatment period (estimate = 0.776, $p = 0.022$, Figure 5.6b) and between the pre-treatment and post-treatment period (estimate = 1.192, $p < 0.001$, Figure 5.6b), whereas the High PAR group only showed a significant increase between the pre-treatment and treatment period (estimate = 0.713, $p = 0.050$, Figure 5.6b). Conversely, the standardised diurnal amplitude of N_2O flux of the Low PAR group decreased significantly from the pre-treatment to the post-treatment period (estimate = -0.684, $p = 0.042$, Figure 5.6c). No significant differences in standardised diurnal amplitude of N_2O flux were found between the periods in the Medium PAR group (Figure 5.6c), whereas in the High PAR group, the standardised diurnal amplitude of N_2O flux increased non-significantly from the pre-treatment to the treatment period (estimate = 0.531, $p = 0.161$) and then decreased significantly from the treatment to the post-treatment period (estimate = -0.820, $p = 0.002$, Figure 5.6c). Detailed results of the model summaries and the pairwise comparisons are supplied in the Appendix III.

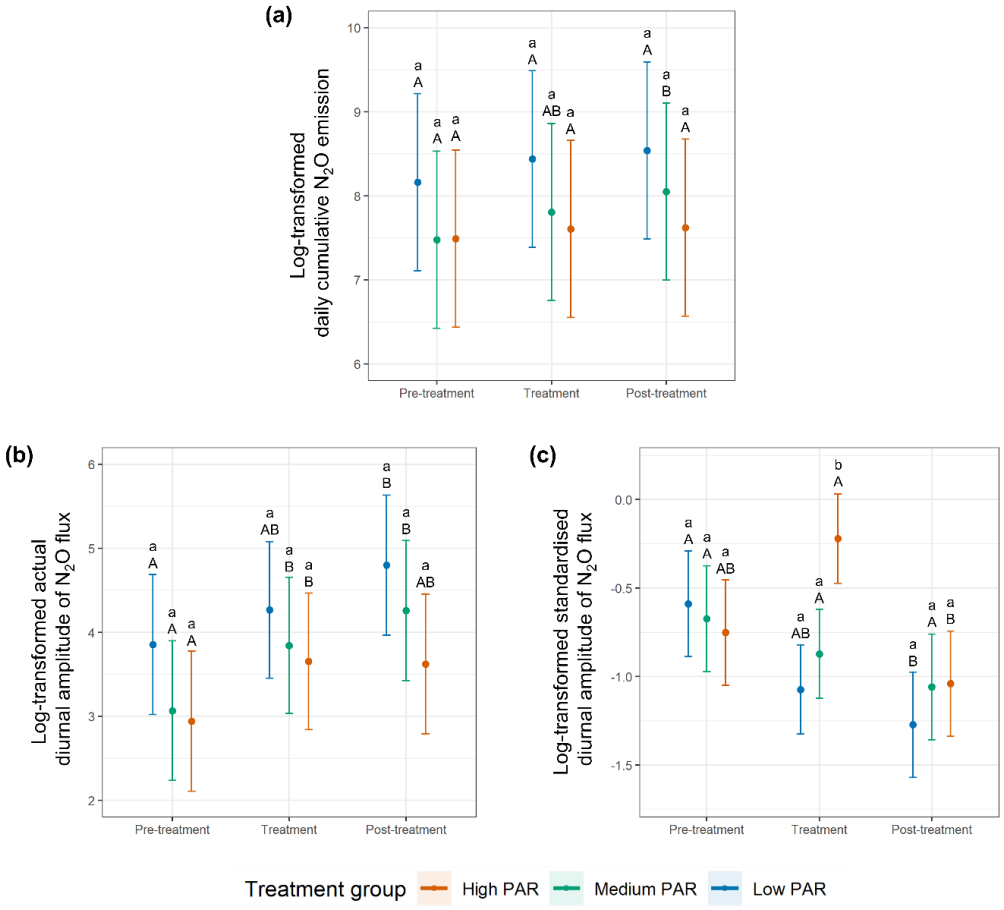

Figure 5.6. Estimated means (dots) and 95% confidence intervals (error bars) of log-transformed (a) daily cumulative N_2O emission (marginal) and (b) actual diurnal amplitude of N_2O flux (marginal) and (c) standardised diurnal amplitude of N_2O flux, and (c) daily cumulative N_2O emission of the treatment groups in the pre-treatment, treatment and post-treatment period. Differences in the lowercase letters above error bars denote significant differences between treatment groups with a treatment period, whereas differences in the uppercase letters above error bars denote significant differences between treatment periods within a treatment group.

5.4.4 Effect of cumulative net ecosystem production (NEP) during photoperiod on diurnal amplitude of N_2O flux

Linear mixed-effects modelling and linear regression modelling were used to examine the effect of cumulative NEP during photoperiod (06:00 – 18:00) on the actual and standardised diurnal amplitude of N_2O flux, respectively (Section 5.3.3). Table 5.3 summarises the results of the two models. While cumulative NEP during photoperiod had no significant effect on the actual diurnal amplitude of N_2O flux (estimate = 0.11, p = 0.576, Figure 5.7a), it had a significant positive effect on the standardised diurnal amplitude of N_2O flux (estimate = 0.41, p = 0.004, Figure 5.7b). However, cumulative NEP during photoperiod explained little in both models (marginal R^2 = 0.001 in the linear mixed-effects model and adjusted R^2 = 0.029 in the linear regression model). Details of model results are supplied in Appendix III.

Table 5.3. Summary of the linear mixed-effects model for the log-transformed actual diurnal amplitude of N_2O flux: lme(fixed = ln(actual diurnal amplitude of N_2O flux) ~ cumulative NEP during photoperiod, random = ~1|mesocosm, correlation = corAR1(form = day|mesocosm), method = 'REML'), and the linear regression model for the log-transformed standardised diurnal amplitude of N_2O flux: lm(ln(standardised diurnal amplitude of N_2O flux) ~ cumulative NEP during photoperiod).

Linear mixed-effects model: log-transformed actual diurnal amplitude of N_2O flux			
Predictors	Estimates	95% confidence intervals	p-value
(Intercept)	3.78	3.32 – 4.24	**<0.001**
Cumulative NEP during photoperiod	0.11	-0.27 – 0.48	0.576
Random effects			
Residual variance (σ^2)		0.87	
Between subject variance (τ_{00}) – Mesocosm		0.55	
Intraclass correlation coefficient (ICC)		0.39	
Number of mesocosm (n)		15	
Observations		255	
Marginal R^2 / Conditional R^2		0.001/ 0.390	
Linear regression model: log-transformed standardised diurnal amplitude of N_2O flux			
Predictors	Estimates	95% confidence intervals	p-value
(Intercept)	-0.86	-0.96 – -0.76	**<0.001**
Cumulative NEP during photoperiod	0.41	0.13 – 0.68	**0.004**
Observations		255	
R^2 / adjusted R^2		0.033/ 0.029	

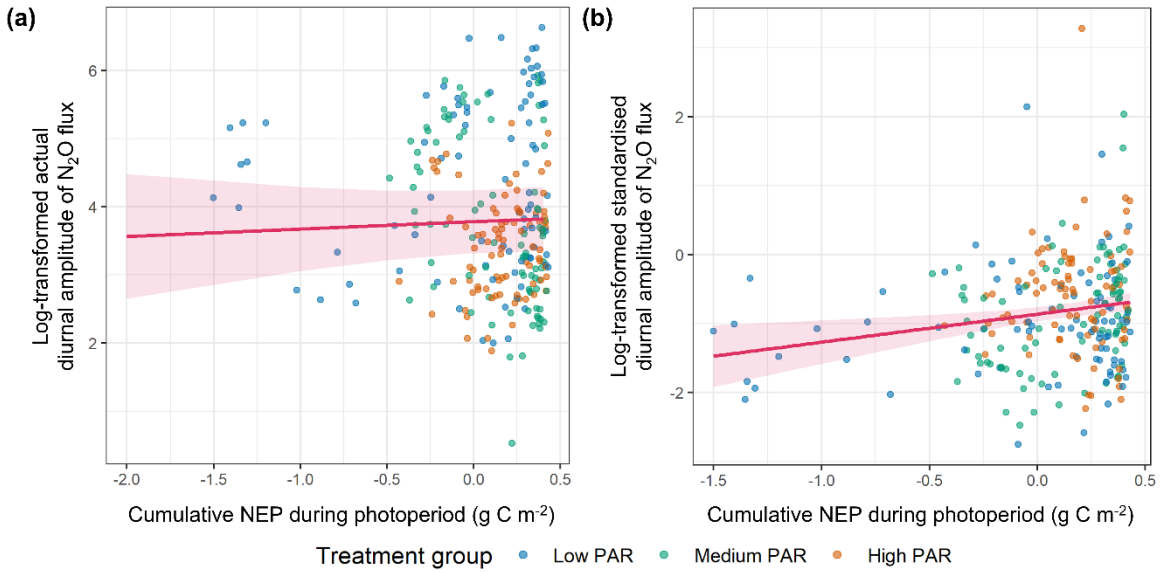

Figure 5.7. Scatterplots of the (a) log-transformed actual diurnal amplitude of N_2O flux and (b) log-transformed standardised diurnal amplitude of N_2O flux against cumulative NEP during photoperiods; data from all three treatment periods are presented. Blue, green and orange dots represent the observations from the Low PAR, Medium PAR and High PAR group, respectively. The pink line and ribbon in (a) represent the marginal fixed effects and 95% confidence intervals, respectively, of cumulative NEP during photoperiods on log-transformed actual diurnal amplitude of N_2O flux in the linear mixed-effects model; and the pink line and ribbon in (b) represent the linear regression curve and 95% confidence intervals, respectively, of cumulative NEP during photoperiods on log-transformed standardised diurnal amplitude of N_2O flux in the linear regression model.

5.5 Discussion

In the experiment, the discrete effects of PAR on diurnal N_2O fluxes were investigated by minimising variations in VWC (≤ 3.0% throughout the experiment with no diurnal oscillation) and soil temperature (< ±1.5 °C in a diurnal course), two environmental variables that would vary substantially more in field conditions and have been attributed to the occurrence (Blackmer, Robbins and Bremner, 1982; Scheer et al., 2014; Williams, Ineson and Coward, 1999) and interruption (van der Weerden, Clough and Styles, 2013) of diurnal patterns of N_2O flux, respectively. This study provides evidence that exposure to PAR (regardless of intensity) of plant-soil mesocosms during regular photoperiods led to daytime peaking of diurnal N_2O fluxes, even when soil temperature and moisture were held constant. Discussion in Section 5.5.1 focuses on the results addressing research question 1, and discussion in Section 5.5.2 focuses on the results addressing research question 2 and 3.

5.5.1 Diurnal pattern and peak timing of N_2O flux

Clear and consistent daytime peaking diurnal patterns of N_2O flux were observed in this experiment (Figure 5.5) regardless of the PAR levels and the experimental periods. This confirmed Q1, that a regular photoperiod induces a consistent daytime peaking of N_2O flux. While small ranges of diurnal oscillation in soil temperature persisted during the experiment (a maximum of ± 1.4 °C diurnal difference), they were not sufficient to cause the extent of diurnal variations in N_2O flux observed in this experiment, considering the temperature sensitivity (Q_{10}) of soil N_2O production is approximately 2.0 (Castaldi, 2000; Phillips et al., 2015a). Given the minimal variations in the VWC and soil temperature in this experiment, the results of the diurnal patterns of N_2O flux (Figure 5.5a, 5.5c and 5.5e) provide empirical evidence that the diurnal variations in PAR levels (i.e., during and outside photoperiods) largely drove the occurrences of daytime peaking of diurnal N_2O fluxes, which also support the postulations of photosynthetic productivity driving the diurnal variations in N_2O flux in multiples studies (Christensen, 1983; Keane et al., 2018; Shurpali et al., 2016; Zona et al., 2013). Compared to the findings of diurnal patterns of N_2O flux in Chapter 3 and 4, and other field-based studies where inconsistent diurnal patterns of N_2O flux were observed (Ball, Scott and Parker, 1999; van der Weerden, Clough and Styles, 2013), the daytime peaking patterns of N_2O flux in this experiment were more consistent and prevalent, occurring very regularly over the majority, with daytime flux peaks (10:00 –

18:00 bins) accounting for 75 – 84% of the total occurrences of diurnal peaks in all three periods. This was in agreement with the consistent daytime peaking of diurnal N_2O patterns observed in previous studies with planted soil cores under controlled temperature (Das et al., 2012; Williams, Ineson and Coward, 1999). The increased consistency of daytime peaking of N_2O flux compared to field studies, was likely due to the removal of climatic factors such as rainfall events, which cause short-term changes in the soil VWC and subsequently interrupting diurnal patterns of N_2O flux by stimulating soil N_2O production (van der Weerden, Clough and Styles, 2013; Zhang et al., 2021). The plant species in this experiment (dominantly *Agrostis stolonifera* and *Poa trivialis*) could offer another explanation to the increased consistency in daytime peaking patterns of N_2O flux observed in this experiment. Pulse-labelling studies with ^{13}C-CO_2 also found that the lag time between photosynthesis and soil respiration of photosynthetically-fixed C is < two hours (Bahn et al., 2009; Staddon et al., 2003), highlighting the promptitude of root exudation of photosynthetically-fixed C from grassland plants following photosynthesis, compared to arable plants (e.g., maize and wheat) which were found to have a lag time of approximately six hours (Gavrichkova and Kuzyakov, 2010; Kuzyakov and Cheng, 2001). This might constitute to the occurrence of daytime peaking patterns of N_2O flux often observed in grassland ecosystems (Chapter 2). Additionally, grassland plants were found to exude higher contents of organic acids (Dietz et al., 2020; Paynel, J Murray and Bernard Cliquet, 2001), which also have a stronger stimulatory effect on denitrification and N_2O production than sugars (Maurer et al., 2021).

All PAR treatment groups predominantly exhibited daytime peaking of N_2O flux with the majority of the diurnal peak fluxes falling between 12:00 – 15:59 or 16:00 – 19:59, which were consistent with the findings in Chapter 3 and 4, as well as existing studies (Keane et al., 2018; Francis Clar and Anex, 2019; van der Weerden, Clough and Styles, 2013). However, there was a notable difference in the peak timing of N_2O flux between the High PAR (majority at the 14:00 bin), the Medium PAR (majority at the 18:00 bin) and the Low PAR (majority at the 18:00 bin) groups during the pre-treatment periods (Figure 5.5b). It was unlikely that the different peak timing was caused by PAR levels since the same level of PAR was imposed at the pre-treatment period. The discrepancy in peak timing might be due to the different time lags between the onset of photoperiod (at 06:00 in this experiment) and root exudation of photosynthate C, which has been shown to range between nine to twelve

hours in grass species (Domanski et al., 2001; Kuzyakov and Cheng, 2001; Kuzyakov and Domanski, 2002). Additionally, the occurrences of diurnal peaks at the 14:00 bin in the High PAR group increased by 14% from the pre-treatment period (Figure 5.5b) to the treatment period (Figure 5.5d) and then decreased by 18% in the post-treatment period (Figure 5.5f), implying the increase in PAR level during the treatment period prompted a more consistent peak time of diurnal N_2O fluxes but the effect was transient. However, the reduction in PAR level in the Low PAR group during the treatment period shifted the majority of the diurnal flux peaks from the 18:00 bin (32%, Figure 5.5b) to the 14:00 bin (43%, Figure 5.5d) and carried over to the post-treatment period (56%, Figure 5.5f), which suggests reduced photosynthesis brought forward the timing of diurnal peaks by several hours. This finding is also consistent with the results in Chapter 4 (Figure 4.4b) where plant shading had similar effects on the peak timing of N_2O flux. The findings of the effects of PAR levels manipulation on the diurnal patterns and peak timing of N_2O flux are novel that have not been observed in other studies so far. It is possible that the changes in PAR level somehow affected plant belowground metabolisms and root exudation behaviour over the diurnal courses (Kuzyakov and Cheng, 2001), leading to the shifting in peak timing of diurnal N_2O flux. Nonetheless, knowledge on the effects of PAR level on the diurnal pattern of root exudation and subsequently that of N_2O flux is still limited and conclusive evidence of the diurnal variations of soil biochemical conditions in response of different level of photosynthesis are required to tease out the underlying mechanisms.

5.5.2 Effects of PAR level and cumulative NEP during photoperiod on diurnal amplitude of N_2O flux

Although a decreasing trend in daily cumulative N_2O emissions and diurnal amplitude of N_2O flux were observed increasing PAR levels (Table 5.1), there was no significant differences between the treatment groups when mesocosm variances were accounted for as random effects in the linear mixed-effects models (Figure 5.6a and 5.6b). This indicates individual mesocosms that were innately high N_2O-emitting were responsible for the high mean daily cumulative N_2O emissions and mean actual diurnal amplitudes of N_2O flux in the Low PAR and Medium PAR group (see Appendix III for N_2O fluxes from all mesocosms), rather than the treatment effects of PAR level, as the divergence in N_2O flux magnitude among the groups also started in the pre-treatment period (Figure 5.3a). The lack of significant differences in the daily cumulative N_2O emission (Figure 5.6a) and actual diurnal

amplitude of N_2O flux (Figure 5.6b) among the treatment groups during the treatment period also indicate PAR levels did not regulate the two aspects of N_2O flux. However, since some mesocosms in the Medium PAR and Low PAR group were emitting N_2O up to 10-fold higher in magnitude before the treatment period, comparisons based on actual diurnal amplitude of N_2O flux (daily maximum flux minus daily minimum flux) might be biased towards high emitting mesocosms due to their high baseline fluxes. Therefore, standardised diurnal amplitude of N_2O flux (actual diurnal amplitude of N_2O flux divided by daily minimum flux) was also assessed. The results indeed showed a significant increase in standardised diurnal amplitude of N_2O flux in the High PAR group against the Medium PAR (estimate = 0.652, $p = 0.011$) and Low PAR (estimate = 0.852, $p < 0.001$) group during the treatment period (Figure 5.6c), which disagrees with the finding on the actual diurnal amplitude of N_2O flux. This disagreement might be due to the High PAR group having comparatively low baseline N_2O fluxes in against the other two groups but similar magnitudes of diurnal increase in N_2O flux during the treatment period. Nonetheless, taking baseline N_2O fluxes into account, similarly with normalising N_2O fluxes (Keane et al., 2018), are commonly performed in studies (Lognoul et al., 2019; Reeves et al., 2016; Reeves and Wang, 2015) to reflect the effects of any treatments on the diurnal amplitude of N_2O flux. Increased diurnal amplitude of N_2O flux with increasing photosynthetic parameter (solar radiation) has been observed before and was attributed to the increased root exudation of photosynthate C fuelling denitrification (Christensen, 1983). However, the results of this experiment suggest this stimulating effect of increased PAR was transient, as no significant differences in the standardised diurnal amplitude of N_2O flux were found between treatment groups in the post-treatment period (Figure 5.6c).

Consistent with the findings in Figure 5.6b and 5.6c, cumulative NEP during photoperiod showed no significant effect on the actual diurnal amplitude of N_2O flux ($p = 0.576$, Table 5.3, Figure 5.7a) but a significant positive effect on the standardised diurnal amplitude of N_2O flux (estimate = 0.41, $p = 0.004$, Table 5.3, Figure 5.7b). This indicates that the magnitude of diurnal variations in N_2O flux was partially regulated by photosynthetic activity and agrees with findings of a positive relationship between diurnal N_2O flux and photosynthetic parameters in previous studies (Christensen, 1983; Keane et al., 2018; Shurpali et al., 2016; Zona et al., 2013). The mechanisms behind the positive control of photosynthesis on diurnal variations in N_2O flux likely involved the rhythmic diurnal

variations in root exudation of labile C (Murray et al., 2004), which could provide energy source to soil heterotrophs including denitrifying bacteria and some nitrifying bacteria (Tiedje, 1983; Tortoso and Hutchinson, 1990), as well as enhance soil O_2 consumption via heterotrophic respiration (Canarini et al., 2019; Mencuccini and Hölttä, 2010), which further stimulate denitrification. It has been demonstrated that the quantity of root exudates varies positively with photosynthetic activity (Kuzyakov and Cheng, 2001), with up to a third of photosynthetically-fixed C being released as root exudates (Guyonnet et al., 2018; Jones, Hodge and Kuzyakov, 2004; Jones, Nguyen and Finlay, 2009). Along with the diurnal oscillating pattern of root exudation, it is plausible that photosynthetic productivity could in part drive the diurnal amplitude of N_2O flux.

Nonetheless, although the relationship between the cumulative NEP during photoperiod and the standardised diurnal amplitude of N_2O flu was positive and significant, it was weak as the adjusted R^2 of the linear regression model was 0.029 (Table 5.3). Much of the variance in the standardised diurnal amplitude of N_2O flux might have been due to the different soil biochemical conditions among the mesocosms as well as over the experiment, which were not regulated by NEP. As indicated by the large differences in N_2O flux magnitude among mesocosms in response to N fertilisation (Figure 5.3a and Appendix III) under similar environmental conditions (in pre-treatment period), the soil microbial communities among the mesocosms might have been largely different despite having collected and randomised the soil cores from the same field (Franklin and Mills, 2003), with some more adapted to heterotrophic N-cycling leading to different diurnal dynamics of N_2O production in response to C deposition by plants (Giles, Daniell and Baggs, 2017). In addition, the quantity and quality of exudate C might vary over the experiment (Louw-Gaume et al., 2017; Micallef et al., 2009) with different levels of variations among the mesocosms as plant composition were not identical among mesocosms, which could also contribute to the unexplained variance in the diurnal amplitude of N_2O flux. The large unexplained variance in the diurnal amplitude of N_2O flux also highlights the complexity of the diurnal variations in the biochemical components (e.g., labile C, inorganic N and O_2 content) in soils, especially in the rhizosphere where most of the microbial activities take place and it is most influenced by plant metabolisms (Mendes, Garbeva and Raaijmakers, 2013), which remains unexplored at present.

5.6 Conclusion

In this study, the discrete effects of PAR on the diurnal dynamics of N_2O flux were explored under tightly controlled environmental conditions. This was necessary as field observations of diurnal patterns of N_2O flux have been inconsistent; and due to changing environmental conditions (PAR, soil temperature, moisture), the drivers of this phenomenon have not been fully elucidated. The results of this study provided conclusive evidence indicating diurnal rhythm of PAR is a driver of diurnal variations in N_2O flux independent of soil temperature and moisture. However, the PAR-driven plant-soil biological mechanisms behind the diurnal variations of N_2O flux are still unclear. This is because current understanding on the complex transitory changes in soil biochemical properties (e.g., soil O_2 status, labile C content, soil inorganic N content, N-cycling gene expression, etc.) over the diurnal course is still lacking. In addition, we possess little knowledge at present on how PAR affects photosynthesis and its subsequent interactions with such biochemical properties influencing N_2O-producing microbial processes including nitrification and denitrification and leading to variations in N_2O flux. Investigating root exudation behaviour and diurnal changes in the soil biochemical conditions, especially in the rhizosphere, in response to plant photosynthesis may provide critical information to understanding the mechanisms driving diurnal variations in soil N_2O flux.

6. General discussion

6.1 Summary of aims and objectives

Failure to address the diurnal variability of N_2O flux in flux measurement regimes can contribute to the large uncertainties in the cumulative N_2O emission estimates (Lammirato et al., 2018; Shurpali et al., 2016). Currently, the uncertainty of N_2O emission estimates sits at ± 37% in the UK (Committee on Climate Change, 2017). Yet, while evidence of diurnal variability of N_2O flux have been rising, it is still rarely considered in standard flux measurement regimes. Furthermore, little is known about the characteristics and driving mechanisms of this phenomenon.

This thesis aimed to (1) investigate the prevalence of diurnal variability of N_2O flux, (2) evaluate the efficacy of different non-diurnal sampling intervals, and (3) examine the potential environmental and biological factors driving the diurnal variability of N_2O flux. Through the systematic review of relevant published literature (Chapter 2) and field- and laboratory-based experiments with sub-daily N_2O flux measurements and manipulations of environmental factors (Chapters 3, 4 and 5), different aspects of the research aims were achieved. Along with knowledge from existing studies, key findings of the previous chapters are compiled and discussed below to synthesis insights into the diurnal variability of N_2O flux and its research implications.

6.2 Prevalence of diurnal variability of N_2O flux

The findings throughout Chapters 2 to 5 highlight that the diurnal variability of N_2O flux is a pervasive phenomenon with distinctive diurnal patterns. Through the synthesis of data extracted from published studies with sub-daily measurements of N_2O flux, Chapter 2 showed that daytime peaking of N_2O flux is a dominant diurnal pattern in general across different terrestrial ecosystems (cropland, grassland and forest), occurring at ~60% of the time, whereas night-time peaking and non-diurnal patterns of N_2O flux each accounted for ~20% of the occurrences (Section 2.3.1, Chapter 2). In line with this finding, daytime peaking of N_2O flux was also observed on ~60% of the measurement days in the first field mesocosm experiment (Figure 3.4b, Chapter 3), which was conducted without artificial manipulations of environmental variables.

Throughout the experiments of Chapters 3 to 5, diurnal peaks of N_2O flux mostly occurred in the afternoon (12:00 – 19:59), which aligns with the findings in Chapter 2 and most of the current studies (Akiyama, Tsuruta and Watanabe, 2000; Hosono et al., 2006; Flessa et al., 2002; Lognoul et al., 2019; Savage, Phillips and Davidson, 2014; van der Weerden, Clough and Styles, 2013) with a few exceptions (Brumme and Beese, 1992; Keane et al., 2019; Peng et al., 2019). Afternoon peaking of N_2O flux is often attributed to the diurnal oscillations of soil temperature in many studies (Alves et al., 2012b; Blackmer, Robbins and Bremner, 1982; Scheer et al., 2014; van der Weerden, Clough and Styles, 2013; Williams, Ineson and Coward, 1999). However, some studies observed stronger relationship of diurnal N_2O flux with photosynthetically active radiation (PAR) and solar radiation instead, and posited that PAR-driven plant metabolic belowground C allocation was the drivers of diurnal patterns of N_2O flux (Christensen, 1983; Keane et al., 2018; Shurpali et al., 2016; Zona et al., 2013). In Chapters 4 and 5 reduced PAR and solar radiation levels were demonstrated to shift the peak timing of N_2O flux from late afternoon (16:00 – 19:59) to early afternoon (12:00 – 15:59), implying that PAR-driven plant metabolism can determine the peak timing of N_2O flux. As current research has not yet investigated the diurnal effects of reduced photosynthesis on the peak timing of diurnal N_2O flux, little is known about the mechanisms behind this phenomenon. Kuzyakov and Cheng (2001) observed asynchronous diurnal rhythms of soil respiration of root-derived C from planted soil in prolonged dark periods, which could offer an explanation to the peak time shift of N_2O flux caused by reduced photosynthesis.

While common, daytime peaking of N_2O flux does not occur consistently under field conditions, which may be attributed to the interruption by non-diurnal events such as rainfall and fertilisation. Prolonged periods (lasting over one day) of high N_2O emissions from recently fertilised soils have been observed in studies following rainfall events (Francis Clar and Anex, 2019; Laville et al., 1999). This is due to the increase in soil moisture during and after rainfall events leading reduce soil aeration, which subsequently stimulates microbial denitrification (Butterbach-Bahl et al., 2013; Cardenas et al., 2017). The observations of increased frequency of daytime peaking of N_2O flux in Chapter 5 (75 – 84% of the occurrences, Section 5.5.1), where temporal fluctuations of soil moisture kept at near-constant in a controlled environment, provide empirical evidence supporting the interruptive effect of rainfall events on diurnal patterns of N_2O flux.

It should also be noted that daytime peaking of N_2O flux is not always the dominant diurnal pattern. Chapter 2 revealed that night-time peaking of N_2O flux was exhibited more commonly in poorly drained soils, accounting for 67% of the occurrences (Figure 2.3a, Chapter 2). This hints at the controls of soil physical properties such as porosity and gas diffusivity over the diurnal patterns of N_2O flux. Since poorly-drained soils have lower levels of gas diffusivity than well drained and imperfectly drained soils (Fujikawa and Miyazaki, 2005), which restricts the O_2 supply from the atmosphere into the soil upon O_2 consumption by plant roots and microbial aerobic respiration (Deepagoda et al., 2011). it is possible that in poorly-drained soils, during daytime when microbial activity is higher (Nakadai et al., 2002; Parkin and Kaspar, 2003), localised anoxic sites are created where produced N_2O are further reduced into N_2 by complete denitrification (Figure 1.3, Chapter 1), resulting in lower N_2O flux during daytime. In the field study by Keane et al. (2019), night-time peaking of N_2O flux with N_2O uptake during daytime were consistently observed from a poorly-drained soil (fine silt over clay), even under dry conditions. This supports the hypothesis proposed above, since N_2O uptake can only be the result of N_2O consumption overtaking N_2O production.

6.3 Implications of diurnal variability of N_2O flux on current measurement practices

High diurnal amplitudes of N_2O flux were observed throughout Chapter 3 to 5. For example, 87% of the measurement days in Chapter 3 exhibited diurnal amplitude of N_2O flux of > 100% (Section 3.4, Chapter 3). As mentioned previously, diurnal patterns of N_2O flux can be irregular under field conditions, which could impact the accuracy of cumulative N_2O emissions estimated with single-daily flux measurements. Current guidelines recommend taking N_2O flux measurements at midmorning (ca. 10:00) to capture the daily mean N_2O flux (Charteris et al., 2020; de Klein & Harvey, 2015; IAEA, 1992; Parkin & Venterea, 2010) based on the assumption that N_2O flux follows soil temperature over the diurnal courses (Alves et al., 2012b; Parkin, 2008; Smith and Dobbie, 2001). While the findings in Chapter 2 agree that measuring N_2O fluxes at 10:00 would produce the least amount of estimation bias (a mean of +2%, Figure 2.5, Chapter 2), the error range is still high (between -29% and +35%). This highlights the potential fallacy in assuming N_2O flux would follow soil temperature diurnally. Chapter 2 showed that diurnal N_2O fluxes only strongly correlate ($R > 0.7$) with soil temperature about one-third of the time (Section 2.4.2, Chapter 2). The lack

of a significant relationship between soil temperature and diurnal N_2O flux in the field campaign of Chapter 3 (Tables 3.2 and 3.3, Chapter 3) further undermines the importance of soil temperature in the regulation of diurnal variations of N_2O flux. Furthermore, some studies observed diurnal N_2O fluxes preceding before soil temperature and peaking in late-morning (Akiyama and Tsuruta, 2003; Keane et al., 2018; Peng et al., 2019), which could result in overestimations of N_2O emissions if flux measurements are made at 10:00.

At present, sub-daily flux measurements are still not considered standard practice for estimating cumulative N_2O emissions. Moreover, estimates of N_2O emissions using weekly to monthly N_2O flux measurements are still commonly reported in studies (Drewer et al., 2012, 2017; Harris et al., 2017; Hergoualc'h et al., 2020; Reinsch et al., 2020). To assess the adequacy of flux measurement frequencies, Barton et al. (2015) defined the acceptable bias for cumulative N_2O emission estimates as within ±10% of those calculated from diurnal N_2O fluxes. Using the diurnal N_2O flux data of Chapter 3, only single-daily measurements at 10:00 were found adequate in estimating cumulative N_2O emissions (+7%, Table 3.1, Chapter 3); any sampling frequencies beyond single-daily would risk under- or overestimations (-46% – +108% with weekly measurements, -75% – +90% with fortnightly measurements). Owing to the large day-to-day variations in N_2O flux, failure to capture the ephemeral episodes of high N_2O emissions (e.g., after rainfall or fertilisation events) would lead to underestimations. Likewise, gap-filling with high N_2O fluxes would result in overestimations. It should also be noted that the cumulative N_2O emissions calculated with diurnal N_2O fluxes amounted to an equivalent of 2.2% of the total N input in the span of 56 days (Section 3.4, Chapter 3), which substantially exceeded the emission factor (annual N_2O emission = 1% of total N input) recommended by the Intergovernmental Panel on Climate Change (IPCC) (Hergoualc'h et al., 2019). This may be because the current IPCC emission factor was estimated based on the data compiled in Bouwman (1996), which largely comprised of N_2O flux data collected at weekly to monthly basis. Adopting N_2O flux data of high temporal resolutions (ideally sub-daily) to estimate cumulative N_2O emissions can help improve the accuracy of N_2O emission factor.

6.4 Relationships of diurnal N_2O flux with environmental and biological parameters

An ongoing area of research regarding the diurnal variability of N_2O flux has been the identifying and understanding the drivers behind this phenomenon. Typically, diurnal variations of N_2O flux (daytime peaking) are attributed to soil temperature in a number of studies (Alves et al., 2012b; Blackmer, Robbins and Bremner, 1982; Livesley et al., 2008; van der Weerden, Clough and Styles, 2013), while only a few studies found stronger relationships between diurnal N_2O flux and photosynthetic parameters (e.g., PAR, solar radiation, net ecosystem production (NEP) and gross primary productivity (GPP)) (Christensen, 1983; Keane et al., 2018; Shurpali et al., 2016; Zona et al., 2013). While microbial denitrification is a temperature dependent process with a Q_{10} of around two to three (Christensen, 1983; Denmead et al., 1979; van der Weerden et al., 2013), which could contribute to the diurnal variations of N_2O flux as soil temperature fluctuates over the diurnal cycles, the magnitudes of diurnal variations (i.e., diurnal amplitudes) of N_2O flux are often observed to overshoot the expected diurnal amplitudes based on diurnal fluctuations of soil temperature (Christensen, 1983; Dobbie & Smith, 2003; Maljanen et al., 2002; Scheer et al., 2012; Shurpali et al., 2016; Williams et al., 1999). The analysis of historical published data in Chapter 2 found the relationship between diurnal N_2O flux and soil temperature was only strong ($R > 0.7$) in 33% of the datasets (Section 2.4.2, Chapter 2). The findings of Chapter 3 and 4 also indicated the lack of a strong relationship between diurnal N_2O flux and soil temperature ($p = 0.113$, Table 3.3, Figure 3.5b, Chapter 3), as well as between diurnal amplitude of N_2O flux and daily average soil temperature ($p = 0.026$, $\eta_p^2 = 0.003$, Table 4.5, Chapter 4). Furthermore, if diurnal variations of N_2O flux are largely driven by soil temperature, daytime soil warming should have resulted in increased diurnal amplitudes of N_2O flux, yet in Chapter 4 soil warming was found to have no significant effects on the diurnal amplitudes of N_2O flux ($p = 0.762$, Table 4.3, Chapter 4). The body of evidence in this thesis suggests the relationship between soil temperature and diurnal N_2O flux is not as strong as some literature postulated to be, or that other environmental or biological variables might be overriding the effects of diurnal fluctuations of soil temperature.

On the other hand, studies that observed stronger relationship between diurnal N_2O flux and photosynthetic parameters such as PAR proposed that by PAR could mediate the root exudation of photosynthate C (Christensen, 1983; Keane et al., 2018), which in turn enhances microbial denitrification by directly providing labile C sources to denitrifiers (Ussiri and Lal, 2013) and indirectly depleting soil O_2 through stimulation of heterotrophic respiration (Farquharson and Baldock, 2008). Evidence of increased microbial denitrification in the afternoon also supports this hypothesis (Ostrom et al., 2010; Yamulki et al., 2001). While PAR-driven diurnal changes of soil biochemical properties (e.g., labile C content in root exudates) were not measured in the experimental chapters of this thesis, the relationship between diurnal N_2O flux and photosynthetic parameters were examined throughout Chapters 3 to 5. In Chapter 3, GPP was found to have a significantly positive relationship with diurnal N_2O flux ($p = 0.009$, Table 3.3, Figure 3.5d); whereas Chapter 4 demonstrated plant shading reduced the diurnal amplitude of N_2O flux by 34%, which alluded to the regulatory effect of PAR on diurnal amplitude of N_2O flux. However, Chapter 4 also presented seemingly conflicting evidence, as the relationship between the diurnal amplitude of N_2O flux and daily cumulative solar radiation was significantly positive ($p = 0.018$, $\eta_p^2 = 0.01$, Table 4.5, Figure 4.5d, Chapter 4) but was significantly negative with daily cumulative NEP ($p = 0.001$, $\eta_p^2 = 0.04$, Table 4.5, Figure 4.5e, Chapter 4). Since NEP is the result of GPP minus ecosystem respiration (Kirschbaum et al., 2001); the latter often reflects soil microbial activity (Phillips and Nickerson, 2015) and can be stimulated by increased C substrates (e.g., root exudation of photosynthate C and its potential priming effect) (Luo and Zhou, 2006). The negative relationship with daily cumulative NEP might hint that the diurnal amplitude of N_2O flux was positively affected by daily cumulative ecosystem respiration rather than daily cumulative GPP. Chapter 5 also provided empirical evidence supporting the positive effect of photosynthetic parameters on the diurnal N_2O flux. When fluctuations of soil temperature and moisture were minimised, increased PAR level was shown to heighten the diurnal amplitude of N_2O flux (Figure 5.6c, Chapter 5).

As expected, soil volumetric water content (VWC) was found to positively regulate diurnal N_2O flux ($p < 0.001$, Figure 3.5a, Chapter 3), as well as its amplitude ($p = 0.002$, Figure 4.5b, Chapter 4). As previously discussed, increasing soil moisture can enhance denitrification by limiting replenishment of soil O_2 from the atmosphere, which would lead to increased N_2O production (Butterbach-Bahl et al., 2013; Schindlbacher, Zechmeister-Boltenstern and

Butterbach-Bahl, 2004). In addition, recent studies have also found that by increasing soil moisture, priming of N_2O could be triggered as the decomposition of soil organic matter releases additional N into the N-cycle which are rapidly denitrified (Roman-Perez and Hernandez-Ramirez, 2021; Thilakarathna and Hernandez-Ramirez, 2021). However, since soil VWC did not show distinctive diurnal patterns in the experiments of this thesis, it was not likely to cause daytime peaking of N_2O flux; rather, the non-diurnal fluctuations of VWC caused by rainfall events interrupted the diurnal patterns of N_2O flux.

6.5 Future work

As the results in this thesis indicate that diurnal amplitude and daytime peaking of N_2O flux were contributed PAR-driven plant belowground metabolism, the overarching question here is: *how do diurnal rhythms of plant metabolism affect diurnal variations of soil N_2O flux?*

Firstly, understanding the diurnal patterns of root exudation of plant primary metabolites (e.g., sugars and amino acids), and their responses to different PAR intensities, could provide useful insight into how microbial denitrification might be regulated over the diurnal courses, as well as address the phenomenon of shifting diurnal N_2O flux peak time potentially caused by plant metabolism. It has been shown that over 60% of N_2O emitted from planted soil originates from the rhizosphere (Xing et al., 2021); however, current research has yet to investigate the diurnal variations in the biochemical compositions within the rhizosphere, which limits deeper understanding of the topic.

Secondly, as microbial denitrification is driven by soil O_2 limitation, monitoring the diurnal variations in soil O_2 concentration could help answer part of the question, as root exudation of photosynthate C could drive diurnal variations in soil O_2 concentration via transient stimulation of heterotrophic respiration. While studies involving diurnal monitoring of O_2 concentration in flooded ecosystems such as wetland and paddy field are abundant (Jørgensen, Struwe and Elberling, 2012; Nikolausz et al., 2008; Zhao et al., 2021), very little research on the diurnal variations of soil O_2 has been conducted on non-flooded cropland and grassland soils. This could be coupled with diurnal flux measurements of ^{13}C-CO_2 from soil under plants pulse-labelled with ^{13}C-CO_2 to trace the lag time between photosynthesis and the arrival and respiration of photosynthate C in the rhizosphere (Griffiths et al., 2004; Kuzyakov and Cheng, 2001). Thirdly, the diurnal dynamics of denitrification and nitrification

could also be explored by measurements of the $\delta^{15}N$ site preference of diurnal N_2O fluxes after the application of ^{15}N-labelled N substrate (Bracken et al., 2021; Ostrom et al., 2010).

By teasing out the underpinning mechanisms involved in the diurnal variability of N_2O flux, a holistic understanding of this phenomenon can be established. This can then improve N_2O flux sampling strategies and accuracy of cumulative N_2O emission estimates. Besides, novel mitigation strategies may be developed on basis of new knowledge on the diurnal variability of N_2O flux. For example, Keane et al. (2019) observed net N_2O uptake during daytime in *Miscanthus* plantations. Understanding the causes of daytime N_2O uptake could provide potential N_2O sinks in agriculture.

6.6 Conclusion

This thesis provides strong evidence that diurnal variability of N_2O flux is prevalent in agricultural soils, with daytime peaking of N_2O flux being a common occurrence. However, under field conditions, diurnal patterns of N_2O flux can be inconsistent owing to interruptions by rainfall events. Due to this inconsistency, single-daily measurements of N_2O flux can still produce uncertain estimates of N_2O emission. If necessary, single-daily measurements of N_2O flux should be conducted in midmorning at 10:00. Apart from diurnal variability, N_2O flux also exhibited large day-to-day variations, making cumulative N_2O emissions estimates based on flux measurements beyond single-daily would result in highly uncertain estimates.

The results from this research also challenge the typical viewpoint that diurnal fluctuations of soil temperature are the driving factor of diurnal variations in N_2O flux. Little relationship was found between diurnal N_2O flux and soil temperature, and increasing the diurnal amplitude of soil temperature via soil warming did not increase that of N_2O flux with significance. Instead, evidence from the laboratory experiment (Chapter 5) indicated that PAR-driven plant metabolism caused diurnal variations of N_2O flux with highly consistent daytime peaking patterns.

However, knowledge of the underlying mechanisms is still not fully-established and would require further investigations of the diurnal changes in soil biochemical properties, such as substrate availability of labile C and inorganic N and soil O_2 concentration, to elucidate the PAR-driven diurnal variability of N_2O flux. A better understanding of the drivers of diurnal variability of N_2O flux could potentially improve strategies for estimating cumulative N_2O emissions and N_2O budget calculations by reducing the uncertainty of current methods.

Appendix I

Appendix I

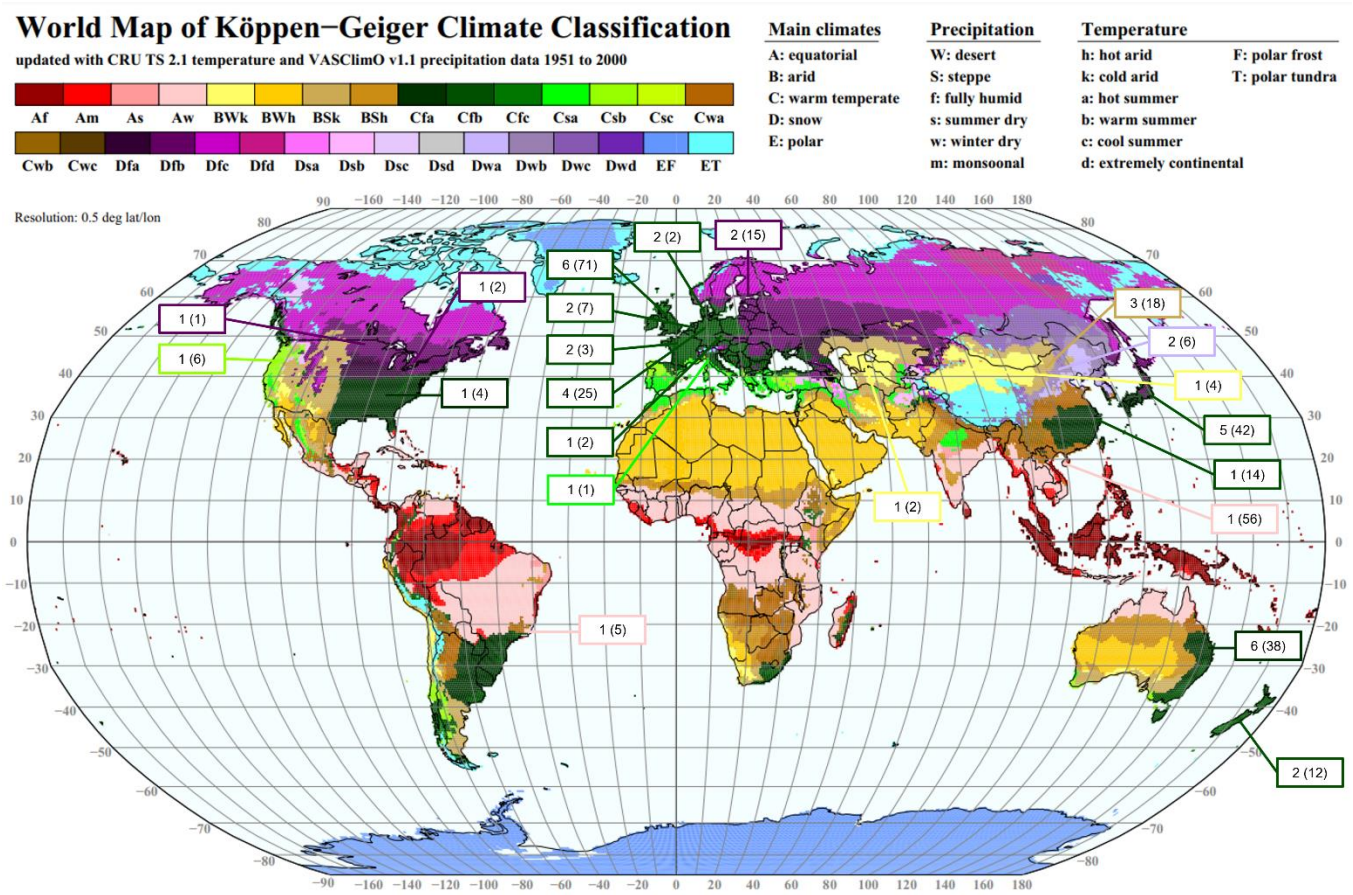

Figure A.1 World map of Köppen-Geiger climate classification (obtained from Kottek et al. (2006)), superimposed with number of reviewed studies (in coloured boxes) and datasets (in brackets) in Chapter 2. Coloured line and boxes indicate locations of studies and their climate classifications, respectively.

Table A.1 Details of non-diurnal factors of each reviewed study in Chapter 2; extracted non-diurnal factors include soil pH, bulk density (BD), texture, measurement season, nitrogen (N) fertilisation, location of study site and the Köppen-Geiger climate classification of the study site.

Reference	Number of datasets	Soil pH	Soil BD (g cm^{-3})	Soil texture	Soil WFPS	Season	N fert.	Land use	Location	Köppen -Geiger
Akiyama et al. (2000)	10	5.9	0.9	NA	35-54.9%	summer	fertilised	cropland	Tsukuba, Japan	Cfb
Akiyama and Tsuruta (2002)	10	5.9	0.9	NA	35-54.9%	summer	fertilised	cropland	Tsukuba, Japan	Cfb
Akiyama and Tsuruta (2003a)	7	5.9	0.9	NA	35-54.9%	summer	fertilised	cropland	Tsukuba, Japan	Cfb
Akiyama and Tsuruta (2003b)	5	5.9	0.9	NA	35-54.9%	summer	fertilised	cropland	Tsukuba, Japan	Cfb
Alves et al.(2012)	5	5.4	1.3	sandy	NA	autumn	fertilised	grassland	Seropédica, Brazil	Aw
Ball et al. (1999)	58	NA	1.2	loam	NA	spring	fertilised	cropland	Edinburgh, UK	Cfb
Brumme and Beese (1992)	16	3	NA	NA	NA	summer	fertilised	forest	Solling, Germany	Cfb
Brummer et al. (2017)*	2	NA	NA	sandy loam (Roskilde), silty sand (Braunschweig)	NA	spring (Roskilde), winter (Braunschweig)	fertilised	cropland, grassland	Braunschweig, Germany (1)/Roskilde, Denmark (1)	Cfb
Christensen (1983)	1	5.3	NA	sandy loam	NA	summer	fertilised	grassland	Lyngby, Denmark	Cfb

Das et al. (2012)	8	NA	1.3	silt loam	35-54.9%	NA	fertilised	grassland	Christchurch, New Zealand	Cfb
Denmead et al. (2010)*	1	5	NA	clay loam	55-74.9%	spring	fertilised	cropland	Northern New South Wales, Australia	Cfa
Du et al. (2006)	4	69	NA	sandy loam	<=34.9% (graph 1, 2, 4), 35-55% (graph 3)	summer, autumn	unfertilised	grassland	Xilin, China	BSk
Flessa et al. (2002)	4	5.9	1.2	silt loam	NA	NA	fertilised	grassland	Scheyern, Germany	Cfb
Hosono et al. (2006)	10	6.5	NA	NA	NA	spring	fertilised	cropland	Nagoya, Japan	Cfb
Huang et al. (2014)	4	NA	NA	silt loam	<=34.9%	spring, summer	fertilised	cropland	Nolensville, TN, USA	Cfa
Keane et al. (2018)	2	NA	1.3	NA	55-74.9%	spring	fertilised	cropland	Lincolnshire, UK	Cfb
Kostyanovsky et al. (2019)	6	5.9	1.2	NA	<=34.9% (dry), >=75% (wet)	summer	fertilised	cropland	Moro, OR, USA	Csb
Laville et al. (1997)*	1	6	NA	loam	55-74.9%	autumn	fertilised	cropland	Pisa, Italy	Csa
Laville et al. (2011)*	1	8.3	1.3	silt loam	35-54.9%	spring	fertilised	cropland	Burgundy, France	Cfb
Laville et al. (2017)*	2	7.7	1.3	silty clay	55-74.9%	summer	fertilised	cropland	Grignon, France	Cfb
Liu et al. (2010)	1	8	1.2	silty clay loam	NA	NA	fertilised	cropland	Shanxi, China	Dwa

Liu et al. (2014)*	5	NA	NA	NA	<=34.9% (cotton year 1-2, wheat maize year 1-2), 35-55% (wheat maize year 3)	NA	fertilised	cropland	Shanxi, China	Dwa
Loftfield et al. (1992)	4	NA	NA	NA	NA	summer	unfertilised	forest	Solling, Germany	Cfb
Lognoul et al. (2019)*	2	NA	NA	silt loam	55-74.9% (spring), 35-54.9% (summer)	spring, summer	fertilised	cropland	Uccle, Belgium	Cfb
Machado et al. (2019)	2	NA	NA	NA	NA	spring	fertilised	cropland	Elora, Ontario, Canada	Dfb
Maljanen et al. (2002)*	13	NA	0.9	NA	NA	summer	fertilised, unfertilised	cropland, grassland, forest	Savonlinna, Finland	Dfb
Peng et al. (2019)	4	5.9	NA	NA	>=75% (spring)	spring, summer	unfertilised	forest	Turpan, China	BWk
Reeves and Wang (2015)*	6	NA	NA	clay loam	NA	NA	fertilised	cropland	Warwick, Queensland, Australia	Cfa
Reeves et al. (2016)*	8	NA	NA	loamy sand (site 1), sandy clay (site 2), silty clay (site 3)	NA	summer	fertilised	cropland	Ingham/Mackay/Bundaberg, Queensland, Australia	Cfa

Savage et al. (2014)*	1	5.7	NA	silt loam	55-74.9%	spring	fertilised	cropland	Mandan, ND, USA	Dfb
Scheer et al. (2008)	2	6.5	1.5	sandy loam	55-74.9%	summer	fertilised	cropland	Urgench, Uzbekistan	BWk
Scheer et al. (2012)	18	7.2	NA	clay	55-74.9%	summer	fertilised	cropland	Toowoomba, Queensland, Australia	Cfa
Scheer et al. (2013)*	1	7.2	NA	clay	55-74.9%	summer	fertilised	cropland	Darling Downs, Queensland, Australia	Cfa
Scheer et al. (2014)	4	7.4	NA	sandy loam	55-74.9%	summer	fertilised	cropland	Gatton, Queensland, Australia	Cfa
Shurpali et al. (2016)*	2	5.8	1.1	clay loam	55-74.9% (spring), 35-54.9% (summer)	spring, summer	fertilised	cropland	Maaninka, Finland	Dfb
Simek et al. (2010)	2	7.3	NA	sandy loam	NA	spring	fertilised	grassland	Borová, Czech Republic	Cfb
Skiba et al. (1996)	2	NA	NA	sandy clay loam	NA	summer	fertilised	cropland	East Lothian, UK	Cfb
Smith et al. (1995)	2	NA	NA	sandy loam	NA	summer	fertilised	grassland	Edinburgh, UK	Cfb
Smith et al. (1998)	4	5.7 (sandy loam), 3.7 (peaty gley)	NA	sandy loam, peaty gley	NA	summer	fertilised	cropland, forest	Midlothian/Northumberland, UK	Cfb

van der Weerden et al. (2013)	4	5.8	1	silt loam	55-74.9%	spring	fertilised	grassland	Mosgiel, New Zealand	Cfb
Wang et al. (2005)	8	6.6	NA	NA	<=34.9%	summer	unfertilised	grassland	Xilin, China	BSk
Williams et al. (1999)	3	8.6	NA	NA	NA	spring	fertilised	grassland	Grange-over-Sands, UK	Cfb
Yang et al. (2018)	6	NA	NA	NA	<=34.9%	summer	unfertilised	forest	Hainan, China	Aw
Yao et al. (2009)	14	8	1.2	sandy loam	55-74.9%	autumn	fertilised	cropland	Jiangdu, China	Cfb
Yeboah et al. (2018)	6	8.4	1.2	sandy loam	NA	spring	fertilised	cropland	Dingxi, China	BSk
Zona et al. (2013)*	5	NA	NA	sandy	55-74.9%	summer, autumn	fertilised	cropland	Lochristi, Belgium	Cfb
*** = study presented diurnal course(s) of average N_2O flux over a period of measurement days**										
NA = data not available										

Appendix II

Daily and total cumulative N_2O emissions:

Date	Sub-daily	Daily 10:00	Every 3 days at 10:00			Weekly at 10:00						
			Scenario 1	Scenario 2	Scenario 3	Scecario 1	Scecario 2	Scecario 3	Scecario 4	Scecario 5	Scecario 6	Scecario 7
26/07/2018	0.27	0.451	0.451	0.451	0.451	0.451	0.451	0.451	0.451	0.451	0.451	0.451
27/07/2018	1.874	0.397	0.397	0.451	0.451	0.397	0.451	0.451	0.451	0.451	0.451	0.451
31/07/2018	4.818	6.41	0.397	6.41	0.451	0.397	6.41	0.451	0.451	0.451	0.451	0.451
01/08/2018	3.391	2.437	0.397	6.41	2.437	0.397	6.41	2.437	0.451	0.451	0.451	0.451
02/08/2018	2.992	3.65	3.65	6.41	2.437	0.397	6.41	2.437	3.65	0.451	0.451	0.451
03/08/2018	3.155	2.667	3.65	3.65	2.437	0.397	6.41	2.437	3.65	2.667	0.451	0.451
04/08/2018	2.923	4.432	3.65	3.65	4.432	0.397	6.41	2.437	3.65	2.667	4.432	0.451
05/08/2018	1.406	1.429	1.429	3.65	4.432	0.397	6.41	2.437	3.65	2.667	4.432	1.429
06/08/2018	0.671	0.628	1.429	0.628	4.432	0.628	6.41	2.437	3.65	2.667	4.432	1.429
07/08/2018	0.677	1.086	1.429	0.628	1.086	0.628	1.086	2.437	3.65	2.667	4.432	1.429
08/08/2018	0.539	0.524	0.524	0.628	1.086	0.628	1.086	0.524	3.65	2.667	4.432	1.429
09/08/2018	0.307	0.195	0.524	0.195	1.086	0.628	1.086	0.524	0.195	2.667	4.432	1.429
10/08/2018	0.379	0.845	0.524	0.195	0.845	0.628	1.086	0.524	0.195	0.845	4.432	1.429
11/08/2018	0.126	0.162	0.162	0.195	0.845	0.628	1.086	0.524	0.195	0.845	0.162	1.429
13/08/2018	0.564	1.208	0.162	1.208	0.845	0.628	1.086	0.524	0.195	0.845	0.162	1.208
14/08/2018	0.684	1.086	0.162	1.208	1.086	1.086	1.086	0.524	0.195	0.845	0.162	1.208
15/08/2018	0.307	0.736	0.736	1.208	1.086	1.086	1.086	0.736	0.195	0.845	0.162	1.208
16/08/2018	0.163	0.582	0.736	0.582	1.086	1.086	1.086	0.736	0.582	0.845	0.162	1.208
17/08/2018	0.181	0.266	0.736	0.582	0.266	1.086	1.086	0.736	0.582	0.266	0.162	1.208
18/08/2018	0.226	0.179	0.179	0.582	0.266	1.086	1.086	0.736	0.582	0.266	0.179	1.208
19/08/2018	0.593	1.156	0.179	1.156	0.266	1.086	1.086	0.736	0.582	0.266	0.179	1.694
20/08/2018	1.003	1.694	0.179	1.156	1.694	1.694	1.086	0.736	0.582	0.266	0.179	1.694
21/08/2018	1.209	2.729	2.729	1.156	1.694	1.694	2.729	0.736	0.582	0.266	0.179	1.694
22/08/2018	2.98	1.132	2.729	1.132	1.694	1.694	2.729	1.132	0.582	0.266	0.179	1.694
23/08/2018	4.702	6.343	2.729	1.132	6.343	1.694	2.729	1.132	6.343	0.266	0.179	1.694
24/08/2018	1.504	1.299	1.299	1.132	6.343	1.694	2.729	1.132	6.343	1.299	0.179	1.694
25/08/2018	2.767	2.959	1.299	2.959	6.343	1.694	2.729	1.132	6.343	1.299	2.959	1.694
26/08/2018	1.22	1.08	1.299	2.959	1.08	1.694	2.729	1.132	6.343	1.299	2.959	1.08
27/08/2018	2.309	3.106	3.106	2.959	1.08	3.106	2.729	1.132	6.343	1.299	2.959	1.08
28/08/2018	2.709	3.468	3.106	3.468	1.08	3.106	3.468	1.132	6.343	1.299	2.959	1.08
29/08/2018	1.621	1.858	3.106	3.468	1.858	3.106	3.468	1.858	6.343	1.299	2.959	1.08
30/08/2018	1.692	1.17	1.17	3.468	1.858	3.106	3.468	1.858	1.17	1.299	2.959	1.08
31/08/2018	0.935	0.518	1.17	0.518	1.858	3.106	3.468	1.858	1.17	0.518	2.959	1.08
01/09/2018	0.533	0.328	1.17	0.518	0.328	3.106	3.468	1.858	1.17	0.518	0.328	1.08
02/09/2018	0.347	0.543	0.543	0.518	0.328	3.106	3.468	1.858	1.17	0.518	0.328	0.543
03/09/2018	1.447	1.118	0.543	1.118	0.328	1.118	3.468	1.858	1.17	0.518	0.328	0.543
04/09/2018	2.024	2.976	0.543	1.118	2.976	1.118	2.976	1.858	1.17	0.518	0.328	0.543
05/09/2018	0.929	0.986	0.986	1.118	2.976	1.118	2.976	0.986	1.17	0.518	0.328	0.543
06/09/2018	0.547	1.083	0.986	1.083	2.976	1.118	2.976	0.986	1.083	0.518	0.328	0.543
07/09/2018	0.183	0.174	0.986	1.083	0.174	1.118	2.976	0.986	1.083	0.174	0.328	0.543
08/09/2018	0.19	-0.054	-0.054	1.083	0.174	1.118	2.976	0.986	1.083	0.174	-0.054	0.543
09/09/2018	0.166	-0.228	-0.054	-0.228	0.174	1.118	2.976	0.986	1.083	0.174	-0.054	-0.228
10/09/2018	0.127	-0.111	-0.054	-0.228	-0.111	-0.111	2.976	0.986	1.083	0.174	-0.054	-0.228
12/09/2018	5.466	6.987	6.987	-0.228	-0.111	-0.111	6.987	0.986	1.083	0.174	-0.054	-0.228
13/09/2018	2.475	2.158	6.987	2.158	-0.111	-0.111	6.987	2.158	1.083	0.174	-0.054	-0.228
14/09/2018	4.118	3.963	6.987	2.158	3.963	-0.111	6.987	2.158	3.963	0.174	-0.054	-0.228
15/09/2018	0.412	0.475	0.475	2.158	3.963	-0.111	6.987	2.158	3.963	0.475	-0.054	-0.228
16/09/2018	2.24	0.141	0.475	0.141	3.963	-0.111	6.987	2.158	3.963	0.475	0.141	-0.228
17/09/2018	1.586	0.299	0.475	0.141	0.299	-0.111	6.987	2.158	3.963	0.475	0.141	0.299
18/09/2018	2.171	2.052	2.052	0.141	0.299	2.052	6.987	2.158	3.963	0.475	0.141	0.299
19/09/2018	0.588	0.524	2.052	0.524	0.299	2.052	0.524	2.158	3.963	0.475	0.141	0.299
20/09/2018	0.882	1.205	2.052	0.524	1.205	2.052	0.524	1.205	3.963	0.475	0.141	0.299
21/09/2018	1.242	0.663	0.663	0.524	1.205	2.052	0.524	1.205	0.663	0.475	0.141	0.299
22/09/2018	2.869	2.809	0.663	2.809	1.205	2.052	0.524	1.205	0.663	2.809	0.141	0.299
23/09/2018	2.319	3.024	0.663	2.809	3.024	2.052	0.524	1.205	0.663	2.809	3.024	0.299
24/09/2018	0.819	1.41	1.41	2.809	3.024	2.052	0.524	1.205	0.663	2.809	3.024	1.41
sum	**84.6**	**90.4**	**83.0**	**89.4**	**97.3**	**69.2**	**176.2**	**75.7**	**123.2**	**53.5**	**65.6**	**45.5**
bias (%)	**0.0**	**6.9**	**-1.9**	**5.7**	**15.0**	**-18.2**	**108.3**	**-10.5**	**45.6**	**-36.7**	**-22.4**	**-46.2**

Appendix II

Date	Fortnightly at 10:00													
	Scenario 1	Scenario 2	Scenario 3	Scenario 4	Scenario 5	Scenario 6	Scenario 7	Scenario 8	Scenario 9	Scenario 10	Scenario 11	Scenario 12	Scenario 13	Scenario 14
26/07/2018	0.451	0.451	0.451	0.451	0.451	0.451	0.451	0.451	0.451	0.451	0.451	0.451	0.451	0.451
27/07/2018	0.397	0.451	0.451	0.451	0.451	0.451	0.451	0.451	0.451	0.451	0.451	0.451	0.451	0.451
31/07/2018	0.397	6.41	0.451	0.451	0.451	0.451	0.451	0.451	0.451	0.451	0.451	0.451	0.451	0.451
01/08/2018	0.397	6.41	2.437	0.451	0.451	0.451	0.451	0.451	0.451	0.451	0.451	0.451	0.451	0.451
02/08/2018	0.397	6.41	2.437	3.65	0.451	0.451	0.451	0.451	0.451	0.451	0.451	0.451	0.451	0.451
03/08/2018	0.397	6.41	2.437	3.65	2.667	0.451	0.451	0.451	0.451	0.451	0.451	0.451	0.451	0.451
04/08/2018	0.397	6.41	2.437	3.65	2.667	4.432	0.451	0.451	0.451	0.451	0.451	0.451	0.451	0.451
05/08/2018	0.397	6.41	2.437	3.65	2.667	4.432	1.429	0.451	0.451	0.451	0.451	0.451	0.451	0.451
06/08/2018	0.397	6.41	2.437	3.65	2.667	4.432	1.429	0.628	0.451	0.451	0.451	0.451	0.451	0.451
07/08/2018	0.397	6.41	2.437	3.65	2.667	4.432	1.429	0.628	1.086	0.451	0.451	0.451	0.451	0.451
08/08/2018	0.397	6.41	2.437	3.65	2.667	4.432	1.429	0.628	1.086	0.524	0.451	0.451	0.451	0.451
09/08/2018	0.397	6.41	2.437	3.65	2.667	4.432	1.429	0.628	1.086	0.524	0.195	0.451	0.451	0.451
10/08/2018	0.397	6.41	2.437	3.65	2.667	4.432	1.429	0.628	1.086	0.524	0.195	0.845	0.451	0.451
11/08/2018	0.397	6.41	2.437	3.65	2.667	4.432	1.429	0.628	1.086	0.524	0.195	0.845	0.162	0.451
13/08/2018	0.397	6.41	2.437	3.65	2.667	4.432	1.429	0.628	1.086	0.524	0.195	0.845	0.162	1.208
14/08/2018	1.086	6.41	2.437	3.65	2.667	4.432	1.429	0.628	1.086	0.524	0.195	0.845	0.162	1.208
15/08/2018	1.086	0.736	2.437	3.65	2.667	4.432	1.429	0.628	1.086	0.524	0.195	0.845	0.162	1.208
16/08/2018	1.086	0.736	0.582	3.65	2.667	4.432	1.429	0.628	1.086	0.524	0.195	0.845	0.162	1.208
17/08/2018	1.086	0.736	0.582	0.266	2.667	4.432	1.429	0.628	1.086	0.524	0.195	0.845	0.162	1.208
18/08/2018	1.086	0.736	0.582	0.266	0.179	4.432	1.429	0.628	1.086	0.524	0.195	0.845	0.162	1.208
19/08/2018	1.086	0.736	0.582	0.266	0.179	1.156	1.429	0.628	1.086	0.524	0.195	0.845	0.162	1.208
20/08/2018	1.086	0.736	0.582	0.266	0.179	1.156	1.694	0.628	1.086	0.524	0.195	0.845	0.162	1.208
21/08/2018	1.086	0.736	0.582	0.266	0.179	1.156	1.694	2.729	1.086	0.524	0.195	0.845	0.162	1.208
22/08/2018	1.086	0.736	0.582	0.266	0.179	1.156	1.694	2.729	1.132	0.524	0.195	0.845	0.162	1.208
23/08/2018	1.086	0.736	0.582	0.266	0.179	1.156	1.694	2.729	1.132	6.343	0.195	0.845	0.162	1.208
24/08/2018	1.086	0.736	0.582	0.266	0.179	1.156	1.694	2.729	1.132	6.343	1.299	0.845	0.162	1.208
25/08/2018	1.086	0.736	0.582	0.266	0.179	1.156	1.694	2.729	1.132	6.343	1.299	2.959	0.162	1.208
26/08/2018	1.086	0.736	0.582	0.266	0.179	1.156	1.694	2.729	1.132	6.343	1.299	2.959	1.08	1.208
27/08/2018	1.086	0.736	0.582	0.266	0.179	1.156	1.694	2.729	1.132	6.343	1.299	2.959	1.08	3.106
28/08/2018	3.468	0.736	0.582	0.266	0.179	1.156	1.694	2.729	1.132	6.343	1.299	2.959	1.08	3.106
29/08/2018	3.468	1.858	0.582	0.266	0.179	1.156	1.694	2.729	1.132	6.343	1.299	2.959	1.08	3.106
30/08/2018	3.468	1.858	1.17	0.266	0.179	1.156	1.694	2.729	1.132	6.343	1.299	2.959	1.08	3.106
31/08/2018	3.468	1.858	1.17	0.518	0.179	1.156	1.694	2.729	1.132	6.343	1.299	2.959	1.08	3.106
01/09/2018	3.468	1.858	1.17	0.518	0.328	1.156	1.694	2.729	1.132	6.343	1.299	2.959	1.08	3.106
02/09/2018	3.468	1.858	1.17	0.518	0.328	0.543	1.694	2.729	1.132	6.343	1.299	2.959	1.08	3.106
03/09/2018	3.468	1.858	1.17	0.518	0.328	0.543	1.118	2.729	1.132	6.343	1.299	2.959	1.08	3.106
04/09/2018	3.468	1.858	1.17	0.518	0.328	0.543	1.118	2.976	1.132	6.343	1.299	2.959	1.08	3.106
05/09/2018	3.468	1.858	1.17	0.518	0.328	0.543	1.118	2.976	0.986	6.343	1.299	2.959	1.08	3.106
06/09/2018	3.468	1.858	1.17	0.518	0.328	0.543	1.118	2.976	0.986	1.083	1.299	2.959	1.08	3.106
07/09/2018	3.468	1.858	1.17	0.518	0.328	0.543	1.118	2.976	0.986	1.083	0.174	2.959	1.08	3.106
08/09/2018	3.468	1.858	1.17	0.518	0.328	0.543	1.118	2.976	0.986	1.083	0.174	-0.054	1.08	3.106
09/09/2018	3.468	1.858	1.17	0.518	0.328	0.543	1.118	2.976	0.986	1.083	0.174	-0.054	-0.228	3.106
10/09/2018	3.468	1.858	1.17	0.518	0.328	0.543	1.118	2.976	0.986	1.083	0.174	-0.054	-0.228	-0.111
12/09/2018	6.987	1.858	1.17	0.518	0.328	0.543	1.118	2.976	0.986	1.083	0.174	-0.054	-0.228	-0.111
13/09/2018	6.987	2.158	1.17	0.518	0.328	0.543	1.118	2.976	0.986	1.083	0.174	-0.054	-0.228	-0.111
14/09/2018	6.987	2.158	3.963	0.518	0.328	0.543	1.118	2.976	0.986	1.083	0.174	-0.054	-0.228	-0.111
15/09/2018	6.987	2.158	3.963	0.475	0.328	0.543	1.118	2.976	0.986	1.083	0.174	-0.054	-0.228	-0.111
16/09/2018	6.987	2.158	3.963	0.475	0.141	0.543	1.118	2.976	0.986	1.083	0.174	-0.054	-0.228	-0.111
17/09/2018	6.987	2.158	3.963	0.475	0.141	0.299	1.118	2.976	0.986	1.083	0.174	-0.054	-0.228	-0.111
18/09/2018	6.987	2.158	3.963	0.475	0.141	0.299	2.052	2.976	0.986	1.083	0.174	-0.054	-0.228	-0.111
19/09/2018	6.987	2.158	3.963	0.475	0.141	0.299	2.052	0.524	0.986	1.083	0.174	-0.054	-0.228	-0.111
20/09/2018	6.987	2.158	3.963	0.475	0.141	0.299	2.052	0.524	1.205	1.083	0.174	-0.054	-0.228	-0.111
21/09/2018	6.987	2.158	3.963	0.475	0.141	0.299	2.052	0.524	1.205	0.663	0.174	-0.054	-0.228	-0.111
22/09/2018	6.987	2.158	3.963	0.475	0.141	0.299	2.052	0.524	1.205	0.663	2.809	-0.054	-0.228	-0.111
23/09/2018	6.987	2.158	3.963	0.475	0.141	0.299	2.052	0.524	1.205	0.663	2.809	3.024	-0.228	-0.111
24/09/2018	6.987	2.158	3.963	0.475	0.141	0.299	2.052	0.524	1.205	0.663	2.809	3.024	1.41	-0.111
sum	**160.6**	**152.9**	**103.6**	**68.6**	**48.0**	**90.9**	**76.9**	**95.4**	**54.9**	**118.5**	**36.7**	**64.0**	**21.5**	**65.2**
bias (%)	**89.9**	**80.7**	**22.5**	**-18.9**	**-43.3**	**7.5**	**-9.1**	**12.8**	**-35.0**	**40.1**	**-56.6**	**-24.4**	**-74.6**	**-23.0**

Appendix II

Correlation matrix of mean N_2O flux, ln(N_2O flux), VWC, ST, PAR and GPP:

Correlation Matrix

		Mean.N2O.flux	N2O.flux.ln	Mean.VWC	Mean.ST	Mean.PAR	Mean.GPP
Mean.N2O.flux	Pearson's r	—					
	p-value	—					
N2O.flux.ln	Pearson's r	0.766	—				
	p-value	< .001	—				
Mean.VWC	Pearson's r	0.273	0.264	—			
	p-value	< .001	< .001	—			
Mean.ST	Pearson's r	0.057	-0.035	0.082	—		
	p-value	0.296	0.535	0.131	—		
Mean.PAR	Pearson's r	0.110	0.114	-0.060	0.265	—	
	p-value	0.043	0.042	0.271	< .001	—	
Mean.GPP	Pearson's r	0.124	0.146	-0.005	0.237	0.880	—
	p-value	0.023	0.009	0.923	< .001	< .001	—

Plot

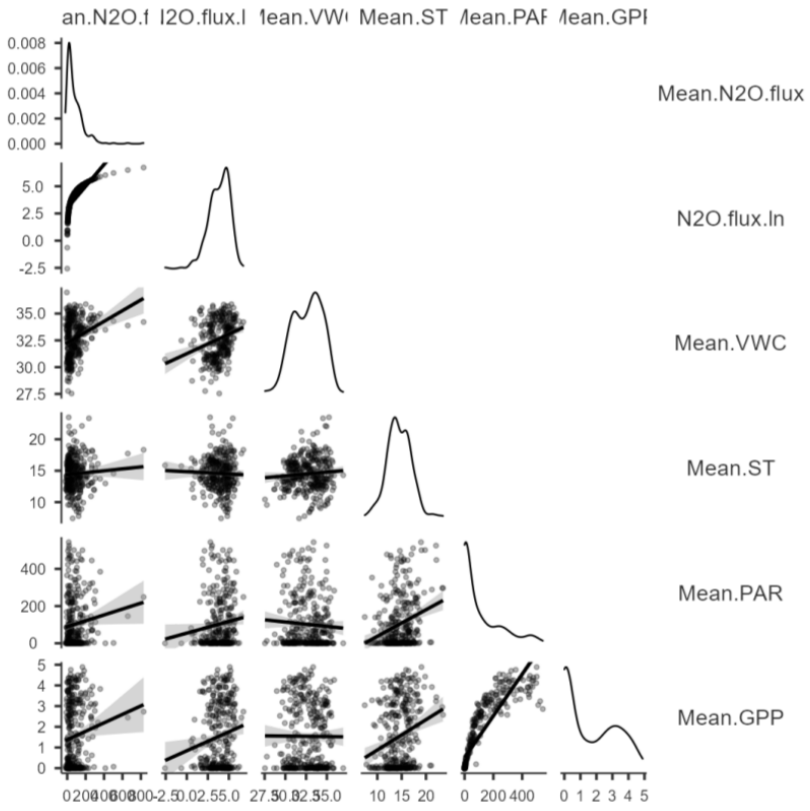

Appendix II

Summary of linear mixed-effects models (ST model, PAR model, GPP model):

Mixed Model

Model Info

Info	
Estimate	Linear mixed model fit by REML
Call	N2O_ln ~ 1 + VWC + ST+(1 | Date)
AIC	429.600
BIC	460.496
LogLikel.	-216.454
R-squared Marginal	0.112
R-squared Conditional	0.759
Converged	yes
Optimizer	bobyqa

Model Results

Fixed Effect Omnibus tests

	F	Num df	Den df	p
VWC	17.69	1	183	< .001
ST	2.53	1	194	0.113

Note. Satterthwaite method for degrees of freedom

Fixed Effects Parameter Estimates

			95% Confidence Interval				
Names	Estimate	SE	Lower	Upper	df	t	p
(Intercept)	4.2176	0.0986	4.02428	4.4109	50.5	42.76	< .001
VWC	0.1589	0.0378	0.08488	0.2330	183.1	4.21	< .001
ST	0.0382	0.0240	-0.00885	0.0852	193.9	1.59	0.113

Random Components

Groups	Name	SD	Variance	ICC
Date	(Intercept)	0.702	0.492	0.729
Residual		0.428	0.183	

Note. Number of Obs: 249 , groups: Date 56

Appendix II

Test for Normality of residuals

Test	Statistics	p
Kolmogorov-Smirnov	0.0499	0.564
Shapiro-Wilk	0.9915	0.161

Q-Q Plot

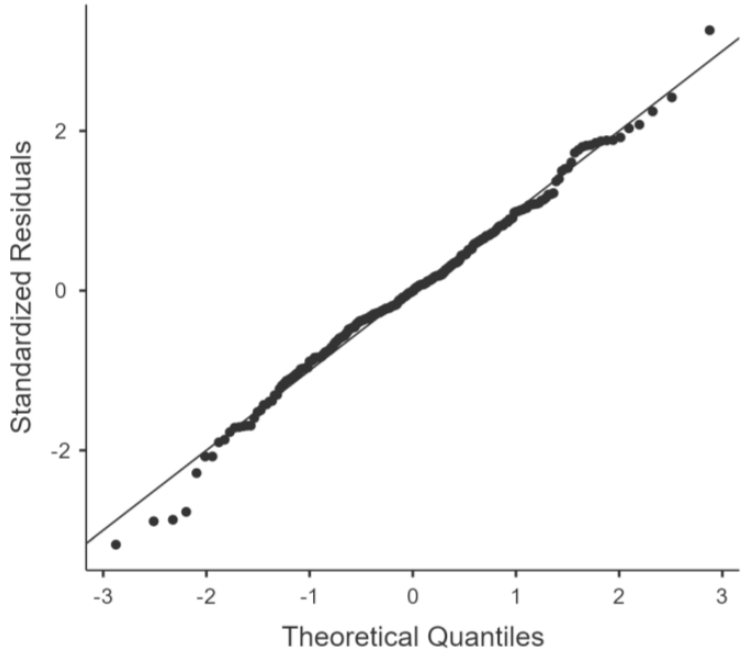

Appendix II

Mixed Model

Model Info

Info	
Estimate	Linear mixed model fit by REML
Call	N2O.flux.ln ~ 1 + VWC + PAR+(1 | Date)
AIC	327.555
BIC	351.597
LogLikel.	-162.775
R-squared Marginal	0.132
R-squared Conditional	0.766
Converged	yes
Optimizer	bobyqa

Model Results

Fixed Effect Omnibus tests

	F	Num df	Den df	p
VWC	20.31	1	150	< .001
PAR	1.48	1	155	0.226

Note. Satterthwaite method for degrees of freedom

Fixed Effects Parameter Estimates

			95% Confidence Interval				
Names	Estimate	SE	Lower	Upper	df	t	p
(Intercept)	4.244	0.0993	4.049	4.439	50.6	42.72	< .001
VWC	0.198	0.0440	0.112	0.285	150.1	4.51	< .001
PAR	0.339	0.2788	-0.207	0.885	154.5	1.22	0.226

Random Components

Groups	Name	SD	Variance	ICC
Date	(Intercept)	0.686	0.471	0.730
Residual		0.417	0.174	

Note. Number of Obs: 183 , groups: Date 54

Appendix II

Test for Normality of residuals

Test	Statistics	p
Kolmogorov-Smirnov	0.0637	0.448
Shapiro-Wilk	0.9881	0.127

Q-Q Plot

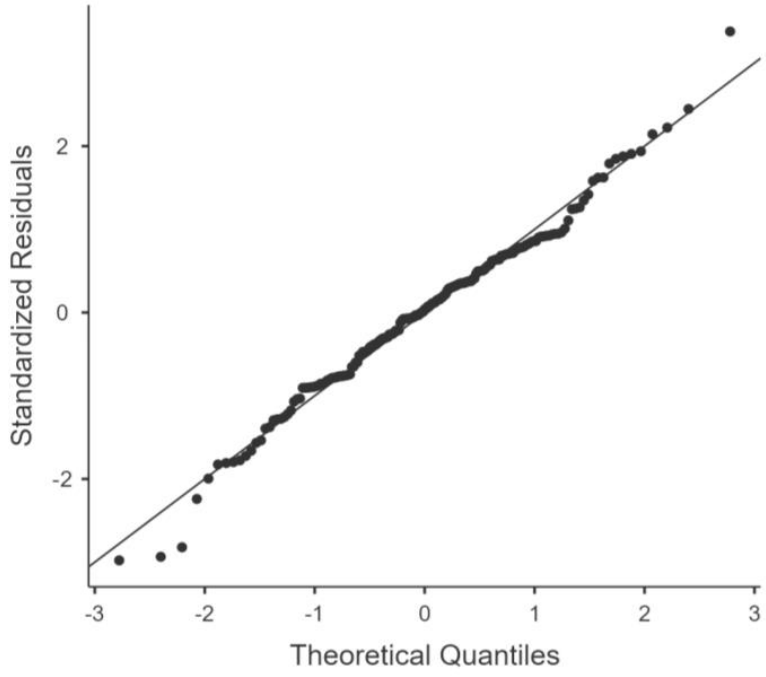

Appendix II

Mixed Model

Model Info

Info	
Estimate	Linear mixed model fit by REML
Call	N2O.flux.ln ~ 1 + VWC + GPP+(1 | Date)
AIC	296.374
BIC	324.864
LogLikel.	-149.593
R-squared Marginal	0.122
R-squared Conditional	0.784
Converged	yes
Optimizer	bobyqa

Model Results

Fixed Effect Omnibus tests

	F	Num df	Den df	p
VWC	15.85	1	144	< .001
GPP	7.04	1	138	0.009

Note. Satterthwaite method for degrees of freedom

Fixed Effects Parameter Estimates

			95% Confidence Interval				
Names	Estimate	SE	Lower	Upper	df	t	p
(Intercept)	4.2286	0.0995	4.0336	4.424	51.3	42.51	< .001
VWC	0.1745	0.0438	0.0886	0.260	144.3	3.98	< .001
GPP	0.0678	0.0256	0.0177	0.118	138.0	2.65	0.009

Random Components

Groups	Name	SD	Variance	ICC
Date	(Intercept)	0.690	0.475	0.754
Residual		0.393	0.155	

Note. Number of Obs: 170 , groups: Date 54

Appendix II

Test for Normality of residuals

Test	Statistics	p
Kolmogorov-Smirnov	0.0600	0.574
Shapiro-Wilk	0.9873	0.128

Q-Q Plot

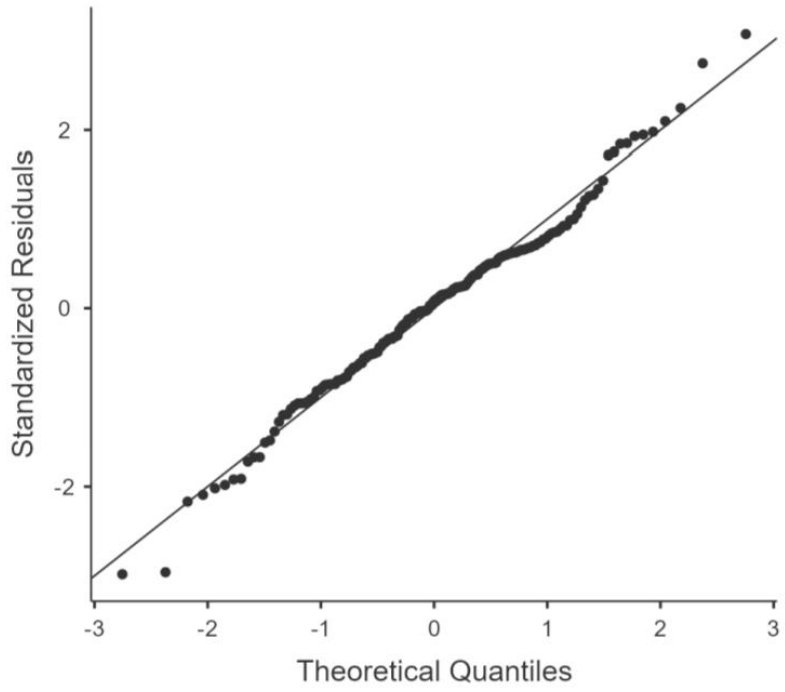

Appendix III

Summary of the pairwise comparisons of the estimated marginal means of log-transformed diurnal amplitude and daily cumulative N_2O emission between the mesocosm groups (CTRL, S, W and SW) during and outside treatment periods.

Log-transformed diurnal amplitude of N_2O flux during treatment periods

Pairwise comparisons	*Estimate*	*Standard error*	*DF*	*p-value*
CTRL – S	0.419	0.190	16	**0.042**
CTRL – W	-0.058	0.186	16	0.762
CTRL – SW	-0.074	0.189	16	0.700
S – W	-0.477	0.194	16	**0.026**
S – SW	-0.493	0.191	16	**0.020**
W – SW	-0.017	0.191	16	0.932

Log-transformed daily cumulative N_2O emission during treatment periods

Pairwise comparisons	*Estimate*	*Standard error*	*DF*	*p-value*
CTRL – S	0.362	0.207	16	0.100
CTRL – W	0.011	0.204	16	0.958
CTRL – SW	-0.106	0.201	16	0.605
S – W	-0.351	0.216	16	0.124
S – SW	-0.468	0.206	16	**0.038**
W – SW	-0.117	0.206	16	0.578

Appendix III

Model 1: Treatment effects on log-transformed diurnal amplitude of N_2O flux during treatment periods

Formula: lme(fixed = ln.inc.N2O.raw ~ avg.VWC + Shading + Warming + Shading:Warming, random = ~ 1|plot, correlation = corAR1(form = ~DOY|plot), na.action = na.omit, data = N2O_daily_on)

Summary:

	ln.inc.N2O.raw		
Predictors	*Estimates*	*CI*	*p*
(Intercept)	4.07	3.18 – 4.96	**<0.001**
avg.VWC	0.05	0.02 – 0.08	**<0.001**
Shading [Y]	-0.42	-0.82 – -0.02	**0.042**
Warming [Y]	0.06	-0.34 – 0.45	0.762
Shading [Y] * Warming [Y]	0.44	-0.13 – 1.00	0.119
Random Effects			
σ^2	0.79		
$\tau_{00\ plot}$	0.00		
ICC	0.00		
$N_{\ plot}$	20		
Observations	290		
Marginal R^2 / Conditional R^2	0.081 / 0.081		

F statistics:

	numDF	denDF	F-value	p-value
(Intercept)	1	269	7082.543	<.0001
avg.VWC	1	269	8.732	0.0034
Shading	1	16	2.032	0.1732
Warming	1	16	4.015	0.0623
Shading:Warming	1	16	2.708	0.1193

Partial eta squared:

	Eta2 (partial)	90% CI
avg.VWC	0.03	[0.01, 0.07]
Shading	0.11	[0.00, 0.38]
Warming	0.20	[0.00, 0.46]
Shading:Warming	0.14	[0.00, 0.41]

Appendix III

Estimated marginal means:

Shading	Warming	emmean	SE	df	lower.CL	upper.CL
N	N	5.63	0.131	19	5.36	5.90
Y	N	5.21	0.136	16	4.92	5.50
N	Y	5.69	0.133	16	5.41	5.97
Y	Y	5.70	0.136	16	5.42	5.99

Degrees-of-freedom method: containment

Confidence level used: 0.95

$contrasts

contrast	estimate	SE	df	t.ratio	p.value
N N - Y N	0.4192	0.190	16	2.209	0.0421
N N - N Y	-0.0575	0.186	16	-0.309	0.7616
N N - Y Y	-0.0741	0.189	16	-0.392	0.7003
Y N - N Y	-0.4766	0.194	16	-2.452	0.0261
Y N - Y Y	-0.4932	0.191	16	-2.579	0.0202
N Y - Y Y	-0.0166	0.191	16	-0.087	0.9317

Degrees-of-freedom method: containment

Appendix III

Model 2: Treatment effects on log-transformed daily cumulative N_2O emission during treatment periods

Formula: lme(fixed = ln.cum.N2O ~ avg.VWC + Shading + Warming + Shading:Warming, random = ~ 1|plot, correlation = corAR1(form = ~DOY|plot), na.action = na.omit, data = N2O_daily_on)

Summary:

	ln.cum.N2O		
Predictors	*Estimates*	*CI*	*p*
(Intercept)	5.74	4.76 – 6.73	**<0.001**
avg.VWC	0.07	0.04 – 0.10	**<0.001**
Shading [Y]	-0.36	-0.80 – 0.08	0.100
Warming [Y]	-0.01	-0.44 – 0.42	0.958
Shading [Y] * Warming [Y]	0.48	-0.13 – 1.09	0.115
Random Effects			
σ^2	0.95		
$\tau_{00\ plot}$	0.00		
ICC	0.00		
$N_{\ plot}$	20		
Observations	285		
Marginal R^2 / Conditional R^2	0.103 / 0.103		

F statistics:

	numDF	denDF	F-value	p-value
(Intercept)	1	264	12052.254	<.0001
avg.VWC	1	264	18.030	<.0001
Shading	1	16	0.506	0.4870
Warming	1	16	2.373	0.1430
Shading:Warming	1	16	2.780	0.1149

Partial eta squared:

	Eta2 (partial)	90% CI
avg.VWC	0.06	[0.02, 0.12]
Shading	0.03	[0.00, 0.26]
Warming	0.13	[0.00, 0.39]
Shading:Warming	0.15	[0.00, 0.41]

Appendix III

Estimated marginal means:

Shading	Warming	emmean	SE	df	lower.CL	upper.CL
N	N	7.94	0.141	19	7.64	8.23
Y	N	7.58	0.150	16	7.26	7.89
N	Y	7.93	0.148	16	7.61	8.24
Y	Y	8.04	0.143	16	7.74	8.35

Degrees-of-freedom method: containment

Confidence level used: 0.95

$contrasts

contrast	estimate	SE	df	t.ratio	p.value
N N - Y N	0.3617	0.207	16	1.747	0.0997
N N - N Y	0.0109	0.204	16	0.054	0.9579
N N - Y Y	-0.1062	0.201	16	-0.528	0.6048
Y N - N Y	-0.3507	0.216	16	-1.626	0.1235
Y N - Y Y	-0.4678	0.206	16	-2.268	0.0375
N Y - Y Y	-0.1171	0.206	16	-0.567	0.5784

Degrees-of-freedom method: containment

Appendix III

Model 3: Effects of environmental and biological variables on log-transformed diurnal amplitude of N_2O flux

Formula: lme(fixed = ln.inc.N2O.raw ~ avg.VWC + avg.ST + cum.SR + cum.Reco + cum.GPP, random = ~ 1|plot, correlation = corAR1(form = ~DOY|plot), na.action = na.omit, data = N2O_daily_lmer)

Model summary:

	ln.inc.N2O.raw		
Predictors	*Estimates*	*CI*	*p*
(Intercept)	4.81	3.54 – 6.08	**<0.001**
avg.VWC	0.05	0.02 – 0.08	**0.002**
avg.ST	-0.07	-0.12 – -0.01	**0.026**
cum.SR	0.10	0.02 – 0.18	**0.018**
cum.NEP	-0.02	-0.03 – -0.01	**0.001**
Random Effects			
σ^2	0.78		
$\tau_{00\ plot}$	0.04		
ICC	0.05		
$N_{\ plot}$	20		
Observations	290		
Marginal R^2 / Conditional R^2	0.090 / 0.132		

F statistics:

	numDF	denDF	F-value	p-value
(Intercept)	1	266	4830.613	<.0001
avg.VWC	1	266	8.722	0.0034
avg.ST	1	266	0.907	0.3417
cum.SR	1	266	3.265	0.0719
cum.NEP	1	266	11.500	0.0008

Appendix III

Partial eta squared:

	Eta2 (partial)	90% CI
avg.VWC	0.03	[0.01, 0.07]
avg.ST	3.40e-03	[0.00, 0.02]
cum.SR	0.01	[0.00, 0.04]
cum.NEP	0.04	[0.01, 0.09]

Correlation Matrix

		ln.inc.N2O.raw	avg.VWC	avg.ST	cum.SR	cum.NEP
ln.inc.N2O.raw	Pearson's r	—				
	p-value	—				
avg.VWC	Pearson's r	0.168	—			
	p-value	0.004	—			
avg.ST	Pearson's r	−0.008	0.027	—		
	p-value	0.889	0.633	—		
cum.SR	Pearson's r	0.097	0.045	0.365	—	0.030
	p-value	0.098	0.434	< .001	—	0.601
cum.NEP	Pearson's r	0.054	−0.152	0.289	0.030	—
	p-value	0.359	0.007	< .001	0.601	—

Collinearity Statistics

	VIF	Tolerance
cum.SR	1.17	0.853
avg.ST	1.30	0.772
avg.VWC	1.04	0.957
cum.NEP	1.16	0.862

Appendix IV

Diurnal N_2O fluxes of mesocosms during pre-treatment period

One-Way ANOVA

One-Way ANOVA (Welch's)

	F	df1	df2	p
N2O_flux_ughm2	158	14	263	< .001

Group Descriptives

	Mesocosm	N	Mean	SD	SE
N2O_flux_ughm2	1	48	70.0	17.88	2.581
	2	48	32.6	12.24	1.766
	3	48	37.2	9.78	1.412
	4	48	54.2	6.85	0.988
	5	47	67.2	43.49	6.343
	6	48	123.3	33.72	4.868
	7	48	200.7	104.83	15.131
	8	48	29.7	6.70	0.967
	9	47	34.1	12.44	1.815
	10	47	18.3	4.69	0.683
	11	47	57.9	13.06	1.906
	12	47	42.2	29.56	4.311
	13	47	176.3	49.87	7.274
	14	47	73.0	37.20	5.427
	15	47	677.7	603.74	88.064

Plots

N2O_flux_ughm2

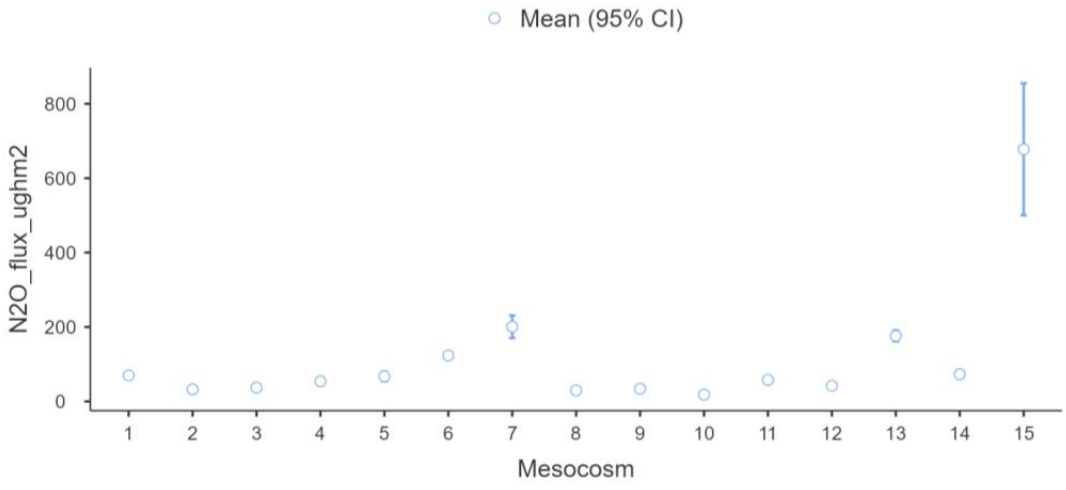

Appendix IV

Diurnal N_2O fluxes of mesocosms during treatment period

One-Way ANOVA

One-Way ANOVA (Welch's)

	F	df1	df2	p
N2O_flux_ughm2	490	14	370	< .001

Group Descriptives

	Mesocosm	N	Mean	SD	SE
N2O_flux_ughm2	1	65	42.1	41.03	5.089
	2	64	115.1	38.17	4.771
	3	67	96.1	46.48	5.679
	4	68	66.8	25.08	3.042
	5	68	73.6	59.93	7.267
	6	67	489.1	188.97	23.086
	7	66	1372.4	429.18	52.828
	8	65	76.2	26.79	3.323
	9	68	78.5	28.48	3.453
	10	68	27.7	7.53	0.913
	11	69	36.5	10.08	1.214
	12	69	122.7	56.99	6.860
	13	68	529.6	282.12	34.213
	14	69	570.5	235.77	28.383
	15	69	2001.1	244.61	29.447

Plots

N2O_flux_ughm2

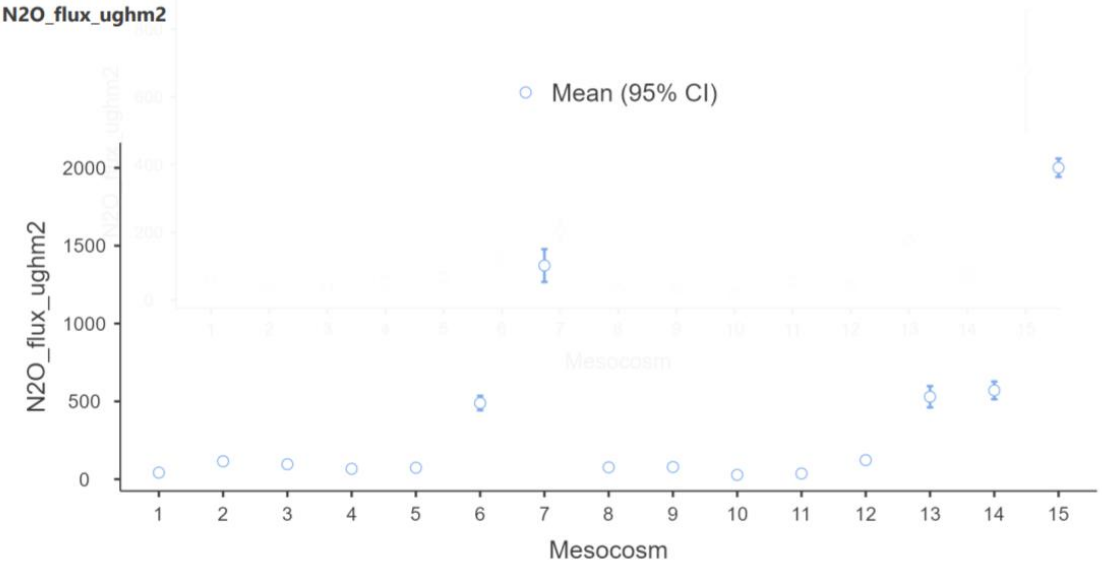

Appendix IV

Diurnal N_2O fluxes of mesocosms during post-treatment period

One-Way ANOVA

One-Way ANOVA (Welch's)

	F	df1	df2	p
N2O_flux_ughm2	1992	14	260	< .001

Group Descriptives

	Mesocosm	N	Mean	SD	SE
N2O_flux_ughm2	1	47	50.5	13.0	1.89
	2	47	168.2	12.9	1.88
	3	47	188.7	32.4	4.72
	4	47	121.2	27.5	4.01
	5	47	307.4	58.9	8.59
	6	47	1005.8	152.8	22.29
	7	47	1943.1	101.4	14.79
	8	47	97.5	18.3	2.67
	9	47	144.9	23.5	3.43
	10	47	34.1	12.0	1.75
	11	47	74.7	16.5	2.40
	12	47	242.9	18.5	2.70
	13	46	1433.1	203.0	29.93
	14	47	1017.9	228.0	33.26
	15	46	1964.6	297.8	43.91

Plots

N2O_flux_ughm2

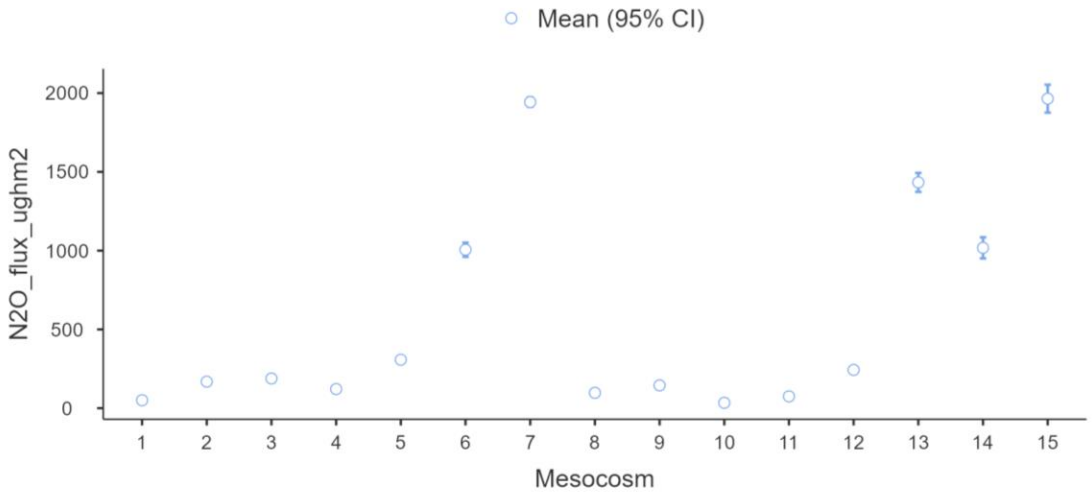

Appendix IV

Summary of the Tukey pairwise comparisons of the estimated means of the log-transformed daily cumulative N_2O emission and actual diurnal amplitude of N_2O flux (marginal means; analysed with linear mixed-effects models), and standardised diurnal amplitude of N_2O flux (means; analysed with a linear regression model) between the treatment groups in the pre-treatment, treatment and post-treatment period, and between the treatment periods in the High PAR, Medium PAR and Low PAR group. Bolded p-values indicate the significances of the differences ($p \leq 0.05$) between pairs.

Linear mixed-effects model: log-transformed daily cumulative N_2O emission (Difference in means (p-value))

	Pre-treatment	*Treatment*	*Post-treatment*
Medium PAR – High PAR	-0.012 (1.000)	0.201 (1.000)	-0.491 (0.999)
Medium PAR – Low PAR	-0.684 (0.988)	-0.630 (0.993)	0.428 (1.000)
Low PAR – High PAR	0.672 (0.990)	0.831 (0.963)	0.918 (0.938)
	Low PAR	*Medium PAR*	*High PAR*
Pre-treatment – Treatment	-0.276 (0.341)	-0.330 (0.134)	-0.117 (0.987)
Treatment – Post-treatment	-0.102 (0.995)	-0.241 (0.535)	-0.014 (1.000)
Pre-treatment – Post-treatment	-0.378 (0.379)	-0.571 (**0.023**)	-0.132 (0.997)

Linear mixed-effects model: log-transformed actual diurnal amplitude of N_2O flux (Difference in means (p-value))

	Pre-treatment	*Treatment*	*Post-treatment*
Medium PAR – High PAR	0.126 (1.000)	0.189 (1.000)	0.636 (0.970)
Medium PAR – Low PAR	-0.787 (0.908)	-0.424 (0.997)	-0.541 (0.988)
Low PAR – High PAR	0.913 (0.824)	0.613 (0.971)	1.177 (0.587)
	Low PAR	*Medium PAR*	*High PAR*
Pre-treatment – Treatment	-0.413 (0.762)	-0.776 (**0.022**)	-0.713 (**0.050**)
Treatment – Post-treatment	-0.533 (0.321)	-0.416 (0.663)	0.031 (1.000)
Pre-treatment – Post-treatment	-0.947 (**0.014**)	-1.192 (**<0.001**)	-0.683 (0.212)

Linear regression model: log-transformed standardised diurnal amplitude of N_2O flux (Difference in means (p-value))

	Pre-treatment	*Treatment*	*Post-treatment*
Medium PAR – High PAR	0.079 (1.000)	-0.652 (**0.011**)	-0.018 (1.000)
Medium PAR – Low PAR	0.401 (0.528)	0.201 (0.972)	0.214 (0.986)
Low PAR – High PAR	0.162 (0.998)	-0.852 (**<0.001**)	-0.232 (0.976)
	Low PAR	*Medium PAR*	*High PAR*
Pre-treatment – Treatment	0.485 (0.265)	0.200 (0.985)	-0.531 (0.161)
Treatment – Post-treatment	-0.199 (0.985)	0.186 (0.995)	0.820 (**0.002**)
Pre-treatment – Post-treatment	-0.684 (**0.042**)	0.307 (0.883)	0.289 (0.915)

Model 1: Effects of PAR treatment and treatment periods on log-transformed diurnal amplitude of N_2O flux (actual)

Formula: lme(fixed = ln.N2O.inc ~ Treatment_group + Treatment_period + Treatment_group:Treatment_period, random = ~ 1|Mesocosm, correlation = corAR1(form = ~Day|Mesocosm), na.action = na.omit, method = 'REML', data = daily)

Summary:

	ln.N2O.inc		
Predictors	*Estimates*	*CI*	*p*
(Intercept)	3.07	2.23 – 3.90	**<0.001**
Treatment_group [Low PAR]	0.79	-0.52 – 2.09	0.213
Treatment_group [High PAR]	-0.13	-1.43 – 1.18	0.836
Treatment_period [Treatment]	0.78	0.33 – 1.22	**0.001**
Treatment_period [Post-treatment]	1.19	0.67 – 1.72	**<0.001**
Treatment_group [Low PAR] * Treatment_period [Treatment]	-0.36	-1.00 – 0.27	0.261
Treatment_group [High PAR] * Treatment_period [Treatment]	-0.06	-0.70 – 0.57	0.846
Treatment_group [Low PAR] * Treatment_period [Post-treatment]	-0.25	-0.99 – 0.50	0.517
Treatment_group [High PAR] * Treatment_period [Post-treatment]	-0.51	-1.25 – 0.23	0.179
Random Effects			
σ^2	0.48		
$\tau_{00\ Mesocosm}$	0.71		
ICC	0.60		
$N_{\ Mesocosm}$	15		
Observations	255		
Marginal R^2 / Conditional R^2	0.192 / 0.674		

Appendix IV
Estimated marginal means:

```
$emmeans

 Treatment_group Treatment_period emmean    SE df lower.CL upper.CL

 Medium PAR      Pre-treatment      3.07 0.423 14     2.16     3.97

 Low PAR         Pre-treatment      3.85 0.423 12     2.93     4.77

 High PAR        Pre-treatment      2.94 0.423 12     2.02     3.86

 Medium PAR      Treatment          3.84 0.412 14     2.96     4.73

 Low PAR         Treatment          4.27 0.412 12     3.37     5.16

 High PAR        Treatment          3.65 0.412 12     2.76     4.55

 Medium PAR      Post-treatment     4.26 0.423 14     3.35     5.17

 Low PAR         Post-treatment     4.80 0.423 12     3.88     5.72

 High PAR        Post-treatment     3.62 0.423 12     2.70     4.54


Degrees-of-freedom method: containment

Confidence level used: 0.95


$contrasts

 contrast                                              estimate    SE  df t.ratio p.value

 (Medium PAR Pre-treatment) - (Low PAR Pre-treatment)     -0.78656 0.598  12 -1.316  0.9080

 (Medium PAR Pre-treatment) - (High PAR Pre-treatment)     0.12609 0.598  12  0.211  1.0000

 (Medium PAR Pre-treatment) - Medium PAR Treatment        -0.77576 0.228 234 -3.408  0.0216

 (Medium PAR Pre-treatment) - Low PAR Treatment           -1.19991 0.590  12 -2.034  0.5504

 (Medium PAR Pre-treatment) - High PAR Treatment          -0.58703 0.590  12 -0.995  0.9792

 (Medium PAR Pre-treatment) - (Medium PAR Post-treatment) -1.19212 0.267 234 -4.463  0.0004

 (Medium PAR Pre-treatment) - (Low PAR Post-treatment)    -1.73328 0.598  12 -2.901  0.1812

 (Medium PAR Pre-treatment) - (High PAR Post-treatment)   -0.55651 0.598  12 -0.931  0.9860

 (Low PAR Pre-treatment) - (High PAR Pre-treatment)        0.91265 0.598  12  1.527  0.8238

 (Low PAR Pre-treatment) - Medium PAR Treatment            0.01080 0.590  12  0.018  1.0000

 (Low PAR Pre-treatment) - Low PAR Treatment              -0.41335 0.228 234 -1.816  0.6718

 (Low PAR Pre-treatment) - High PAR Treatment              0.19953 0.590  12  0.338  1.0000

 (Low PAR Pre-treatment) - (Medium PAR Post-treatment)    -0.40556 0.598  12 -0.679  0.9982

 (Low PAR Pre-treatment) - (Low PAR Post-treatment)       -0.94672 0.267 234 -3.544  0.0138

 (Low PAR Pre-treatment) - (High PAR Post-treatment)       0.23005 0.598  12  0.385  1.0000

 (High PAR Pre-treatment) - Medium PAR Treatment          -0.90186 0.590  12 -1.529  0.8233

 (High PAR Pre-treatment) - Low PAR Treatment             -1.32601 0.590  12 -2.247  0.4355

 (High PAR Pre-treatment) - High PAR Treatment            -0.71313 0.228 234 -3.132  0.0498

 (High PAR Pre-treatment) - (Medium PAR Post-treatment)   -1.31822 0.598  12 -2.206  0.4568

 (High PAR Pre-treatment) - (Low PAR Post-treatment)      -1.85937 0.598  12 -3.112  0.1318

 (High PAR Pre-treatment) - (High PAR Post-treatment)     -0.68261 0.267 234 -2.555  0.2116
```

Appendix IV

Medium PAR Treatment - Low PAR Treatment	-0.42415	0.582	12	-0.728	0.9971
Medium PAR Treatment - High PAR Treatment	0.18873	0.582	12	0.324	1.0000
Medium PAR Treatment - (Medium PAR Post-treatment)	-0.41636	0.228	234	-1.829	0.6629
Medium PAR Treatment - (Low PAR Post-treatment)	-0.95752	0.590	12	-1.623	0.7774
Medium PAR Treatment - (High PAR Post-treatment)	0.21925	0.590	12	0.372	1.0000
Low PAR Treatment - High PAR Treatment	0.61288	0.582	12	1.052	0.9713
Low PAR Treatment - (Medium PAR Post-treatment)	0.00779	0.590	12	0.013	1.0000
Low PAR Treatment - (Low PAR Post-treatment)	-0.53337	0.228	234	-2.343	0.3211
Low PAR Treatment - (High PAR Post-treatment)	0.64340	0.590	12	1.090	0.9650
High PAR Treatment - (Medium PAR Post-treatment)	-0.60509	0.590	12	-1.026	0.9752
High PAR Treatment - (Low PAR Post-treatment)	-1.14625	0.590	12	-1.943	0.6017
High PAR Treatment - (High PAR Post-treatment)	0.03052	0.228	234	0.134	1.0000
(Medium PAR Post-treatment) - (Low PAR Post-treatment)	-0.54116	0.598	12	-0.906	0.9882
(Medium PAR Post-treatment) - (High PAR Post-treatment)	0.63561	0.598	12	1.064	0.9695
(Low PAR Post-treatment) - (High PAR Post-treatment)	1.17677	0.598	12	1.969	0.5866

Degrees-of-freedom method: containment

P value adjustment: tukey method for comparing a family of 9 estimates

QQ plot of model residuals:

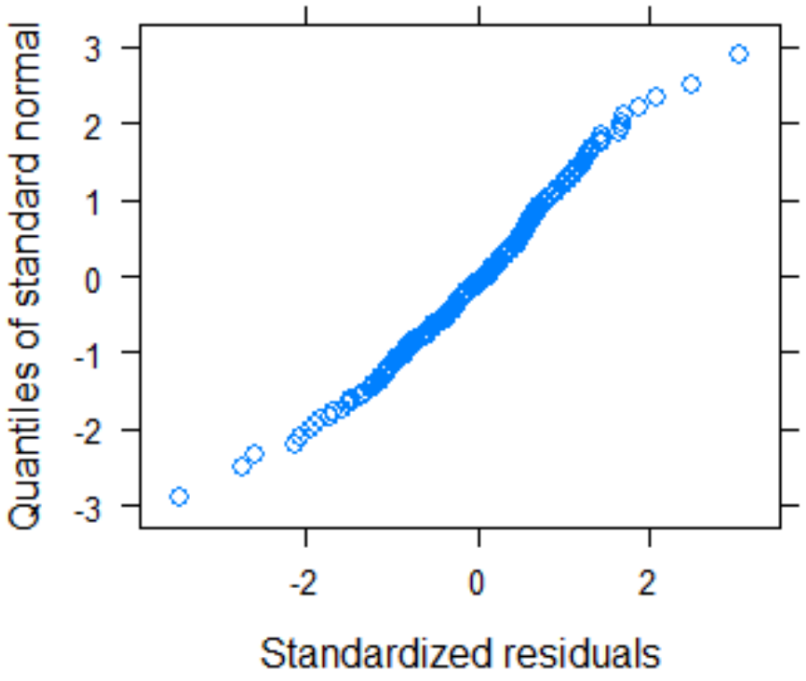

Appendix IV

Model 2: Effects of PAR treatment and treatment periods on log-transformed diurnal amplitude of N_2O flux (standardised)

Formula: lm(ln.N2O.inc.std ~ Treatment_group + Treatment_period + Treatment_group:Treatment_period, data = daily)

Summary:

	ln.N2O.inc.std		
Predictors	*Estimates*	*CI*	*p*
(Intercept)	-0.67	-0.97 – -0.37	**<0.001**
Treatment_group [Low PAR]	0.08	-0.34 – 0.50	0.698
Treatment_group [High PAR]	-0.08	-0.50 – 0.34	0.712
Treatment_period [Treatment]	-0.20	-0.59 – 0.19	0.314
Treatment_period [Post-treatment]	-0.39	-0.81 – 0.04	0.072
Treatment_group [Low PAR] * Treatment_period [Treatment]	-0.28	-0.84 – 0.27	0.311
Treatment_group [High PAR] * Treatment_period [Treatment]	0.73	0.18 – 1.28	**0.010**
Treatment_group [Low PAR] * Treatment_period [Post-treatment]	-0.30	-0.89 – 0.30	0.327
Treatment_group [High PAR] * Treatment_period [Post-treatment]	0.10	-0.50 – 0.69	0.748
Observations	255		
R^2 / R^2 adjusted	0.149 / 0.121		

Appendix IV

```
  Tukey multiple comparisons of means

    95% family-wise confidence level

Fit: aov(formula = lm.inc.std)

$Treatment_group

                          diff         lwr       upr     p adj

Medium PAR-Low PAR  0.1212603 -0.15248126 0.3950018 0.5495322

High PAR-Low PAR    0.3716768  0.09793534 0.6454183 0.0043971

High PAR-Medium PAR 0.2504166 -0.02332491 0.5241581 0.0807858


$Treatment_period

                                    diff        lwr        upr     p adj

Treatment-Pre-treatment      -0.05126983 -0.3210724  0.2185327 0.8952990

Post-treatment-Pre-treatment -0.45292711 -0.7443472 -0.1615070 0.0008824

Post-treatment-Treatment     -0.40165728 -0.6714599 -0.1318547 0.0015386


$`Treatment_group:Treatment_period`

                                                          diff         lwr         upr     p adj

Medium PAR:Pre-treatment-Low PAR:Pre-treatment     -0.08329658 -0.75323203  0.58663888 0.9999850

High PAR:Pre-treatment-Low PAR:Pre-treatment       -0.16244300 -0.83237846  0.50749245 0.9977877

Low PAR:Treatment-Low PAR:Pre-treatment            -0.48452879 -1.10476850  0.13571092 0.2647466

Medium PAR:Treatment-Low PAR:Pre-treatment         -0.28337995 -0.90361965  0.33685976 0.8853118

High PAR:Treatment-Low PAR:Pre-treatment            0.36835966 -0.25188004  0.98859937 0.6427544

Low PAR:Post-treatment-Low PAR:Pre-treatment       -0.68353146 -1.35346691 -0.01359600 0.0415441

Medium PAR:Post-treatment-Low PAR:Pre-treatment    -0.46955842 -1.13949387  0.20037704 0.4131500

High PAR:Post-treatment-Low PAR:Pre-treatment      -0.45143103 -1.12136648  0.21850443 0.4696764

High PAR:Pre-treatment-Medium PAR:Pre-treatment    -0.07914643 -0.74908188  0.59078903 0.9999899

Low PAR:Treatment-Medium PAR:Pre-treatment         -0.40123222 -1.02147193  0.21900749 0.5277711

Medium PAR:Treatment-Medium PAR:Pre-treatment      -0.20008337 -0.82032308  0.42015634 0.9847213

High PAR:Treatment-Medium PAR:Pre-treatment         0.45165624 -0.16858347  1.07189595 0.3589763

Low PAR:Post-treatment-Medium PAR:Pre-treatment    -0.60023488 -1.27017034  0.06970057 0.1194557

Medium PAR:Post-treatment-Medium PAR:Pre-treatment -0.38626184 -1.05619729  0.28367361 0.6792617

High PAR:Post-treatment-Medium PAR:Pre-treatment   -0.36813445 -1.03806991  0.30180100 0.7338810

Low PAR:Treatment-High PAR:Pre-treatment           -0.32208579 -0.94232550  0.29815392 0.7901565

Medium PAR:Treatment-High PAR:Pre-treatment        -0.12093694 -0.74117665  0.49930277 0.9995437

High PAR:Treatment-High PAR:Pre-treatment           0.53080267 -0.08943704  1.15104237 0.1610862

Low PAR:Post-treatment-High PAR:Pre-treatment      -0.52108846 -1.19102391  0.14884700 0.2702638

Medium PAR:Post-treatment-High PAR:Pre-treatment   -0.30711541 -0.97705087  0.36282004 0.8833511

High PAR:Post-treatment-High PAR:Pre-treatment     -0.28898803 -0.95892348  0.38094743 0.9149063

Medium PAR:Treatment-Low PAR:Treatment              0.20114885 -0.36504995  0.76734765 0.9720463
```

High PAR:Treatment-Low PAR:Treatment	0.85288846	0.28668966	1.41908726	0.0001396
Low PAR:Post-treatment-Low PAR:Treatment	-0.19900267	-0.81924238	0.42123704	0.9852433
Medium PAR:Post-treatment-Low PAR:Treatment	0.01497038	-0.60526933	0.63521009	1.0000000
High PAR:Post-treatment-Low PAR:Treatment	0.03309776	-0.58714195	0.65333747	1.0000000
High PAR:Treatment-Medium PAR:Treatment	0.65173961	0.08554081	1.21793841	0.0112631
Low PAR:Post-treatment-Medium PAR:Treatment	-0.40015151	-1.02039122	0.22008820	0.5315635
Medium PAR:Post-treatment-Medium PAR:Treatment	-0.18617847	-0.80641818	0.43406124	0.9904421
High PAR:Post-treatment-Medium PAR:Treatment	-0.16805108	-0.78829079	0.45218863	0.9952058
Low PAR:Post-treatment-High PAR:Treatment	-1.05189112	-1.67213083	-0.43165141	0.0000087
Medium PAR:Post-treatment-High PAR:Treatment	-0.83791808	-1.45815779	-0.21767837	0.0010946
High PAR:Post-treatment-High PAR:Treatment	-0.81979069	-1.44003040	-0.19955098	0.0015755
Medium PAR:Post-treatment-Low PAR:Post-treatment	0.21397304	-0.45596241	0.88390850	0.9856685
High PAR:Post-treatment-Low PAR:Post-treatment	0.23210043	-0.43783502	0.90203588	0.9760446
High PAR:Post-treatment-Medium PAR:Post-treatment	0.01812739	-0.65180807	0.68806284	1.0000000

QQ plot of model residuals:

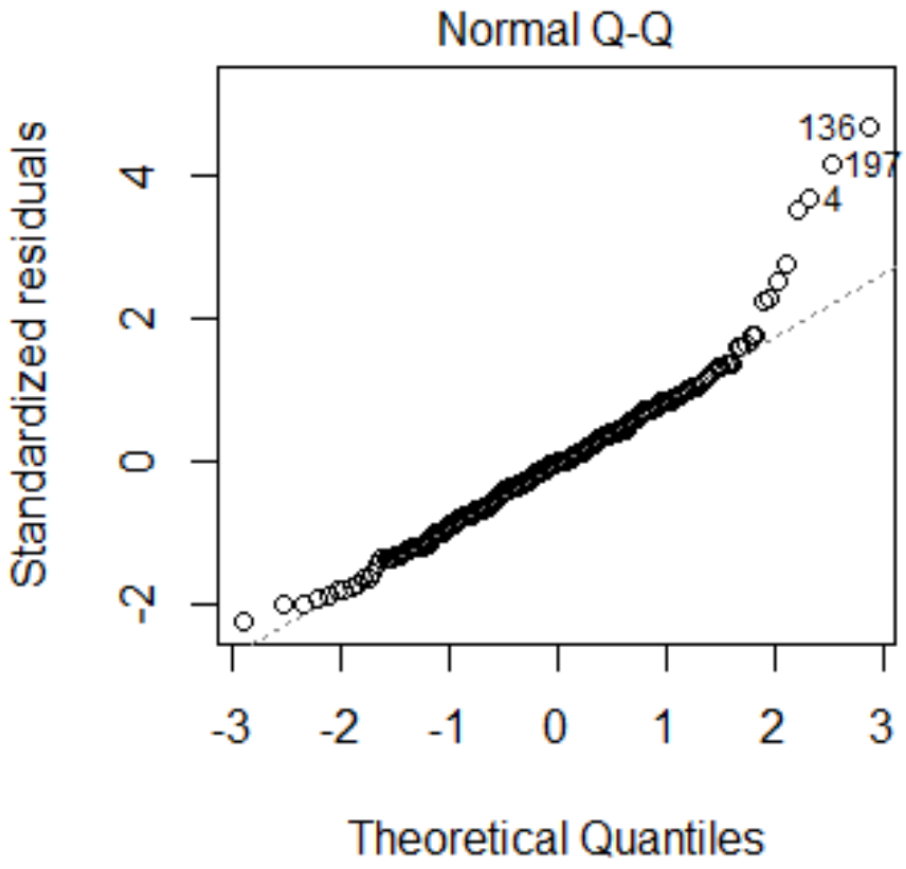

Appendix IV

Model 3: Effects of PAR treatment and treatment periods on log-transformed daily cumulative N_2O emission

Formula: lme(fixed = ln.N2O.cum ~ Treatment_group + Treatment_period + Treatment_group:Treatment_period, random = ~ 1|Mesocosm, correlation = corAR1(form = ~Day|Mesocosm), na.action = na.omit, method = 'REML', data = daily)

Summary:

	ln.N2O.cum		
Predictors	*Estimates*	*CI*	*p*
(Intercept)	7.48	6.42 – 8.53	**<0.001**
Treatment_group [Low PAR]	0.68	-0.96 – 2.33	0.384
Treatment_group [High PAR]	0.01	-1.64 – 1.66	0.988
Treatment_period [Treatment]	0.33	0.09 – 0.57	**0.006**
Treatment_period [Post-treatment]	0.57	0.24 – 0.90	**0.001**
Treatment_group [Low PAR] * Treatment_period [Treatment]	-0.05	-0.39 – 0.28	0.752
Treatment_group [High PAR] * Treatment_period [Treatment]	-0.21	-0.55 – 0.12	0.210
Treatment_group [Low PAR] * Treatment_period [Post-treatment]	-0.19	-0.66 – 0.28	0.419
Treatment_group [High PAR] * Treatment_period [Post-treatment]	-0.44	-0.91 – 0.03	0.066
Random Effects			
σ^2	1.64		
$\tau_{00\ Mesocosm}$	0.00		
ICC	0.00		
$N_{\ Mesocosm}$	15		
Observations	255		
Marginal R^2 / Conditional R^2	0.080 / 0.080		

Appendix IV
Estimated marginal means:

```
$emmeans

 Treatment_group Treatment_period emmean    SE df lower.CL upper.CL

 Medium PAR      Pre-treatment      7.48 0.535 14     6.33     8.62

 Low PAR         Pre-treatment      8.16 0.535 12     7.00     9.33

 High PAR        Pre-treatment      7.49 0.535 12     6.32     8.65

 Medium PAR      Treatment          7.81 0.534 14     6.66     8.95

 Low PAR         Treatment          8.44 0.534 12     7.27     9.60

 High PAR        Treatment          7.61 0.534 12     6.44     8.77

 Medium PAR      Post-treatment     8.05 0.535 14     6.90     9.20

 Low PAR         Post-treatment     8.54 0.535 12     7.37     9.70

 High PAR        Post-treatment     7.62 0.535 12     6.46     8.79


Degrees-of-freedom method: containment

Confidence level used: 0.95


$contrasts

 contrast                                              estimate    SE  df t.ratio p.value

 (Medium PAR Pre-treatment) - (Low PAR Pre-treatment)      -0.6835 0.756  12 -0.904  0.9883

 (Medium PAR Pre-treatment) - (High PAR Pre-treatment)     -0.0116 0.756  12 -0.015  1.0000

 (Medium PAR Pre-treatment) - Medium PAR Treatment         -0.3298 0.120 234 -2.756  0.1344

 (Medium PAR Pre-treatment) - Low PAR Treatment            -0.9597 0.756  12 -1.270  0.9226

 (Medium PAR Pre-treatment) - High PAR Treatment           -0.1288 0.756  12 -0.170  1.0000

 (Medium PAR Pre-treatment) - (Medium PAR Post-treatment)  -0.5709 0.168 234 -3.393  0.0226

 (Medium PAR Pre-treatment) - (Low PAR Post-treatment)     -1.0616 0.756  12 -1.404  0.8765

 (Medium PAR Pre-treatment) - (High PAR Post-treatment)    -0.1432 0.756  12 -0.189  1.0000

 (Low PAR Pre-treatment) - (High PAR Pre-treatment)         0.6719 0.756  12  0.889  0.9895

 (Low PAR Pre-treatment) - Medium PAR Treatment             0.3538 0.756  12  0.468  0.9999

 (Low PAR Pre-treatment) - Low PAR Treatment               -0.2762 0.120 234 -2.308  0.3413

 (Low PAR Pre-treatment) - High PAR Treatment               0.5547 0.756  12  0.734  0.9969

 (Low PAR Pre-treatment) - (Medium PAR Post-treatment)      0.1127 0.756  12  0.149  1.0000

 (Low PAR Pre-treatment) - (Low PAR Post-treatment)        -0.3781 0.168 234 -2.247  0.3790

 (Low PAR Pre-treatment) - (High PAR Post-treatment)        0.5403 0.756  12  0.715  0.9975

 (High PAR Pre-treatment) - Medium PAR Treatment           -0.3182 0.756  12 -0.421  0.9999

 (High PAR Pre-treatment) - Low PAR Treatment              -0.9481 0.756  12 -1.255  0.9271

 (High PAR Pre-treatment) - High PAR Treatment             -0.1172 0.120 234 -0.980  0.9874

 (High PAR Pre-treatment) - (Medium PAR Post-treatment)    -0.5592 0.756  12 -0.740  0.9968

 (High PAR Pre-treatment) - (Low PAR Post-treatment)       -1.0500 0.756  12 -1.389  0.8824

 (High PAR Pre-treatment) - (High PAR Post-treatment)      -0.1316 0.168 234 -0.782  0.9973
```

Appendix IV

Medium PAR Treatment - Low PAR Treatment	-0.6299	0.755	12	-0.834	0.9929
Medium PAR Treatment - High PAR Treatment	0.2010	0.755	12	0.266	1.0000
Medium PAR Treatment - (Medium PAR Post-treatment)	-0.2411	0.120	234	-2.015	0.5345
Medium PAR Treatment - (Low PAR Post-treatment)	-0.7318	0.756	12	-0.968	0.9823
Medium PAR Treatment - (High PAR Post-treatment)	0.1866	0.756	12	0.247	1.0000
Low PAR Treatment - High PAR Treatment	0.8309	0.755	12	1.100	0.9632
Low PAR Treatment - (Medium PAR Post-treatment)	0.3889	0.756	12	0.515	0.9998
Low PAR Treatment - (Low PAR Post-treatment)	-0.1019	0.120	234	-0.851	0.9951
Low PAR Treatment - (High PAR Post-treatment)	0.8165	0.756	12	1.081	0.9667
High PAR Treatment - (Medium PAR Post-treatment)	-0.4420	0.756	12	-0.585	0.9994
High PAR Treatment - (Low PAR Post-treatment)	-0.9328	0.756	12	-1.234	0.9327
High PAR Treatment - (High PAR Post-treatment)	-0.0144	0.120	234	-0.120	1.0000
(Medium PAR Post-treatment) - (Low PAR Post-treatment)	-0.4907	0.756	12	-0.649	0.9987
(Medium PAR Post-treatment) - (High PAR Post-treatment)	0.4276	0.756	12	0.566	0.9995
(Low PAR Post-treatment) - (High PAR Post-treatment)	0.9184	0.756	12	1.214	0.9380

Degrees-of-freedom method: containment

P value adjustment: tukey method for comparing a family of 9 estimates #

QQ plot of model residuals:

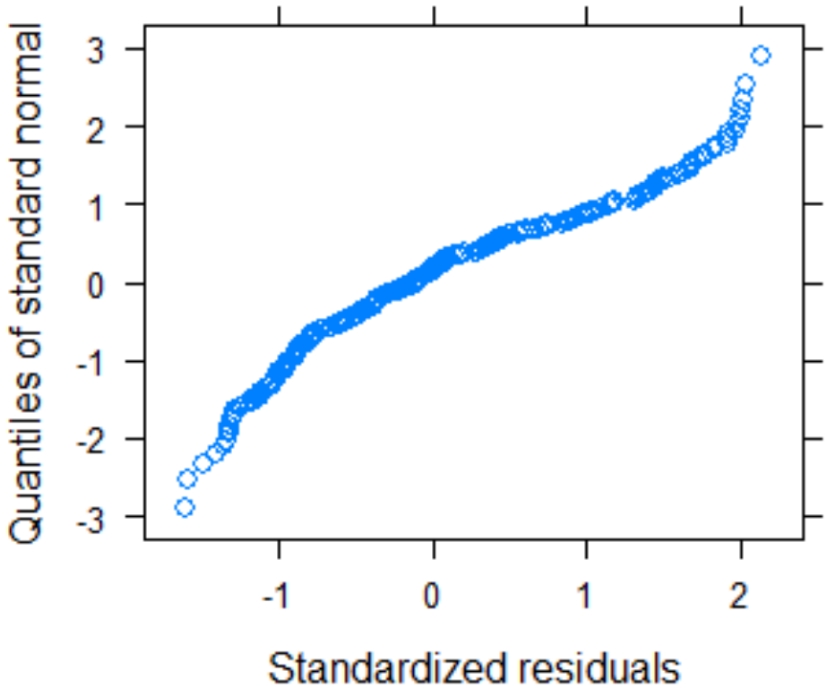

Appendix IV

Model 4: Effect of NEP during photoperiods on log-transformed diurnal amplitude of N_2O flux (actual)

Formula: lme(fixed = ln.N2O.inc ~ NEP.cum.photo, random = ~ 1|Mesocosm, correlation = corAR1(form = ~Day|Mesocosm), na.action = na.omit, method = 'REML', data = daily)

Summary:

		ln.N2O.inc	
Predictors	*Estimates*	*CI*	*p*
(Intercept)	3.78	3.32 – 4.24	**<0.001**
NEP.cum.photo	0.11	-0.27 – 0.48	0.576
Random Effects			
σ^2	0.87		
$\tau_{00\ Mesocosm}$	0.55		
ICC	0.39		
$N_{\ Mesocosm}$	15		
Observations	255		
Marginal R^2 / Conditional R^2	0.001 / 0.390		

QQ plot of model residuals:

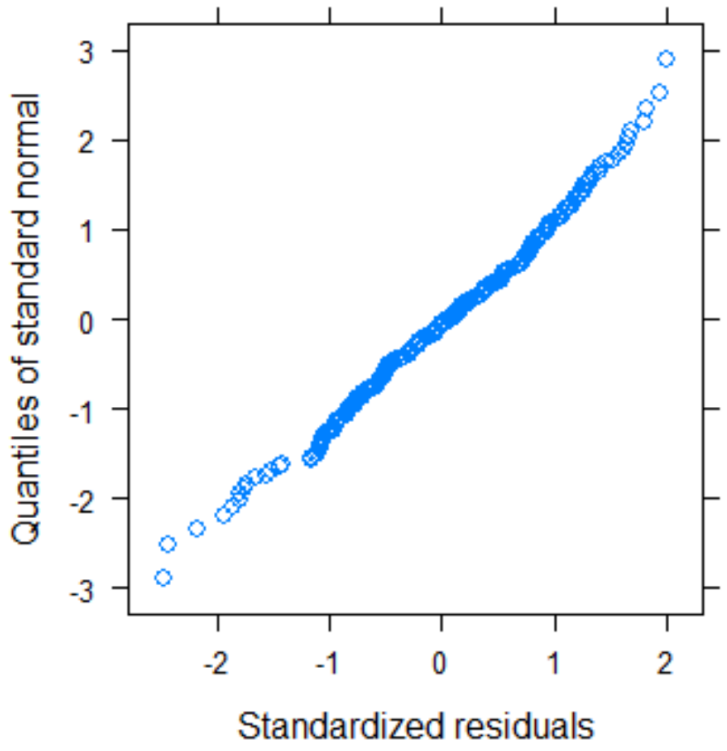

Appendix IV

Model 5: Effect of NEP during photoperiods on log-transformed diurnal amplitude of N_2O flux (standardised)

Formula: lm(ln.N2O.inc.std ~ NEP.cum.photo, data = daily)

Summary:

	ln.N2O.inc.std		
Predictors	*Estimates*	*CI*	*p*
(Intercept)	-0.86	-0.96 – -0.76	**<0.001**
NEP.cum.photo	0.41	0.13 – 0.68	**0.004**
Observations	255		
R^2 / R^2 adjusted	0.033 / 0.029		

QQ plot of model residuals:

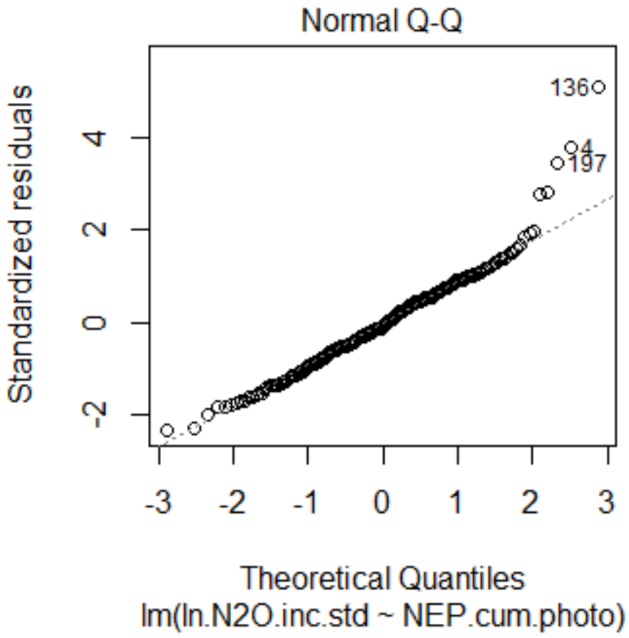

References

Abdalla, M., Smith, P. and Williams, M. (2011). Emissions of Nitrous Oxide from Agriculture: Responses to Management and Climate Change. *ACS Symposium Series*, 1072, pp.343–370. [Online]. Available at: doi:10.1021/bk-2011-1072.ch018.

Abdelhamed, H. et al. (2021). The role of denitrification genes in anaerobic growth and virulence of Flavobacterium columnare. *Journal of Applied Microbiology*, 130 (4), pp.1062–1074. [Online]. Available at: doi:10.1111/jam.14855.

Agresti, A. (2002). *Categorical data analysis*, Wiley series in probability and statistics. 2nd ed. New York: Wiley-Interscience.

AHDB. (2021). *The growth stages of oilseed rape | AHDB*. [Online]. Available at: https://ahdb.org.uk/knowledge-library/the-growth-stages-of-oilseed-rape [Accessed 18 October 2021].

Ai, C. et al. (2020). Wheat rhizodeposition stimulates soil nitrous oxide emission and denitrifiers harboring the nosZ clade I gene. *Soil Biology and Biochemistry*, 143, p.107738. [Online]. Available at: doi:10.1016/j.soilbio.2020.107738.

Aires, A. et al. (2009). Initial in vitro evaluations of the antibacterial activities of glucosinolate enzymatic hydrolysis products against plant pathogenic bacteria. *Journal of Applied Microbiology*, 106 (6), pp.2096–2105. [Online]. Available at: doi:10.1111/j.1365-2672.2009.04181.x.

Akiyama, H. and Tsuruta, H. (2002). Effect of chemical fertilizer form on N2O, NO and NO2 fluxes from Andisol field. *Nutrient Cycling in Agroecosystems*, 63 (2), pp.219–230. [Online]. Available at: doi:10.1023/A:1021102925159.

Akiyama, H. and Tsuruta, H. (2003). Effect of organic matter application on N2O, NO, and NO2 fluxes from an Andisol field. *Global Biogeochemical Cycles*, 17 (4). [Online]. Available at: doi:10.1029/2002GB002016.

Akiyama, H., Tsuruta, H. and Watanabe, T. (2000). N2O and NO emissions from soils after the application of different chemical fertilizers. *Chemosphere - Global Change Science*, 2 (3), pp.313–320. [Online]. Available at: doi:10.1016/S1465-9972(00)00010-6.

Alves, B. J. R. et al. (2012a). Selection of the most suitable sampling time for static chambers for the estimation of daily mean N_2O flux from soils. *Soil Biology and Biochemistry*, 46, pp.129–135. [Online]. Available at: doi:10.1016/j.soilbio.2011.11.022.

Alves, B. J. R. et al. (2012b). Selection of the most suitable sampling time for static chambers for the estimation of daily mean N2O flux from soils. *Soil Biology and Biochemistry*, 46, pp.129–135. [Online]. Available at: doi:10.1016/j.soilbio.2011.11.022.

Ambus, P. and Zechmeister-Boltenstern, S. (2007). Denitrification and N-Cycling in Forest Ecosystems. In: Bothe, H., Ferguson, S. J. and Newton, W. E. B. T.-B. of the N. C. (Eds). *Biology of the Nitrogen Cycle*. Amsterdam: Elsevier. pp.343–358. [Online]. Available at: doi:https://doi.org/10.1016/B978-044452857-5.50023-0.

Azam, F. et al. (2002). Nitrification and denitrification as sources of atmospheric nitrous oxide - Role of oxidizable carbon and applied nitrogen. *Biology and Fertility of Soils*, 35 (1), pp.54–61. [Online]. Available at: doi:10.1007/s00374-001-0441-5.

Babu, Y. J. et al. (2006). Field Validation of DNDC Model for Methane and Nitrous Oxide Emissions from Rice-based Production Systems of India. *Nutrient Cycling in Agroecosystems*, 74 (2), pp.157–174. [Online]. Available at: doi:10.1007/s10705-005-6111-5.

Badri, D. V. and Vivanco, J. M. (2009). Regulation and function of root exudates. *Plant, Cell & Environment*, 32 (6), pp.666–681. [Online]. Available at: doi:https://doi.org/10.1111/j.1365-3040.2009.01926.x.

Baggs, E. M., Pihlatie, M. and Cadisch, G. (2003). Nitrous oxide emissions following application of residues and fertiliser under zero and conventional tillage. *CEUR Workshop Proceedings*, 254, pp.361–370. [Online]. Available at: doi:10.1023/A.

Bahn, M. et al. (2009). Does photosynthesis affect grassland soil-respired CO2 and its carbon isotope composition on a diurnal timescale? *New Phytologist*, 182 (2), pp.451–460. [Online]. Available at: doi:https://doi.org/10.1111/j.1469-8137.2008.02755.x.

Bakken, L. R. et al. (2012). Regulation of denitrification at the cellular level: a clue to the understanding of N2O emissions from soils. *Philosophical Transactions of the Royal Society B-Biological Sciences*, 367 (1593), pp.1226–1234. [Online]. Available at: doi:10.1098/rstb.2011.0321.

Balaine, N. et al. (2013). Changes in Relative Gas Diffusivity Explain Soil Nitrous Oxide Flux Dynamics. *Soil Science Society of America Journal*, 77. [Online]. Available at: doi:10.2136/sssaj2013.04.0141.

Balaine, N. et al. (2016). Soil Gas Diffusivity Controls N2O and N2 Emissions and their Ratio. *Soil Science Society of America Journal*, 80 (3), pp.529–540. [Online]. Available at: doi:10.2136/sssaj2015.09.0350.

Ball, B. C., Crichton, I. and Horgan, G. W. (2008). Dynamics of upward and downward N2O and CO2 fluxes in ploughed or no-tilled soils in relation to water-filled pore space, compaction and crop presence. *Soil and Tillage Research*, 101 (1), pp.20–30. [Online]. Available at: doi:10.1016/j.still.2008.05.012.

Ball, B. C., Scott, A. and Parker, J. P. (1999). Field N2O, CO2 and CH4 fluxes in relation to tillage, compaction and soil quality in Scotland. *Soil and Tillage Research*, 53 (1), pp.29–39. [Online]. Available at: doi:10.1016/S0167-1987(99)00074-4.

Banning, N. C. et al. (2015). Ammonia-oxidising bacteria not archaea dominate nitrification activity in semi-arid agricultural soil. *Scientific Reports*, 5 (1), p.11146. [Online]. Available at: doi:10.1038/srep11146.

Barnard, R., Leadley, P. W. and Hungate, B. A. (2005). Global change, nitrification, and denitrification: A review. *Global Biogeochemical Cycles*, 19 (1). [Online]. Available at: doi:10.1029/2004GB002282 [Accessed 14 September 2021].

Barrat, H. A. et al. The impact of drought and rewetting on N2O emissions from soil in temperate and Mediterranean climates. *European Journal of Soil Science*, n/a (n/a). [Online]. Available at: doi:10.1111/ejss.13015 [Accessed 23 November 2021].

Bárta, J. et al. (2017). Microbial communities with distinct denitrification potential in spruce and beech soils differing in nitrate leaching. *Scientific Reports*, 7 (1), p.9738. [Online]. Available at: doi:10.1038/s41598-017-08554-1.

Barton, L. et al. (2008). Nitrous oxide emissions from a cropped soil in a semi-arid climate. *Global Change Biology*, 14 (1), pp.177–192. [Online]. Available at: doi:10.1111/j.1365-2486.2007.01474.x.

Barton, L. et al. (2015). Sampling frequency affects estimates of annual nitrous oxide fluxes. *Scientific Reports*, 5. [Online]. Available at: doi:10.1038/srep15912 [Accessed 20 November 2020].

Bateman, E. J. and Baggs, E. M. (2005). Contributions of nitrification and denitrification to N2O emissions from soils at different water-filled pore space. *Biology and Fertility of Soils*, 41 (6), pp.379–388. [Online]. Available at: doi:10.1007/s00374-005-0858-3.

Bell, M. et al. (2012). Simulation of soil nitrogen, nitrous oxide emissions and mitigation scenarios at 3 European cropland sites using the ECOSSE model. *Nutrient Cycling in Agroecosystems*, 92, pp.161–181. [Online]. Available at: doi:10.1007/s10705-011-9479-4.

Bell, M. J. et al. (2016). Quantifying N2O emissions from intensive grassland production: the role of synthetic fertilizer type, application rate, timing and nitrification inhibitors. *The Journal of Agricultural Science*, 154 (5), pp.812–827. [Online]. Available at: doi:10.1017/S0021859615000945.

van den Berg, E. M. et al. (2016). DNRA and Denitrification Coexist over a Broad Range of Acetate/N-NO(3)(-) Ratios, in a Chemostat Enrichment Culture. *Frontiers in microbiology*, 7, p.1842. [Online]. Available at: doi:10.3389/fmicb.2016.01842.

van den Berg, E. M. et al. (2017). Role of nitrite in the competition between denitrification and DNRA in a chemostat enrichment culture. *AMB Express*, 7 (1), p.91. [Online]. Available at: doi:10.1186/s13568-017-0398-x.

Bergaust, L. et al. (2010). Denitrification response patterns during the transition to anoxic respiration and posttranscriptional effects of suboptimal ph on nitrogen oxide reductase in paracoccus denitrificans. *Applied and Environmental Microbiology*, 76 (19), pp.6387–6396. [Online]. Available at: doi:10.1128/AEM.00608-10.

Bickel, K. et al. (2006). *Chapter 3: Consistent Representation of Lands*. 4, Kanagawa, Japan: IPCC.

Birch, H. F. and Friend, M. T. (1956). Humus Decomposition in East African Soils. *Nature*, 178 (4531), pp.500–501. [Online]. Available at: doi:10.1038/178500a0.

Blackmer, A. M., Robbins, S. G. and Bremner, J. M. (1982). Diurnal Variability in Rate of Emission of Nitrous Oxide from Soils. *Soil Science Society of America Journal*, 46 (5), pp.937–

942. [Online]. Available at: doi:https://doi.org/10.2136/sssaj1982.03615995004600050011x.

Bollag, J.-M. and Henninger, N. M. (1978). Effects of nitrite toxicity on soil bacteria under aerobic and anaerobic conditions. *Soil Biology and Biochemistry*, 10 (5), pp.377–381. [Online]. Available at: doi:https://doi.org/10.1016/0038-0717(78)90061-5.

Bollmann, A. and Conrad, R. (1998). Influence of O2 availability on NO and N2O release by nitrification and denitrification in soils. *Global Change Biology*, 4 (4), pp.387–396. [Online]. Available at: doi:10.1046/j.1365-2486.1998.00161.x.

Bonin, P. (1996). Anaerobic nitrate reduction to ammonium in two strains isolated from coastal marine sediment: A dissimilatory pathway. *FEMS Microbiology Ecology*, 19 (1), pp.27–38. [Online]. Available at: doi:10.1111/j.1574-6941.1996.tb00195.x.

Borken, W. and Matzner, E. (2009). Reappraisal of drying and wetting effects on C and N mineralization and fluxes in soils. *Global Change Biology*, 15 (4), pp.808–824. [Online]. Available at: doi:10.1111/j.1365-2486.2008.01681.x.

Bouskill, N. J. et al. (2012). Trait-based representation of biological nitrification: model development testing, and predicted community composition. *Frontiers in Microbiology*, 3. [Online]. Available at: doi:10.3389/fmicb.2012.00364.

Bouwman, A. (1996). Direct emission of nitrous oxide from agricultural soils. *Nutrient Cycling in Agroecosystems*, 46, pp.53–70. [Online]. Available at: doi:10.1007/BF00210224.

Bouwman, A. F., Boumans, L. J. M. and Batjes, N. H. (2002). Emissions of N2O and NO from fertilized fields: summary of available measurement data. *Global Biogeochemical Cycles*, 16. [Online]. Available at: doi:10.1029/2001GB001811 [Accessed 23 November 2021].

Brabban, A. D. and Edwards, C. (1995). The effects of glucosinolates and their hydrolysis products on microbial growth. *The Journal of Applied Bacteriology*, 79 (2), pp.171–177. [Online]. Available at: doi:10.1111/j.1365-2672.1995.tb00931.x.

Bracken, C. J. et al. (2021). Source partitioning using N2O isotopomers and soil WFPS to establish dominant N2O production pathways from different pasture sward compositions. *Science of The Total Environment*, 781, p.146515. [Online]. Available at: doi:10.1016/j.scitotenv.2021.146515.

Bradford, M. (2013). Thermal adaptation of decomposer communities in warming soils. *Frontiers in Microbiology*, 4. [Online]. Available at: https://www.frontiersin.org/article/10.3389/fmicb.2013.00333 [Accessed 17 April 2022].

Braker, G., Schwarz, J. and Conrad, R. (2010). Influence of temperature on the composition and activity of denitrifying soil communities. *FEMS Microbiology Ecology*, 73 (1), pp.134–148. [Online]. Available at: doi:10.1111/j.1574-6941.2010.00884.x.

Bremner, J. M. and Blackmer, A. M. (1978). Nitrous Oxide: Emission from Soils During Nitrification of Fertilizer Nitrogen. *Science*, 199 (4326), pp.295–296. [Online]. Available at: doi:10.1126/science.199.4326.295.

Bressan, M. et al. (2009). Exogenous glucosinolate produced by Arabidopsis thaliana has an impact on microbes in the rhizosphere and plant roots. *The ISME Journal*, 3 (11), pp.1243–1257. [Online]. Available at: doi:10.1038/ismej.2009.68.

Bronson, K., Neue, H.-U. and Singh, U. (1997). Automated Chamber Measurements of Methane and Nitrous Oxide Flux in a Flooded Rice Soil: I. Residue, Nitrogen, and Water Management. *Soil Science Society of America Journal - SSSAJ*, 61. [Online]. Available at: doi:10.2136/sssaj1997.03615995006100030038x.

Bruijn, A. et al. (2009). Model evaluation of different mechanisms driving freeze-thaw N2O emissions. *Agriculture, Ecosystems & Environment*, 133. [Online]. Available at: doi:10.1016/j.agee.2009.04.023.

Brumme, R. and Beese, F. (1992). Effects of liming and nitrogen-fertilization on emissions of CO2 and N2O from a temporate forest. *Journal of Geophysical Research-Atmospheres*, 97 (D12), pp.12851–12858. [Online]. Available at: doi:10.1029/92JD01217.

Brummer, C. et al. (2017). Gas chromatography vs. quantum cascade laser-based N2O flux measurements using a novel chamber design. *Biogeosciences*, 14 (6), pp.1365–1381. [Online]. Available at: doi:10.5194/bg-14-1365-2017.

Brunet, R. C. and Garcia-Gil, L. J. (1996). Sulfide-induced dissimilatory nitrate reduction to ammonia in anaerobic freshwater sediments. *FEMS Microbiology Ecology*, 21 (2), pp.131–138. [Online]. Available at: doi:10.1016/0168-6496(96)00051-7.

Burton, D. L. et al. (2008). Effect of split application of fertilizer nitrogen on N2O emissions from potatoes. *Canadian Journal of Soil Science*, 88 (2), pp.229–239. [Online]. Available at: doi:10.4141/CJSS06007.

Butterbach-Bahl, K. et al. (2013). Nitrous oxide emissions from soils: how well do we understand the processes and their controls? *Philosophical Transactions of the Royal Society B: Biological Sciences*, 368 (1621). [Online]. Available at: doi:10.1098/rstb.2013.0122 [Accessed 29 March 2021].

Butterbach-Bahl, K. and Dannenmann, M. (2011). Denitrification and associated soil N2O emissions due to agricultural activities in a changing climate. *Current Opinion in Environmental Sustainability*, 3 (5), pp.389–395. [Online]. Available at: doi:10.1016/j.cosust.2011.08.004.

Cai, Z. et al. (2003). Field validation of the DNDC model for greenhouse gas emissions in East Asian cropping systems. *Global Biogeochemical Cycles*, 17 (4). [Online]. Available at: doi:10.1029/2003GB002046 [Accessed 27 August 2021].

Caldwell, M. M. and Flint, S. D. (1994). Stratospheric ozone reduction, solar UV-B radiation and terrestrial ecosystems. *Climatic Change*, 28 (4), pp.375–394. [Online]. Available at: doi:10.1007/BF01104080.

de Campos, S. B. et al. (2013). Changes in Root Bacterial Communities Associated to Two Different Development Stages of Canola (Brassica napus L. var oleifera) Evaluated through

Next-Generation Sequencing Technology. *Microbial Ecology*, 65 (3), pp.593–601. [Online]. Available at: doi:10.1007/s00248-012-0132-9.

Canarini, A. et al. (2019). Root Exudation of Primary Metabolites: Mechanisms and Their Roles in Plant Responses to Environmental Stimuli. *Frontiers in Plant Science*, 10. [Online]. Available at: doi:10.3389/fpls.2019.00157 [Accessed 22 March 2021].

Caranto, J. D. and Lancaster, K. M. (2017). Nitric oxide is an obligate bacterial nitrification intermediate produced by hydroxylamine oxidoreductase. *Proceedings of the National Academy of Sciences*, 114 (31), pp.8217–8222. [Online]. Available at: doi:10.1073/pnas.1704504114.

Cardenas, L. M. et al. (2017). Effect of soil saturation on denitrification in a grassland soil. *Biogeosciences*, 14 (20), pp.4691–4710. [Online]. Available at: doi:10.5194/bg-14-4691-2017.

Cardenas, L. M. et al. (2019). Nitrogen use efficiency and nitrous oxide emissions from five UK fertilised grasslands. *Science of The Total Environment*, 661, pp.696–710. [Online]. Available at: doi:10.1016/j.scitotenv.2019.01.082.

Carey, J. C. et al. (2016). Temperature response of soil respiration largely unaltered with experimental warming. *Proceedings of the National Academy of Sciences*, 113 (48), pp.13797–13802. [Online]. Available at: doi:10.1073/pnas.1605365113.

Cassia, R. et al. (2018). Climate Change and the Impact of Greenhouse Gasses: CO2 and NO, Friends and Foes of Plant Oxidative Stress. *Frontiers in Plant Science*, 9, p.273. [Online]. Available at: doi:10.3389/fpls.2018.00273.

Castaldi, S. (2000). Responses of nitrous oxide, dinitrogen and carbon dioxide production and oxygen consumption to temperature in forest and agricultural light-textured soils determined by model experiment. *Biology and Fertility of Soils*, 32 (1), pp.67–72. [Online]. Available at: doi:10.1007/s003740000218.

Castignetti, D. and Hollocher, T. C. (1984). Heterotrophic nitrification among denitrifiers. *Applied and Environmental Microbiology*, 47 (4), pp.620–623.

Chabbi, A. and Rumpel, C. (2009). Organic Matter Dynamics in Agro-Ecosystems – the Knowledge Gaps. *European Journal of Soil Science*, 60, pp.153–157. [Online]. Available at: doi:10.1111/j.1365-2389.2008.01116.x.

Chamindu Deepagoda, T. K. K. et al. (2011). Density-Corrected Models for Gas Diffusivity and Air Permeability in Unsaturated Soil. *Vadose Zone Journal*, 10 (1), pp.226–238. [Online]. Available at: doi:10.2136/vzj2009.0137.

Chamindu Deepagoda, T. K. K. et al. (2019). Soil-gas diffusivity and soil-moisture effects on N2O emissions from intact pasture soils. *Soil Science Society of America Journal*. [Online]. Available at: doi:10.2136/sssaj2018.

Chamindu Deepagoda, T. k. k. et al. (2020). Soil-gas diffusivity and soil-moisture effects on N2O emissions from repacked pasture soils. *Soil Science Society of America Journal*, 84 (2), pp.371–386. [Online]. Available at: doi:10.1002/saj2.20024.

Chang, J. et al. (2016). Biochar reduced nitrous oxide and carbon dioxide emissions from soil with different water and temperature cycles. *Agronomy journal*, 108, p.2214.

Charteris, A. F. et al. (2020). Global Research Alliance N2O chamber methodology guidelines: Recommendations for deployment and accounting for sources of variability. *Journal of Environmental Quality*, 49 (5), pp.1092–1109. [Online]. Available at: doi:https://doi.org/10.1002/jeq2.20126.

Chen, H. et al. (2013). Soil nitrous oxide emissions following crop residue addition: A meta-analysis. *Global Change Biology*, 19 (10), pp.2956–2964. [Online]. Available at: doi:10.1111/gcb.12274.

Chen, J. and Strous, M. (2013). Denitrification and aerobic respiration, hybrid electron transport chains and co-evolution. *Biochimica et Biophysica Acta (BBA) - Bioenergetics*, 1827 (2), pp.136–144. [Online]. Available at: doi:10.1016/j.bbabio.2012.10.002.

Chen, T. et al. (2019). Seasonal variations in N2 and N2O emissions from a wheat–maize cropping system. *Biology and Fertility of Soils*, 55 (6), pp.539–551. [Online]. Available at: doi:10.1007/s00374-019-01373-8.

Chen, Y. et al. (1995). Nitrous oxide emission from an agricultural soil subjected to different freeze-thaw cycles. *Agriculture, Ecosystems & Environment*, 55 (2), pp.123–128. [Online]. Available at: doi:10.1016/0167-8809(95)00611-U.

Chen, Z. et al. (2017). Extreme rainfall and snowfall alter responses of soil respiration to nitrogen fertilization: A 3-year field experiment. *Global Change Biology*, 23, pp.3403–3417. [Online]. Available at: doi:10.1111/gcb.13620.

Chen, Z. et al. (2018). Nitrous oxide emissions following seasonal freeze-thaw events from arable soils in Northeast China. *Journal of Integrative Agriculture*, 17 (1), pp.231–246. [Online]. Available at: doi:10.1016/S2095-3119(17)61738-6.

Chèneby, D. et al. (2000). 16S rDNA analysis for characterization of denitrifying bacteria isolated from three agricultural soils. *FEMS Microbiology Ecology*, 34 (2), pp.121–128. [Online]. Available at: doi:10.1111/j.1574-6941.2000.tb00761.x.

Chenu, C., Hassink, J. and Bloem, J. (2001). Short-term changes in the spatial distribution of microorganisms in soil aggregates as affected by glucose addition. *Biol. Fertil. Soils 34 (2001), 5: 349-356*, 34. [Online]. Available at: doi:10.1007/s003740100419.

Choudhary, M. A., Akramkhanov, A. and Saggar, S. (2002). Nitrous oxide emissions from a New Zealand cropped soil: tillage effects, spatial and seasonal variability. *Agriculture, Ecosystems & Environment*, 93 (1), pp.33–43. [Online]. Available at: doi:10.1016/S0167-8809(02)00005-1.

Christensen, S. (1983). Nitrous oxide emission from a soil under permanent grass: Seasonal and diurnal fluctuations as influenced by manuring and fertilization. *Soil Biology and Biochemistry*, 15 (5), pp.531–536. [Online]. Available at: doi:10.1016/0038-0717(83)90046-9.

Chu, H. et al. (2021). Representativeness of Eddy-Covariance flux footprints for areas surrounding AmeriFlux sites. *Agricultural and Forest Meteorology*, 301–302, p.108350. [Online]. Available at: doi:10.1016/j.agrformet.2021.108350.

Chuang, S. C., Lee, H. and Chen, J. H. (2004). Diurnal rhythm and effect of temperature on oxygen consumption in earthworms, Amynthas gracilis and Pontoscolex corethrurus. *Journal of Experimental Zoology Part A: Comparative Experimental Biology*, 301A (9), pp.737–744. [Online]. Available at: doi:10.1002/jez.a.96.

Ciais, P. et al. (2013). Carbon and other biogeochemical cycles. *Climate Change 2013: The Physical Science Basis*, pp.465–570.

Clar, J. T. F. and Anex, R. P. (2020). Flux intensity and diurnal variability of soil N2O emissions in a highly fertilized cropping system. *Soil Science Society of America Journal*, n/a (n/a). [Online]. Available at: doi:https://doi.org/10.1002/saj2.20132 [Accessed 15 December 2020].

Cleveland, C. C. et al. (2007). Increases in Soil Respiration following Labile Carbon Additions Linked to Rapid Shifts in Soil Microbial Community Composition. *Biogeochemistry*, 82 (3), pp.229–240.

Clough, T. J. et al. (2006). Diffusion of 15N-labelled N2O into soil columns: a promising method to examine the fate of N2O in subsoils. *Soil Biology and Biochemistry*, 38 (6), pp.1462–1468. [Online]. Available at: doi:10.1016/j.soilbio.2005.11.002.

Collier, S. M. et al. (2014). Measurement of Greenhouse Gas Flux from Agricultural Soils Using Static Chambers. *Journal of Visualized Experiments : JoVE*, (90), p.52110. [Online]. Available at: doi:10.3791/52110.

Committee on Climate Change. (2017). *Quantifying Greenhouse Gas Emissions*. London, UK: Committe on Climate Change., pp.1–72. [Online]. Available at: https://www.theccc.org.uk/wp-content/uploads/2017/04/Quantifying-Greenhouse-Gas-Emissions-Committee-on-Climate-Change-April-2017.pdf [Accessed 27 November 2021].

Congreves, K. A. et al. (2017). Differences in field-scale N2O flux linked to crop residue removal under two tillage systems in cold climates. *GCB Bioenergy*, 9 (4), pp.666–680. [Online]. Available at: doi:10.1111/gcbb.12354.

Cowan, N. et al. (2019). Application of Bayesian statistics to estimate nitrous oxide emission factors of three nitrogen fertilisers on UK grasslands. 2019/05/08 ed. *Environment international*, 128, pp.362–370. *PubMed* [Online]. Available at: doi:10.1016/j.envint.2019.04.054.

Coyotzi, S. et al. (2017). Agricultural soil denitrifiers possess extensive nitrite reductase gene diversity. *Environmental Microbiology*, 19 (3), pp.1189–1208. [Online]. Available at: doi:10.1111/1462-2920.13643.

Cua, L. S. and Stein, L. Y. (2014). Characterization of denitrifying activity by the alphaproteobacterium, Sphingomonas wittichii RW1. *Frontiers in Microbiology*, 5. [Online]. Available at: https://www.frontiersin.org/article/10.3389/fmicb.2014.00404 [Accessed 10 May 2022].

Čuhel, J. et al. (2010). Insights into the Effect of Soil pH on N2O and N2 Emissions and Denitrifier Community Size and Activity. *Applied and Environmental Microbiology*, 76 (6), p.1870 LP – 1878.

Dąbrowska, G. B. et al. (2021). The Impact of Forest Fungi on Promoting Growth and Development of Brassica napus L. *Agronomy*, 11 (12), p.2475. [Online]. Available at: doi:10.3390/agronomy11122475.

Dalal, R. C. et al. (2003). Nitrous oxide emission from Australian agricultural lands and mitigation options: a review. *Soil Research*, 41 (2), pp.165–195. [Online]. Available at: doi:10.1071/sr02064.

Dalsgaard, T. and Bak, F. (1994). Nitrate Reduction in a Sulfate-Reducing Bacterium, Desulfovibrio desulfuricans, Isolated from Rice Paddy Soil: Sulfide Inhibition, Kinetics, and Regulation. *Applied and Environmental Microbiology*, 60 (1), pp.291–297. [Online]. Available at: doi:10.1128/aem.60.1.291-297.1994.

Das, B. T. et al. (2012). Influence of photosynthetically active radiation on diurnal N2O emissions under ruminant urine patches. *New Zealand Journal of Agricultural Research*, 55 (4), pp.319–331. [Online]. Available at: doi:10.1080/00288233.2012.697068.

Davidson, E. A. (1993). Soil Water Content and the Ratio of Nitrous Oxide to Nitric Oxide Emitted from Soil. In: Oremland, R. S. (Ed). *Biogeochemistry of Global Change: Radiatively Active Trace Gases Selected Papers from the Tenth International Symposium on Environmental Biogeochemistry, San Francisco, August 19–24, 1991*. Boston, MA: Springer US. pp.369–386. [Online]. Available at: doi:10.1007/978-1-4615-2812-8_20.

Davidson, E. A. et al. (2000). Testing a conceptual model of soil emissions of nitrous and nitric oxides: using two functions based on soil nitrogen availability and soil water content, the hole-in-the-pipe model characterizes a large fraction of the observed variation of nitric oxide . *BioScience*, 50 (8), pp.667–680.

Davidson, E. A. and Verchot, L. V. (2000). Testing the Hole-in-the-Pipe Model of nitric and nitrous oxide emissions from soils using the TRAGNET Database. *Global Biogeochemical Cycles*, 14 (4), pp.1035–1043. [Online]. Available at: doi:10.1029/1999GB001223.

De Boer, W. and Kowalchuk, G. A. (2001). Nitrification in acid soils: micro-organisms and mechanisms. *Soil Biology and Biochemistry*, 33 (7), pp.853–866. [Online]. Available at: doi:10.1016/S0038-0717(00)00247-9.

De Klein, C. and Harvey, M. (2015). *Nitrous Oxide Chamber Methodology Guidelines.*

Dechassa, N. and Schenk, M. K. (2004). Exudation of organic anions by roots of cabbage, carrot, and potato as influenced by environmental factors and plant age. *Journal of Plant Nutrition and Soil Science*, 167 (5), pp.623–629. [Online]. Available at: doi:10.1002/jpln.200420424.

Deepagoda, T. K. K. C. et al. (2011). Density-Corrected Models for Gas Diffusivity and Air Permeability in Unsaturated Soil. *Vadose Zone Journal*, 10 (1), pp.226–238. [Online]. Available at: doi:https://doi.org/10.2136/vzj2009.0137.

Defra. (2019). *Agricultural Statistics and Climate Change*. Department for Environment Food and Rural Affairs., pp.1–109. [Online]. Available at: https://assets.publishing.service.gov.uk/government/uploads/system/uploads/attachment_data/file/835762/agriclimate-9edition-02oct19.pdf [Accessed 27 September 2021].

DEFRA. (2020). *Farming statistics - provisional arable crop areas as at 1 June 2020, England*. DEFRA. [Online]. Available at: https://www.gov.uk/government/statistics/farming-statistics-provisional-arable-crop-areas-as-at-1-june-2020-england [Accessed 17 April 2022].

Del Grosso, S. et al. (2012). DayCent Model Simulations for Estimating Soil Carbon Dynamics and Greenhouse Gas Fluxes from Agricultural Production Systems. In: *Managing Agricultural Greenhouse Gases*. pp.241–250. [Online]. Available at: doi:10.1016/B978-0-12-386897-8.00014-0.

Del Grosso, S. j et al. (2001). *Simulated Interaction of Carbon Dynamics and Nitrogen Trace Gas Fluxes Using the DAYCENT Model*. In: pp.303–332. [Online]. Available at: doi:10.1201/9781420032635.ch8.

Denmead, O. T. (1979). Chamber Systems for Measuring Nitrous Oxide Emission from Soils in the Field. *Soil Science Society of America Journal*, 43 (1), pp.89–95. [Online]. Available at: doi:https://doi.org/10.2136/sssaj1979.03615995004300010016x.

Denmead, O. T. et al. (2010). Emissions of methane and nitrous oxide from Australian sugarcane soils. *Agricultural and Forest Meteorology*, 150 (6), pp.748–756. [Online]. Available at: doi:10.1016/j.agrformet.2009.06.018.

Dennis, P. G., Miller, A. J. and Hirsch, P. R. (2010). Are root exudates more important than other sources of rhizodeposits in structuring rhizosphere bacterial communities? *FEMS Microbiology Ecology*, 72 (3), pp.313–327. [Online]. Available at: doi:10.1111/j.1574-6941.2010.00860.x.

Di, H. J. et al. (2009). Nitrification driven by bacteria and not archaea in nitrogen-rich grassland soils. *Nature Geoscience*, 2 (9), pp.621–624. [Online]. Available at: doi:10.1038/ngeo613.

Dietz, S. et al. (2020). Root exudate composition of grass and forb species in natural grasslands. *Scientific Reports*, 10 (1), p.10691. [Online]. Available at: doi:10.1038/s41598-019-54309-5.

Dilkes, N. B., Jones, D. L. and Farrar, J. (2004). Temporal Dynamics of Carbon Partitioning and Rhizodeposition in Wheat. *Plant Physiology*, 134 (2), pp.706–715. [Online]. Available at: doi:10.1104/pp.103.032045.

Ding, F., Sun, W. and Huang, Y. (2019). Net N2O production from soil particle size fractions and its response to changing temperature. *Science of The Total Environment*, 650, pp.97–104. [Online]. Available at: doi:10.1016/j.scitotenv.2018.08.428.

Dlugokencky, E. J. et al. (2018). Long-lived greenhouse gases. In: Blunden, J., Arndt, D. S. and Hartfield, G. (Eds). *State of the climate in 2017*. Bulletin of the American Meteorological Society. pp.46–49. [Online]. Available at: doi:10.1175/2018BAMSStateoftheClimate.1.

Dobbie, K. E. and Smith, K. A. (2003). Impact of different forms of N fertilizer on N2O emissions from intensive grassland. *Nutrient Cycling in Agroecosystems*, 67 (1), pp.37–46. [Online]. Available at: doi:10.1023/A:1025119512447.

Domanski, G. et al. (2001). Carbon flows in the rhizosphere of ryegrass (Lolium perenne). *Journal of Plant Nutrition and Soil Science*, 164, pp.381–387. [Online]. Available at: doi:10.1002/1522-2624(200108)164:43.0.CO;2-5.

Dorich, C. D. et al. (2020). Improving N2O emission estimates with the global N2O database. *Current Opinion in Environmental Sustainability*, 47, pp.13–20. [Online]. Available at: doi:10.1016/j.cosust.2020.04.006.

Drewer, J. et al. (2012). How do soil emissions of N2O, CH4 and CO2 from perennial bioenergy crops differ from arable annual crops? *GCB Bioenergy*, 4 (4), pp.408–419. [Online]. Available at: doi:10.1111/j.1757-1707.2011.01136.x.

Drewer, J. et al. (2017). Difference in Soil Methane (CH4) and Nitrous Oxide (N2O) Fluxes from Bioenergy Crops SRC Willow and SRF Scots Pine Compared with Adjacent Arable and Fallow in a Temperate Climate. *BioEnergy Research*, 10 (2), pp.575–582. [Online]. Available at: doi:10.1007/s12155-017-9824-9.

Du, R., Lu, D. and Wang, G. (2006). Diurnal, seasonal, and inter-annual variations of N2O fluxes from native semi-arid grassland soils of inner Mongolia. *Soil Biology and Biochemistry*, 38 (12), pp.3474–3482. [Online]. Available at: doi:10.1016/j.soilbio.2006.06.012.

Ehhalt, D. et al. (2001). *Chapter 4: Atmospheric Chemistry and Greenhouse Gases*. The International Panel on Climate Change (IPCC). [Online]. Available at: https://www.ipcc.ch/report/ar3/wg1/.

Ellis, E. C. et al. (2010). Anthropogenic transformation of the biomes, 1700 to 2000. *Global Ecology and Biogeography*, 19 (5), pp.589–606. [Online]. Available at: doi:10.1111/j.1466-8238.2010.00540.x.

Enwall, K. et al. (2010). Soil Resources Influence Spatial Patterns of Denitrifying Communities at Scales Compatible with Land Management. *Applied and Environmental Microbiology*, 76 (7), p.2243 LP – 2250.

European Environment Agency. (2019). *Trends in atmospheric concentrations of CO2 (ppm), CH4 (ppb) and N2O (ppb), between 1800 and 2017*.

Farquharson, R. and Baldock, J. (2008). Concepts in modelling N2O emissions from land use. *Plant and Soil*, 309 (1), pp.147–167. [Online]. Available at: doi:10.1007/s11104-007-9485-0.

Farrell, M. et al. (2013). Oligopeptides Represent a Preferred Source of Organic N Uptake: A Global Phenomenon? *Ecosystems*, 16 (1), pp.133–145. [Online]. Available at: doi:10.1007/s10021-012-9601-8.

Felix, J. D. and Elliott, E. M. (2013). The agricultural history of human-nitrogen interactions as recorded in ice core δ15N-NO3−. *Geophysical Research Letters*, 40 (8), pp.1642–1646. [Online]. Available at: doi:10.1002/grl.50209.

Firestone, M. and Davidson, E. (1989). Microbiological Basis of NO and N2O Production and Consumption in Soil. *Exchange of Trace Gases between terrestrial Ecosystems and the Atmosphere,* 47.

Firestone, M. K., Firestone, R. B. and Tiedje, J. M. (1980). Nitrous Oxide from Soil Denitrification: Factors Controlling Its Biological Production. *Science*, 208 (4445), p.749 LP – 751.

Flessa, H. et al. (2002). N2O and CH4 fluxes in potato fields: Automated measurement, management effects and temporal variation. *Geoderma*, 105, pp.307–325. [Online]. Available at: doi:10.1016/S0016-7061(01)00110-0.

Flessa, H., Dörsch, P. and Beese, F. (1995). Seasonal variation of N2O and CH4 fluxes in differently managed arable soils in southern Germany. *Journal of Geophysical Research: Atmospheres*, 100 (D11), pp.23115–23124. [Online]. Available at: doi:10.1029/95JD02270.

Florian, G. et al. (2021). *Core and indicative bacterial and fungal taxa define characteristic soil communities of arable land, grassland, and forest*. bioRxiv., p.2021.06.07.447343. [Online]. Available at: doi:10.1101/2021.06.07.447343 [Accessed 10 May 2022].

Fóti, S. et al. (2018). Temporal Variability of CO2 and N2O Flux Spatial Patterns at a Mowed and a Grazed Grassland. *Ecosystems*, 21 (1), pp.112–124. [Online]. Available at: doi:10.1007/s10021-017-0138-8.

Francis Clar, J. T. and Anex, R. P. (2019). *Measuring frequently during peak soil N2O emissions is more important than choosing the time of day to sample*. preprint, Biogeochemistry: Greenhouse Gases. [Online]. Available at: doi:10.5194/bg-2019-396 [Accessed 28 August 2021].

Franklin, R. B. and Mills, A. L. (2003). Multi-scale variation in spatial heterogeneity for microbial community structure in an eastern Virginia agricultural field. *FEMS Microbiology Ecology*, 44 (3), pp.335–346. [Online]. Available at: doi:10.1016/S0168-6496(03)00074-6.

Fujikawa, T. and Miyazaki, T. (2005). Effects of Bulk Density and Soil Type on the Gas Diffusion Coefficient in Repacked and Undisturbed Soils. *Soil Science*, 170, pp.892–901. [Online]. Available at: doi:10.1097/01.ss.0000196771.53574.79.

Fuß, R. et al. (2011). Pulse emissions of N2O and CO2 from an arable field depending on fertilization and tillage practice. *Agriculture, Ecosystems & Environment*, 144 (1), pp.61–68. [Online]. Available at: doi:10.1016/j.agee.2011.07.020.

Gargallo-Garriga, A. et al. (2018). Root exudate metabolomes change under drought and show limited capacity for recovery. *Scientific Reports*, 8 (1), p.12696. [Online]. Available at: doi:10.1038/s41598-018-30150-0.

Gavrichkova, O. and Kuzyakov, Y. (2010). Respiration costs associated with nitrate reduction as estimated by 14 CO 2 pulse labeling of corn at various growth stages. *Plant and Soil*, 329 (1), pp.433–445. [Online]. Available at: doi:10.1007/s11104-009-0169-9.

Gavrichkova, O. and Kuzyakov, Y. (2017). The above-belowground coupling of the C cycle: fast and slow mechanisms of C transfer for root and rhizomicrobial respiration. *Plant and Soil*, 410 (1), pp.73–85. [Online]. Available at: doi:10.1007/s11104-016-2982-2.

Gelfand, I. et al. (2015). Short-term drought response of N2O and CO2 emissions from mesic agricultural soils in the US Midwest. *Agriculture, Ecosystems & Environment*, 212, pp.127–133. [Online]. Available at: doi:10.1016/j.agee.2015.07.005.

Geng, S. et al. (2017). Rainfall reduction amplifies the stimulatory effect of nitrogen addition on N2O emissions from a temperate forest soil. *Scientific Reports*, 7, p.43329. [Online]. Available at: doi:10.1038/srep43329.

Geßler, A. et al. (2002). Diurnal courses of ammonium net uptake by the roots of adult beech (Fagus sylvatica) and spruce (Picea abies) trees. *Plant and Soil*, 240 (1), pp.23–32. [Online]. Available at: doi:10.1023/A:1015831304911.

Giles, M. et al. (2012). Soil nitrate reducing processes – drivers, mechanisms for spatial variation, and significance for nitrous oxide production. *Frontiers in Microbiology*, 3, p.407. [Online]. Available at: doi:10.3389/fmicb.2012.00407.

Giles, M. E., Daniell, T. J. and Baggs, E. M. (2017). Compound driven differences in N2 and N2O emission from soil; the role of substrate use efficiency and the microbial community. *Soil Biology and Biochemistry*, 106, pp.90–98.

Gilhespy, S. L. et al. (2014). First 20 years of DNDC (DeNitrification DeComposition): Model evolution. *Ecological Modelling*, 292, pp.51–62. [Online]. Available at: doi:10.1016/j.ecolmodel.2014.09.004.

Giltrap, D. L., Li, C. S. and Saggar, S. (2010). DNDC: A process-based model of greenhouse gas fluxes from agricultural soils. *Agriculture Ecosystems & Environment*, 136 (3–4), pp.292–300. [Online]. Available at: doi:10.1016/j.agee.2009.06.014.

Global Monitoring Laboratory. *Trends in Atmospheric Carbon Dioxide*. National Oceanic & Atmospheric Administration. [Online]. Available at: https://gml.noaa.gov/ccgg/trends/ [Accessed 21 May 2021].

Goldberg, S. D., Knorr, K.-H. and Gebauer, G. (2008). N2O concentration and isotope signature along profiles provide deeper insight into the fate of N2O in soils. *Isotopes in Environmental and Health Studies*, 44 (4), pp.377–391. [Online]. Available at: doi:10.1080/10256010802507433.

Gough, C. et al. (1997). Specific flavonoids promote intercellular root colonization of Arabidopsis thaliana by Azorhizobium caulinodans ORS571. *Molecular plant-microbe interactions: MPMI*, 10 (5), pp.560–570. [Online]. Available at: doi:10.1094/MPMI.1997.10.5.560.

Grace, P. R. et al. (2020). Global Research Alliance N2O chamber methodology guidelines: Considerations for automated flux measurement. *Journal of Environmental Quality*, 49 (5), pp.1126–1140. [Online]. Available at: doi:10.1002/jeq2.20124.

Griffis, T. J. et al. (2017). Nitrous oxide emissions are enhanced in a warmer and wetter world. *Proceedings of the National Academy of Sciences*, 114 (45), pp.12081–12085. [Online]. Available at: doi:10.1073/pnas.1704552114.

Griffiths, R. I. et al. (2004). 13CO2 pulse labelling of plants in tandem with stable isotope probing: methodological considerations for examining microbial function in the rhizosphere. *Journal of Microbiological Methods*, 58 (1), pp.119–129. [Online]. Available at: doi:10.1016/j.mimet.2004.03.011.

Grinfelde, I. et al. (2017). *Automated cavity ring down spectroscopy usage for nitrous oxide emission measurements from soil using recirculation system*. In: 24 May 2017. [Online]. Available at: doi:10.22616/ERDev2017.16.N235.

Groenendyk, D. G. et al. (2015). Hydrologic-Process-Based Soil Texture Classifications for Improved Visualization of Landscape Function. *PLoS ONE*, 10 (6). [Online]. Available at: doi:10.1371/journal.pone.0131299 [Accessed 1 December 2020].

Groffman, P. M. et al. (2009). Challenges to incorporating spatially and temporally explicit phenomena (hotspots and hot moments) in denitrification models. *Biogeochemistry*, 93 (1), pp.49–77. [Online]. Available at: doi:10.1007/s10533-008-9277-5.

Gruber, N. and Galloway, J. N. (2008). An Earth-system perspective of the global nitrogen cycle. *Nature*, 451 (7176), pp.293–296. [Online]. Available at: doi:10.1038/nature06592.

Guyonnet, J. P. et al. (2018). Root exudation rate as functional trait involved in plant nutrient-use strategy classification. *Ecology and Evolution*, 8 (16), pp.8573–8581. [Online]. Available at: doi:10.1002/ece3.4383.

Hamerlynck, E. et al. (January 12). Nocturnal soil CO2 uptake and its relationship to subsurface soil and ecosystem carbon fluxes in a Chihuahuan Desert shrubland. *Journal of Geophysical Research: Biogeosciences*, 118. [Online]. Available at: doi:10.1002/2013JG002495.

Hamonts, K. et al. (2013). Effect of nitrogen and waterlogging on denitrifier gene abundance, community structure and activity in the rhizosphere of wheat. *FEMS Microbiology Ecology*, 83 (3), pp.568–584. [Online]. Available at: doi:10.1111/1574-6941.12015.

van Haren, J. et al. (2005). Drought-induced nitrous oxide flux dynamics in an enclosed tropical forest. *Global Change Biology*, 11. [Online]. Available at: doi:10.1111/j.1365-2486.2005.00987.x.

Harris, E. et al. (2021). Denitrifying pathways dominate nitrous oxide emissions from managed grassland during drought and rewetting. *Science Advances*, 7 (6), p.eabb7118. [Online]. Available at: doi:10.1126/sciadv.abb7118.

Harris, Z. M. et al. (2017). Land-use change to bioenergy: grassland to short rotation coppice willow has an improved carbon balance. *GCB Bioenergy*, 9 (2), pp.469–484. [Online]. Available at: doi:10.1111/gcbb.12347.

Hayatsu, M., Tago, K. and Saito, M. (2008). Various players in the nitrogen cycle: Diversity and functions of the microorganisms involved in nitrification and denitrification. *Soil Science and Plant Nutrition*, 54 (1), pp.33–45. [Online]. Available at: doi:10.1111/j.1747-0765.2007.00195.x.

van Hees, P. A. W. et al. (2005). The carbon we do not see—the impact of low molecular weight compounds on carbon dynamics and respiration in forest soils: a review. *Soil Biology and Biochemistry*, 37 (1), pp.1–13. [Online]. Available at: doi:10.1016/j.soilbio.2004.06.010.

Hegewald, H. et al. (2016). Impacts of high intensity crop rotation and N management on oilseed rape productivity in Germany. *Crop and Pasture Science*, 67 (4), pp.439–449. [Online]. Available at: doi:10.1071/CP15214.

Helal, H. M. and Sauerbeck, D. (1986). Effect of plant roots on carbon metabolism of soil microbial biomass. *Zeitschrift für Pflanzenernährung und Bodenkunde*, 149 (2), pp.181–188. [Online]. Available at: doi:https://doi.org/10.1002/jpln.19861490205.

Hénault, C. et al. (2012). Nitrous Oxide Emission by Agricultural Soils: A Review of Spatial and Temporal Variability for Mitigation. *Pedosphere*, 22, pp.426–433. [Online]. Available at: doi:10.1016/S1002-0160(12)60029-0.

Hénault, C. et al. (2019). Management of soil pH promotes nitrous oxide reduction and thus mitigates soil emissions of this greenhouse gas. *Scientific Reports*, 9 (1), p.20182. [Online]. Available at: doi:10.1038/s41598-019-56694-3.

Henderson, S. L. et al. (2010). Changes in Denitrifier Abundance, Denitrification Gene mRNA Levels, Nitrous Oxide Emissions, and Denitrification in Anoxic Soil Microcosms Amended with Glucose and Plant Residues. *Applied and Environmental Microbiology*, 76 (7), p.2155. [Online]. Available at: doi:10.1128/AEM.02993-09.

Henry, H. A. L. (2008). Climate change and soil freezing dynamics: historical trends and projected changes. *Climatic Change*, 87 (3), pp.421–434. [Online]. Available at: doi:10.1007/s10584-007-9322-8.

Henry, S. et al. (2008). Disentangling the rhizosphere effect on nitrate reducers and denitrifiers: insight into the role of root exudates. *Environmental Microbiology*, 10 (11), pp.3082–3092. [Online]. Available at: doi:https://doi.org/10.1111/j.1462-2920.2008.01599.x.

Hensen, A., Skiba, U. and Famulari, D. (2013). Low cost and state of the art methods to measure nitrous oxide emissions. *Environmental Research Letters*, 8 (2), p.025022. [Online]. Available at: doi:10.1088/1748-9326/8/2/025022.

Hergoualc'h, K. et al. (2019). Chapter 11: N2O Emissions from Managed Soils, and CO2 Emissions from Lime and Urea Application. In: *2019 Refinement to the 2006 IPCC Guidelines for National Greenhouse Gas Inventories*. Agriculture, Forestry and Other Land Use. 4. Intergovernmental Panel on Climate Change (IPCC). pp.1–48. [Online]. Available at: https://www.ipcc-nggip.iges.or.jp/public/2019rf/pdf/4_Volume4/19R_V4_Ch11_Soils_N2O_CO2.pdf [Accessed 27 August 2021].

Hergoualc'h, K. et al. (2020). Spatial and temporal variability of soil N2O and CH4 fluxes along a degradation gradient in a palm swamp peat forest in the Peruvian Amazon. *Global Change Biology*, 26 (12), pp.7198–7216. [Online]. Available at: doi:10.1111/gcb.15354.

van den Heuvel, R. N. et al. (2009). N2O emission hotspots at different spatial scales and governing factors for small scale hotspots. *The Science of the Total Environment*, 407 (7), pp.2325–2332. [Online]. Available at: doi:10.1016/j.scitotenv.2008.11.010.

Heylen, K. et al. (2007). Nitric oxide reductase (norB) gene sequence analysis reveals discrepancies with nitrite reductase (nir) gene phylogeny in cultivated denitrifiers. *Environmental Microbiology*, 9 (4), pp.1072–1077. [Online]. Available at: doi:10.1111/j.1462-2920.2006.01194.x.

Hill, P. et al. (2007). Response of root respiration and root exudation to alterations in root C supply and demand in wheat. *Plant and Soil*, 291 (1), pp.131–141. [Online]. Available at: doi:10.1007/s11104-006-9180-6.

Hill, P. W., Farrell, M. and Jones, D. L. (2012). Bigger may be better in soil N cycling: Does rapid acquisition of small l-peptides by soil microbes dominate fluxes of protein-derived N in soil? *Soil Biology and Biochemistry*, 48, pp.106–112. [Online]. Available at: doi:10.1016/j.soilbio.2012.01.023.

Hirsch, P. R. et al. (2017). Soil resilience and recovery: rapid community responses to management changes. *Plant and Soil*, 412 (1), pp.283–297. [Online]. Available at: doi:10.1007/s11104-016-3068-x.

Hobbie, E. A. (2006). Carbon allocation to ectomycorrhizal fungi correlates with belowground allocation in culture studies. *Ecology*, 87 (3), pp.563–569. [Online]. Available at: doi:10.1890/05-0755.

Holmes, D. E., Dang, Y. and Smith, J. A. (2019). Chapter Four - Nitrogen cycling during wastewater treatment. In: Gadd, G. M. and Sariaslani, S. (Eds). *Advances in Applied*

Microbiology. 106. Academic Press. pp.113–192. [Online]. Available at: doi:10.1016/bs.aambs.2018.10.003 [Accessed 1 October 2021].

Honda, N. et al. (1998). Antifungal effect of a heterotrophic nitrifier Alcaligenes faecalis. *Biotechnology Letters*, 20 (7), pp.703–705. [Online]. Available at: doi:10.1023/A:1005382810088.

Hosono, T. et al. (2006). Measurements of N2O and NO emissions during tomato cultivation using a flow-through chamber systemin a glasshouse. *Nutrient Cycling in Agroecosystems*, 75 (1), pp.115–134. [Online]. Available at: doi:10.1007/s10705-006-9016-z.

Hu, H. W., Chen, D. and He, J. Z. (2015). Microbial regulation of terrestrial nitrous oxide formation: Understanding the biological pathways for prediction of emission rates. *FEMS Microbiology Reviews*, 39 (5), pp.729–749. [Online]. Available at: doi:10.1093/femsre/fuv021.

Hu, H.-W., Xu, Z.-H. and He, J.-Z. (2014). Ammonia-Oxidizing Archaea Play a Predominant Role in Acid Soil Nitrification. In: Sparks, D. L. B. T.-A. in A. (Ed). *Advances in Agronomy*. 125. Academic Press. pp.261–302. [Online]. Available at: doi:https://doi.org/10.1016/B978-0-12-800137-0.00006-6.

Huang, H. et al. (2014). Nitrous oxide emissions from a commercial cornfield (*Zea mays*) measured using the eddy covariance technique. *Atmospheric Chemistry and Physics*, 14 (23), pp.12839–12854. [Online]. Available at: doi:10.5194/acp-14-12839-2014.

Huang, L. et al. (2021). Ammonia-oxidizing archaea are integral to nitrogen cycling in a highly fertile agricultural soil. *ISME Communications*, 1 (1), pp.1–12. [Online]. Available at: doi:10.1038/s43705-021-00020-4.

Huhe et al. (2016). Microbial Nitrogen-Cycle Gene Abundance in Soil of Cropland Abandoned for Different Periods. *PLOS ONE*, 11 (5), p.e0154697.

Hütsch, B. W., Augustin, J. and Merbach, W. (2002). Plant rhizodeposition — an important source for carbon turnover in soils. *Journal of Plant Nutrition and Soil Science*, 165 (4), pp.397–407. [Online]. Available at: doi:10.1002/1522-2624(200208)165:4<397::AID-JPLN397>3.0.CO;2-C.

IAEA. (1992). *Manual on measurement of methane and nitrous oxide emissions from agriculture. A joint undertaking by the Food and Agriculture Organization of the United Nations and the International Atomic Energy Agency*. Vienna, Austria: International Atomic Energy Agency.

Islam, A., Chen, D. and White, R. E. (2007). Heterotrophic and autotrophic nitrification in two acid pasture soils. *Soil Biology and Biochemistry*, 39 (4), pp.972–975. [Online]. Available at: doi:https://doi.org/10.1016/j.soilbio.2006.11.003.

Ito, A. et al. (2018). Emissions of nitrous oxide (N2O) from soil surfaces and their historical changes in East Asia: a model-based assessment. *Progress in Earth and Planetary Science*, 5 (1), p.55. [Online]. Available at: doi:10.1186/s40645-018-0215-4.

Jia, X. et al. (2014). Effects of Substrate Addition on Soil Respiratory Carbon Release Under Long-Term Warming and Clipping in a Tallgrass Prairie. *PLoS ONE*, 9 (12), p.e114203. [Online]. Available at: doi:10.1371/journal.pone.0114203.

Johnson, D. et al. (2002). In situ13CO2 pulse-labelling of upland grassland demonstrates a rapid pathway of carbon flux from arbuscular mycorrhizal mycelia to the soil. *New Phytologist*, 153 (2), pp.327–334. [Online]. Available at: doi:https://doi.org/10.1046/j.0028-646X.2001.00316.x.

Jones, D. L., Hodge, A. and Kuzyakov, Y. (2004). Plant and mycorrhizal regulation of rhizodeposition. *New Phytologist*, 163 (3), pp.459–480. [Online]. Available at: doi:10.1111/j.1469-8137.2004.01130.x.

Jones, D. L., Nguyen, C. and Finlay, R. D. (2009). Carbon flow in the rhizosphere: carbon trading at the soil–root interface. *Plant and Soil*, 321 (1), pp.5–33. [Online]. Available at: doi:10.1007/s11104-009-9925-0.

Jones, S. K. et al. (2011). Nitrous oxide emissions from managed grassland: a comparison of eddy covariance and static chamber measurements. *Atmospheric Measurement Techniques*, 4 (10), pp.2179–2194. [Online]. Available at: doi:10.5194/amt-4-2179-2011.

Jørgensen, C., Struwe, S. and Elberling, B. (2012). Temporal trends in N2O flux dynamics in a Danish wetland – effects of plant-mediated gas transport of N2O and O2 following changes in water level and soil mineral-N availability. *Global Change Biology*, 18. [Online]. Available at: doi:10.1111/j.1365-2486.2011.02485.x.

Jung, M.-Y. et al. (2014). Isotopic signatures of N2O produced by ammonia-oxidizing archaea from soils. 2013/11/14 ed. *The ISME journal*, 8 (5), pp.1115–1125. [Online]. Available at: doi:10.1038/ismej.2013.205.

Jungkunst, H. F. et al. (2018). How to best address spatial and temporal variability of soil-derived nitrous oxide and methane emissions. *Journal of Plant Nutrition and Soil Science*, 181 (1), pp.7–11. [Online]. Available at: doi:10.1002/jpln.201700607.

Jurasinski, G. et al. (2015). *Package 'flux'*. R. [Online]. Available at: https://cran.r-project.org/web/packages/flux/flux.pdf [Accessed 18 February 2021].

Kaiser, C. et al. (2015). Exploring the transfer of recent plant photosynthates to soil microbes: mycorrhizal pathway vs direct root exudation. *New Phytologist*, 205 (4), pp.1537–1551. [Online]. Available at: doi:https://doi.org/10.1111/nph.13138.

Karimi, B. et al. (2018). Biogeography of soil bacteria and archaea across France. *Science Advances*, 4 (7), p.eaat1808. [Online]. Available at: doi:10.1126/sciadv.aat1808.

Katayanagi, N. and Hatano, R. (2012). N2O emissions during the freezing and thawing periods from six fields in a livestock farm, southern Hokkaido, Japan. *Soil Science and Plant Nutrition*, 58 (2), pp.261–271. [Online]. Available at: doi:10.1080/00380768.2012.670810.

Kavdir, Y., Hellebrand, H. J. and Kern, J. (2008). Seasonal variations of nitrous oxide emission in relation to nitrogen fertilization and energy crop types in sandy soil. *Soil and Tillage Research*, 98 (2), pp.175–186. [Online]. Available at: doi:10.1016/j.still.2007.11.002.

Keane, B. J. et al. (2017). Greenhouse gas emissions from the energy crop oilseed rape (*Brassica napus*); the role of photosynthetically active radiation in diurnal N_2O flux variation. *GCB Bioenergy*, 44, pp.1–14. [Online]. Available at: doi:10.1111/gcbb.12491.

Keane, B. J. et al. (2018). Greenhouse gas emissions from the energy crop oilseed rape (Brassica napus); the role of photosynthetically active radiation in diurnal N2O flux variation. *GCB Bioenergy*, 10 (5), pp.306–319. [Online]. Available at: doi:https://doi.org/10.1111/gcbb.12491.

Keane, J. B. et al. (2019). Real-time monitoring of greenhouse gas emissions with tall chambers reveals diurnal N2O variation and increased emissions of CO2 and N2O from Miscanthus following compost addition. *GCB Bioenergy*, 11 (12), pp.1456–1470. [Online]. Available at: doi:https://doi.org/10.1111/gcbb.12653.

Kelting, D. L., Burger, J. A. and Edwards, G. S. (1998). Estimating root respiration, microbial respiration in the rhizosphere, and root-free soil respiration in forest soils. *Soil Biology and Biochemistry*, 30 (7), pp.961–968. [Online]. Available at: doi:10.1016/S0038-0717(97)00186-7.

Khalil, K., Mary, B. and Renault, P. (2004). Nitrous oxide production by nitrification and denitrification in soil aggregates as affected by O2 concentration. *Soil Biology and Biochemistry*, 36 (4), pp.687–699. [Online]. Available at: doi:10.1016/j.soilbio.2004.01.004.

Khalil, M. I. et al. (2007). Daytime, Temporal, and Seasonal Variations of N2O Emissions in an Upland Cropping System of the Humid Tropics. *Communications in Soil Science and Plant Analysis*, 38 (1–2), pp.189–204. [Online]. Available at: doi:10.1080/00103620601094122.

Kirschbaum, M. U. F. et al. (2001). *Definitions Of Some Ecological Terms Commonly Used In Carbon Accounting*. p.4.

Kissel, D. E. (2014). *The Historical Development and Significance of the Haber Bosch Process*. 98 (2), p.3.

Klefoth, R. et al. (2014). Soil Bulk Density and Moisture Content Influence Relative Gas Diffusivity and the Reduction of Nitrogen-15 Nitrous Oxide. *Vadose Zone Journal*, 13. [Online]. Available at: doi:10.2136/vzj2014.07.0089.

de Klein, C. A. M. et al. (2020). Global Research Alliance N2O chamber methodology guidelines: Introduction, with health and safety considerations. *Journal of Environmental Quality*, 49 (5), pp.1073–1080. [Online]. Available at: doi:10.1002/jeq2.20131.

de Klein, C. et al. (2006). N2O Emissions from Managed Soils, and CO2 Emissions from Lime and Urea Application. *2006 IPCC Guidelines for National Greenhouse Gas Inventories*, 4.

Knowles, R. (1982). Denitrification. *Microbiological reviews*, 46 (1), pp.43–70. *PubMed*.

Koga, N. et al. (2004). N2O emission and CH4 uptake in arable fields managed under conventional and reduced tillage cropping systems in northern Japan. *Global Biogeochemical Cycles - GLOBAL BIOGEOCHEM CYCLE*, 18. [Online]. Available at: doi:10.1029/2004GB002260.

Koo, B.-. J. et al. (2005). ROOT EXUDATES AND MICROORGANISMS. In: Hillel, D. (Ed). *Encyclopedia of Soils in the Environment*. Oxford: Elsevier. pp.421–428. [Online]. Available at: doi:10.1016/B0-12-348530-4/00461-6 [Accessed 10 May 2021].

Kool, D. M. et al. (2010). Nitrifier denitrification can be a source of N2O from soil: a revised approach to the dual-isotope labelling method. *European Journal of Soil Science*, 61 (5), pp.759–772. [Online]. Available at: doi:10.1111/j.1365-2389.2010.01270.x.

Köster, J. et al. (2015). Anaerobic digestates lower N2O emissions compared to cattle slurry by affecting rate and product stoichiometry of denitrification – An N2O isotopomer case study. *Soil Biology and Biochemistry*, 84. [Online]. Available at: doi:10.1016/j.soilbio.2015.01.021.

Kostyanovsky, K. I. et al. (2019). Emissions of N2O and CO2 Following Short-Term Water and N Fertilization Events in Wheat-Based Cropping Systems. *Frontiers in Ecology and Evolution*, 7. [Online]. Available at: doi:10.3389/fevo.2019.00063 [Accessed 27 April 2021].

Kottek, M. et al. (2006). World Map of the Köppen-Geiger Climate Classification Updated. *Meteorologische Zeitschrift*, 15, pp.259–263. [Online]. Available at: doi:10.1127/0941-2948/2006/0130.

Kraft, B., Strous, M. and Tegetmeyer, H. E. (2011). Microbial nitrate respiration – Genes, enzymes and environmental distribution. *Journal of Biotechnology*, 155 (1), pp.104–117. [Online]. Available at: doi:https://doi.org/10.1016/j.jbiotec.2010.12.025.

Kreba, S. A. et al. (2017). Soil Gas Diffusivity, Air-Filled Porosity, and Pore Continuity: Land Use and Spatial Patterns. *Soil Science Society of America Journal*, 81 (3), pp.477–489. [Online]. Available at: doi:10.2136/sssaj2016.10.0344.

Kuzyakov, Y. and Cheng, W. (2001). Photosynthesis controls of rhizosphere respiration and organic matter decomposition. *Soil Biology and Biochemistry*, 33 (14), pp.1915–1925. [Online]. Available at: doi:10.1016/S0038-0717(01)00117-1.

Kuzyakov, Y. and Domanski, G. (2000). Carbon input by plants into the soil. Review. *Journal of Plant Nutrition and Soil Science*, 163 (4), pp.421–431. [Online]. Available at: doi:10.1002/1522-2624(200008)163:4<421::AID-JPLN421>3.0.CO;2-R.

Kuzyakov, Y. and Domanski, G. (2002). Model for rhizodeposition and CO2 efflux from planted soil and its validation by 14C pulse labelling of ryegrass. *Plant and Soil*, 239 (1), pp.87–102. [Online]. Available at: doi:10.1023/A:1014939120651.

Kuzyakov, Y. and Gavrichkova, O. (2010). REVIEW: Time lag between photosynthesis and carbon dioxide efflux from soil: a review of mechanisms and controls. *Global Change Biology*, 16 (12), pp.3386–3406. [Online]. Available at: doi:https://doi.org/10.1111/j.1365-2486.2010.02179.x.

Kyveryga, P. M. et al. (2004). Soil pH Effects on Nitrification of Fall-Applied Anhydrous Ammonia . *Soil Science Society of America Journal*, 68, pp.545–551. [Online]. Available at: doi:10.2136/sssaj2004.0545.

Lai, T. V. and Denton, M. D. (2018). N2O and N2 emissions from denitrification respond differently to temperature and nitrogen supply. *Journal of Soils and Sediments*, 18 (4), pp.1548–1557. [Online]. Available at: doi:10.1007/s11368-017-1863-5.

Lammirato, C. et al. (2018). Analysis of uncertainty for N2O fluxes measured with the closed-chamber method under field conditions: Calculation method, detection limit, and spatial variability. *Journal of Plant Nutrition and Soil Science*, 181 (1), pp.78–89. [Online]. Available at: doi:10.1002/jpln.201600499.

Langarica-Fuentes, A. et al. (2018). Effect of model root exudate on denitrifier community dynamics and activity at different water-filled pore space levels in a fertilised soil. *Soil Biology and Biochemistry*, 120, pp.70–79. [Online]. Available at: doi:10.1016/j.soilbio.2018.01.034.

Larsen, K. S. et al. (2007). Ecosystem respiration depends strongly on photosynthesis in a temperate heath. *Biogeochemistry*, 85 (2), pp.201–213. [Online]. Available at: doi:10.1007/s10533-007-9129-8.

Laville, P. et al. (1999). Nitrous oxide fluxes from a fertilised maize crop using micrometeorological and chamber methods. *Agricultural and Forest Meteorology*, 96 (1), pp.19–38. [Online]. Available at: doi:10.1016/S0168-1923(99)00054-4.

Laville, P. et al. (2017). Temporal integration of soil N_2O fluxes: validation of IPNOA station automatic chamber prototype. *Environmental Monitoring and Assessment*, 189 (10). [Online]. Available at: doi:10.1007/s10661-017-6181-2.

Lebegue, B. et al. (2016). Comparison of nitrous oxide (N_2O) analyzers for high-precision measurements of atmospheric mole fractions. *Atmospheric Measurement Techniques*, 9 (3), pp.1221–1238. [Online]. Available at: doi:10.5194/amt-9-1221-2016.

Lehtovirta-Morley, L. E. (2018). Ammonia oxidation: Ecology, physiology, biochemistry and why they must all come together. *FEMS Microbiology Letters*, 365 (9). [Online]. Available at: doi:10.1093/femsle/fny058 [Accessed 29 September 2021].

Leininger, S. et al. (2006). Archaea predominate among ammonia-oxidizing prokaryotes in soils. *Nature*, 442 (7104), pp.806–809. [Online]. Available at: doi:10.1038/nature04983.

Leitner, S. et al. (2017). Linking NO and N2O emission pulses with the mobilization of mineral and organic N upon rewetting dry soils. *Soil Biology and Biochemistry*, 115, pp.461–466. [Online]. Available at: doi:10.1016/j.soilbio.2017.09.005.

Lesschen, J. P. et al. (2011). Differentiation of nitrous oxide emission factors for agricultural soils. *Environmental Pollution*, 159 (11), pp.3215–3222. [Online]. Available at: doi:10.1016/j.envpol.2011.04.001.

LG Seeds. (2019). *Essential Guide to Forage Crops*. [Online]. Available at: https://www.lgseeds.co.uk/uploads/Forage-Brochure_Singles.pdf [Accessed 17 October 2021].

Li, C. et al. (2006). Modeling nitrate leaching with a biogeochemical model modified based on observations in a row-crop field in Iowa. *Ecological Modelling*, 196 (1), pp.116–130. [Online]. Available at: doi:10.1016/j.ecolmodel.2006.02.007.

Li, C., Frolking, S. and Frolking, T. A. (1992). A model of nitrous oxide evolution from soil driven by rainfall events: 1. Model structure and sensitivity. *Journal of Geophysical Research: Atmospheres*, 97 (D9), pp.9759–9776. [Online]. Available at: doi:10.1029/92JD00509.

Li, D. and Wang, X. (2008). Nitrogen isotopic signature of soil-released nitric oxide (NO) after fertilizer application. *Atmospheric Environment*, 42 (19), pp.4747–4754. [Online]. Available at: doi:10.1016/j.atmosenv.2008.01.042.

Li, T. et al. (2017). Changes in soil bacterial community structure as a result of incorporation of Brassica plants compared with continuous planting eggplant and chemical disinfection in greenhouses. *PLOS ONE*, 12 (3), p.e0173923. [Online]. Available at: doi:10.1371/journal.pone.0173923.

Li, X. et al. (2010). Partitioning soil respiration and assessing the carbon balance in a Setaria italica (L.) Beauv. Cropland on the Loess Plateau, Northern China. *Soil Biology and Biochemistry*, 42 (2), pp.337–346. [Online]. Available at: doi:10.1016/j.soilbio.2009.11.013.

Li, Z. et al. (2011). Contrasting diurnal variations in soil organic carbon decomposition and root respiration due to a hysteresis effect with soil temperature in a Gossypium s. (cotton) plantation. *Plant and Soil*, 343 (1), pp.347–355. [Online]. Available at: doi:10.1007/s11104-011-0722-1.

Liang, L. L. et al. (2018). Nitrous oxide fluxes determined by continuous eddy covariance measurements from intensively grazed pastures: Temporal patterns and environmental controls. *Agriculture, Ecosystems & Environment*, 268, pp.171–180. [Online]. Available at: doi:10.1016/j.agee.2018.09.010.

Liu, B. et al. (2010). Denitrification gene pools, transcription and kinetics of NO, N2O and N2 production as affected by soil pH. *FEMS Microbiology Ecology*, 72 (3), pp.407–417.

Liu, B., Frostegård, Å. and Bakken, L. R. (2014). Impaired reduction of N2O to N2 in acid soils is due to a posttranscriptional interference with the expression of nosZ. *mBio*, 5 (3), pp.e01383-01314. [Online]. Available at: doi:10.1128/mBio.01383-14.

Liu, H. et al. (2019). Heterotrophic nitrification and denitrification are the main sources of nitrous oxide in two paddy soils. *Plant and Soil*, 445 (1), pp.39–53. [Online]. Available at: doi:10.1007/s11104-018-3860-x.

Liu, R. et al. (2016). Nitrification Is a Primary Driver of Nitrous Oxide Production in Laboratory Microcosms from Different Land-Use Soils. *Frontiers in Microbiology*, 7, p.1373. [Online]. Available at: doi:10.3389/fmicb.2016.01373.

Liu, X. et al. (2014). Response of soil N2O emissions to precipitation pulses under different nitrogen availabilities in a semiarid temperate steppe of Inner Mongolia, China. *Journal of Arid Land*, 6 (4), pp.410–422. [Online]. Available at: doi:10.1007/s40333-013-0211-x.

Livesley, S. et al. (2008). Trace gas flux and the influence of short-term soil water and temperature dynamics in Australian sheep grazed pastures of differing productivity. *Plant and Soil*, 309, pp.89–103. [Online]. Available at: doi:10.1007/s11104-008-9647-8.

Lloyd, J. and Taylor, J. A. (1994). On the Temperature Dependence of Soil Respiration. *Functional Ecology*, 8 (3), pp.315–323. [Online]. Available at: doi:10.2307/2389824.

Loescher, H. W. et al. (2006). Uncertainties in, and interpretation of, carbon flux estimates using the eddy covariance technique. *Journal of Geophysical Research: Atmospheres*, 111 (D21). [Online]. Available at: doi:10.1029/2005JD006932 [Accessed 22 November 2021].

Lognoul, M. et al. (2019). N2O flux short-term response to temperature and topsoil disturbance in a fertilized crop: An eddy covariance campaign. *Agricultural and Forest Meteorology*, 271, pp.193–206. [Online]. Available at: doi:10.1016/j.agrformet.2019.02.033.

Louw-Gaume, A. E. et al. (2017). Temporal differences in plant growth and root exudation of two Brachiaria grasses in response to low phosphorus supply. *Tropical Grasslands-Forrajes Tropicales*, 5 (3), pp.103–116. [Online]. Available at: doi:10.17138/tgft(5)103-116.

Lu, X. et al. (2013). Responses of Soil CO2 Fluxes to Short-Term Experimental Warming in Alpine Steppe Ecosystem, Northern Tibet. *PLOS ONE*, 8 (3), p.e59054. [Online]. Available at: doi:10.1371/journal.pone.0059054.

Luo, Y. and Zhou, X. (2006). CHAPTER 7 - Responses to Disturbances. In: Luo, Y. and Zhou, X. (Eds). *Soil Respiration and the Environment*. Burlington: Academic Press. pp.133–158. [Online]. Available at: doi:10.1016/B978-012088782-8/50007-3 [Accessed 28 November 2021].

Ma, J. et al. (2020). Herbaceous layer determines the relationship between soil respiration and photosynthesis in a shrub-dominated desert plant community. *Plant and Soil*, 449. [Online]. Available at: doi:10.1007/s11104-020-04484-6.

Maag, M. and Vinther, F. P. (1996). Nitrous oxide emission by nitrification and denitrification in different soil types and at different soil moisture contents and temperatures. *Applied Soil Ecology*, 4 (1), pp.5–14. [Online]. Available at: doi:10.1016/0929-1393(96)00106-0.

Macduff, J. H. and Bakken, A. K. (2003). Diurnal variation in uptake and xylem contents of inorganic and assimilated N under continuous and interrupted N supply to Phleum pratense and Festuca pratensis. *Journal of Experimental Botany*, 54 (381), pp.431–444. [Online]. Available at: doi:10.1093/jxb/erg058.

Maeda, K. et al. (2015). N2O production, a widespread trait in fungi. *Scientific Reports*, 5, p.9697.

Makita, N. et al. (2018). Seasonal and diurnal patterns of soil respiration in an evergreen coniferous forest: Evidence from six years of observation with automatic chambers. *PLOS ONE*, 13 (2), p.e0192622. [Online]. Available at: doi:10.1371/journal.pone.0192622.

Makita, N., Kosugi, Y. and Kamakura, M. (2014). Linkages between diurnal patterns of root respiration and leaf photosynthesis in Quercus crispula and Fagus crenata seedlings. *Journal of Agricultural Meteorology*, 70 (3), pp.151–162. [Online]. Available at: doi:10.2480/agrmet.D-14-00006.

Maljanen, M. et al. (2002). Short-term variation in fluxes of carbon dioxide, nitrous oxide and methane in cultivated and forested organic boreal soils. *Soil Biology and Biochemistry*, 34 (5), pp.577–584. [Online]. Available at: doi:10.1016/S0038-0717(01)00213-9.

di Marco, C. et al. (2005). Field scale N2O flux measurements from grassland using eddy covariance. *Water, Air, & Soil Pollution: Focus*, 4 (6), pp.143–149. [Online]. Available at: doi:10.1007/s11267-005-3024-x.

Marsden, K. A. et al. (2018). Sheep urine patch N2O emissions are lower from extensively-managed than intensively-managed grasslands. *Agriculture, Ecosystems & Environment*, 265, pp.264–274. [Online]. Available at: doi:10.1016/j.agee.2018.06.025.

Martens, D. A. (2005). Denitrification. In: Hillel, D. B. T.-E. of S. in the E. (Ed). *Encyclopedia of Soils in the Environment*. Oxford: Elsevier. pp.378–382. [Online]. Available at: doi:https://doi.org/10.1016/B0-12-348530-4/00138-7.

Maurer, D. et al. (2021). Interactive regulation of root exudation and rhizosphere denitrification by plant metabolite content and soil properties. *Plant and Soil*, 467 (1), pp.107–127. [Online]. Available at: doi:10.1007/s11104-021-05069-7.

McDaniel, M. D. et al. (2017). Quantifying and predicting spatio-temporal variability of soil CH4 and N2O fluxes from a seemingly homogeneous Australian agricultural field. *Agriculture, Ecosystems & Environment*, 240, pp.182–193. [Online]. Available at: doi:10.1016/j.agee.2017.02.017.

McGinn, S. M. (2006). Measuring greenhouse gas emissions from point sources in agriculture. *Canadian Journal of Soil Science*, 86 (3), pp.355–371. [Online]. Available at: doi:10.4141/S05-099.

McKenney, D. J., Shuttleworth, K. F. and Findlay, W. I. (1980). Temperature dependence of nitrous oxide production from brookston clay. *Canadian Journal of Soil Science*, 60, pp.665–674. [Online]. Available at: doi:10.4141/cjss80-076.

McLain, J. E. T. and Martens, D. A. (2006). N2O production by heterotrophic N transformations in a semiarid soil. *Applied Soil Ecology*, 32 (2), pp.253–263. [Online]. Available at: doi:10.1016/j.apsoil.2005.06.005.

McMillan, A. et al. (2014). *Automated N2O/N2 analysis- a new tool for studying denitrification dynamics and testing mitigation strategies*.

McMillen, R. T. (1988). An eddy correlation technique with extended applicability to non-simple terrain. *Boundary-Layer Meteorology*, 43 (3), pp.231–245. [Online]. Available at: doi:10.1007/BF00128405.

Meinhardt, K. A. et al. (2018). Ammonia-oxidizing bacteria are the primary N2O producers in an ammonia-oxidizing archaea dominated alkaline agricultural soil. *Environmental Microbiology*, 20 (6), pp.2195–2206. [Online]. Available at: doi:10.1111/1462-2920.14246.

Melling, L. et al. (2014). Soil CO2 Fluxes from Different Ages of Oil Palm in Tropical Peatland of Sarawak, Malaysia. In: Hartemink, A. E. and McSweeney, K. (Eds). *Soil Carbon*. Progress in Soil Science. Cham: Springer International Publishing. pp.447–455. [Online]. Available at: doi:10.1007/978-3-319-04084-4_44 [Accessed 22 November 2021].

Mencuccini, M. and Hölttä, T. (2010). The significance of phloem transport for the speed with which canopy photosynthesis and belowground respiration are linked. *New Phytologist*, 185 (1), pp.189–203. [Online]. Available at: doi:10.1111/j.1469-8137.2009.03050.x.

Mendes, R., Garbeva, P. and Raaijmakers, J. M. (2013). The rhizosphere microbiome: significance of plant beneficial, plant pathogenic, and human pathogenic microorganisms. *FEMS Microbiology Reviews*, 37 (5), pp.634–663. [Online]. Available at: doi:10.1111/1574-6976.12028.

Metivier, K. A., Pattey, E. and Grant, R. F. (2009). Using the ecosys mathematical model to simulate temporal variability of nitrous oxide emissions from a fertilized agricultural soil. *Soil Biology and Biochemistry*, 41, pp.2370–2386. [Online]. Available at: doi:10.1016/j.soilbio.2009.03.007.

Micallef, S. A. et al. (2009). Plant age and genotype impact the progression of bacterial community succession in the Arabidopsis rhizosphere. *Plant Signaling & Behavior*, 4 (8), pp.777–780.

Miller, M. et al. (2009). Denitrifier Community Dynamics in Soil Aggregates under Permanent Grassland and Arable Cropping Systems. *Soil Science Society of America Journal - SSSAJ*, 73. [Online]. Available at: doi:10.2136/sssaj2008.0357.

Minick, K. et al. (2016). Dissimilatory nitrate reduction to ammonium and N2O flux: effect of soil redox potential and N fertilization in loblolly pine forests. *Biology and Fertility of Soils*, 52. [Online]. Available at: doi:10.1007/s00374-016-1098-4.

Mithen, R. F., Lewis, B. G. and Fenwick, G. R. (1986). In vitro activity of glucosinolates and their products against Leptosphaeria maculans. *Transactions of the British Mycological Society*, 87 (3), pp.433–440. [Online]. Available at: doi:10.1016/S0007-1536(86)80219-4.

Moldrup, P. et al. (2000). Predicting the Gas Diffusion Coefficient in Undisturbed Soil from Soil Water Characteristics. *Soil Science Society of America Journal*, 64 (1), pp.94–100. [Online]. Available at: doi:10.2136/sssaj2000.64194x.

Morley, N. et al. (2008). Production of NO, N2O and N2 by extracted soil bacteria, regulation by NO2(-) and O2 concentrations. *FEMS microbiology ecology*, 65 (1), pp.102–112. [Online]. Available at: doi:10.1111/j.1574-6941.2008.00495.x.

Mosier, A. R. (1994). Nitrous oxide emissions from agricultural soils. *Fertilizer research*, 37 (3), pp.191–200. [Online]. Available at: doi:10.1007/BF00748937.

Mosier, A. R. et al. (1998). Assessing and Mitigating N2O Emissions from Agricultural Soils. *Climatic Change*, 40 (1), pp.7–38. [Online]. Available at: doi:10.1023/A:1005386614431.

Mrkonjic Fuka, M., Gesche Braker, S. H. and Philippot, L. (2007). *Chapter 20 - Molecular Tools to Assess the Diversity and Density of Denitrifying Bacteria in Their Habitats*. In: Bothe, H., Ferguson, S. J. and Newton, W. E. B. T.-B. of the N. C. (Eds). Amsterdam: Elsevier. pp.313–330. [Online]. Available at: doi:https://doi.org/10.1016/B978-044452857-5.50021-7.

Müller, C. et al. (2009). Effect of elevated CO2 on soil N dynamics in a temperate grassland soil. *Soil Biology & Biochemistry*, 41 (9), pp.1996–2001.

Murray, P. et al. (2004). Effect of defoliation on patterns of carbon exudation from Agrostis capillaris. *Journal of Plant Nutrition and Soil Science*, 167 (4), pp.487–493. [Online]. Available at: doi:10.1002/jpln.200320371.

Myhre, G. et al. (2013). *Anthropogenic and Natural Radiative Forcing*. Cambridge, United Kingdom and New York, NY, USA: Intergovernmental Panel on Climate Change.

Myrold, D. D. and Tiedje, J. M. (1985). Establishment of denitrification capacity in soil: Effects of carbon, nitrate and moisture. *Soil Biology and Biochemistry*, 17 (6), pp.819–822. [Online]. Available at: doi:https://doi.org/10.1016/0038-0717(85)90140-3.

Myrstener, M., Jonsson, A. and Bergström, A.-K. (2016). The effects of temperature and resource availability on denitrification and relative N2O production in boreal lake sediments. *Journal of Environmental Sciences*, 47. [Online]. Available at: doi:10.1016/j.jes.2016.03.003.

Nakadai, T. et al. (2002). Diurnal changes of carbon dioxide flux from bare soil in agricultural field in Japan. *Applied Soil Ecology*, 19 (2), pp.161–171. [Online]. Available at: doi:10.1016/S0929-1393(01)00180-9.

Nakayama, M. and Tateno, R. (2018). Solar radiation strongly influences the quantity of forest tree root exudates. *Trees*, 32 (3), pp.871–879. [Online]. Available at: doi:10.1007/s00468-018-1685-0.

Neales, T. F. and Davies, J. A. (1966). The effect of photoperiod duration upon the respiratory activity of the roots of wheat seedlings. *Aust. J. Biol. Sci.*, 19, pp.471–480.

Necpálová, M. et al. (2015). Understanding the DayCent model: Calibration, sensitivity, and identifiability through inverse modeling. *Environmental Modelling & Software*, 66, pp.110–130. [Online]. Available at: doi:10.1016/j.envsoft.2014.12.011.

Neill, C. et al. (2005). Rates and controls of nitrous oxide and nitric oxide emissions following conversion of forest to pasture in Rondônia. *Nutrient Cycling in Agroecosystems*, 71 (1), pp.1–15. [Online]. Available at: doi:10.1007/s10705-004-0378-9.

Newman, E. I. (1985). The rhizosphere: carbon sources and microbial populations. *Ecological interactions in soil: plants, microbes and animals*, pp.107–121.

Nguyen, C. (2009). Rhizodeposition of Organic C by Plant: Mechanisms and Controls. In: Lichtfouse, E. et al. (Eds). *Sustainable Agriculture*. Dordrecht: Springer Netherlands. pp.97–123. [Online]. Available at: doi:10.1007/978-90-481-2666-8_9 [Accessed 9 May 2022].

Nikolausz, M. et al. (2008). Diurnal redox fluctuation and microbial activity in the rhizosphere of wetland plants. *European Journal of Soil Biology*, 44 (3), pp.324–333. [Online]. Available at: doi:10.1016/j.ejsobi.2008.01.003.

NOAA National Centers for Environmental information. *Climate at a Glance: Global Time Series*. NOAA National Centers for Environmental information. [Online]. Available at: https://www.ncdc.noaa.gov/cag/ [Accessed 21 May 2021].

Norton, J. and Ouyang, Y. (2019). Controls and Adaptive Management of Nitrification in Agricultural Soils. *Frontiers in Microbiology*, 10, p.1931. [Online]. Available at: doi:10.3389/fmicb.2019.01931.

Nunan, N. et al. (2003). Spatial distribution of bacterial communities and their relationships with the micro-architecture of soil. *FEMS Microbiology Ecology*, 44 (2), pp.203–215. [Online]. Available at: doi:10.1016/S0168-6496(03)00027-8.

O'Brien, F. J. M. et al. (2018). Rhizosphere Bacterial Communities Differ According to Fertilizer Regimes and Cabbage (Brassica oleracea var. capitata L.) Harvest Time, but Not Aphid Herbivory. *Frontiers in Microbiology*, 9, p.1620. [Online]. Available at: doi:10.3389/fmicb.2018.01620.

Oburger, E. et al. (2014). Root exudation of phytosiderophores from soil-grown wheat. *New Phytologist*, 203 (4), pp.1161–1174. [Online]. Available at: doi:https://doi.org/10.1111/nph.12868.

O'Callaghan, K. J. et al. (2000). Effects of Glucosinolates and Flavonoids on Colonization of the Roots of Brassica napus by Azorhizobium caulinodans ORS571. *Applied and Environmental Microbiology*, 66 (5), pp.2185–2191.

Okubo, A., Matsusaka, M. and Sugiyama, S. (2016). Impacts of root symbiotic associations on interspecific variation in sugar exudation rates and rhizosphere microbial communities: a comparison among four plant families. *Plant and Soil*, 399 (1), pp.345–356. [Online]. Available at: doi:10.1007/s11104-015-2703-2.

Okuyama, Y., Ozawa, K. and Takagaki, M. (2015). Diurnal changes in nitrogen and potassium absorption rates of plants grown in a greenhouse. *Journal of Agricultural Meteorology*, 71 (4), pp.256–262. [Online]. Available at: doi:10.2480/agrmet.D-14-00039.

O'Leary, J. W. (1966). Temperature Effects on Root Pressure Exudation. *Annals of Botany*, 30 (119), pp.419–423.

Opdyke, M. R., Ostrom, N. E. and Ostrom, P. H. (2009). Evidence for the predominance of denitrification as a source of N2O in temperate agricultural soils based on isotopologue measurements. *Global Biogeochemical Cycles*, 23 (4). [Online]. Available at: doi:10.1029/2009GB003523 [Accessed 1 October 2021].

Or, D. et al. (2007). Physical constraints affecting bacterial habitats and activity in unsaturated porous media – a review. *Adv. Water Resour.*, 30.

Ostrom, N. et al. (2010). Isotopologue data reveal bacterial denitrification as the primary source of N2O during a high flux event following cultivation of a native temperate grassland. *Soil Biology and Biochemistry*, 42, pp.499–506. [Online]. Available at: doi:10.1016/j.soilbio.2009.12.003.

Pajares, S. and Bohannan, B. J. M. (2016). Ecology of Nitrogen Fixing, Nitrifying, and Denitrifying Microorganisms in Tropical Forest Soils. *Frontiers in Microbiology*, 7, p.1045. [Online]. Available at: doi:10.3389/fmicb.2016.01045.

Pandey, C. B. et al. (2020). DNRA: A short-circuit in biological N-cycling to conserve nitrogen in terrestrial ecosystems. *The Science of the Total Environment*, 738, p.139710. [Online]. Available at: doi:10.1016/j.scitotenv.2020.139710.

Papastylianou, I. (1995). Diurnal variation of nitrate concentration in cereals grown under rainfed mediterranean conditions. *Communications in Soil Science and Plant Analysis*, 26 (7–8), pp.1121–1131. [Online]. Available at: doi:10.1080/00103629509369359.

Park, S. et al. (2012). Trends and seasonal cycles in the isotopic composition of nitrous oxide since 1940. *Nature Geoscience*, 5 (4), pp.261–265. [Online]. Available at: doi:10.1038/ngeo1421.

Parker, S. S. and Schimel, J. P. (2011). Soil nitrogen availability and transformations differ between the summer and the growing season in a California grassland. *Applied Soil Ecology*, 48 (2), pp.185–192.

Parkin, T. B. (2008). Effect of Sampling Frequency on Estimates of Cumulative Nitrous Oxide Emissions. *Journal of Environmental Quality*, 37 (4), pp.1390–1395. [Online]. Available at: doi:10.2134/jeq2007.0333.

Parkin, T. B. and Kaspar, T. C. (2006). Nitrous Oxide Emissions from Corn–Soybean Systems in the Midwest. *Journal of Environmental Quality*, 35 (4), pp.1496–1506. [Online]. Available at: doi:10.2134/jeq2005.0183.

Parkin, T. B. and Venterea, R. T. (2010). *Chapter 3. Chamber-based trace gas flux measurements*. Washington D.C., USA: USDA., pp.1–39.

Parkin, T. and Kaspar, T. (2003). Temperature Controls on Diurnal Carbon Dioxide Flux: Implications for Estimating Soil Carbon Loss. *Soil Science Society of America Journal - SSSAJ*, 67.

Patel, K. F. et al. (2021). Repeated freeze–thaw cycles increase extractable, but not total, carbon and nitrogen in a Maine coniferous soil. *Geoderma*, 402, p.115353. [Online]. Available at: doi:10.1016/j.geoderma.2021.115353.

Pausch, J. et al. (2013). Estimation of rhizodeposition at field scale: upscaling of a 14C labeling study. *Plant and Soil*, 364 (1), pp.273–285. [Online]. Available at: doi:10.1007/s11104-012-1363-8.

Pavelka, M. et al. (2018). Standardisation of chamber technique for CO2, N2O and CH4 fluxes measurements from terrestrial ecosystems. *International Agrophysics*, 32 (4), pp.569–587. [Online]. Available at: doi:10.1515/intag-2017-0045.

Paynel, F., J Murray, P. and Bernard Cliquet, J. (2001). Root exudates: a pathway for short-term N transfer from clover and ryegrass. *Plant and Soil*, 229 (2), pp.235–243. [Online]. Available at: doi:10.1023/A:1004877214831.

Pedersen, H., Dunkin, K. A. and Firestone, M. K. (1999). The relative importance of autotrophic and heterotrophic nitrification in a conifer forest soil as measured by 15N tracer and pool dilution techniques. *Biogeochemistry*, 44 (2), pp.135–150. [Online]. Available at: doi:10.1023/A:1006059930960.

Peng, B. et al. (2019). N2O emission from a temperate forest soil during the freeze-thaw period: a mesocosm study. *Science of the Total Environment*, 648, pp.350–357. [Online]. Available at: doi:10.1016/j.scitotenv.2018.08.155.

Pester, M. et al. (2013). NxrB encoding the beta subunit of nitrite oxidoreductase as functional and phylogenetic marker for nitrite-oxidizing Nitrospira. *Environmental Microbiology*, 16 (10), pp.3055–3071. [Online]. Available at: doi:10.1111/1462-2920.12300.

Peterjohn, W. T. et al. (1994). Responses of Trace Gas Fluxes and N Availability to Experimentally Elevated Soil Temperatures. *Ecological Applications*, 4 (3), pp.617–625. [Online]. Available at: doi:https://doi.org/10.2307/1941962.

Petrescu, A. M. R. et al. (2020). European anthropogenic AFOLU greenhouse gas emissions: a review and benchmark data. *Earth System Science Data*, 12 (2), pp.961–1001. [Online]. Available at: doi:10.5194/essd-12-961-2020.

Phillips, C. L. and Nickerson, N. (2015). Soil Respiration. In: *Reference Module in Earth Systems and Environmental Sciences*. Elsevier. [Online]. Available at: doi:10.1016/B978-0-12-409548-9.09442-2 [Accessed 11 May 2021].

Phillips, R. et al. (2015a). Temperature effects on N $_2$ O and N $_2$ denitrification end-products for a New Zealand pasture soil. *New Zealand Journal of Agricultural Research*, 58 (1), pp.89–95. [Online]. Available at: doi:10.1080/00288233.2014.969380.

Phillips, R. L. et al. (2015b). Temperature effects on N_2O and N_2 denitrification end-products for a New Zealand pasture soil. *New Zealand Journal of Agricultural Research*, 58 (1), pp.89–95. [Online]. Available at: doi:10.1080/00288233.2014.969380.

Pishgar, R. et al. (2019). Denitrification performance and microbial versatility in response to different selection pressures. *Bioresource Technology*, 281, pp.72–83. [Online]. Available at: doi:10.1016/j.biortech.2019.02.061.

Portmann, R. W., Daniel, J. S. and Ravishankara, A. R. (2012). Stratospheric ozone depletion due to nitrous oxide: Influences of other gases. *Philosophical Transactions of the Royal Society B: Biological Sciences*, 367 (1593), pp.1256–1264. [Online]. Available at: doi:10.1098/rstb.2011.0377.

del Prado, A. et al. (2006). N2O and NO emissions from different N sources and under a range of soil water contents. *Nutrient Cycling in Agroecosystems*, 74 (3), pp.229–243. [Online]. Available at: doi:10.1007/s10705-006-9001-6.

Prendergast-Miller, M. T., Baggs, E. M. and Johnson, D. (2011). Nitrous oxide production by the ectomycorrhizal fungi Paxillus involutus and Tylospora fibrillosa. *FEMS Microbiology Letters*, 316 (1), pp.31–35. [Online]. Available at: doi:10.1111/j.1574-6968.2010.02187.x.

Prescott, C. E. et al. (2020). Surplus Carbon Drives Allocation and Plant–Soil Interactions. *Trends in Ecology & Evolution*, 35 (12), pp.1110–1118. [Online]. Available at: doi:10.1016/j.tree.2020.08.007.

Prosser, J. I. et al. (2020). Nitrous oxide production by ammonia oxidizers: Physiological diversity, niche differentiation and potential mitigation strategies. *Global Change Biology*, 26 (1), pp.103–118. [Online]. Available at: doi:10.1111/gcb.14877.

Prosser, J. I. and Nicol, G. W. (2008). Relative contributions of archaea and bacteria to aerobic ammonia oxidation in the environment. *Environmental Microbiology*, 10 (11), pp.2931–2941. [Online]. Available at: doi:10.1111/j.1462-2920.2008.01775.x.

Prosser, J. I. and Nicol, G. W. (2012). Archaeal and bacterial ammonia-oxidisers in soil: the quest for niche specialisation and differentiation. *Trends in Microbiology*, 20 (11), pp.523–531. [Online]. Available at: doi:10.1016/j.tim.2012.08.001.

Putz, M. et al. (2018). Relative abundance of denitrifying and DNRA bacteria and their activity determine nitrogen retention or loss in agricultural soil. *Soil Biology and Biochemistry*, 123, pp.97–104. [Online]. Available at: doi:10.1016/j.soilbio.2018.05.006.

Ravishankara, A. R., Daniel, J. S. and Portmann, R. W. (2009). Nitrous oxide (N2O): The dominant ozone-depleting substance emitted in the 21st century. *Science*, 326 (5949), pp.123–125. [Online]. Available at: doi:10.1126/science.1176985.

Reay, D. S. et al. (2012). Global agriculture and nitrous oxide emissions. *Nature Climate Change*, 2 (6), pp.410–416. [Online]. Available at: doi:10.1038/nclimate1458.

Redeker, K. R., Baird, A. J. and Teh, Y. A. (2015). Quantifying wind and pressure effects on trace gas fluxes across the soil–atmosphere interface. *Biogeosciences*, 12 (24), pp.7423–7434. [Online]. Available at: doi:10.5194/bg-12-7423-2015.

Reeves, S. et al. (2016). Quantifying nitrous oxide emissions from sugarcane cropping systems: Optimum sampling time and frequency. *Atmospheric Environment*, 136, pp.123–133. [Online]. Available at: doi:10.1016/j.atmosenv.2016.04.008.

Reeves, S. and Wang, W. (2015). Optimum sampling time and frequency for measuring N2O emissions from a rain-fed cereal cropping system. *The Science of the Total Environment*, 530–531, pp.219–226. [Online]. Available at: doi:10.1016/j.scitotenv.2015.05.117.

Regina, K. et al. (2004). Fluxes of N2O from farmed peat soils in Finland. *European Journal of Soil Science*, 55 (3), pp.591–599. [Online]. Available at: doi:10.1111/j.1365-2389.2004.00622.x.

Reichman, R. et al. (2013). Effects of soil moisture on the diurnal pattern of pesticide emission: Comparison of simulations with field measurements. *Atmospheric Environment*, 66, pp.52–62. [Online]. Available at: doi:10.1016/j.atmosenv.2012.04.047.

Reichman, S. M. and Parker, D. R. (2007). Probing the effects of light and temperature on diurnal rhythms of phytosiderophore release in wheat. *New Phytologist*, 174 (1), pp.101–108. [Online]. Available at: doi:10.1111/j.1469-8137.2007.01990.x.

Reichstein, M. et al. (2005). On the separation of net ecosystem exchange into assimilation and ecosystem respiration: review and improved algorithm. *Global Change Biology*, 11 (9), pp.1424–1439. [Online]. Available at: doi:https://doi.org/10.1111/j.1365-2486.2005.001002.x.

Reinsch, T. et al. (2020). Nitrous oxide emissions from grass–clover swards as influenced by sward age and biological nitrogen fixation. *Grass and Forage Science*, 75 (4), pp.372–384. [Online]. Available at: doi:10.1111/gfs.12496.

Richter, M. et al. (2012). Temporal Variability of Nitrous Oxide from Fertilized Croplands: Hot Moment Analysis. *Soil Science Society of America Journal*, 76, p.1728. [Online]. Available at: doi:10.2136/sssaj2012.0039.

Ridl, J. et al. (2016). Plants Rather than Mineral Fertilization Shape Microbial Community Structure and Functional Potential in Legacy Contaminated Soil. *Frontiers in Microbiology*, 7, p.995. [Online]. Available at: doi:10.3389/fmicb.2016.00995.

Riley, W. J., Zhu, Q. and Tang, J. Y. (2018). Weaker land–climate feedbacks from nutrient uptake during photosynthesis-inactive periods. *Nature Climate Change*, 8 (11), pp.1002–1006. [Online]. Available at: doi:10.1038/s41558-018-0325-4.

Ringuet, S., Sassano, L. and Johnson, Z. I. (2011). A suite of microplate reader-based colorimetric methods to quantify ammonium, nitrate, orthophosphate and silicate concentrations for aquatic nutrient monitoring. *Journal of Environmental Monitoring*, 13 (2), pp.370–376. [Online]. Available at: doi:10.1039/C0EM00290A.

Risk, N., Snider, D. and Wagner-Riddle, C. (2013). Mechanisms leading to enhanced soil nitrous oxide fluxes induced by freeze–thaw cycles. *Canadian Journal of Soil Science*, 93 (4), pp.401–414. [Online]. Available at: doi:10.4141/cjss2012-071.

Roberts, K. J. and Anderson, R. C. (2001). Effect of Garlic Mustard [Alliaria Petiolata (Beib. Cavara & Grande)] Extracts on Plants and Arbuscular Mycorrhizal (AM) Fungi. *The American Midland Naturalist*, 146 (1), pp.146–152.

Rochette, P. (2011). Towards a standard non-steady-state chamber methodology for measuring soil N2O emissions. *Animal Feed Science and Technology*, 166–167, pp.141–146. [Online]. Available at: doi:10.1016/j.anifeedsci.2011.04.063.

Roman-Perez, C. C. and Hernandez-Ramirez, G. (2021). Sources and priming of nitrous oxide production across a range of moisture contents in a soil with high organic matter. *Journal of Environmental Quality*, 50 (1), pp.94–109. [Online]. Available at: doi:10.1002/jeq2.20172.

Rowlings, D. W. et al. (2015). Rainfall variability drives interannual variation in N2O emissions from a humid, subtropical pasture. *Science of The Total Environment*, 512–513, pp.8–18. [Online]. Available at: doi:10.1016/j.scitotenv.2015.01.011.

Roxy, M. S., Sumithranand, V. B. and Renuka, G. (2010). Variability of soil moisture and its relationship with surface albedo and soil thermal diffusivity at Astronomical Observatory, Thiruvananthapuram, south Kerala. *Journal of Earth System Science*, 119 (4), pp.507–517. [Online]. Available at: doi:10.1007/s12040-010-0038-1.

Ruiz-Rueda, O., Hallin, S. and Bañeras, L. (2009). Structure and function of denitrifying and nitrifying bacterial communities in relation to the plant species in a constructed wetland. *FEMS Microbiology Ecology*, 67 (2), pp.308–319. [Online]. Available at: doi:10.1111/j.1574-6941.2008.00615.x.

Ruser, R. et al. (2001). Effect of crop-specific field management and N fertilization on N2O emissions from a fine-loamy soil. *Nutrient Cycling in Agroecosystems*, 59 (2), pp.177–191. [Online]. Available at: doi:10.1023/A:1017512205888.

Ruser, R. et al. (2006). Emission of N2O, N2 and CO2 from soil fertilized with nitrate: effect of compaction, soil moisture and rewetting. *Soil Biology and Biochemistry*, 38 (2), pp.263–274. [Online]. Available at: doi:10.1016/j.soilbio.2005.05.005.

Ruser, R. et al. (2017). Nitrous oxide emissions from winter oilseed rape cultivation. *Agriculture, Ecosystems & Environment*, 249, pp.57–69. [Online]. Available at: doi:10.1016/j.agee.2017.07.039.

Rütting, T. et al. (2011). Assessment of the importance of dissimilatory nitrate reduction to ammonium for the terrestrial nitrogen cycle. *Biogeosciences*, 8 (7), pp.1779–1791. [Online]. Available at: doi:10.5194/bg-8-1779-2011.

Saikawa, E. et al. (2014). Global and regional emissions estimates for N₂O. *Atmospheric Chemistry and Physics*, 14 (9), pp.4617–4641. [Online]. Available at: doi:10.5194/acp-14-4617-2014.

Savage, K., Phillips, R. and Davidson, E. (2014). High temporal frequency measurements of greenhouse gas emissions from soils. *Biogeosciences*, 11 (10), pp.2709–2720. [Online]. Available at: doi:10.5194/bg-11-2709-2014.

Scanlon, T. M. and Kiely, G. (2003). Ecosystem-scale measurements of nitrous oxide fluxes for an intensely grazed, fertilized grassland. *Geophysical Research Letters*, 30 (16). [Online]. Available at: doi:10.1029/2003GL017454 [Accessed 22 November 2021].

Scheer, C. et al. (2008). Nitrous oxide emissions from fertilized, irrigated cotton (Gossypium hirsutum L.) in the Aral Sea Basin, Uzbekistan: Influence of nitrogen applications and irrigation practices. *Soil Biology and Biochemistry*, 40 (2), pp.290–301. [Online]. Available at: doi:10.1016/j.soilbio.2007.08.007.

Scheer, C. et al. (2011). Effect of biochar amendment on the soil-atmosphere exchange of greenhouse gases from an intensive subtropical pasture in northern New South Wales, Australia. *Plant and Soil*, 345 (1), pp.47–58. [Online]. Available at: doi:10.1007/s11104-011-0759-1.

Scheer, C. et al. (2012). Nitrous oxide emissions from irrigated wheat in Australia: impact of irrigation management. *Plant and Soil*, 359 (1), pp.351–362. [Online]. Available at: doi:10.1007/s11104-012-1197-4.

Scheer, C. et al. (2014). Impact of nitrification inhibitor (DMPP) on soil nitrous oxide emissions from an intensive broccoli production system in sub-tropical Australia. *Soil Biology and Biochemistry*, 77, pp.243–251. [Online]. Available at: doi:10.1016/j.soilbio.2014.07.006.

Schimel, J., Balser, T. C. and Wallenstein, M. (2007). Microbial Stress-Response Physiology and Its Implications for Ecosystem Function. *Ecology*, 88 (6), pp.1386–1394. [Online]. Available at: doi:10.1890/06-0219.

Schimel, J. P. and Bennett, J. (2004). Nitrogen mineralization: Challenges of a changing paradigm. *Ecology*, 85 (3), pp.591–602. [Online]. Available at: doi:10.1890/03-8002.

Schindlbacher, A., Zechmeister-Boltenstern, S. and Butterbach-Bahl, K. (2004). Effects of soil moisture and temperature on NO, NO2, and N2O emissions from European forest soils. *Journal of Geophysical Research: Atmospheres*, 109 (D17). [Online]. Available at: doi:10.1029/2004JD004590.

Schindlbacher, A., Zechmeister-Boltenstern, S. and Butterbach-Bahl, K. (2004). Effects of soil moisture and temperature on NO, NO2, and N2O emissions from European forest soils. *Journal of Geophysical Research: Atmospheres*, 109 (D17). [Online]. Available at: doi:https://doi.org/10.1029/2004JD004590 [Accessed 29 March 2021].

Schleper, C. and Nicol, G. W. (2010). Ammonia-Oxidising Archaea – Physiology, Ecology and Evolution. In: Poole, R. K. (Ed). *Advances in Microbial Physiology*. 57. Academic Press. pp.1–41. [Online]. Available at: doi:10.1016/B978-0-12-381045-8.00001-1 [Accessed 1 October 2021].

Schlüter, S. et al. (2018). Denitrification in Soil Aggregate Analogues-Effect of Aggregate Size and Oxygen Diffusion. *Frontiers in Environmental Science*, 6 (17). [Online]. Available at: doi:10.3389/fenvs.2018.00017.

Schütz, H. et al. (1989). A 3-year continuous record on the influence of daytime, season, and fertilizer treatment on methane emission rates from an Italian rice paddy. *Journal of Geophysical Research*, 94, p.16,405-16,416. [Online]. Available at: doi:10.1029/JD094iD13p16405.

Schützenmeister, K. et al. (2020). N2O emissions from plants are reduced under photosynthetic activity. *Plant-Environment Interactions*, 1 (1), pp.48–56. [Online]. Available at: doi:https://doi.org/10.1002/pei3.10015.

Schwenke, G. D. et al. (2016). Greenhouse gas (N2O and CH4) fluxes under nitrogen-fertilised dryland wheat and barley on subtropical Vertosols: risk, rainfall and alternatives. *Soil Research*, 54 (5), pp.634–650. [Online]. Available at: doi:10.1071/SR15338.

Senwo, Z. N. and Tabatabai, M. A. (1998). Amino acid composition of soil organic matter. *Biology and Fertility of Soils*, 26 (3), pp.235–242. [Online]. Available at: doi:10.1007/s003740050373.

Serquet, G. et al. (2011). Seasonal trends and temperature dependence of the snowfall/ precipitation-day ratio in Switzerland. *Geophysical Research Letters*, 38. [Online]. Available at: doi:10.1029/2011GL046976.

Sgouridis, F. et al. (2011). Denitrification and dissimilatory nitrate reduction to ammonium (DNRA) in a temperate re-connected floodplain. *Water Research*, 45 (16), pp.4909–4922. [Online]. Available at: doi:10.1016/j.watres.2011.06.037.

Sharma, S. et al. (2005). Diversity of Transcripts of Nitrite Reductase Genes (nirK and nirS) in Rhizospheres of Grain Legumes. *Applied and Environmental Microbiology*, 71 (4), p.2001 LP – 2007.

Sharpe, D. (2019). Chi-Square Test is Statistically Significant: Now What? *Practical Assessment, Research, and Evaluation*, 20 (1). [Online]. Available at: doi:https://doi.org/10.7275/tbfa-x148.

Shcherbak, I. and Robertson, G. P. (2019). Nitrous Oxide (N2O) Emissions from Subsurface Soils of Agricultural Ecosystems. *Ecosystems*, 22 (7), pp.1650–1663. [Online]. Available at: doi:10.1007/s10021-019-00363-z.

Shen, J.-P. et al. (2012). A review of ammonia-oxidizing bacteria and archaea in Chinese soils. *Frontiers in Microbiology*, 3, p.296. [Online]. Available at: doi:10.3389/fmicb.2012.00296.

Shepherd, T. and Davies, H. V. (1993). Carbon Loss from the Roots of Forage Rape (Brassica napus L.) Seedlings Following Pulse-labelling with 14CO2. *Annals of Botany*, 72 (2), pp.155–163. [Online]. Available at: doi:10.1006/anbo.1993.1094.

Shukla, P. R. et al. (2019). *Summary for Policymakers*. In press: IPCC.

Shurpali, N. J. et al. (2016). Neglecting diurnal variations leads to uncertainties in terrestrial nitrous oxide emissions. *Scientific Reports*, 6 (1), p.25739. [Online]. Available at: doi:10.1038/srep25739.

Signor, D., Cerri, C. E. P. and Conant, R. (2013). N $_2$ O emissions due to nitrogen fertilizer applications in two regions of sugarcane cultivation in Brazil. *Environmental Research Letters*, 8 (1), p.015013. [Online]. Available at: doi:10.1088/1748-9326/8/1/015013.

Silver, W. L., Herman, D. J. and Firestone, M. K. (2001). Dissimilatory Nitrate Reduction to Ammonium in Upland Tropical Forest Soils. *Ecology*, 82 (9), pp.2410–2416. [Online]. Available at: doi:10.1890/0012-9658(2001)082[2410:DNRTAI]2.0.CO;2.

Šimek, M., Brůček, P. and Hynšt, J. (2010). Diurnal fluxes of CO_2 and N_2O from cattle-impacted soil and implications for emission estimates. *Plant, Soil and Environment*, 56 (No. 10), pp.451–457. [Online]. Available at: doi:10.17221/127/2010-PSE.

Skiba, U. et al. (1996). Measurement of field scale N2O emission fluxes from a wheat crop using micrometeorological techniques. *Plant and Soil*, 181 (1), pp.139–144. [Online]. Available at: doi:10.1007/BF00011300.

Skiba, U. et al. (2012). UK emissions of the greenhouse gas nitrous oxide. *Philosophical Transactions of the Royal Society B: Biological Sciences*, 367 (1593), pp.1175–1185. [Online]. Available at: doi:10.1098/rstb.2011.0356.

Skiba, U. et al. (2013). Comparison of soil greenhouse gas fluxes from extensive and intensive grazing in a temperate maritime climate. *Biogeosciences*, 10 (2), pp.1231–1241. [Online]. Available at: doi:10.5194/bg-10-1231-2013.

Skiba, U. M. et al. (1998). Some key environmental variables controlling nitrous oxide emissions from agricultural and semi-natural soils in Scotland. *Atmospheric Environment*, 32 (19), pp.3311–3320. [Online]. Available at: doi:10.1016/S1352-2310(97)00364-6.

Skiba, U. and Smith, K. A. (2000). The control of nitrous oxide emissions from agricultural and natural soils. *Chemosphere - Global Change Science*, 2 (3), pp.379–386. [Online]. Available at: doi:10.1016/S1465-9972(00)00016-7.

Smith, J. et al. (2010). Estimating changes in national soil carbon stocks using ECOSSE – a new model that includes upland organic soils. Part I. Model description and uncertainty in national scale simulations of Scotland. *Climate Research*, 45, pp.179–192.

Smith, K. A. et al. (1995). The measurement of nitrous oxide emissions from soil by using chambers. *Philosophical Transactions of the Royal Society of London. Series A: Physical and Engineering Sciences*, 351 (1696), pp.327–338. [Online]. Available at: doi:10.1098/rsta.1995.0037.

Smith, K. A. et al. (1998). Effects of temperature, water content and nitrogen fertilisation on emissions of nitrous oxide by soils. *Atmospheric Environment*, 32 (19), pp.3301–3309. [Online]. Available at: doi:10.1016/S1352-2310(97)00492-5.

Smith, K. A. (2017). Changing views of nitrous oxide emissions from agricultural soil: key controlling processes and assessment at different spatial scales. *European Journal of Soil Science*, 68 (2), pp.137–155. [Online]. Available at: doi:10.1111/ejss.12409.

Smith, K. A. and Dobbie, K. E. (2001). The impact of sampling frequency and sampling times on chamber-based measurements of N2O emissions from fertilized soils. *Global Change Biology*, 7 (8), pp.933–945. [Online]. Available at: doi:10.1046/j.1354-1013.2001.00450.x.

Smith, K., Bouwman, L. and Braatz, B. (2000). *N2O: Direct emissions from agricultural soils*. IPCC., pp.361–380. [Online]. Available at: https://www.ipcc-nggip.iges.or.jp/public/gp/bgp/4_5_N2O_Agricultural_Soils.pdf [Accessed 21 September 2021].

Smith, M. S. and Tiedje, J. M. (1979). Phases of denitrification following oxygen depletion in soil. *Soil Biology and Biochemistry*, 11 (3), pp.261–267. [Online]. Available at: doi:10.1016/0038-0717(79)90071-3.

Smith, W. N. et al. (2004). Estimates of the interannual variations of N2O emissions from agricultural soils in Canada. *Nutrient Cycling in Agroecosystems*, 68 (1), pp.37–45. [Online]. Available at: doi:10.1023/B:FRES.0000012230.40684.c2.

Snider, D. M. et al. (2015). From the Ground Up: Global Nitrous Oxide Sources are Constrained by Stable Isotope Values. *PLOS ONE*, 10 (3), p.e0118954. [Online]. Available at: doi:10.1371/journal.pone.0118954.

Snyder, C. S. et al. (2009). Review of greenhouse gas emissions from crop production systems and fertilizer management effects. *Agriculture, Ecosystems & Environment*, 133 (3), pp.247–266. [Online]. Available at: doi:10.1016/j.agee.2009.04.021.

Staddon, P. L. et al. (2003). The speed of soil carbon throughput in an upland grassland is increased by liming. *Journal of Experimental Botany*, 54 (386), pp.1461–1469. [Online]. Available at: doi:10.1093/jxb/erg153.

Stehfest, E. and Bouwman, L. (2006). N_2O and NO emission from agricultural fields and soils under natural vegetation: summarizing available measurement data and modeling of global annual emissions. *Nutrient Cycling in Agroecosystems*, 74 (3), pp.207–228. [Online]. Available at: doi:10.1007/s10705-006-9000-7.

Stein, L. Y. (2011). Heterotrophic Nitrification and Nitrifier Denitrification. In: *Nitrification*. John Wiley & Sons, Ltd. pp.95–114. [Online]. Available at: doi:10.1128/9781555817145.ch5 [Accessed 30 August 2021].

Stein, L. Y. and Klotz, M. G. (2016). The nitrogen cycle. *Current Biology*, 26 (3), pp.R94–R98. [Online]. Available at: doi:10.1016/j.cub.2015.12.021.

Stevenson, F. J. and Cole, M. A. (1999). The Carbon Cycle. In: *Cycles of Soil: Carbon, Nitrogen, Phosphorus, Sulfur, Micronutrients*. 2nd ed. John Wiley & Sons, Ltd. pp.1–19.

Sun, L. et al. (2017). Relationship between fine-root exudation and respiration of two Quercus species in a Japanese temperate forest. *Tree Physiology*, 37 (8), pp.1011–1020. [Online]. Available at: doi:10.1093/treephys/tpx026.

Sun, X. et al. (2018). Effect of rice-straw biochar on nitrous oxide emissions from paddy soils under elevated CO 2 and temperature. *Science of the Total Environment*, 628, pp.629–1009. [Online]. Available at: doi:10.1016/j.scitotenv.2018.02.046.

Suseela, V. et al. (2012). Effects of soil moisture on the temperature sensitivity of heterotrophic respiration vary seasonally in an old-field climate change experiment. *Global Change Biology*, 18 (1), pp.336–348. [Online]. Available at: doi:10.1111/j.1365-2486.2011.02516.x.

Sutka, R. L. et al. (2006). Distinguishing Nitrous Oxide Production from Nitrification and Denitrification on the Basis of Isotopomer Abundances. *Applied and Environmental Microbiology*, 72 (1), p.638. [Online]. Available at: doi:10.1128/AEM.72.1.638-644.2006.

Suzuki, I., Dular, U. and Kwok, S. C. (1974). Ammonia or ammonium ion as substrate for oxidation by Nitrosomonas europaea cells and extracts. *Journal of bacteriology*, 120 (1), pp.556–558.

Swiss Re Institute. (2021). *The economics of climate change: no action not an option*. Swiss Re Institute. [Online]. Available at: https://www.swissre.com/dam/jcr:e73ee7c3-7f83-4c17-a2b8-8ef23a8d3312/swiss-re-institute-expertise-publication-economics-of-climate-change.pdf [Accessed 20 September 2021].

Syakila, A. and Kroeze, C. (2011). The global nitrous oxide budget revisited. *Greenhouse Gas Measurement and Management*, 1 (1), pp.17–26. [Online]. Available at: doi:10.3763/ghgmm.2010.0007.

Syväsalo, E. et al. (2004). Emissions of nitrous oxide from boreal agricultural clay and loamy sand soils. *Nutrient Cycling in Agroecosystems*, 69 (2), pp.155–165. [Online]. Available at: doi:10.1023/B:FRES.0000029675.24465.fc.

Tang, J. et al. (2003). Assessing soil CO2 efflux using continuous measurements of CO2 profiles in soils with small solid-state sensors. *Agricultural and Forest Meteorology*, 118 (3), pp.207–220. [Online]. Available at: doi:10.1016/S0168-1923(03)00112-6.

Tang, J., Baldocchi, D. D. and Xu, L. (2005). Tree photosynthesis modulates soil respiration on a diurnal time scale. *Global Change Biology*, 11 (8), pp.1298–1304. [Online]. Available at: doi:https://doi.org/10.1111/j.1365-2486.2005.00978.x.

Tarre, S. and Green, M. (2004). High-Rate Nitrification at Low pH in Suspended- and Attached-Biomass Reactors. *Applied and Environmental Microbiology*, 70 (11), pp.6481–6487. [Online]. Available at: doi:10.1128/AEM.70.11.6481-6487.2004.

Teepe, R., Brumme, R. and Beese, F. (2001). Nitrous oxide emissions from soil during freezing and thawing periods. *Soil Biology & Biochemistry - SOIL BIOL BIOCHEM*, 33, pp.1269–1275. [Online]. Available at: doi:10.1016/S0038-0717(01)00084-0.

Thilakarathna, S. K. et al. (2020). Nitrous oxide emissions and nitrogen use efficiency in wheat: Nitrogen fertilization timing and formulation, soil nitrogen, and weather effects. *Soil Science Society of America Journal*, 84 (6), pp.1910–1927. [Online]. Available at: doi:10.1002/saj2.20145.

Thilakarathna, S. K. and Hernandez-Ramirez, G. (2021). Primings of soil organic matter and denitrification mediate the effects of moisture on nitrous oxide production. *Soil Biology and Biochemistry*, 155, p.108166. [Online]. Available at: doi:10.1016/j.soilbio.2021.108166.

Tiedje, J. M. (1983). Denitrification. In: *Methods of Soil Analysis*. John Wiley & Sons, Ltd. pp.1011–1026. [Online]. Available at: doi:10.2134/agronmonogr9.2.2ed.c47 [Accessed 30 August 2021].

Tiedje, J. M. et al. (1983). Denitrification: ecological niches, competition and survival. *Antonie van Leeuwenhoek*, 48 (6), pp.569–583. [Online]. Available at: doi:10.1007/BF00399542.

Tiedje, J. M. (1988). Ecology of denitrification and dissimilatory nitrate reduction to ammonium. In: Zehnder, A. J. B. (Ed). *Environmental Microbiology of Anaerobes*. (January 1988). New York: John Wiley & Sons, Ltd. pp.179–244.

Tierens, K. F. M.-J. et al. (2001). Study of the Role of Antimicrobial Glucosinolate-Derived Isothiocyanates in Resistance of Arabidopsis to Microbial Pathogens1. *Plant Physiology*, 125 (4), pp.1688–1699. [Online]. Available at: doi:10.1104/pp.125.4.1688.

Toma, Y. et al. (2011). Nitrous oxide emission derived from soil organic matter decomposition from tropical agricultural peat soil in central Kalimantan, Indonesia. *Soil Science and Plant Nutrition*, 57 (3), pp.436–451. [Online]. Available at: doi:10.1080/00380768.2011.587203.

Tortoso, A. C. and Hutchinson, G. L. (1990). Contributions of Autotrophic and Heterotrophic Nitrifiers to Soil NO and N2O Emissions. *Applied and Environmental Microbiology*, 56 (6), pp.1799–1805.

Uchida, Y. et al. (2013). Contribution of nitrification and denitrification to nitrous oxide emissions in Andosol and from Fluvisol after coated urea application. *Soil Science and Plant Nutrition*, 59 (1), pp.46–55. [Online]. Available at: doi:10.1080/00380768.2012.708646.

Ueno, D. and Ma, J. F. (2009). Secretion time of phytosiderophore differs in two perennial grasses and is controlled by temperature. *Plant and Soil*, 323, pp.335–341. [Online]. Available at: doi:10.1007/s11104-009-9962-8.

Uksa, M. et al. (2015). Prokaryotes in Subsoil-Evidence for a Strong Spatial Separation of Different Phyla by Analysing Co-occurrence Networks. *Frontiers in Microbiology*, 6, p.1269. [Online]. Available at: doi:10.3389/fmicb.2015.01269.

Urban, M. C. (2015). Accelerating extinction risk from climate change. *Science*, 348 (6234), pp.571–573. [Online]. Available at: doi:10.1126/science.aaa4984.

Ussiri, D. and Lal, R. (2012). Formation and Release of Nitrous Oxide from Terrestial and Aquatic Ecossytems. In: *Soil Emission of Nitrous Oxide and its Mitigation*. 1st ed. Springer. pp.63–96. [Online]. Available at: doi:10.1007/978-94-007-5364-8.

Ussiri, D. and Lal, R. (2013). *Soil Emission of Nitrous Oxide and its Mitigation*. [Online]. Available at: doi:10.1007/978-94-007-5364-8.

Van Groenigen, J. W. et al. (2005). Vertical gradients of δ15N and δ18O in soil atmospheric N2O—temporal dynamics in a sandy soil. *Rapid Communications in Mass Spectrometry*, 19 (10), pp.1289–1295. [Online]. Available at: doi:10.1002/rcm.1929.

Van Groenigen, J. W. et al. (2015). The soil N cycle: new insights and key challenges. *SOIL*, 1, pp.235–256. [Online]. Available at: doi:10.5194/soil-1-235-2015.

Vanparys, B. et al. (2007). The phylogeny of the genus Nitrobacter based on comparative rep-PCR, 16S rRNA and nitrite oxidoreductase gene sequence analysis. *Systematic and Applied Microbiology*, 30 (4), pp.297–308. [Online]. Available at: doi:https://doi.org/10.1016/j.syapm.2006.11.006.

Venterea, R. T. (2007). Nitrite-driven nitrous oxide production under aerobic soil conditions: kinetics and biochemical controls. *Global Change Biology*, 13 (8), pp.1798–1809. [Online]. Available at: doi:10.1111/j.1365-2486.2007.01389.x.

Venterea, R. T. et al. (2012). Challenges and opportunities for mitigating nitrous oxide emissions from fertilized cropping systems. *Frontiers in Ecology and the Environment*, 10 (10), pp.562–570. [Online]. Available at: doi:10.1890/120062.

Venterea, R. T. et al. (2020). Global Research Alliance N2O chamber methodology guidelines: Flux calculations. *Journal of Environmental Quality*, 49 (5), pp.1141–1155. [Online]. Available at: doi:10.1002/jeq2.20118.

Vicca, S. et al. (2009). Temperature dependence of greenhouse gas emissions from three hydromorphic soils at different groundwater levels. *Geobiology*, 7 (4), pp.465–476. [Online]. Available at: doi:https://doi.org/10.1111/j.1472-4669.2009.00205.x.

Vierheilig, H. et al. (2000). Differences in glucosinolate patterns and arbuscular mycorrhizal status of glucosinolate-containing plant species. *The New Phytologist*, 146 (2), pp.343–352. [Online]. Available at: doi:10.1046/j.1469-8137.2000.00642.x.

de Vries, F. T. et al. (2019). Changes in root-exudate-induced respiration reveal a novel mechanism through which drought affects ecosystem carbon cycling. *The New Phytologist*, 224 (1), pp.132–145. [Online]. Available at: doi:10.1111/nph.16001.

Wagner-Riddle, C. et al. (2010). Nitrous oxide fluxes related to soil freeze and thaw periods identified using heat pulse probes. *Canadian Journal of Soil Science*, 90 (3), pp.409–418. [Online]. Available at: doi:10.4141/CJSS09016.

Wagner-Riddle, C. et al. (2017). Globally important nitrous oxide emissions from croplands induced by freeze–thaw cycles. *Nature Geoscience*, 10 (4), pp.279–283. [Online]. Available at: doi:10.1038/ngeo2907.

Wagner-Riddle, C. and Thurtell, G. W. (1998). Nitrous oxide emissions from agricultural fields during winter and spring thaw as affected by management practices. *Nutrient Cycling in Agroecosystems*, 52 (2), pp.151–163. [Online]. Available at: doi:10.1023/A:1009788411566.

Waldo, S. et al. (2019). N2O Emissions From Two Agroecosystems: High Spatial Variability and Long Pulses Observed Using Static Chambers and the Flux-Gradient Technique. *Journal of Geophysical Research: Biogeosciences*, 124 (7), pp.1887–1904. [Online]. Available at: doi:10.1029/2019JG005032.

Wang, C. et al. (2021). Factors That Influence Nitrous Oxide Emissions from Agricultural Soils as Well as Their Representation in Simulation Models: A Review. *Agronomy*, 11 (4), p.770. [Online]. Available at: doi:10.3390/agronomy11040770.

Wang, L. et al. (2005). Effects of disturbance and glucose addition on nitrous oxide and carbon dioxide emissions from a paddy soil. *Soil and Tillage Research*, 82 (2), pp.185–194. [Online]. Available at: doi:https://doi.org/10.1016/j.still.2004.06.001.

Wang, L. (2008). N2O and CO2 Emission from an Arable Soil Amended with Glucose and Alanine Addition. In: *2008 2nd International Conference on Bioinformatics and Biomedical Engineering*. 2008. pp.3864–3867. [Online]. Available at: doi:10.1109/ICBBE.2008.467.

Wang, L. and Cai, Z. (2008). Nitrous oxide production at different soil moisture contents in an arable soil in China. *Soil Science and Plant Nutrition*, 54 (5), pp.786–793. [Online]. Available at: doi:10.1111/j.1747-0765.2008.00297.x.

Wang, W. J. et al. (2003). Relationships of soil respiration to microbial biomass, substrate availability and clay content. *Soil Biology and Biochemistry*, 35 (2), pp.273–284. [Online]. Available at: doi:10.1016/S0038-0717(02)00274-2.

Wang, Y. et al. (2017). Responses of denitrifying bacterial communities to short-term waterlogging of soils. *Scientific Reports*, 7 (1), p.803. [Online]. Available at: doi:10.1038/s41598-017-00953-8.

Wang, Z. et al. (2016). Soil Respiration in Semiarid Temperate Grasslands under Various Land Management. *PloS one*, 11, p.e0147987. [Online]. Available at: doi:10.1371/journal.pone.0147987.

van der Weerden, T. J. et al. (1999). Nitrous oxide emissions and methane oxidation by soil following cultivation of two different leguminous pastures. *Biology and Fertility of Soils*, 30 (1), pp.52–60. [Online]. Available at: doi:10.1007/s003740050587.

van der Weerden, T. J., Clough, T. J. and Styles, T. M. (2013). Using near-continuous measurements of N2O emission from urine-affected soil to guide manual gas sampling regimes. *New Zealand Journal of Agricultural Research*, 56 (1), pp.60–76. [Online]. Available at: doi:10.1080/00288233.2012.747548.

van der Weerden, T. J., Kelliher, F. M. and Klein, C. A. M. de. (2012). Influence of pore size distribution and soil water content on nitrous oxide emissions. *Soil Research*, 50 (2), pp.125–135. [Online]. Available at: doi:10.1071/SR11112.

Weier, K. L. et al. (1993). Denitrification and the Dinitrogen/Nitrous Oxide Ratio as Affected by Soil Water, Available Carbon, and Nitrate. *Soil Science Society of America Journal*, 57, pp.66–72. [Online]. Available at: doi:10.2136/sssaj1993.03615995005700010013x.

Weisler, F., Behrens, T. and Horst, W. J. (2001). The Role of Nitrogen-Efficient Cultivars in Sustainable Agriculture. *TheScientificWorldJOURNAL*, 1, pp.61–69. [Online]. Available at: doi:10.1100/tsw.2001.264.

Williams, D. Ll., Ineson, P. and Coward, P. A. (1999). Temporal variations in nitrous oxide fluxes from urine-affected grassland. *Soil Biology and Biochemistry*, 31 (5), pp.779–788. [Online]. Available at: doi:10.1016/S0038-0717(98)00186-2.

Windham-Myers, L. et al. (2018). Potential for negative emissions of greenhouse gases (CO 2 , CH 4 and N 2 O) through coastal peatland re-establishment: Novel insights from high frequency flux data at meter and kilometer scales. *Environmental Research Letters*, 13 (4), p.045005. [Online]. Available at: doi:10.1088/1748-9326/aaae74.

Winiwarter, W. et al. (2018). Technical opportunities to reduce global anthropogenic emissions of nitrous oxide. *Environmental Research Letters*, 13 (1), p.014011. [Online]. Available at: doi:10.1088/1748-9326/aa9ec9.

Winkler, J. P., Cherry, R. S. and Schlesinger, W. H. (1996). The Q10 relationship of microbial respiration in a temperate forest soil. *Soil Biology and Biochemistry*, 28 (8), pp.1067–1072. [Online]. Available at: doi:10.1016/0038-0717(96)00076-4.

Włodarczyk, T. et al. (2021). Sequence and preference in the use of electron acceptors in flooded agricultural soils. *International Agrophysics*, 35 (1), pp.61–71. [Online]. Available at: doi:10.31545/intagr/132372.

Wrage, N. et al. (2001). Role of nitrifier denitrification in the production of nitrous oxide. *Soil Biology and Biochemistry*, 33 (12), pp.1723–1732. [Online]. Available at: doi:https://doi.org/10.1016/S0038-0717(01)00096-7.

Wrage, N. et al. (2005). A novel dual-isotope labelling method for distinguishing between soil sources of N2O. *Rapid Communications in Mass Spectrometry*, 19 (22), pp.3298–3306. [Online]. Available at: doi:10.1002/rcm.2191.

Wrage-Mönnig, N. et al. (2018). The role of nitrifier denitrification in the production of nitrous oxide revisited. *Soil Biology and Biochemistry*, 123, pp.A3–A16. [Online]. Available at: doi:10.1016/j.soilbio.2018.03.020.

Wright, A. F. and Bailey, J. S. (2001). Organic carbon, total carbon, and total nitrogen determinations in soils of variable calcium carbonate contents using a Leco CN-2000 dry combustion analyzer. *Communications in Soil Science and Plant Analysis*, 32 (19–20), pp.3243–3258. [Online]. Available at: doi:10.1081/CSS-120001118.

Wu, H. et al. (2017a). Effect of carbon and nitrogen addition on nitrous oxide and carbon dioxide fluxes from thawing forest soils. *International Agrophysics*, 31 (3), pp.339–349. [Online]. Available at: doi:https://doi.org/10.1515/intag-2016-0065.

Wu, K. et al. (2017b). CO2-induced alterations in plant nitrate utilization and root exudation stimulate N2O emissions. *Soil Biology and Biochemistry*, 106, pp.9–17. [Online]. Available at: doi:10.1016/j.soilbio.2016.11.018.

Wu, X. et al. (2017c). Responses of CH4 and N2O fluxes to land-use conversion and fertilization in a typical red soil region of southern China. *Scientific Reports*, 7 (1), p.10571. [Online]. Available at: doi:10.1038/s41598-017-10806-z.

Wu, Y.-F. et al. (2021). Diurnal variability in soil nitrous oxide emissions is a widespread phenomenon. *Global Change Biology*, 27 (20), pp.4950–4966. [Online]. Available at: doi:10.1111/gcb.15791.

Xia, J. et al. (2009). Effects of diurnal warming on soil respiration are not equal to the summed effects of day and night warming in a temperate steppe. *Biogeosciences*, 6 (8), pp.1361–1370. [Online]. Available at: doi:10.5194/bg-6-1361-2009.

Xing, L. et al. (2021). An improved microelectrode method reveals significant emission of nitrous oxide from the rhizosphere of a long-term fertilized soil in the North China Plain. *Science of The Total Environment*, 783, p.147011. [Online]. Available at: doi:10.1016/j.scitotenv.2021.147011.

Xu, J. et al. (2016). Diurnal pattern of nitrous oxide emissions from soils under different vertical moisture distribution conditions. *Chilean journal of agricultural research*, 76, pp.84–92. [Online]. Available at: doi:10.4067/S0718-58392016000100012.

Xu, X. et al. (2008). Root-derived respiration and non-structural carbon of rice seedlings. *European Journal of Soil Biology*, 44 (1), pp.22–29. [Online]. Available at: doi:10.1016/j.ejsobi.2007.09.008.

Yamulki, S. et al. (2001). Diurnal fluxes and the isotopomer ratios of N2O in a temperate grassland following urine amendment. *Rapid Communications in Mass Spectrometry*, 15 (15), pp.1263–1269. [Online]. Available at: doi:10.1002/rcm.352.

Yang, L. and Cai, Z. (2006). Effects of Shading Soybean Plants on N2O Emission from Soil. *Plant and Soil*, 283 (1–2), pp.265–274. [Online]. Available at: doi:10.1007/s11104-006-0017-0.

Yao, Z. et al. (2009). Comparison of manual and automated chambers for field measurements of N2O, CH4, CO2 fluxes from cultivated land. *Atmospheric Environment*, 43 (11), pp.1888–1896. [Online]. Available at: doi:10.1016/j.atmosenv.2008.12.031.

Yao, Z. et al. (2010). Soil-atmosphere exchange potential of NO and N_2O in different land use types of Inner Mongolia as affected by soil temperature, soil moisture, freeze-thaw, and drying-wetting events. *Journal of Geophysical Research Atmospheres*, 115 (17), pp.1–17. [Online]. Available at: doi:10.1029/2009JD013528.

Yin, H. et al. (2013). Enhanced root exudation stimulates soil nitrogen transformations in a subalpine coniferous forest under experimental warming. *Global Change Biology*, 19 (7), pp.2158–2167. [Online]. Available at: doi:10.1111/gcb.12161.

Yu, Z. et al. (2012). Effect of Scirpus mariqueter on nitrous oxide emissions from a subtropical monsoon estuarine wetland. *Journal of Geophysical Research: Biogeosciences*, 117 (G2). [Online]. Available at: doi:10.1029/2011JG001850 [Accessed 24 March 2020].

Yue, P. et al. (2018). Impact of elevated precipitation, nitrogen deposition and warming on soil respiration in a temperate desert. *Biogeosciences*, 15 (7), pp.2007–2019. [Online]. Available at: doi:10.5194/bg-15-2007-2018.

Zeng, R. S., Mallik, A. U. and Setliff, E. (2003). Growth stimulation of ectomycorrhizal fungi by root exudates of Brassicaceae plants: role of degraded compounds of indole glucosinolates. *Journal of Chemical Ecology*, 29 (6), pp.1337–1355. [Online]. Available at: doi:10.1023/a:1024257218558.

Zhalnina, K. et al. (2012). Drivers of archaeal ammonia-oxidizing communities in soil. *Frontiers in Microbiology*, 3, p.210. [Online]. Available at: doi:10.3389/fmicb.2012.00210.

Zhang, H. et al. (2021). Precipitation and nitrogen application stimulate soil nitrous oxide emission. *Nutrient Cycling in Agroecosystems*, 120 (3), pp.363–378. [Online]. Available at: doi:10.1007/s10705-021-10155-4.

Zhang, J. et al. (2014). The substrate is an important factor in controlling the significance of heterotrophic nitrification in acidic forest soils. *Soil Biology and Biochemistry*, 76, pp.143–148. [Online]. Available at: doi:10.1016/j.soilbio.2014.05.001.

Zhang, J., Müller, C. and Cai, Z. (2015). Heterotrophic nitrification of organic N and its contribution to nitrous oxide emissions in soils. *Soil Biology and Biochemistry*, 84, pp.199–209. [Online]. Available at: doi:10.1016/j.soilbio.2015.02.028.

Zhang, L.-M. et al. (2012a). Ammonia-oxidizing archaea have more important role than ammonia-oxidizing bacteria in ammonia oxidation of strongly acidic soils. 2011/12/01 ed. *The ISME journal*, 6 (5), pp.1032–1045. [Online]. Available at: doi:10.1038/ismej.2011.168.

Zhang, W. et al. (2017). Effects of drying and wetting cycles on the transformations of extraneous inorganic N to soil microbial residues. *Scientific Reports*, 7 (1), p.9477. [Online]. Available at: doi:10.1038/s41598-017-09944-1.

Zhang, Y. et al. (2012b). Nitrous oxide emissions from a maize field during two consecutive growing seasons in the North China Plain. *Journal of Environmental Sciences*, 24 (1), pp.160–168. [Online]. Available at: doi:10.1016/S1001-0742(10)60594-3.

Zhang, Z. et al. (2016). Do warming-induced changes in quantity and stoichiometry of root exudation promote soil N transformations via stimulation of soil nitrifiers, denitrifiers and ammonifiers? *European Journal of Soil Biology*, 74, pp.60–68. [Online]. Available at: doi:10.1016/j.ejsobi.2016.03.007.

Zhao, K. et al. (2021). Light exposure mediates circadian rhythms of rhizosphere microbial communities. *The ISME Journal*, 15 (9), pp.2655–2664. [Online]. Available at: doi:10.1038/s41396-021-00957-3.

Zhao, P. et al. (2018). On the calculation of daytime CO2 fluxes measured by automated closed transparent chambers. *Agricultural and Forest Meteorology*, 263, pp.267–275. [Online]. Available at: doi:10.1016/j.agrformet.2018.08.022.

Zhou, Y. et al. (2020). Nitrifying Microbes in the Rhizosphere of Perennial Grasses Are Modified by Biological Nitrification Inhibition. *Microorganisms*, 8 (11), p.1687. [Online]. Available at: doi:10.3390/microorganisms8111687.

Zhu, X. et al. (2013). Ammonia oxidation pathways and nitrifier denitrification are significant sources of N2O and NO under low oxygen availability. *Proceedings of the National Academy of Sciences of the United States of America*, 110 (16), pp.6328–6333. [Online]. Available at: doi:10.1073/pnas.1219993110.

Zhu-Barker, X. and Steenwerth, K. L. (2018). Chapter Six - Nitrous Oxide Production From Soils in the Future: Processes, Controls, and Responses to Climate Change. In: Horwath, W. R. and Kuzyakov, Y. (Eds). *Developments in Soil Science*. Climate Change Impacts on Soil Processes and Ecosystem Properties. 35. Elsevier. pp.131–183. [Online]. Available at: doi:10.1016/B978-0-444-63865-6.00006-5 [Accessed 28 September 2021].

Zimmermann, M. et al. (2009). Litter contribution to diurnal and annual soil respiration in a tropical montane cloud forest. *Soil Biology and Biochemistry*, 41 (6), pp.1338–1340. [Online]. Available at: doi:10.1016/j.soilbio.2009.02.023.

Zona, D. et al. (2013). N2O fluxes of a bio-energy poplar plantation during a two years rotation period. *GCB Bioenergy*, 5 (5), pp.536–547. [Online]. Available at: doi:https://doi.org/10.1111/gcbb.12019.

Zuo, J. et al. (2022). Responses of N2O Production and Abundances of Associated Microorganisms to Soil Profiles and Water Regime in Two Paddy Soils. *Agronomy*, 12 (3), p.743. [Online]. Available at: doi:10.3390/agronomy12030743.